PLASTIC POLLUTION IN THE BAY AREAS

EDITED BY: Daoji Li, Xiangrong Xu, Lincoln Fok, Bin Cao and Xiaoshan Zhu
PUBLISHED IN: Frontiers in Marine Science

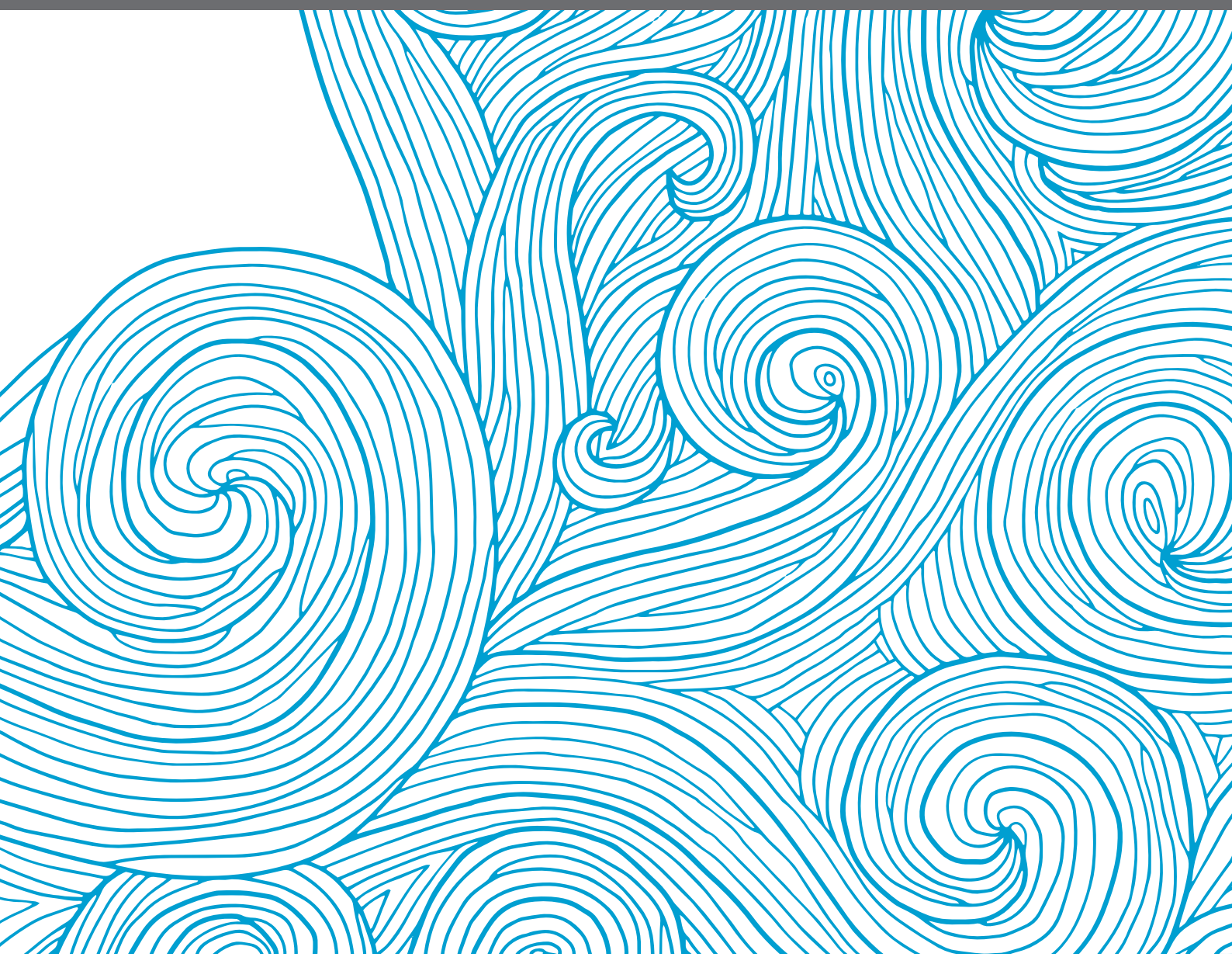

frontiers Research Topics

ISSN 1664-8714
ISBN 978-2-88976-122-7
DOI 10.3389/978-2-88976-122-7

About Frontiers

Frontiers is more than just an open-access publisher of scholarly articles: it is a pioneering approach to the world of academia, radically improving the way scholarly research is managed. The grand vision of Frontiers is a world where all people have an equal opportunity to seek, share and generate knowledge. Frontiers provides immediate and permanent online open access to all its publications, but this alone is not enough to realize our grand goals.

Frontiers Journal Series

The Frontiers Journal Series is a multi-tier and interdisciplinary set of open-access, online journals, promising a paradigm shift from the current review, selection and dissemination processes in academic publishing. All Frontiers journals are driven by researchers for researchers; therefore, they constitute a service to the scholarly community. At the same time, the Frontiers Journal Series operates on a revolutionary invention, the tiered publishing system, initially addressing specific communities of scholars, and gradually climbing up to broader public understanding, thus serving the interests of the lay society, too.

Dedication to Quality

Each Frontiers article is a landmark of the highest quality, thanks to genuinely collaborative interactions between authors and review editors, who include some of the world's best academicians. Research must be certified by peers before entering a stream of knowledge that may eventually reach the public - and shape society; therefore, Frontiers only applies the most rigorous and unbiased reviews.
Frontiers revolutionizes research publishing by freely delivering the most outstanding research, evaluated with no bias from both the academic and social point of view. By applying the most advanced information technologies, Frontiers is catapulting scholarly publishing into a new generation.

What are Frontiers Research Topics?

Frontiers Research Topics are very popular trademarks of the Frontiers Journals Series: they are collections of at least ten articles, all centered on a particular subject. With their unique mix of varied contributions from Original Research to Review Articles, Frontiers Research Topics unify the most influential researchers, the latest key findings and historical advances in a hot research area! Find out more on how to host your own Frontiers Research Topic or contribute to one as an author by contacting the Frontiers Editorial Office: frontiersin.org/about/contact

PLASTIC POLLUTION IN THE BAY AREAS

Topic Editors:
Daoji Li, East China Normal University, China
Xiangrong Xu, South China Sea Institute of Oceanology, Chinese Academy of Sciences, China
Lincoln Fok, The Education University of Hong Kong, Hong Kong, SAR China
Bin Cao, Nanyang Technological University, Singapore
Xiaoshan Zhu, Tsinghua University, China

Citation: Li, D., Xu, X., Fok, L., Cao, B., Zhu, X., eds. (2022). Plastic Pollution in the Bay Areas. Lausanne: Frontiers Media SA. doi: 10.3389/978-2-88976-122-7

Table of Contents

frontiers | Frontiers in Marine Science

EDITORIAL
published: 19 April 2022
doi: 10.3389/fmars.2022.901687

Editorial: Plastic Pollution in the Bay Areas

Xiaoshan Zhu[1,2], *Xiangrong Xu*[3*], *Lincoln Fok*[4], *Bin Cao*[5] *and Daoji Li*[6]

[1] Shenzhen Key Laboratory of Marine IntelliSense and Computation, Shenzhen International Graduate School, Tsinghua University, Shenzhen, China, [2] College of Ecology and Environment, Hainan University, Haikou, China, [3] Key Laboratory of Tropical Marine Bio-Resources and Ecology, Guangdong Provincial Key Laboratory of Applied Marine Biology, South China Sea Institute of Oceanology, Chinese Academy of Sciences, Guangzhou, China, [4] Department of Science and Environmental Studies (SES), The Education University of Hong Kong, Hong Kong, Hong Kong SAR, China, [5] School of Civil and Environmental Engineering and Singapore Centre for Environmental Life Sciences Engineering, Nanyang Technological University, Singapore, Singapore, [6] State Key Laboratory of Estuarine and Coastal Research, East China Normal University, Shanghai, China

Keywords: plastics, microplastics, bay, sources, occurrence, ecological effects

Editorial on the Research Topic

Plastic Pollution in the Bay Areas

MOTIVATION

Bays are special portions of the ocean partly enclosed by the land, varying in size, shape, and depth. Bay areas are characterized by high productivity and rich biodiversity of species and habitats, with high economic and cultural values. More than half of the world's population are living in estuarine, coastal or bay areas, in which the resources, environment and space have formed the important material basis for the sustainable development of human society. The bay ecosystem is relatively fragile and has become one of the most sensitive and concerned ecosystems. In recent decades, the bay ecosystem has been increasingly subject to a large amount of plastic waste which has caused a worldwide problem today. Mass production of plastic products and inappropriate disposal lead to the accumulation of plastic waste in the bay, and thus the bay areas have been acted as one of sinks for plastics. Upon entering the marine environment, plastics will be gradually fragmented and/or degraded into microplastics (generally < 5 mm) and even nanoplastics (generally < 1 μm), greatly increasing the ingestion potential by marine species and causing ecological consequences in the bay areas.

A Research Topic in the Frontiers in Marine Science with the topic "Plastic Pollution in the Bay Areas" was therefore designed, in which 13 papers have been included, covering detection, occurrence, distribution, environmental fates, and ecological effects of plastics in bay areas has thus produced.

SOURCES, OCCURRENCE, DISTRIBUTION, AND ECOLOGICAL EFFECTS

Plastics have been discharged into bay areas from a wide range of sources including runoff, sewage discharge, industrial effluents, and atmospheric deposition. Particularly, surface runoff is considered one major pathway for plastics transport to coast (Okoffo et al., 2019). This is corroborated by the

OPEN ACCESS

Edited and reviewed by:
Ilaria Corsi,
University of Siena, Italy

***Correspondence:**
Xiangrong Xu
xuxr@scsio.ac.cn

Specialty section:
This article was submitted to Marine Pollution, a section of the journal Frontiers in Marine Science

Received: *22 March 2022*
Accepted: *28 March 2022*
Published: *19 April 2022*

Citation:
Zhu X, Xu X, Fok L, Cao B and Li D (2022) Editorial: Plastic Pollution in the Bay Areas. Front. Mar. Sci. 9:901687. doi: 10.3389/fmars.2022.901687

study of Li et al. showing the flux of microplastics into the Jiulong River (a small-/medium-sized river in China) and then into the Xiamen Bay (Xiamen, China). Interestingly, the riverine flux of small microplastics (0.044–5 mm) was found to be about eight times greater than that of large particles (0.33–5.0 mm) (Li et al.). Human activity is undoubtedly deemed for this blame for plastics pollution, which was supported by a significant positive correlation between microplastic abundance and both population density and per capita gross domestic product in Chinese coastal seawaters (Zhu et al.).

Given the concerns of massive inputs of plastics into marine environment, local to middle and large-scale investigations on plastics occurrence and distribution in sea water, sediment, beaches, mangroves or organisms have been actively carried out based on diverse detection technologies (Adyel and Macreadie; Chai et al.; Lei et al.; Li et al.; Liu et al.; Zhang et al.; Zhu et al.). These studies demonstrated that plastics, especially those with small sizes, seem to be ubiquitous and have a wide concentration range in marine environments. In particular, the authors pointed out that mangrove forest is under immense threat of plastic pollution. The world's largest single mangrove forest, the UNESCO Marine World Heritage-listed Sundarbans between Bangladesh and India, is becoming plastic cesspit. In addition, it has been found that weather plays an important role in controlling the distribution of plastics in coastal waters. For example, extreme storms, such as tropical cyclones, are responsible for a significant portion of the plastic debris transported from land to the sea (Nakajima et al.).

In addition to the widespread presence in surface water and sediments, plastics were also detected in the body of various marine organisms, such as corals (Lei et al.). barnacles and bivalves (Zhang et al.). The considerable quantity of plastic found in wild organisms greatly raises the concern of ecological risk and encourages the studies on plastic toxicity effects, which are diverse, including growth inhibition, oxidative stress, metabolic changes, and DNA damage (Su et al.; Zhang et al.). The toxicity mechanisms of plastic are also complicated because plastics are not only an exogenous foreign body but also a vector or carrier for metals and persistent organic pollutants (Han et al.; Han et al.; Su et al.). For instance, a synergistic effect was found between microplastics at 100 mg/L and benzo[a]pyrene (BaP) at 150 μg/L on the microalgae, *Chaetoceros muelleri* (Su et al.). However, most present ecological impact assessments today merely focus on the individual organism level under simplified conditions, further efforts are needed to understand the effects of plastics on complex ecosystems.

CONTRIBUTION AND PERSPECTIVES

In this special issue, we introduce the Research Topic "Plastic Pollution in the Bay Areas" covering the estimation of riverine fluxes, spatio-temporal distribution, toxicity, and environmental behaviors of plastics in the bay areas. New sampling and analytical methodologies for microplastic identification are also discussed. Through the 13 papers adopted, the special issue provides a better understanding of the status, fate, and potential risks of plastics in the bay areas. We hope that this special issue can provide a scientific support for the formulation of prevention and control measures of plastic pollution.

AUTHOR CONTRIBUTIONS

All authors listed have made a substantial, direct and intellectual contribution to the work, and approved it for publication.

ACKNOWLEDGMENTS

We wish to thank all the editors in Marine Science Editorial Office of the Journal, and all the reviewers for their valuable supports on this Research Topic, and thank Dr. Yifan Tong for his help in preparing this Editorial. The work was also supported by the Innovation Group Project of Southern Marine Science and Engineering Guangdong Laboratory (Zhuhai) (No. 311021004) and the National Natural Science Foundation of China (41877352 and 42077227).

REFERENCE

Okoffo, E., O'Brien, S., O'Brien, J., Tscharke, B., and Thomas, K. (2019). Wastewater Treatment Plants as a Source of Plastics in the Environment: A Review of Occurrence, Methods for Identification, Quantification and Fate. *Environ. Sci: Water Res. Technol.* 5., 1908–1931.

Conflict of Interest: The authors declare that the research was conducted in the absence of any commercial or financial relationships that could be construed as a potential conflict of interest.

frontiers in Marine Science

ORIGINAL RESEARCH
published: 23 July 2021
doi: 10.3389/fmars.2021.712727

Mid-Level Riverine Outflow Matters: A Case of Microplastic Transport in the Jiulong River, China

Yifan Li[1,2,3†], Siguang Liu[3,4†], Mengyang Liu[1], Wei Huang[5], Kai Chen[1], Yongcheng Ding[6], Fangzhu Wu[5], Hongwei Ke[1], Linghao Lou[1], Yan Lin[1], Mingyu Zhang[1], Fengjiao Liu[7], Chunhui Wang[1] and Minggang Cai[1,2,3,6]*

[1] College of Ocean and Earth Sciences, Xiamen University, Xiamen, China, [2] State Key Laboratory of Marine Environmental Science, Xiamen University, Xiamen, China, [3] Fujian Provincial Key Laboratory for Coastal Ecology and Environmental Studies, Xiamen University, Xiamen, China, [4] Fujian Institute of Oceanography, Xiamen, China, [5] Second Institute of Oceanography, Ministry of Natural Resources, Hangzhou, China, [6] Coastal and Ocean Management Institute, Xiamen University, Xiamen, China, [7] College of Chemistry and Environment, Minnan Normal University, Zhangzhou, China

OPEN ACCESS

Edited by:
Xiaoshan Zhu, Tsinghua University, China

Reviewed by:
Jianxiang Feng, Sun Yat-sen University Zhuhai Campus, China
Xiaoshou Liu, Ocean University of China, China
Jingli Mu, Minjiang University, China

***Correspondence:**
Minggang Cai
mgcai@xmu.edu.cn

[†]These authors share first authorship

Specialty section:
This article was submitted to Marine Pollution, a section of the journal Frontiers in Marine Science

Received: *21 May 2021*
Accepted: *29 June 2021*
Published: *23 July 2021*

Citation:
Li Y, Liu S, Liu M, Huang W, Chen K, Ding Y, Wu F, Ke H, Lou L, Lin Y, Zhang M, Liu F, Wang C and Cai M (2021) Mid-Level Riverine Outflow Matters: A Case of Microplastic Transport in the Jiulong River, China. Front. Mar. Sci. 8:712727. doi: 10.3389/fmars.2021.712727

Riverine outflow is one of the major pathways for microplastic transportation to coastal environments. Research on the output of microplastics in small- or medium-sized rivers will help accurately understand the status of their marine loads. In this study, we used both trawling and pumping methods to collect microplastics of different sizes in the Jiulong River Estuary and Xiamen Bay. We found that the abundance of small microplastics (44 μm–5.0 mm) was at least 20 times higher than the large particles (0.33–5.0 mm). The abundance of the large particles ranges from 4.96 to 16.3 particles/m^3, and that of the small particles ranged from 82.8 to 918 particles/m^3. Granule was the dominant shape (>60%), and polyethylene (PE), polypropylene (PP), and polyethylene terephthalate (PET) were the most common components. The riverine flux of small microplastics (44 μm–5 mm, 472 ± 230 t/y) was at a medium level and was eight times greater than that of large particles (0.33–5.0 mm, 61.2 ± 2.6 t/y). The behavior of the large microplastics was relatively conservative, whose abundance had a significant correlation with salinity (R^2 = 0.927) and was mainly influenced by physical factors. In contrast, results of statistical analysis revealed that more complicated factors influenced the small microplastics.

Keywords: microplastics, Xiamen Bay, Jiulong River, riverine outflow, export dynamics

INTRODUCTION

Microplastics have become a global concern due to their ecological threats and ubiquitous existence in marine environments (Cole et al., 2015; Galloway and Lewis, 2016; Pagter et al., 2020; Qi et al., 2020). In addition to direct ingestion and physical damage, microplastic may increase the bioaccumulation of persistent organic pollutants and heavy metals along the food chain (Zettler et al., 2013; Bakir et al., 2014; Brennecke et al., 2016; Fu et al., 2020). Rivers connect most land surfaces, and estuarine areas are the most significant socio-economic development belts around the world (Zayen et al., 2020). As for marine plastics, they are mainly from the land-based sources, thus estuarine-coastal environments act as important converters (Schmidt et al., 2017). Riverine outflow

is regarded as one of the major pathways for plastics entering coastal environments, and the annual flux reaches 57000 MT worldwide (Mai et al., 2020).

Several studies have estimated the microplastic flux of riverine flows into the sea. The flux of plastic waste into marine waters globally is estimated to range between 4.8 and 12.7 Mt in 2010, 46.7–126.4 in 2015 on model predictions (Yonkos et al., 2014; Jambeck et al., 2015; Lebreton et al., 2017; Mai et al., 2019; Zhao et al., 2019). These data can help estimate the real value of the reserves of plastics and the plastic pollution in the ocean. However, the results could be more accurate if combined with field data representing the actual situation of watershed-offshore microplastic transportation. Although small- and medium-sized rivers have become essential parts of freshwater systems, most estimations currently focus on major rivers, and outflows in small- or medium-sized rivers are less well known. Therefore, to better study riverine discharges of microplastics and provide robust suggestions on microplastic management, it is essential to consider more small- or medium-sized rivers (Huang et al., 2012).

Xiamen Bay is located in one of the fastest-growing areas in Southeast Asia, the southeast coast of China, and borderers the Jiulong River in the west and the Taiwan Strait in the east. It is a semi-enclosed bay with a normal semi-diurnal tide, and which is divided into the Western Harbor and the Eastern Sea (Chen et al., 2021). Xiamen Bay receives considerable domestic, agricultural, and industrial wastes, and undergoes increasing threats to its environments and ecosystem (Chen et al., 2013). The levels of various contaminants, such as nutrients, persistent organic pollutants, heavy metals, and microplastics, have been reported (Klumpp et al., 2002; Ya et al., 2014; Tang et al., 2018; Wu et al., 2021). Especially, it has been verified that the abundance of microplastics has a relationship with socio-economic development and human activities along the Taiwan Strait Coast (Wu et al., 2021). Because of the intense pollutant release and weak hydrological conditions, more studies are focusing on the transport and fate of contaminants in the Xiamen Bay.

Jiulong River represents a small- or medium-sized river, whose lower reach is connected with Xiamen Bay and further flows into the Taiwan Strait (Li et al., 2015). From the first study on microplastics in this area, the abundance of microplastics by trawling ranges from 103 to 2017 particles/m^3 (Tang et al., 2018). Under the influence of different water exchange dynamics, foam is the most common shape, and the compositions of PP and PE occupied the highest proportions. According to a study on microplastics in seawater and two sides of the Taiwan Strait, particles from the west coast, such as Xiamen Bay, are more prone to transport to the central Taiwan Strait (Wu et al., 2021). Since microplastics with different sizes usually have various buoyancy and vertical transport behavior, further research is needed on the export dynamics of microplastics to support the future management and control (Poulain et al., 2019).

This study focuses on the outflow of microplastics from the Jiulong River. The objectives are (1) to obtain the current status of microplastic pollution in the Jiulong River Estuary and Xiamen Bay, (2) to estimate the flux of microplastics from the river into the sea, and (3) to analyze the factors affecting microplastics of different particle sizes with the help of a variety of correlation analysis methods.

MATERIALS AND METHODS

Microplastic Sampling

Microplastic sampling was conducted at 22 sites in the Jiulong River Estuary and Xiamen Bay by R/V *Haiyang II* in April 2019 (**Figure 1** and **Supplementary Table 1**). We both used trawling and pumping methods to collect microplastics in different sizes (trawling: 0.33–5.0 mm, pumping: 44 μm–5.0 mm); pumping was conducted at all sites, and trawling was conducted at 10 sites.

Surface trawling samples were collected with a 1 m wide and 0.25 deep Manta net with a mesh size of 0.33 mm, at a speed of approximately 2 knots for 15 min. The passing water volume was calculated by the following function:

$$V = v \times t \times S$$

$$S = \text{width} \times \text{depth}$$

where V is the volume of the passing water; v is the shipping speed; t is the time of trawling; and S is the cross-sectional area, which is related to the width and depth of the net.

After trawling, the contents were transferred into a precleaned glass bottle with Milli-Q water, fixed in 2.5% formaldehyde solution, and kept in the dark until further processing was conducted in the laboratory (Lattin et al., 2004).

The particles, which include smaller ones (44 μm–5.0 mm), were collected from the surface water of all 22 sites by pumping. The pumping machine extracted surface water and filtered it in the field. The passing water volume was recorded by a calibrated flow meter (HYDRO-BIOS in Germany) at the mesh port (150–200 L/sample). Relying on a centrifugal pump made of titanium and stainless steel connected to a dual water meter and water hose (Cai et al., 2018). The seawater pump was located 0.5 m below the quarterdeck and bow waterline. The substances remaining on the 5 mm mesh were discarded. Those remaining on the 44 μm mesh were obtained, wrapped, and isolated with aluminum foil, and then stored at a low temperature for further analysis. In addition, according to the data recorded in the two water meters and the sampling duration, the water discharge could be estimated.

Microplastic Pretreatment

The pretreatment method used in this study was the same as that used in our previous studies (Cai et al., 2018; Tang et al., 2018) and is briefly described here. The trawling samples on nets and the pumping samples on meshes were washed three times with Milli-Q water using an ultrasonic cleaning instrument for 2 min. Then all washing solutions were transferred to a precleaned 1 L beaker and prefiltered through a 5 mm metallic mesh to discard the large debris (>5.0 mm). The remaining samples were collected by passing them through a filter consisting of a sand core sandwiched between nylon filter papers (47 mm) and connected to a vacuum pump (Millipore, 20 μm).

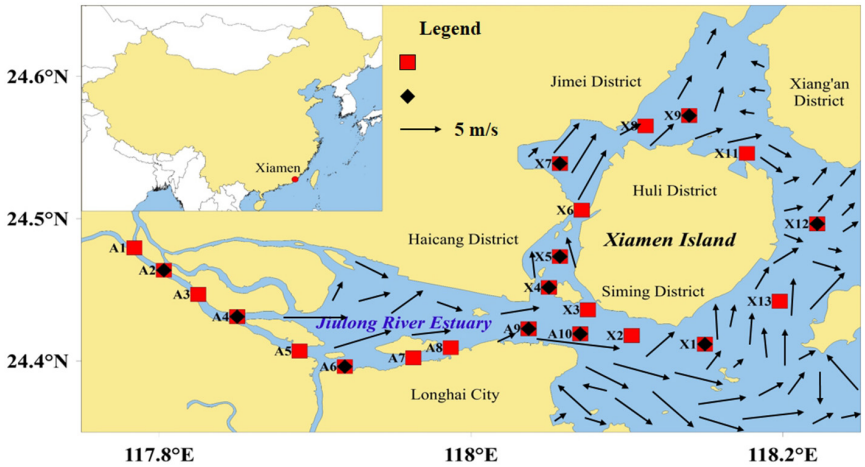

FIGURE 1 | Map of the sampling sites. X1-X9 and X11-X13 are located in Xiamen Bay, and A1-A10 are located in the Jiulong River Estuary. Pumping samples were collected at all sites, and trawling samples were collected at half of the sites, marked in black.

The particles on the nylon filters (20 μm) were disposed of with digestion and flotation to eliminate non-plastic components. Next, the filter contents were treated with a 30% H_2O_2 solution and placed on a 75°C heating plate for 24–48 h for oxidation and digestion (Nuelle et al., 2014; Zhao et al., 2014). After filtering the digestion solution again with a nylon filter (20 μm), the filter contents were density-separated by a saturated NaCl solution (with a density of 1.2 g/cm^3). The upper liquid was collected through nylon filters. Then, the obtained filter membranes and solid retention were placed in capsules for further observation and analysis (Hidalgo-Ruz et al., 2012).

Observation and Identification

The particles collected on the filter papers from the trawling and pumping samples were observed with a microscope (ZEISS, Scope A1, Germany) at approximately 40× magnification, and the microscope was connected with a computer to take photos in "zigzag" mode until every position had been covered and photographed. The number of microplastics in each photo was calculated manually. The possible number of microplastics in each sample was obtained by integration, and they were classified according to their different colors and shapes. According to the color, microplastics can be classified into five categories: black, white, brown, transparent, and others; and the shapes of microplastics can be categorized into four groups: fibers, foams, films, and granules. The size of pumping samples is 44 μm–5.0 mm, and the size of trawling samples is 0.33–5.0 mm.

For identification of polymer type, 10 particles were picked randomly from each filter sample. Three different sections were detected for each particle with a micro-Fourier Transform Infrared Spectroscopy (micro-FTIR) (Nicolet iN10, Thermo Fisher Scientific, United States). Then the obtained spectra were processed by OMNIC Picta software, and were compared to the OMNIC polymer reference spectra library. The sample was regarded as plastics only when the matching rate to a plastic component was higher than 70%, and the polymer type was identified as the type with the maximum matching rate. Finally, statistical data was used to calculate the proportion of particles in each sample.

Quality Assurance and Quality Control

All the sampling devices were thoroughly cleaned with Milli-Q water before use. At each sampling site, the meshes and nets were immediately folded and sealed with aluminum foil in a compact bag, or their contents were directly transferred to glass bottles for further processing. In addition, blank samples were collected at selected sites by filtering 20 L Milli-Q water to analyze potential contamination, e.g., from the air and workers' clothes. The mean abundance of the blank microplastic samples was 0 particles/m^3.

During the laboratory pretreatment and analysis, all researchers wore non-plastic coats and gloves to prevent external pollution. The laboratory platform was cleaned, each instrument was washed with Milli-Q water at least three times before use. All analysis devices and sample containers were covered by aluminum foil when not in use. In addition, after each microscopic examination was complete, we immediately placed the lid on the sample (Nuelle et al., 2014).

The lab blanks, consisting of 250 mL Milli-Q water in place of seawater samples, were treated the same as other samples during the whole process. No particles were found on the filters during the examination, which meant that contamination from the containers, operations, and laboratories could be ignored.

Data Processing

Estimation of the Flux of Microplastics Into the Sea

The flux of microplastics into the sea indicates a situation of microplastic pollution. The following equation is used to calculate the flux of microplastics per unit time (Zhao et al., 2019):

$$\text{Flux} = \sum wt. \times 10^{-6} \times Dischage \times Discharge_{ratio-i} \times 3.1536 \times 10^{7}$$

$$Discharge_{ratio-i} = \frac{h}{H}$$

where *Flux* (t/year) is the annual plastic flux input to the ocean; $\Sigma wt.$ (g/m^3) is the average weight of microplastics in the Jiulong River per square meter. *Discharge* (m^3/s) is the average annual discharge of the river, and $Discharge_{ratio-i}$ is the proportional discharge rate through sampling depth. The discharge rate is assumed to be the same for all depths, h is the depth of sampling, and H is the average water depth of each sampling station. $Discharge_{ratio-i}$ is calculated by the ratio of h to H (Miller et al., 2017).

To estimate the microplastics flux of the Jiulong River estuary, we used the abundance of microplastic from our data and the average weight of microplastic in different components (Eriksen et al., 2013) to calculate $\Sigma wt.$ (**Supplementary Table 7**). Flux of the Jiulong River could be obtained from the previous record, which is 469.3 m^3/s. Moreover, the h for the trawl is 0.25 m deep, and for the pump is 0.5 m deep, and H is different in each site, which shows in **Supplementary Table 2**. Therefore, the $Discharge_{ratio-i}$ can be got in this study.

Data Analysis and Graphing

Cluster analysis, Pearson correlation analysis, and principal component analysis were performed to study the correlations between appearance and composition characteristics of microplastics and other water quality parameters by SPSS version 22.0 (IBM Corporation). The characteristics of microplastics include their abundance, shapes, components, and the water quality parameters include salinity, PH, DO, nutrients, chlorophyll-α, and so on. Microsoft Excel (2019), Golden Software Grapher, and Surfer were used to record and calculate data, and graph.

RESULTS AND DISCUSSION

Microplastic Abundance and Spatial Distribution

Microplastics were widely detected in water samples collected from the Jiulong River and Xiamen Bay, and there were significant spatial variations in distributions of the microplastics (**Figure 2** and **Supplementary Figure 1**).

Xiamen Bay

The abundances of large microplastics collected by trawling varied from 5.52 to 14.8 particles/m^3, and the average value was 12.2 particles/m^3. Microplastic abundance decreased along with river flow, and the abundance in the populated western harbor was higher than those in the eastern area ($p < 0.05$). It was also found in a previous study that there is a significant positive correlation between the abundance of microplastics and population density (Browne et al., 2011).

For the small microplastics collected by pumping, the abundances varied from 82.8 to 918 particles/m^3, and the average value was 340 particles/m^3. Most of the high values were also concentrated in the western harbor, far away from the sea. The abundance of the northwestern island was higher than that of the southwestern island, which indicates that terrestrial inputs near industrialized and populated coastal areas may transport more microplastics in the northwest of the island, while gathering of streams may provide fewer microplastics in the southwest of the island (Browne et al., 2011; Cheung et al., 2016).

The results of other studies can be compared with our data: the average value was 0.490 ± 0.430 particles/m^3 by neuston net with 333μm mesh size in Chabahar Bay, Iran (Aliabad et al., 2019), 8.90 ± 4.70 particles/m^3 collected by plankton net tows with 330 μm in Xiangshan Bay, China (Chen et al., 2018), 0.240 ± 0.350 particles/m^3 by using a Manta trawl with a 335 μm mesh net in the Bay of Brest, France (Frere et al., 2017), 0.140 ± 0.120 particles/m^3 by trawl nets with 330 μm mesh size in Hangzhou Bay, China (Wang et al., 2020), 514 ± 520 particles/m^3 by a manta trawl with 330 μm mesh in Xiamen Bay, China (Tang et al., 2018); the range of abundance was 0.0100–0.700 particles/m^3 by a manta trawl with 333 μm in Todos Santos Bay, Mexico (Ramirez-Alvarez et al., 2020) and 20.0–120 particles/m^3 collected by a 20μm mesh in Jiaozhou Bay, China (Zheng et al., 2019). It can be found that most previous research used the trawl to collect the microplastic, and the sizes of them mainly larger than 330 μm, and that is why the data we obtained by pumping was high than others. The data we obtained by trawling was at the middle level among the abundance observed in other bays with a nearly similar sea.

Jiulong River Estuary

The abundance of large microplastics varied from 4.96 to 16.3 particles/m^3, and the average was 11.1 particles/m^3, which was slightly lower than that observed in Xiamen Bay. Compared with those collected from in large-scale rivers, microplastic abundance observed in the Jiulong River Estuary was lower than that in the Yangtze River Estuary, which was 79.4 ± 60.8 particles/m^3 (0.3–5 mm) (Zhao et al., 2019). This difference may be due to human activities and the scales of these two rivers. In addition, as samples were collected further downstream in the Jiulong River, the abundances decreased gradually due to the dilution effect.

For small microplastics, the distribution varied significantly and irregularly. The abundances ranged from 93.4 to 511 particles/m^3, and the average was 232 particles/m^3, at a moderate level compared with the results of other estuaries with similar sampling methods. For example, the average abundance was 157 ± 75.8 particles/m^3 in the Yangtze River Estuary (60 μm–5.0 mm) (Zhao et al., 2019), 8.90 × 10^3 particles/m^3 (50 μm–5.0 mm) in the Pearl River Estuary (Yan et al., 2019), and 30.0 particles/m^3 (80 μm–5.0 mm) in the Qin River Estuary (Zhang et al., 2020).

The abundance of small microplastics (44 μm–0.33 mm) accounted for a much large proportion of the total collected microplastics than that of large microplastics. This result was in accordance with previous studies, that the dominant size of microplastics in the Saigon River was found to be <0.25 mm (Lahens et al., 2018), and Lindeque et al. (2020) found that United Kingdom data revealed a 2.5-fold increase in microplastics using 100 μm nets compared to 333 μm nets. Different environmental conditions influenced the microplastic

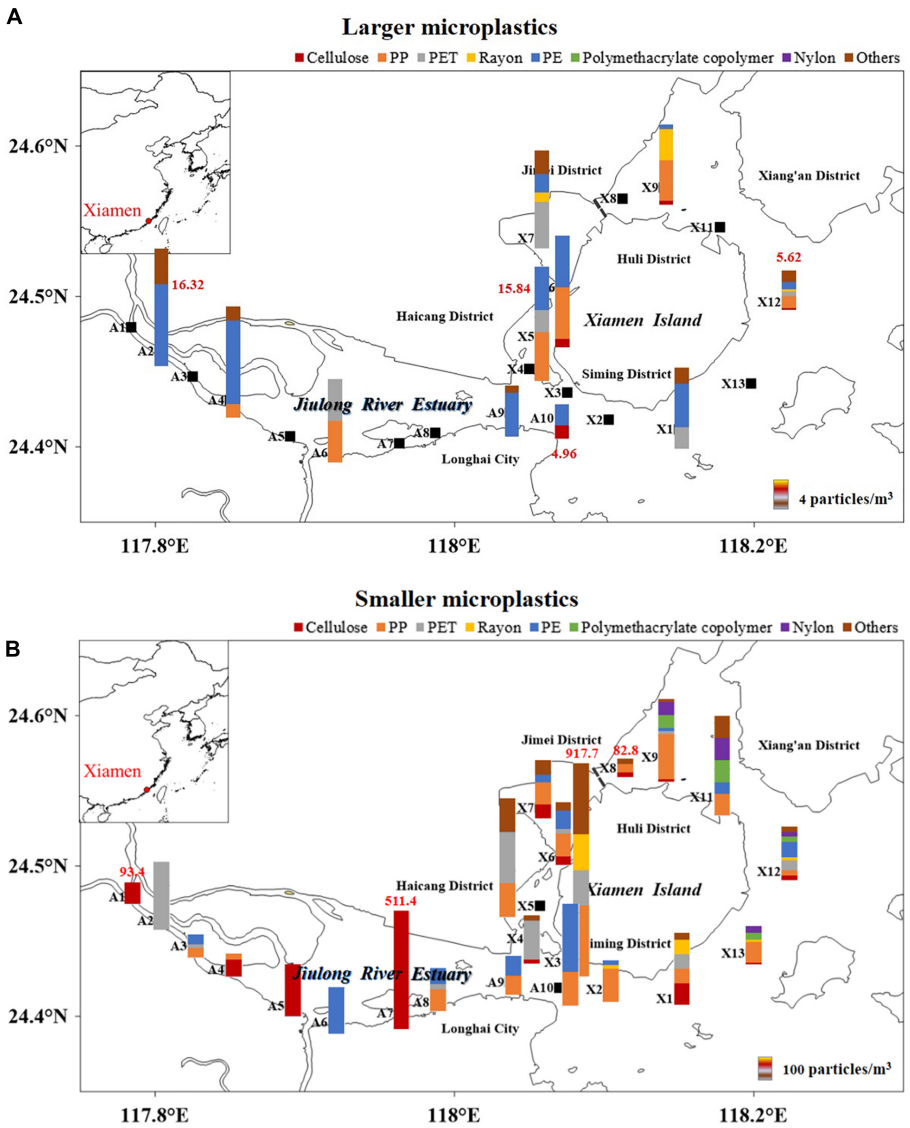

FIGURE 2 | The abundances of larger **(A)** or smaller **(B)** microplastics in Xiamen Bay and the Jiulong River Estuary. The length of vertical bars indicates microplastic abundance, and different colors in the figures represent different compositions of microplastics.

abundance with different sizes. For the Manta trawling, the turbulence caused by the vessel's wake could influence the data, while for the pumping, air can get sucked in when the waves are higher, therefore affecting the certainty of the sampled volume.

Appearance Characteristics and Chemical Compositions

Colors and Shapes

In this study, the colors and shapes of both the large and small microplastics were recorded. Color has been considered an essential aspect affecting the ingestion of microplastics by organisms (Abayomi et al., 2017). Therefore, the various colors of microplastics found in the samples were divided into five categories: brown, black, white, transparent, and others.

In Xiamen Bay, transparent (29.5%) and white (26.6%) were the dominant colors of large microplastics. For small particles, the proportion of each color was almost the same, except for the "others" category. However, in the Jiulong River Estuary, transparent (28.0%) and white (33.2%) colors were the most prominent in the large and small microplastics (**Supplementary Figure 2** and **Supplementary Table 3**).

In addition, the abundance of large microplastics of "other" colors was much higher than that of small microplastics, while the opposite trend occurred on black particles. Brown, transparent, and white particles did not display apparent differences between the two particle sizes. This result indicated that compared to the black microplastics, colored particles had more difficulty physically breaking into small pieces.

Microplastics of different shapes were observed: films, foams, fibers, and granules. A granule is a spherical or cylindrical piece of plastic debris or fragment, and when a particle could not be defined as one of the other shapes, it was identified as a granule (Yan et al., 2019). **Supplementary Figure 3** and **Supplementary Table 4** show the proportions of all shapes in our study. Granule particles were the most common at all sites (>60%), followed by film particles (>15%). However, small microplastics with fiber shapes were few. The shape pattern founded in this study was not in accordance with the typical pattern described in the literature, where fiber and fragment are the most abundant, implying the strong sinking and export processes in the estuarine-coastal area (Kooi and Koelmans, 2019).

Chemical Composition Patterns

Ten components of microplastics in Xiamen Bay and the Jiulong River were identified by micro-FTIR spectral analysis (**Supplementary Tables 5, 6**). For the large microplastics, polyethylene (PE), polypropylene (PP), and polyethylene terephthalate (PET) accounted for over 80% of the samples. Among them, PE was of the highest proportion (43%), followed by PP (22%) and PET (22%). The other component types included Rayon, cellulose, nitrocellulose (NC), acrylics (ACR), polyacrylonitrile (PAN), polystyrene (PS), and phenoxy resin.

For the small microplastics, 13 kinds of components were identified; this number was greater than that of the large microplastics. PP (27%), cellulose (19%), PE (18%), and PET (17%) were the major components, and a few items were found to be composed of ACR, polyacrylic acid (PAA), polyvinyl chloride (PVC), NC, and PS.

No significant difference was observed when comparing the component results between the large and small microplastics (**Figure 2**, $p = 0.05$). PE, PP, and PET particles were the most common component in all samples. The densities of PP and PE were approximately 0.90 and 0.95 g/cmł, respectively, so most of them remained on the seawater surface. Previous studies also reported that PP and PE could be treated as the most common microplastic types due to the wide application and ease of transport (Hidalgo-Ruz et al., 2012; Cozar et al., 2014). However, cellulose accounted for a high proportion of small microplastics but a relatively low proportion of large microplastics, which may mean that it is easy for cellulose plastic to break into small pieces physically. In addition, there were 14 component types found in Xiamen Bay and only 8 types collected in the Jiulong River, and the composition of microplastics in Xiamen Bay was rather complicated. Xiamen Bay is more influenced by intensive human activities, such as tourism, port transportation, and domestic discharge. Therefore there are more multiple pollution sources than the Jiulong River Estuary. Besides, compared to the estuarine area, the weak hydrological dynamics would lead to plastic accumulation in the inner bay (Tang et al., 2018).

Moreover, oxidation decomposition and density separation are the steps of the pretreatment to remove organic and non-plastic inorganic matters, which will inevitably affect the original characteristics of the collected microplastics, including the amount, size, color, shape, and composition. Moreover, it has been confirmed that using 30% H_2O_2 solution for treatment can alter the characteristics of microplastics, especially for fibers, or even dissolve the polymers (Crawford and Quinn, 2017). Thus, these steps were only undertaken when the impurities of samples had high degrees of non-plastics.

Flux Estimation of Riverine Outflow

In the Jiulong River Estuary, the flux of microplastics was estimated based on the field data (**Supplementary Table 7**). The flux of microplastics that includes the smaller microplastics (44 μm–5.0 mm) was 472 ± 230 t/y (River section S < 5), while that for the large particles (0.33–5.0 mm), the flux was 61.2 ± 2.6 t/y (River section S < 5). Thus, the flux of small particles was approximately 8 times greater than that of large particles, which can be explained by the fact that a few large particles can be physically broken into a large number of small particles. In addition, different sampling methods may cause changes in the observed concentrations (Cai et al., 2018), so the observed gap between the sizes between the two kinds of particles is acceptable.

In addition, the small-sized particle data were used to calculate the flux of microplastics from the Jiulong River Estuary into the sea. Compared with the other rivers (**Supplementary Figure 4** and **Supplementary Table 8**), the Jiulong River is a typical small- or medium-sized river whose flux of microplastics (472 ± 230 t/y) is at the medium level for large-sized rivers. For example, the microplastic flux is 538–906 t/y in the Yangtze River Estuary according to samples collected by pumping (60 μm–5.0 mm) (Zhao et al., 2019); 2.83×10^3 t/y from the Qiantang River to the Hangzhou Bay (45 μm–5.0 mm) (Zhao et al., 2020); 66.0 t/y in the Pearl River delta, as measured by a Manta trawl (0.3 mm–5 mm) (Mai et al., 2019); 22.0 t/y in the Rhone River (0.3–5 mm) (Constant et al., 2020); and 120 t/y in the Po River (0.3–5 mm) (Van der Wal et al., 2015).

Three main factors affect flux values and give rise to the estimation uncertainties: The first is the size of the sampling net. The minimum net size in our pumping method (44 μm) is small than those in other studies, but particles with a small size (<44 μm) are still neglected in this study. Hence, the actual value of the total amount of microplastics is less than the real value. The second factor is the flow of the river, which varies among different seasons and in the rainy and dry seasons. For example, our sampling took place during the rainy season in summer when there is great runoff. The rain washes away many microplastics, which may lead to the calculated result being higher than the actual value. Last but not least, the representativeness of the field data is an important factor influencing flux values as well. Microplastic abundance was influenced by rainfall, tide and other environmental factors, and it has daily and monthly fluctuations. Since field sampling was carried out only once, attention should be paid to the representativeness of microplastic abundance.

Moreover, it is inaccurate to equate a high flux with a high abundance because the components and sizes of microplastics vary greatly among different rivers. The average weight estimated in the study (Eriksen et al., 2013) is much higher than that used for the Yangtze River (0.00000330 g/particles) (Zhao et al., 2019) or other rivers. The measured average weight per particle was significantly different from that obtained by modeling

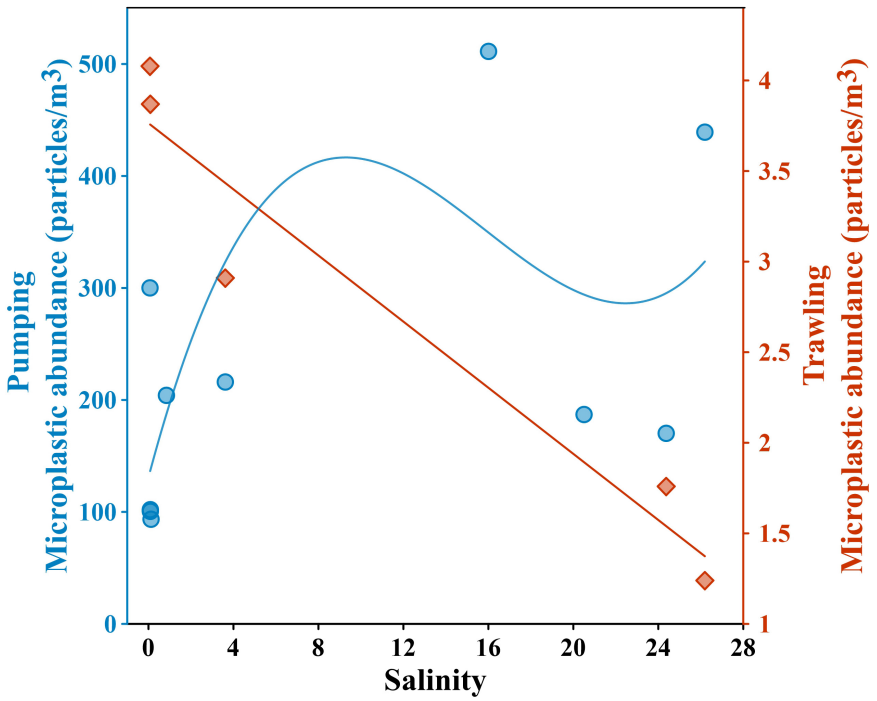

FIGURE 3 | The relationship between the abundance of microplastics and the salinity of the water from which they were sampled in the Jiulong River Estuary. The red squares refer to the large particles that were collected by trawling, and the blue dots refer to the small particles that were collected by pumping.

(Lebreton et al., 2017). Hence, there would be some inevitable errors in the modeled flux results.

The Relationship Between Microplastic Abundance and Hydrology

The Relationship Between Changes in Microplastic Abundance and Salinity

Here we further analyzed the correlation between salinity (shown in **Supplementary Table 9**) and the abundance of microplastics in the Jiulong River Estuary, and the result is shown in **Figure 3**. The abundance of large microplastics decreased as the river flowed into the sea, while the salinity gradually increased (R^2 = 0.927). As large microplastics are affected by light, wind, and waves, they could gradually decompose into small microplastics. Some of these microplastics are too small-sized for their surface features to be distinguished, so it is difficult to identify their sources (Zhao et al., 2019). The Jiulong River Estuary is dominated by semi-diurnal tides. The water columns were approximately well-mixed during the last flood and were stratified during the early ebb, leading to distinct differences in the magnitude and vertical structure (Cheng et al., 2020). The mixture and stratification processes between the saline and freshwater would influence the distribution of buoyant plastics, and the strong tidal currents could influence their residence time and transport processes between high and low tides (Browne et al., 2011; Sadri and Thompson, 2014). Based on the analysis, the dilution effect and physical weathering were the main reasons for the loss of large microplastics in the Jiulong River Estuary; moreover, physical processes occurred more often along coastlines or in marine environments (Corcoran et al., 2009).

The Small Particles Are Affected by a Variety of Factors

The linear relationship between small microplastics and salinity was not significant but showed a slightly positive trend, and its variation was much more complicated in the estuary. On the one hand, the physical properties of microplastics, such as density, shape, and size, determine their bio-fouling celerity and residence time, influencing their transport and fate in the marine environments (Chubarenko et al., 2016). When exposed to ultraviolet light for a long time, plastic could be less elastic and more brittle (Torikai et al., 2000). In addition, the smaller microplastics may be absorbed by microorganisms and ingested by fish, and the diversity of organisms that can ingest plastic particles would increase with the particle size being smaller (Auta et al., 2017; Jabeen et al., 2018). On the another hand, the environmental variation and extra discharge would change microplastic abundances. The fragmentation of microplastics could be accelerated where winds, waves, and currents are strong. An additional input source of microplastics (e.g., fibers in wastewater might be from domestic sewage), leading to abnormally high abundances at stations A2 and A7.

Correlation of Characteristics With Water Quality Parameters

Principal component analysis (PCA) and Pearson correlation analysis were performed to explore the potential relationship

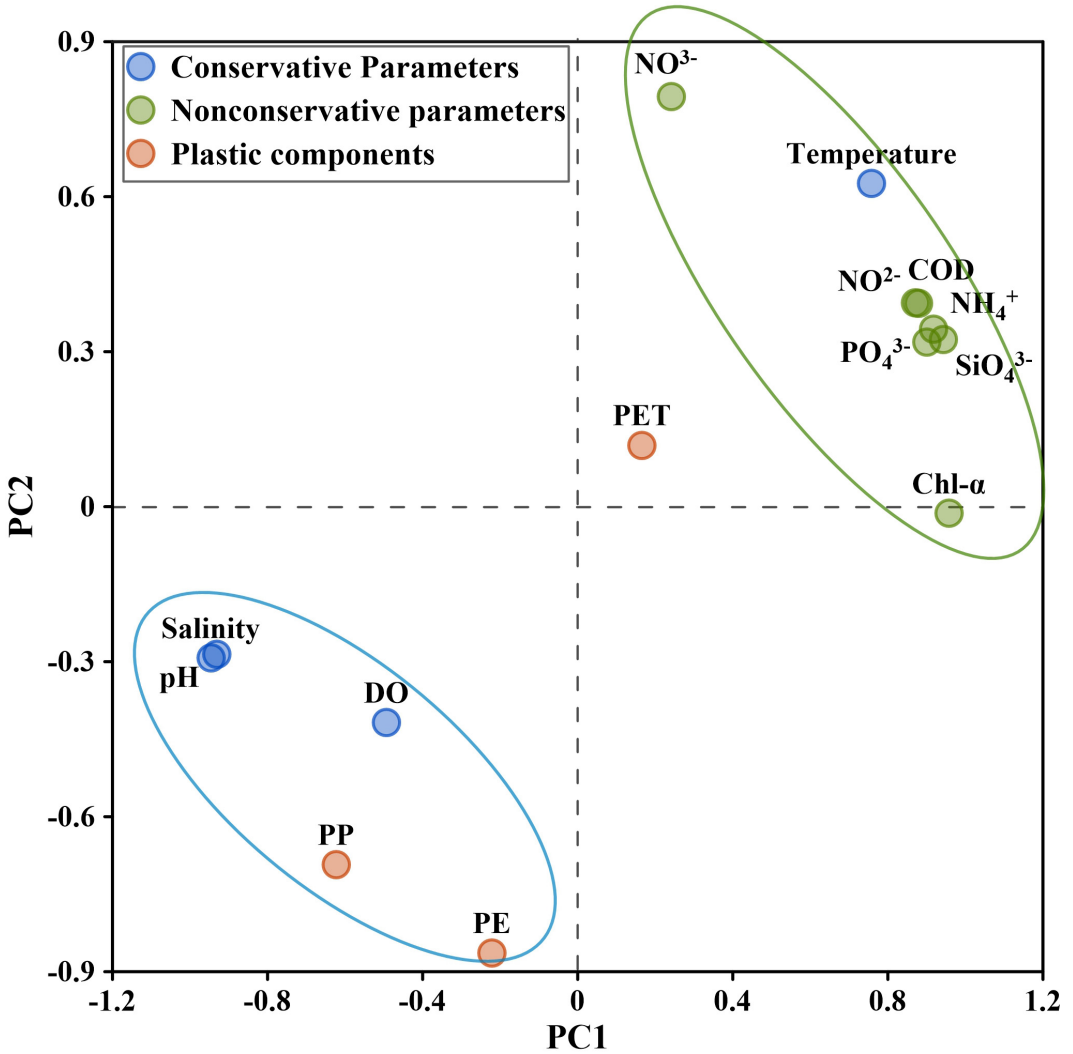

FIGURE 4 | Loadings of microplastic parameters on principal component 1 (PC1) and principal component 2 (PC2). The parameters were classified into 3 types: conservative (such as temperature and salinity), nonconservative (such as nutrients), and plastic components (including PET, PP, and PE).

between the microplastic characteristics and the physicochemical properties of the estuarine waters.

Principal Component Analysis (PCA)

Three principal components were extracted in this study, and their cumulative variance was 90% (**Supplementary Table 10**). The first principal component (PC1) showed more non-conservative properties dominated by nutrients, while the second component (PC2) showed more conservative properties (**Figure 4**). PC1 explained 60% of the data variability and was positively related to temperature, NO_2^-, NH_4^+, PO_4^{3-}, SiO_4^{3-}, and Chl-α and negatively related to pH and salinity. The parameters that had maximums in the PC1 showed decreasing trends from the Jiulong River Estuary to the sea, suggesting that they were mainly associated with riverine inputs. Abundant nutrients in the Jiulong River are mostly from the land-derived runoffs and release from sediments, leading to frequent blooms in the estuarine-coastal area (Li, 2019; Lin et al., 2010). Microplastics could be present in the natural aggregates, increasing their sinking rates and enhancing their vertical export.

PC2, which explained 20% of the data variability, was positively related to NO_3^- and was negatively related to PP and PE. NO_3^- is a typical pollutant and mainly originates from outfalls. Domestic sewage, offshore aquaculture, and fertilizer are the potential sources of NO_3^- in Zhanjiang Bay (Zhang et al., 2019), and manure, sewage, and soil are the sources of NO_3^- in surface waters. Therefore, it can be speculated that part of PP and PET, which have remarkable correlations with NO_3^- potentially come from sewage in outfalls.

PC3, explaining 10% of the data variability, was positively related to dissolved oxygen and PET. Dissolved oxygen in water has two primary sources, air and photosynthesis. Air-sea exchange process can bring or take away dissolved oxygen in seawater, which is influenced by temperature, wind, and some

physical factors. And Photosynthesis is a process capture and store solar energy on a massive scale and produces O_2 by plants, algae, cyanobacteria, and anoxygenic photosynthetic bacteria (Hoganson and Babcock, 1997). Therefore, it is speculated that biological and chemical factors (oxidation) are the main factors affecting PET.

Pearson Correlation Analysis

Pearson correlation analysis shows that PP and foam were significantly correlated with some water quality parameters (**Supplementary Table 11**). PP had negative correlations with temperature, NO_2^-, NO_3^-, NH_4^+, PO_4^{3-}, SiO_4^{3-} and chemical oxygen demand (COD) and positively correlated with pH and salinity. The foam was positively correlated with pH and negatively correlated with NO_2^-, NH_4^+, PO_4^{3-} and Chl-α.

After the Jiulong River entering the sea, the seawater salinity gradually rose, and the nutrient concentration gradually decreased. It has been revealed that NO_3^-, SiO_4^3, and dissolved inorganic nitrogen (DIN) behave conservatively in the predominantly P-limited Jiulong River Estuarine (Chen et al., 2013). The results of the Pearson correlation analysis showed that there are new sources of PP and foam occurring during the transmission process, and PP has a new source near the river estuary. For the foam, it is more likely that large particles are broken into small particles during transport from the estuary to the sea, leading to the increase of small particles' abundance along the direction of flow.

CONCLUSION

Microplastics were studied in water samples collected from Xiamen Bay and the Jiulong River Estuary. Microplastic pollution is mainly caused by the smaller microplastics, whose abundance is considered high (for the large particles) and medium (for the small particles) compared with other bays globally. Furthermore, the abundance of the Jiulong River is considered medium to low levels compared with other rivers worldwide. The flux of the small particles was approximately 8 times greater than that of the large particles, which are 472 ± 230 t/y and 61.2 ± 2.6 t/y, respectively. It means that the transportation of microplastic in the ocean by small and medium-sized rivers cannot be ignored, and the management of plastic discharge in these kinds of rivers should also be strengthened. In addition, the behavior of large microplastics is more conservative. In contrast, that of small microplastics is more complex, because various components of small microplastics have different sources and influencing factors, which also provides theoretical support for the treatment of microplastics pollution.

DATA AVAILABILITY STATEMENT

The original contributions presented in the study are included in the article/**Supplementary Material**, further inquiries can be directed to the corresponding author/s.

AUTHOR CONTRIBUTIONS

YFL: writing—original draft. SL: field investigation. ML: graphing, writing—editing, and revising. WH: instrumental analysis. KC: statistical analysis. YD: field sampling and pretreatment. FW: instrumental analysis. HK: supervision. LL: field investigation. YL: consulting. MZ: pretreatment. FL: funding support. CW: lab management. MC: supervision. All authors contributed to the article and approved the submitted version.

FUNDING

This work was financially supported by the National Natural Science Foundation of China (U2005207, 41776088, 41976216, and 41961144011), Natural Science Foundation of Fujian Province (2020J0141 and 2019Y4010), Dean's Research Funding of Xiamen University (20720190105), and Training Program of Innovation and Entrepreneurship for Undergraduates, Xiamen University (S202010384579 and S202010384769).

ACKNOWLEDGMENTS

We thank the crew of *R/V Haiyang II* for their help during the sampling process. We are thankful to Wenlu Zhao and Xuan Ni for their help during the instrumental analysis and Peng Huang for his assistance with data processing.

SUPPLEMENTARY MATERIAL

The Supplementary Material for this article can be found online at: https://www.frontiersin.org/articles/10.3389/fmars.2021.712727/full#supplementary-material

REFERENCES

Abayomi, O. A., Range, P., Al-Ghouti, M. A., Obbard, J. P., Almeer, S. H., and Ben-Hamadou, R. (2017). Microplastics in coastal environments of the Arabian Gulf. *Mar. Pollut. Bull.* 124, 181–188. doi: 10.1016/j.marpolbul.2017.07.011

Aliabad, M. K., Nassiri, M., and Kor, K. (2019). Microplastics in the surface seawaters of Chabahar Bay, Gulf of Oman (Makran Coasts). *Mar. Pollut. Bull.* 143, 125–133. doi: 10.1016/j.marpolbul.2019.04.037

Auta, H. S., Emenike, C. U., and Fauziah, S. H. (2017). Distribution and importance of microplastics in the marine environment: a review of the sources, fate, effects, and potential solutions. *Environ. Int.* 102, 165–176. doi: 10.1016/j.envint.2017.02.013

Bakir, A., Rowland, S. J., and Thompson, R. C. (2014). Enhanced desorption of persistent organic pollutants from microplastics under simulated physiological conditions. *Environ. Pollut.* 185, 16–23. doi: 10.1016/j.envpol.2013.10.007

Brennecke, D., Duarte, B., Paiva, F., Cacador, I., and Canning-Clode, J. (2016). Microplastics as vector for heavy metal contamination from the marine environment. *Estuar. Coast. Shelf Sci.* 178, 189–195. doi: 10.1016/j.ecss.2015.12.003

Browne, M. A., Crump, P., Niven, S. J., Teuten, E., Tonkin, A., Galloway, T., et al. (2011). Accumulation of microplastic on shorelines woldwide: sources and sinks. *Environ. Sci. Technol.* 45, 9175–9179. doi: 10.1021/es201811s

Cai, M., He, H., Liu, M., Li, S., Tang, G., Wang, W., et al. (2018). Lost but can't be neglected: huge quantities of small microplastics hide in the South China Sea. *Sci. Total Environ.* 633, 1206–1216. doi: 10.1016/j.scitotenv.2018.03.197

Chen, B. H., Ji, W. D., Chen, J. M., Lin, C., Huang, H. N., Huo, Y. L., et al. (2013). Characteristics of nutrients in the Jiulong River and its impact on Xiamen Water, China. *Chin. J. Oceanol. Limnol.* 31, 1055–1063. doi: 10.1007/s00343-013-2263-3

Chen, B., Kang, W., Xu, D., and Hui, L. (2021). Long-term changes in red tide outbreaks in Xiamen Bay in China from 1986 to 2017. *Estuar. Coast. Shelf Sci.* 249:107095. doi: 10.1016/j.ecss.2020.107095

Chen, M., Jin, M., Tao, P., Wang, Z., Xie, W., Yu, X., et al. (2018). Assessment of microplastics derived from mariculture in Xiangshan Bay, China. *Environ. Pollut.* 242 (Pt B), 1146–1156. doi: 10.1016/j.envpol.2018.07.133

Cheng, P., Yu, F. L., Chen, N. W., and Wang, A. J. (2020). Observational study of tidal mixing asymmetry and eddy viscosity-shear covariance-induced residual flow in the Jiulong River estuary. *Cont. Shelf Res.* 193:104035. doi: 10.1016/j.csr.2019.104035

Cheung, P. K., Cheung, L. T. O., and Fok, L. (2016). Seasonal variation in the abundance of marine plastic debris in the estuary of a subtropical macro-scale drainage basin in South China. *Sci. Total Environ.* 562, 658–665. doi: 10.1016/j.scitotenv.2016.04.048

Chubarenko, I., Bagaev, A., Zobkov, M., and Esiukova, E. (2016). On some physical and dynamical properties of microplastic particles in marine environment. *Mar. Pollut. Bull.* 108, 105–112. doi: 10.1016/j.marpolbul.2016.04.048

Cole, M., Lindeque, P., Fileman, E., Halsband, C., and Galloway, T. S. (2015). The impact of polystyrene microplastics on feeding, function and fecundity in the marine copepod *Calanus helgolandicus*. *Environ. Sci. Technol.* 49, 1130–1137. doi: 10.1021/es504525u

Constant, M., Ludwig, W., Kerherve, P., Sola, J., Charriere, B., Sanchez-Vidal, A., et al. (2020). Microplastic fluxes in a large and a small Mediterranean river catchment: the Tet and the Rhone, Northwestern Mediterranean Sea. *Sci. Total Environ.* 716:136984. doi: 10.1016/j.scitotenv.2020.136984

Corcoran, P. L., Biesinger, M. C., and Grifi, M. (2009). Plastics and beaches: a degrading relationship. *Mar. Pollut. Bull.* 58, 80–84. doi: 10.1016/j.marpolbul.2008.08.022

Cozar, A., Echevarria, F., Ignacio Gonzalez-Gordillo, J., Irigoien, X., Ubeda, B., Hernandez-Leon, S., et al. (2014). Plastic debris in the open ocean. *Proc. Natl. Acad. Sci. U.S.A.* 111, 10239–10244.

Crawford, C. B., and Quinn, B. (eds.). (2017). "Microplastic identification techniques" in *Microplastic Pollutants*, (Elsevier) 219–267. doi: 10.1016/B978-0-12-809406-8.00010-4

Eriksen, M., Cummins, A., Maximenko, N., Thiel, M., Lattin, G., Wilson, S., et al. (2013). Plastic pollution in the South Pacific subtropical gyre. *Mar. Pollut. Bull.* 68, 71–76. doi: 10.1016/j.marpolbul.2012.12.021

Frere, L., Paul-Pont, I., Rinnert, E., Petton, S., Jaffre, J., Bihannic, I., et al. (2017). Influence of environmental and anthropogenic factors on the composition, concentration and spatial distribution of microplastics: a case study of the Bay of Brest (Brittany, France). *Environ. Pollut.* 225, 211–222. doi: 10.1016/j.envpol.2017.03.023

Fu, Z., Chen, G., Wang, W., and Wang, J. (2020). Microplastic pollution research methodologies, abundance, characteristics and risk assessments for aquatic biota in China. *Environ. Pollut.* 266:115098. doi: 10.1016/j.envpol.2020.115098

Galloway, T. S., and Lewis, C. N. (2016). Marine microplastics spell big problems for future generations. *Proc. Natl. Acad. Sci. U.S.A.* 113, 2331–2333. doi: 10.1073/pnas.1600715113

Hidalgo-Ruz, V., Gutow, L., Thompson, R. C., and Thiel, M. (2012). Microplastics in the marine environment: a review of the methods used for identification and quantification. *Environ. Sci. Technol.* 46, 3060–3075. doi: 10.1021/es2031505

Hoganson, C. W., and Babcock, G. T. (1997). A metallo radical mechanism for the generation of oxygen from water in photosynthesis. *Science* 277, 1953–1956. doi: 10.1126/science.277.5334.1953

Huang, J., Li, Q., Huang, L., Wang, J., Hu, Y., and Feng, Y. (2012). Preliminary delineation and classification of estuarine drainage areas for major coastal rivers in China. *Acta Ecol. Sin.* 32, 3516–3527. **** journal wrong doi: 10.5846/stxb201105100610

Jabeen, K., Li, B. W., Chen, Q. Q., Su, L., Wu, C. X., Hollert, H., et al. (2018). Effects of virgin microplastics on goldfish (*Carassius auratus*). *Chemosphere* 213, 323–332. doi: 10.1016/j.chemosphere.2018.09.031

Jambeck, J. R., Geyer, R., Wilcox, C., Siegler, T. R., Perryman, M., Andrady, A., et al. (2015). Plastic waste inputs from land into the ocean. *Science* 347, 768–771. doi: 10.1126/science.1260352

Klumpp, D. W., Hong, H. S., Humphrey, C., Wang, X. H., and Codi, S. (2002). Toxic contaminants and their biological effects in coastal waters of Xiamen, China. I. Organic pollutants in mussel and fish tissues. *Mar. Pollut. Bull.* 44, 752–760. doi: 10.1016/s0025-326x(02)00053-x

Kooi, M., and Koelmans, A. A. (2019). Simplifying microplastic via continuous probability distributions for size, shape, and density. *Environ. Sci. Technol. Lett.* 6, 551–557. doi: 10.1021/acs.estlett.9b00379

Lahens, L., Strady, E., Kieu-Le, T.-C., Dris, R., Boukerma, K., Rinnert, E., et al. (2018). Macroplastic and microplastic contamination assessment of a tropical river (Saigon River, Vietnam) transversed by a developing megacity. *Environ. Pollut.* 236, 661–671. doi: 10.1016/j.envpol.2018.02.005

Lattin, G. L., Moore, C. J., Zellers, A. F., Moore, S. L., and Weisberg, S. B. (2004). A comparison of neustonic plastic and zooplankton at different depths near the southern California shore. *Mar. Pollut. Bull.* 49, 291–294. doi: 10.1016/j.marpolbul.2004.01.020

Lebreton, L. C. M., Van der Zwet, J., Damsteeg, J. W., Slat, B., Andrady, A., and Reisser, J. (2017). River plastic emissions to the world's oceans. *Nat. Commun.* 8:15611.

Li, G. (2019). Fast acclimation of phytoplankton assemblies to acute salinity stress in the Jiulong River estuary. *Acta Oceanol. Sin.* 38, 78–85. doi: 10.1007/s13131-019-1389-3

Li, Y., Chen, Y. N., Ruan, M. N., and Chen, J. W. (2015). The Jiulong River plume as cross-strait exporter and along-strait barrier for suspended sediment: evidence from the endmember analysis of in-situ particle size. *Estuar. Coast. Shelf Sci.* 166, 146–152. doi: 10.1016/j.ecss.2015.03.002

Lin, H., Zhang, C. H., Qi, W. D., Zhou, Q. L., Lin, L. B., Lu, M. L., et al. (2010). Changing trends of DIN and PO4-P content in Xiamen Seawaters. *J. Ocean. Taiw. Strait.* 29, 314–319.

Lindeque, P. K., Cole, M., Coppock, R. L., Lewis, C. N., Miller, R. Z., Watts, A. J. R., et al. (2020). Are we underestimating microplastic abundance in the marine environment? A comparison of microplastic capture with nets of different mesh-size. *Environ. Pollut.* 265:114721. doi: 10.1016/j.envpol.2020.114721

Mai, L., He, H., Bao, L. J., Liu, L. Y., and Zeng, E. Y. (2020). Plastics are an insignificant carrier of riverine organic pollutants to the coastal oceans. *Environ. Sci. Technol.* 54, 15852–15860. doi: 10.1021/acs.est.0c05446

Mai, L., You, S. N., He, H., Bao, L. J., Liu, L. Y., and Zeng, E. Y. (2019). Riverine microplastic pollution in the Pearl River Delta, China: are modeled estimates accurate? *Environ. Sci. Technol.* 53, 11810–11817. doi: 10.1021/acs.est.9b04838

Miller, R. Z., Watts, A. J. R., Winslow, B. O., Galloway, T. S., and Barrows, A. P. W. (2017). Mountains to the sea: River study of plastic and non-plastic microfiber pollution in the northeast USA. *Mar. Pollut. Bull.* 124, 245–251. doi: 10.1016/j.marpolbul.2017.07.028

Nuelle, M. T., Dekiff, J. H., Remy, D., and Fries, E. (2014). A new analytical approach for monitoring microplastics in marine sediments. *Environ. Pollut.* 184, 161–169. doi: 10.1016/j.envpol.2013.07.027

Pagter, E., Frias, J., Kavanagh, F., and Nash, R. (2020). Differences in microplastic abundances within demersal communities highlight the importance of an ecosystem-based approach to microplastic monitoring. *Mar. Pollut. Bull.* 160:111644. doi: 10.1016/j.marpolbul.2020.111644

Poulain, M., Mercier, M. J., Brach, L., Martignac, M., Routaboul, C., Perez, E., et al. (2019). Small microplastics as a main contributor to plastic mass balance in the North Atlantic subtropical gyre. *Environ. Sci. Technol.* 53, 1157–1164. doi: 10.1021/acs.est.8b05458

Qi, R., Jones, D., Li, Z., Liu, Q., and Yan, C. (2020). Behavior of microplastics and plastic film residues in the soil environment: a critical review. *Sci. Total Environ.* 703:134722. doi: 10.1016/j.scitotenv.2019.134722

Ramirez-Alvarez, N., Mendoza, L. M. R., Vinicio Macias-Zamora, J., Oregel-Vazquez, L., Alvarez-Aguilar, A., Augusto Hernandez-Guzman, F., et al. (2020). Microplastics: sources and distribution in surface waters and sediments of Todos Santos Bay, Mexico. *Sci. Total Environ.* 703:134838. doi: 10.1016/j.scitotenv.2019.134838

Sadri, S. S., and Thompson, R. C. (2014). On the quantity and composition of floating plastic debris entering and leaving the Tamar Estuary, Southwest England. *Mar. Pollut. Bull.* 81, 55–60. doi: 10.1016/j.marpolbul.2014.02.020

Schmidt, C., Krauth, T., and Wagner, S. (2017). Export of plastic debris by rivers into the sea. *Environ. Sci. Technol.* 51, 12246–12253. doi: 10.1021/acs.est.7b02368

Tang, G., Liu, M., Zhou, Q., He, H., Chen, K., Zhang, H., et al. (2018). Microplastics and polycyclic aromatic hydrocarbons (PAHs) in Xiamen coastal areas: implications for anthropogenic impacts. *Sci. Total Environ.* 634, 811–820. doi: 10.1016/j.scitotenv.2018.03.336

Torikai, N., Matsushita, Y., Langridge, S., Bucknall, D., Penfold, J., and Takeda, M. (2000). Interfacial structures of block and graft copolymers with lamellar microphase-separated structures. *Physica B* 283, 12–16. doi: 10.1016/s0921-4526(99)01882-7

Van der Wal, M., Van del Meulen, M., Tweehuijsen, G., Peterlin, M., Palatinus, A., Virsek, M. K., et al. (2015). *Identification and Assessment of Riverine Input of (Marine) Litter.* Final Report for the European Commission DG Environment under Framework Contract No ENV. D (Vol. 25). 2/FRA/2012. Bristol: Eunomia Research & Consulting Ltd.

Wang, T., Hu, M., Song, L., Yu, J., Liu, R., Wang, S., et al. (2020). Coastal zone use influences the spatial distribution of microplastics in Hangzhou Bay, China. *Environ. Pollut.* 266(Pt 2):115137. doi: 10.1016/j.envpol.2020.115137

Wu, Q., Liu, S., Chen, P., Liu, M., Cheng, S. Y., Ke, H., et al. (2021). Microplastics in seawater and two sides of the Taiwan Strait: reflection of the social-economic development. *Mar. Pollut. Bull.* 169:112588.

Ya, M. L., Wang, X. H., Wu, Y. L., Ye, C. X., and Li, Y. Y. (2014). Enrichment and partitioning of polycyclic aromatic hydrocarbons in the sea surface microlayer and subsurface water along the coast of Xiamen Island, China. *Mar. Pollut. Bull.* 78, 110–117. doi: 10.1016/j.marpolbul.2013.10.053

Yan, M., Nie, H., Xu, K., He, Y., Hu, Y., Huang, Y., et al. (2019). Microplastic abundance, distribution and composition in the Pearl River along Guangzhou city and Pearl River estuary, China. *Chemosphere* 217, 879–886. doi: 10.1016/j.chemosphere.2018.11.093

Yonkos, L. T., Friedel, E. A., Perez-Reyes, A. C., Ghosal, S., and Arthur, C. D. (2014). Microplastics in four estuarine rivers in the Chesapeake Bay, USA. *Environ. Sci. Technol.* 48, 14195–14202. doi: 10.1021/es5036317

Zayen, A., Sayadi, S., Chevalier, C., Boukthir, M., Ben Ismail, S., and Tedetti, M. (2020). Microplastics in surface waters of the Gulf of Gabes, southern Mediterranean Sea: distribution, composition and influence of hydrodynamics. *Estuar. Coast. Shelf Sci.* 242:106832. doi: 10.1016/j.ecss.2020.106832

Zettler, E. R., Mincer, T. J., and Amaral-Zettler, L. A. (2013). Life in the "Plastisphere": microbial communities on plastic marine debris. *Environ. Sci. Technol.* 47, 7137–7146. doi: 10.1021/es401288x

Zhang, L., Liu, J., Xie, Y., Zhong, S., Yang, B., Lu, D., et al. (2020). Distribution of microplastics in surface water and sediments of Qin River in Beibu Gulf, China. *Sci. Total Environ.* 708:135176. doi: 10.1016/j.scitotenv.2019.135176

Zhang, P., Wei, L., Lai, J., Dai, P., Chen, Y., and Zhang, J. (2019). Concentration, compoition and fluxes of land-based nitrogen and phosphorus source pollutants input into Zhanjiang Bay in summer. *J. Guangdong Ocean Univ.* 039, 63–72.

Zhao, S., Wang, T., Zhu, L., Xu, P., Wang, X., Gao, L., et al. (2019). Analysis of suspended microplastics in the Changjiang estuary: implications for riverine plastic load to the ocean. *Water Res.* 161, 560–569. doi: 10.1016/j.watres.2019.06.019

Zhao, S., Zhu, L., Wang, T., and Li, D. (2014). Suspended microplastics in the surface water of the Yangtze estuary system, China: first observations on occurrence, distribution. *Mar. Pollut. Bull.* 86, 562–568. doi: 10.1016/j.marpolbul.2014.06.032

Zhao, W., Huang, W., Yin, M., Huang, P., Ding, Y., Ni, X., et al. (2020). Tributary inflows enhance the microplastic load in the estuary: a case from the Qiantang River. *Mar. Pollut. Bull.* 156:111152. doi: 10.1016/j.marpolbul.2020.111152

Zheng, Y., Li, J., Cao, W., Liu, X., Jiang, F., Ding, J., et al. (201x9). Distribution characteristics of microplastics in the seawater and sediment: a case study in Jiaozhou Bay, China. *Sci. Total Environ.* 674, 27–35. doi: 10.1016/j.scitotenv.2019.04.008

Conflict of Interest: The authors declare that the research was conducted in the absence of any commercial or financial relationships that could be construed as a potential conflict of interest.

Publisher's Note: All claims expressed in this article are solely those of the authors and do not necessarily represent those of their affiliated organizations, or those of the publisher, the editors and the reviewers. Any product that may be evaluated in this article, or claim that may be made by its manufacturer, is not guaranteed or endorsed by the publisher.

frontiers in Marine Science

OPINION
published: 12 October 2021
doi: 10.3389/fmars.2021.766876

World's Largest Mangrove Forest Becoming Plastic Cesspit

Tanveer M. Adyel and Peter I. Macreadie*

Centre for Integrative Ecology, School of Life and Environmental Sciences, Deakin University, Melbourne, VIC, Australia

Keywords: Bay of Bengal, blue carbon ecosystem, mangrove, plastic, the Sundarbans

PLASTICS AS NEW CONCERN FOR THE SUNDARBANS

Plastic is considered as hazardous waste (Rochman et al., 2013) and planetary transboundary pollution (Villarrubia-Gómez et al., 2018; Tessnow-von Wysocki and Le Billon, 2019). Plastics in different forms—including marine litter, plastic debris, meso-plastics, and microplastics—are now ubiquitously distributed in the environment (Jambeck et al., 2015; Napper and Thompson, 2020). The world's largest single mangrove forest, the UNESCO Marine World Heritage-listed Sundarbans between Bangladesh and India, is under immense threat of plastic pollution. A Ramsar site and a Class 3 Tiger Conservation Landscape of global priority for endangered and flagship species Royal Bengal Tiger (*Panthera tigris*)—the Sundarbans, is historically threatened by many challenges, like over-exploitation, commercial farming and development activities, climate change-induced hazards, and natural disasters (Sen, 2019; Mukul et al., 2020).

Bangladesh and India, the benefit and management sharing countries of the Sundarbans, are ranked among the top twelve mismanaged plastic waste (herein also "plastics") generating nations (Jambeck et al., 2015) and are discharging plastic waste downstream through rivers and coasts (**Figure 1A**) making the Sundarbans a cesspit for plastic waste. Moreover, this mangrove is formed and modified by the super confluence of the world's 15th longest river Brahmaputra/Jamuna, along the transboundary rivers Ganges/Padma and Meghna. These rivers are among the top ten global plastic waste carriers, transporting over 72,000 tonnes of plastics annually before emptying into the Bay of Bengal (Schmidt et al., 2017). A recent study estimated that the combined flows of the Ganges, Brahmaputra and Meghna rivers can discharge up to 3 billion pieces of microplastics per day into the Bay of Bengal (Napper et al., 2021). Moreover, all the river systems in Bangladesh and India discharge about 4 million tonnes of plastic waste to the Bay of Bengal per annum. The Sundarbans Bangladesh has 177 rivers receiving water from three main rivers and flowing through it to the Bay of Bengal (Banglapedia, 2012) making the Sundarbans as a basin for the long-term accumulation of plastic waste. If current business as usual trend of 2015 and consumer demand for plastic increases with economy continue, Bangladesh and India can generate about 3 and 52 million tonnes of plastics, respectively by 2060 (**Figures 1B,C**) (Lebreton and Andrady, 2019).

The Bay of Bengal is the largest bay in the world and several littoral countries including Bangladesh, India, Indonesia, Myanmar, Sri Lanka, and Thailand uses its resources. Different river systems of these countries also release plastics to the Bay of Bengal (**Figure 1D**). Rivers are key vectors for transporting plastics to oceans and bays (Lebreton et al., 2017; Meijer et al., 2021). The discharge of plastics from the littoral countries around the Bay of Bengal is projected to increase up to 5-times by 2025 compared to that of 2010 (Jambeck et al., 2015). Data-driven mechanistic and Plastics-to-Ocean (P_2O) models indicated that over 85 million tonnes of plastics per year can be discharged to the global aquatic systems by the next 20 years if no strong initiatives are taken now in waste management (Borrelle et al., 2020; Lau et al., 2020). Moreover, recently a Lagrangian particle transport model indicated that plastics can be drifted/washed from the oceans to the coasts (Onink et al., 2021). There is a probability of some of these plastics can be drifted or washed toward the

OPEN ACCESS

Edited by:
Xiaoshan Zhu,
Tsinghua University, China

Reviewed by:
Ping Li,
Shenzhen University, China

****Correspondence:***
Tanveer M. Adyel
t.adyel@deakin.edu.au

Specialty section:
This article was submitted to Marine Pollution, a section of the journal Frontiers in Marine Science

Received: *30 August 2021*
Accepted: *20 September 2021*
Published: *12 October 2021*

Citation:
Adyel TM and Macreadie PI (2021) World's Largest Mangrove Forest Becoming Plastic Cesspit. Front. Mar. Sci. 8:766876. doi: 10.3389/fmars.2021.766876

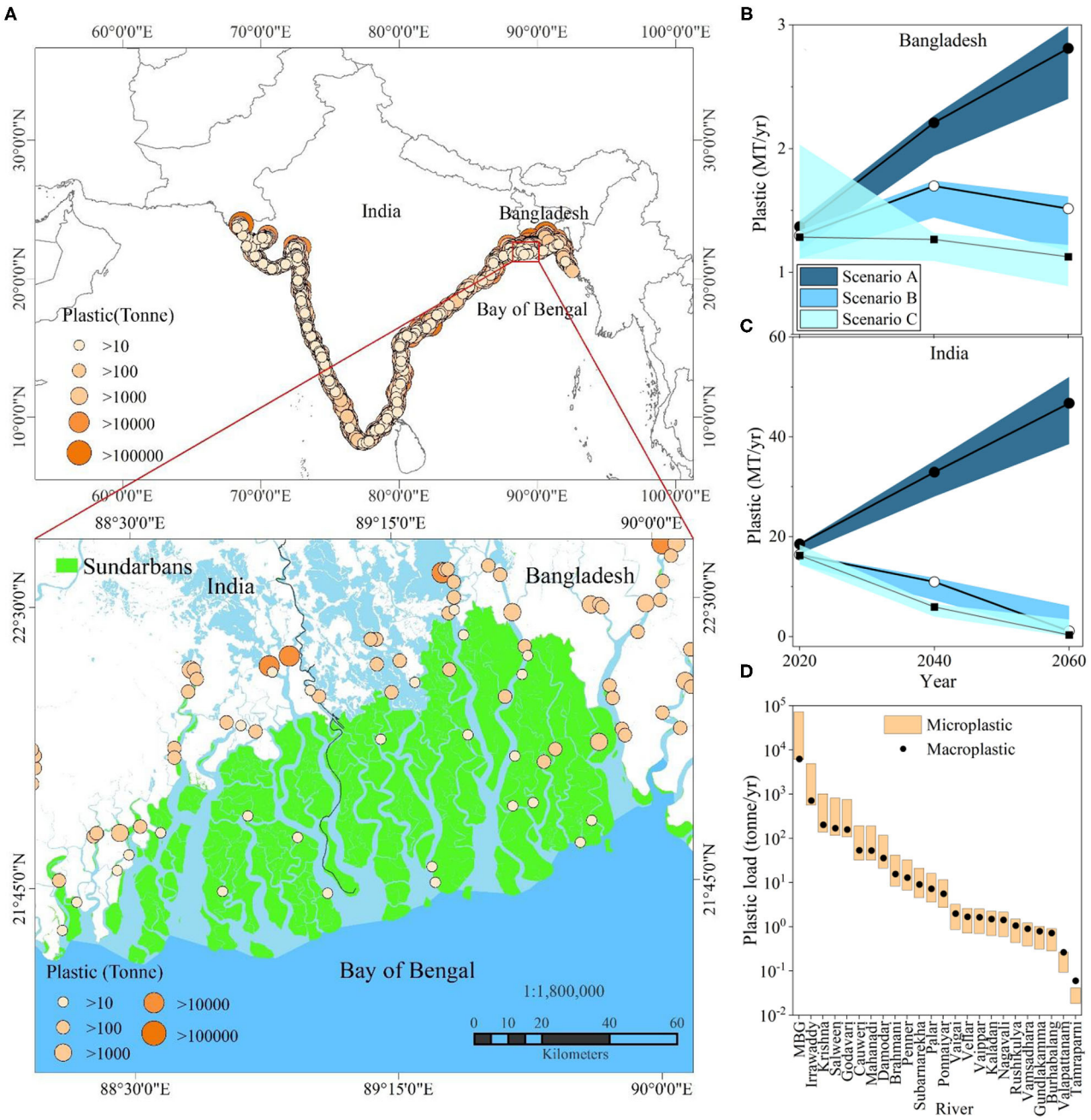

FIGURE 1 | (A) Current status of plastic waste across the coast of India and Bangladesh including the Sundarbans based on Lebreton et al. (2017), **(B, C)** Possible plastic waste generation in 2020, 2040 and 2060 under three scenarios as per Lebreton and Andrady (2019). Scenario A represents a "business-as-usual" case of 2015 while consumer demand for plastic increases with economy. Scenario B indicates that infrastructures for plastic waste management will advance according to per capita gross domestic product grows. Finally, scenario C corresponds a reduction in plastic demand per capita with fraction of plastic in municipal solid waste capped at 10 and 5% by 2020 and 2040, respectively as well plastic waste management gradually improves as indicated in scenario B. **(D)** The discharge of plastic waste as microplastic and macro plastic to the Bay of Bengal through different rivers as per 2017. The lower and upper bar indicates microplastics released based on global model based on data of Schmidt et al. (2017). MBG indicates the Meghna, Brahmaputra and Ganges combined.

nearby Sundarbans from the Bay of Bengal. Discharged transboundary marine litter like fishing net and lost fishing gears within the Bay of Bengal's Exclusive Economic Zones (Nelms et al., 2021) could also wash into the Sundarbans. Therefore, there is a concern for the integrity of this fragile and diverse ecosystems.

The Sundarbans mangroves supports around 1,136 animals and 334 plant species (Mukul et al., 2020), comprising 35% of Bangladesh's biodiversity. These mangrove forests provide unique habitat for breeding and nursing ground of mammals, fishes, turtles, birds, and other exotic species, including threatened, vulnerable or endangered species, e.g., Ganges river dolphin, Irrawaddy dolphin, water monitor lizard, olive ridley turtle, estuarine crocodile, and others. Over 800 marine species are affected by plastics (CBD, 2016), which can occur, for example, through: ingestion; entangled causing severe physical injuries; deaths due to starvation following ingestion; or more subtle effects on behavior and ecological interactions-e.g., the ability to escape from predators or migrate, reducing feeding and depleting energy stores, effects for fertility and growth (Galloway et al., 2017; Napper and Thompson, 2020). Plastics pose the potential to alter wildlife populations and fisheries stocks impairing genetic expression, tissues, reproduction, population size, and community structure (Rochman et al., 2016). Alarmingly, microplastics were found in fish and coral species within the Bay of Bengal and the surrounding area (Hossain et al., 2019; Ghosh et al., 2021). It is estimated that 291 diverse fishery species supported by 177 tidal streams and channels of this forest could be impacted by plastic waste, putting at risk the livelihoods of about 200,000 subsistence fishermen (Sen, 2019). Although microplastics ingestions by biota within the Sundarbans is not reported, however, the scenario is different in the Bay of Bengal. For instance, microplastics are found in gastrointestinal tracts of marine commercial fishes (Hossain et al., 2019) and shrimps (Hossain et al., 2020) collected from the Northern Bay of Bengal at Bangladesh. Microplastics are also reported in zooplankton, and different finfishes and shellfishes collected from Port Blair Bay situated in the Bay of Bengal of Indian territory (Goswami et al., 2020). Therefore, interdisciplinary investigations of plastics and microplastics levels in different trophic levels in the Sundarbans are urgently needed.

Some key features for the local and global significance of the Sundarbans along with plastic issues include:

- Area: About 10,000 km^2 (Bangladesh: 6,017 km^2 and India: 4,260 km^2)
- Sanctuaries of the Sundarbans: Sundarbans East, Sundarbans South and Sundarbans West Wildlife Sanctuaries (Bangladesh), Sundarbans National Park and Sajnakhali Wildlife Sanctuary (India)
- Biodiversity (Mukul et al., 2020): Around 334 species of plants. 355 species of birds, 291 species of fishes, 49 species of mammals, 87 species of reptiles, and 14 amphibians
- Dominant floral species (Sen, 2019): *Heritiera fomes, Avicennia, Xylocarpus mekongensis, Xylocarpus granatum, Sonneratia apetala, Bruguiera gymnorhiza, Ceriops decandra, Aegiceras corniculatum, Rhizophora mucronate,* and *Nypa fruticans* palms
- Globally threatened, vulnerable or endangered species (Aziz and Paul, 2015; Sen, 2019; Mukul et al., 2020): Royal Bengal Tiger (*Panthera tigris*), Ganges river dolphin (*Platanista gangetica*), Irrawaddy dolphin (*Orcaella brevirostris*), Water monitor lizard (*Varanus salvator*), Olive ridley turtle (*Lepidochelys olivacea*), Estuarine crocodile (*Crocodilus porosus*) and others
- Carbon sink capacity (Atwood et al., 2017; UNESCO, 2020): Soil C stocks (Mg C/ha): about 120 to 180 (Bangladesh) and about 140 to 250 (India). Total soil C stock (Tg C): 20.92 $\pm$ 5.11 (Bangladesh) and 19.99 $\pm$ 7.16 (India)
- Plastic discharge to the Bay of Bengal and through the Sundarbans: To the Bay of Bengal from Bangladesh and India: about 4 million tonnes/yr
- Plastic discharge through the Sundarbans (Lebreton et al., 2017): about 1.7×10^{-8} tonnes plastic/ha-yr

Root and sediment within mangroves are efficient at trapping plastics, while root features i.e., density, thickness and height can influence the plastic accumulation and dispersion in the mangroves (Duan et al., 2021). Stationary plastic in forest fringe or sediment can hamper oxygen penetration within the rhizosphere and therefore, create an anoxic condition and subsequently can cause mangrove suffocation (Smith, 2012) leading to pneumatophore deformation or low growth (van Bijsterveldt et al., 2021). Therefore, there is a possibility that the juvenile mosaic of Sterculiaceae and Euphorbiaceae mangroves including Sundari (*Heritiera fomes*) and looking-glass (*Heritiera littoralis*) in the Sundarbans could face plastic-induced stress condition that needs further investigation.

The Sundarbans mangrove ecosystem is a major global carbon sink (Atwood et al., 2017). The Sundarbans (Bangladesh) and the Sundarbans National Park (India) mangroves comprise at least 168 million Mg carbon, and the mangrove area within Bangladesh jurisdiction stores about 28% of total mangrove carbon stocks within all marine World Heritage sites (UNESCO, 2020). The Sundarbans in Bangladesh and India site can sequester about 118 to 180 and 141 to 252 M g C/ha, respectively (Atwood et al., 2017; UNESCO, 2020). Plastics impact carbon cycling in the terrestrial ecosystem by disrupting soil microbial processes, plant growth, or litter decomposition (Rillig et al., 2021). The waterways within the Sundarbans can transport about 1.7×10^{-8} tonne plastic/ha annually from upstream rivers to the Bay of Bengal (Lebreton et al., 2017). Alarmingly, a recent study predicted that global plastic-carbon will be equal to global blue carbon sink by 2035 if the current plastic accumulation trend continues (Stubbins et al., 2021). However, it is not well-established whether plastics could hamper carbon sequestration capacity of this mangrove.

The Sundarbans and its resources provide provisional (genetic resources, food and fiber, timer, fuel wood, etc.) services directly and indirectly to 3.5 million people of Bangladesh for their livelihood (Sen, 2019). In addition, 10,000 km^2 of the Sundarbans coastline borders India, is supporting a further 4.5 million people. There is a growing demand for tourism within the Sundarbans (Hossain et al., 2021). However, direct plastic dumping by $\sim$250,000 tourists annually with an increasing number of 30,000 per year just in the Sundarbans Bangladesh-side (Sachin, 2020) is exacerbating forest's threat. Ecosystem services including the aesthetic appeal of mangroves can be hampered due to plastic deposition in the forest floor. Although Bangladesh

Forest Department is currently working to minimise plastic dumping within the forest floor, conservationists fear that the overall monitoring and enforcement initiatives are not sufficient. Additionally, episodic events can also contribute to plastic accumulation in the Sundarbans. For example, over 26 tonnes of plastics waste from post-cyclone Amphan relief material was discarded from the Indian side in the forest recently (Singh, 2020).

LOOKING FORWARD

If local and transboundary plastics continue to receive voluntary and undefined support (Borrelle et al., 2017) and downplayed by resource-sharing countries of the Sundarbans, this previously IUCN-advised "heritage in danger (IUCN, 2019)" will be impacted heavily. Although Bangladesh, for the first time in the world, banned the use of thin plastic bag in 2002, but plastic waste management is still a concern for the country (Chowdhury et al., 2020). Cross-border solutions, policy-frameworks, and implementation of action-plans under international environment and development agreements, like the Basel Convention, the United Nations Environment Assembly resolutions on Marine Litter and Microplastics and Agenda 2030, are immediately needed to protect the last habitat of the endangered Royal Bengal Tigers and other species. For instance, the 2030 Agenda for Sustainable Development Goals calls for action to implement integrated water resources management at all levels, including involvement of transboundary cooperation as appropriate (Target 6.5), protect and restore water-related ecosystems, including forests, wetlands, and rivers (Target 6.6), substantially reduce waste generation through prevention, reduction, recycling and reuse (Target 12.5), and prevent and significantly reduce marine pollution of all kinds, in particular from land-based activities, including marine debris (Target 14.1). The Bay of Bengal Initiative for Multi-Sectoral Technical and Economic Cooperation (BIMSTEC), Joint River Commission, India-Bangladesh Joint Working Group on Conservation of the Sundarbans, and South Asian Association for Regional Cooperation (SAARC) can lead transboundary plastic discharge minimisation and raise public awareness on plastic pollution. Local and national responses, like effective eco-tourism, plastic sorting and disposal program, and inclusive and participatory decision-making and forest-management/conservation are also critical to protect the future of this invaluable blue carbon ecosystem. Plastics reduction approaches at local level have recently been suggested (Lebreton and Andrady, 2019; Lau et al., 2020; Simon et al., 2021). For instance, Lebreton and Andrady (2019) proposed a scenario (Scenario B) where facilities or infrastructures for plastic waste management need to be improved according to per capita gross domestic product grows (**Figure 1B**). In addition to Scenario B, the portion of plastic waste in overall municipal solid waste needs to be lowered at 10 and 5% by 2020 and 2040, respectively (Scenario C), (**Figure 1C**), (Lebreton and Andrady, 2019). Therefore, we call the countries sharing the Sundarbans and Bay of Bengal to: eliminate plastic discharge to the environment; reduce plastic production; improve plastic waste collection and recycling infrastructure; and develop public awareness on plastic waste control. Periodic plastic clean-up program needs to strengthen to remove existing plastic waste in the environment and block the plastic discharge downstream. Strong monitoring and incentive scheme for the organisation involved with plastics recycling needs to be encouraged.

AUTHOR CONTRIBUTIONS

TA: conceptualization, funding acquisition, data curation, formal analysis, writing—original draft, writing—review, and editing. PM: writing—original draft, writing—review and editing, resources, supervision, and project administration. All authors contributed to the article and approved the submitted version.

FUNDING

TA received support from the Deakin University under the Alfred Deakin Postdoctoral Research Fellowship (ADPRF) scheme and ECR Enabler Grant.

REFERENCES

Atwood, T. B., Connolly, R. M., Almahasheer, H., Carnell, P. E., Duarte, C. M., Lewis, C. J. E., et al. (2017). Global patterns in mangrove soil carbon stocks and losses. *Nat. Clim. Chang.* 7, 523–528. doi: 10.1038/nclimate3326

Aziz, A., and Paul, A. R. (2015). Bangladesh sundarbans: present status of the environment and biota. *Diversity* 7, 242–269. doi: 10.3390/d7030242

Banglapedia (2012) *National Encyclopedia of Bangladesh*, 2nd edn. Bangladesh: Asiatic Society of Bangladesh. Available online at: https://en.banglapedia.org/index.php/River (accessed August 30, 2021).

Borrelle, S. B., Ringma, J., Law, K. L., Monnahan, C. C., Lebreton, L., McGivern, A., et al. (2020). Predicted growth in plastic waste exceeds efforts to mitigate plastic pollution. *Science* 369, 1515–1518. doi: 10.1126/science.aba3656

Borrelle, S. B., Rochman, C. M., Liboiron, M., Bond, A. L., Lusher, A., Bradshaw, H., et al. (2017). Opinion: why we need an international agreement on marine plastic pollution. *Proc. Nat. Acad. Sci. U.S.A.* 114, 9994–9997. doi: 10.1073/pnas.1714450114

CBD (2016). *Marine Debris: Understanding, Preventing and Mitigating the Significant Adverse Impacts on Marine and Coastal Biodiversity*. Technical Series No.83. Montreal: Secretariat of the Convention on Biological Diversity.

Chowdhury, G. W., Koldewey, H. J., Duncan, E., Napper, I. E., Niloy, M. N. H., Nelms, S. E., et al. (2020). Plastic pollution in aquatic systems in Bangladesh: a review of current knowledge. *Sci. Total Environ.* 761:143285. doi: 10.1016/j.scitotenv.2020.143285

Duan, J., Han, J., Cheung, S. G., Chong, R. K. Y., Lo, C.-M., Lee, F. W.-F., et al. (2021). How mangrove plants affect microplastic distribution in sediments of coastal wetlands: case study in Shenzhen Bay, South China. *Sci. Total Environ.* 767:144695. doi: 10.1016/j.scitotenv.2020.144695

Galloway, T., Cole, M., Lewis, C., Atkinson, A., and Allen, J. (2017). Interactions of microplastic debris throughout the marine ecosystem. *Nat. Ecol. Evol.* 1:116. doi: 10.1038/s41559-017-0116

Ghosh, G. C., Akter, S. M., Islam, R. M., Habib, A., Chakraborty, T. K., Zaman, S., et al. (2021). Microplastics contamination in commercial marine fish from the Bay of Bengal. *Reg. Stud. Mar. Sci.* 44:101728. doi: 10.1016/j.rsma.2021.101728

Goswami, P., Vinithkumar, N. V., and Dharani, G. (2020). First evidence of microplastics bioaccumulation by marine organisms in the Port Blair Bay, Andaman Islands. *Mar. Pollut. Bull.* 155:111163. doi: 10.1016/j.marpolbul.2020.111163

Hossain, M., Ahmed, M., Islam, T., Uddin, M. Z., Ahmed, Z. U., and Saha, C. (2021). Paradigm shift in the management of the Sundarbans mangrove forest of Bangladesh: issues and challenges. *Trees Forests People* 5:100094. doi: 10.1016/j.tfp.2021.100094

Hossain, M. S., Rahman, M. S., Uddin, M. N., Sharifuzzaman, S., Chowdhury, S. R., Sarker, S., et al. (2020). Microplastic contamination in Penaeid shrimp from the Northern Bay of Bengal. *Chemosphere* 238:124688. doi: 10.1016/j.chemosphere.2019.124688

Hossain, M. S., Sobhan, F., Uddin, M. N., Sharifuzzaman, S., Chowdhury, S. R., Sarker, S., et al. (2019). Microplastics in fishes from the Northern Bay of Bengal. *Sci. Total Environ.* 690, 821–830. doi: 10.1016/j.scitotenv.2019.07.065

IUCN (2019). *IUCN Advises "in Danger" Status for Three World Heritage sites. International Union for Conservation of Nature*. Available online at: https://www.iucn.org/news/iucn-43whc/201906/iucn-advises-danger-status-three-world-heritage-sites (accessed August 30, 2021).

Jambeck, J. R., Geyer, R., Wilcox, C., Siegler, T. R., Perryman, M., Andrady, A., et al. (2015). Plastic waste inputs from land into the ocean. *Science* 347, 768–771. doi: 10.1126/science.1260352

Lau, W. W., Shiran, Y., Bailey, R. M., Cook, E., Stuchtey, M. R., Koskella, J., et al. (2020). Evaluating scenarios toward zero plastic pollution. *Science* 369, 1455–1461. doi: 10.1126/science.aba9475

Lebreton, L., and Andrady, A. (2019). Future scenarios of global plastic waste generation and disposal. *Palgrave Commun.* 5, 1–11. doi: 10.1057/s41599-018-0212-7

Lebreton, L. C., Van Der Zwet, J., Damsteeg, J.-W., Slat, B., Andrady, A., and Reisser, J. (2017). River plastic emissions to the world's oceans. *Nat. Commun.* 8, 1–10. doi: 10.1038/ncomms15611

Meijer, L. J., van Emmerik, T., van der Ent, R., Schmidt, C., and Lebreton, L. (2021). More than 1,000 rivers account for 80% of global riverine plastic emissions into the ocean. *Sci. Adv.* 7:eaaz5803. doi: 10.1126/sciadv.aaz5803

Mukul, S. A., Huq, S., Herbohn, J., Seddon, N., and Laurance, W. F. (2020). Saving the sundarbans from development. *Science* 368, 1198–1198. doi: 10.1126/science.abb9448

Napper, I. E., Baroth, A., Barrett, A. C., Bhola, S., Chowdhury, G. W., Davies, B. F., et al. (2021). The abundance and characteristics of microplastics in surface water in the transboundary Ganges River. *Environ. Pollut.* 274:116348. doi: 10.1016/j.envpol.2020.116348

Napper, I. E., and Thompson, R. C. (2020). Plastic debris in the marine environment: history and future challenges. *Glob. Chall.* 4:1900081. doi: 10.1002/gch2.201900081

Nelms, S. E., Duncan, E. M., Patel, S., Badola, R., Bhola, S., Chakma, S., et al. (2021). Riverine plastic pollution from fisheries: Insights from the Ganges River system. *Sci. Total Environ.* 756:143305. doi: 10.1016/j.scitotenv.2020.143305

Onink, V., Jongedijk, C. E., Hoffman, M. J., van Sebille, E., and Laufkötter, C. (2021). Global simulations of marine plastic transport show plastic trapping in coastal zones. *Environ. Res. Lett.* 16:064053. doi: 10.1088/1748-9326/abecbd

Rillig, M. C., Leifheit, E., and Lehmann, J. (2021). Microplastic effects on carbon cycling processes in soils. *PLoS Biol.* 19:e3001130. doi: 10.1371/journal.pbio.3001130

Rochman, C. M., Browne, M. A., Halpern, B. S., Hentschel, B. T., Hoh, E., Karapanagioti, H. K., et al. (2013). Classify plastic waste as hazardous. *Nature* 494, 169–171. doi: 10.1038/494169a

Rochman, C. M., Browne, M. A., Underwood, A. J., Van Franeker, J. A., Thompson, R. C., and Amaral-Zettler, L. A. (2016). The ecological impacts of marine debris: unraveling the demonstrated evidence from what is perceived. *Ecology* 97, 302–312. doi: 10.1890/14-2070.1

Sachin, S. (2020). *Annual Visitor Arrivals at Sundarbans Rise to 250,000 but Drawbacks Remain*. Available online at: https://www.bdnews24.com (accessed August 30, 2021).

Schmidt, C., Krauth, T., and Wagner, S. (2017). Export of plastic debris by rivers into the sea. *Environ. Sci. Tech.* 51, 12246–12253. doi: 10.1021/acs.est.7b02368

Sen, H. (2019). *The Sundarbans: A Disaster-Prone Eco-Region*. Berlin: Springer. doi: 10.1007/978-3-030-00680-8

Simon, N., Raubenheimer, K., Urho, N., Unger, S., Azoulay, D., Farrelly, T., et al. (2021). A binding global agreement to address the life cycle of plastics. *Science* 373, 43–47. doi: 10.1126/science.abi9010

Singh, G. (2020). *Plastic Waste From Post-Amphan Relief Material Could Add to Pollution in Sundarbans*. Menlo Park, CA: MONGABAY.

Smith, S. D. (2012). Marine debris: a proximate threat to marine sustainability in Bootless Bay, Papua New Guinea. *Mar. Pollut. Bull.* 64, 1880–1883. doi: 10.1016/j.marpolbul.2012.06.013

Stubbins, A., Law, K. L., Muñoz, S. E., Bianchi, T. S., and Zhu, L. (2021). Plastics in the Earth system. *Science* 373, 51–55. doi: 10.1126/science.abb0354

Tessnow-von Wysocki, I., and Le Billon, P. (2019). Plastics at sea: treaty design for a global solution to marine plastic pollution. *Environ. Sci. Policy* 100, 94–104. doi: 10.1016/j.envsci.2019.06.005

UNESCO (2020). *UNESCO Marine World Heritage: Custodians of the Globe's Blue Carbon Assets*. Paris: UNESCO.

van Bijsterveldt, C. E., van Wesenbeeck, B. K., Ramadhani, S., Raven, O. V., van Gool, F. E., Pribadi, R., et al. (2021). Does plastic waste kill mangroves? A field experiment to assess the impact of macro plastics on mangrove growth, stress response and survival. *Sci. Total Environ.* 756:143826. doi: 10.1016/j.scitotenv.2020.143826

Villarrubia-Gómez, P., Cornell, S. E., and Fabres, J. (2018). Marine plastic pollution as a planetary boundary threat–The drifting piece in the sustainability puzzle. *Mar. Policy* 96, 213–220. doi: 10.1016/j.marpol.2017.11.035

Conflict of Interest: The authors declare that the research was conducted in the absence of any commercial or financial relationships that could be construed as a potential conflict of interest.

frontiers in Marine Science

ORIGINAL RESEARCH
published: 13 October 2021
doi: 10.3389/fmars.2021.728745

Abundance and Characteristics of Microplastics in Seawater and Corals From Reef Region of Sanya Bay, China

*Xinming Lei[1,2], Hao Cheng[3], Yong Luo[1,2], Yuyang Zhang[1,2], Lei Jiang[1,2], Youfang Sun[1,2], Guowei Zhou[1,2] and Hui Huang[1,2]**

[1] CAS Key Laboratory of Tropical Marine Bio-resources and Ecology, Guangdong Provincial Key Laboratory of Applied Marine Biology, South China Sea Institute of Oceanology, Innovation Academy of South China Sea Ecology and Environmental Engineering, Chinese Academy of Sciences, Guangzhou, China, [2] CAS-HKUST Sanya Joint Laboratory of Marine Science Research and Key Laboratory of Tropical Marine Biotechnology of Hainan Province, Tropical Marine Biological Research Station in Hainan, Chinese Academy of Sciences, Sanya, China, [3] State Key Laboratory of Tropical Oceanography, South China Sea Institute of Oceanology, Chinese Academy of Sciences, Guangzhou, China

OPEN ACCESS

Edited by:
Xiaoshan Zhu,
Tsinghua University, China

Reviewed by:
Youji Wang,
Shanghai Ocean University, China
Zhi Zhou,
Hainan University, China
Licheng Peng,
Hainan University, China

***Correspondence:**
Hui Huang
huanghui@scsio.ac.cn

Specialty section:
This article was submitted to Marine Pollution, a section of the journal Frontiers in Marine Science

Received: *22 June 2021*
Accepted: *16 September 2021*
Published: *13 October 2021*

Citation:
Lei X, Cheng H, Luo Y, Zhang Y, Jiang L, Sun Y, Zhou G and Huang H (2021) Abundance and Characteristics of Microplastics in Seawater and Corals From Reef Region of Sanya Bay, China. Front. Mar. Sci. 8:728745. doi: 10.3389/fmars.2021.728745

Microplastics (MPs) contamination is widespread in the coral reef ecosystems leading to the exposure of both corals and other biotas. Knowledge gaps still exist concerning patterns in MPs abundance spatially. This work quantified the MPs abundance and characteristics in the seawater and corals in the Sanya Bay, Hainan Island. MPs abundance was detected in the seawater and coral samples ranging from 15.50 to 22.14 items L^{-1}, and 0.01 to 3.60 items $polyp^{-1}$, respectively. We found the predominant size and type of MPs in seawater and corals were smaller than 2 mm and fiber. Further analysis revealed that the characteristics of MPs in the corals were significantly different from those in the seawater environment, indicating that the MPs are selectively enriched in corals. Furthermore, the MPs particles ingested and retained in coral tissue may be related to the polyp size. This study shows that MPs are present in the whole coral reef region and the coral community structure would be potentially harmed by these contaminants.

Keywords: microplastics, seawater, corals, Sanya Bay, distribution

INTRODUCTION

Plastic debris was first noted as a potential coastal water problem in 1971 (Carpenter et al., 1972), and MPs (plastic fragments < 5 mm, MPs) are now a widespread form of contamination in marine ecosystems (Moore, 2008; Andrady, 2011), from the Arctic waters (Lusher et al., 2015) to the remote Islands (Ding et al., 2019; Saliu et al., 2019; Tan et al., 2020; Oldenburg et al., 2021) and the coastal waters (Sutton et al., 2016; Yan et al., 2019; Qi et al., 2020; Tsang et al., 2020; Xie et al., 2021). MPs could enter the marine environment via multiple ways, such as ship transportation, fisheries, and domestic sewage discharges (Lusher et al., 2015; Sutton et al., 2016). MPs can be ingested by

diverse marine organisms and potentially be transferred through the food web (Setala et al., 2014; Rochman et al., 2015; Tanaka and Takada, 2016). It is a matter of great concern that the MPs may negatively affect the health of marine organisms (Moore, 2008) by blocking of the intestines (Carpenter et al., 1972), by acting as a vector for diseases (Lamb et al., 2018), and by acting as a carrier for the transport of heavy metals and chemical contaminants (Andrady, 2011; Saliu et al., 2019; Xie et al., 2021). Furthermore, colonization of MPs by sessile organisms provided carriers for the transport of alien species in the marine environment and may threaten the marine ecosystems (Moore, 2008).

Coral reefs are among the most biologically diverse region in the ocean, providing important ecosystem services to many millions of people, while coral reefs are degrading rapidly in response to various environmental and anthropogenic drivers (Hoegh-Guldberg et al., 2007; Hughes et al., 2017). Recently, high MPs abundance was reported in different coral reef ecosystems (Ding et al., 2019; Saliu et al., 2019; Oldenburg et al., 2021; Tang et al., 2021). MPs could be ingested by corals in the laboratory and natural habitats (Rotjan et al., 2019), which poses another threat to these vital organisms globally (Soares et al., 2020). Experimental study indicated that MPs could reduce growth performance, deteriorate health status and change the photosynthetic performance of corals (Reichert et al., 2019). Lamb et al. (2018) found the likelihood of disease increased when corals are in contact with plastic. Rotjan et al. (2019) found MPs ingestion could inhibit food intake of coral. In addition, there was evidence that MPs had negative impacts on their symbiotic association (Okubo et al., 2020; Su et al., 2020). All the research suggested that MPs ingestion might have negative physiological (Reichert et al., 2018; Su et al., 2020; Liao et al., 2021; Tang et al., 2021; Xiao et al., 2021) and ecological (Lamb et al., 2018; Saliu et al., 2019; Soares et al., 2020) consequences for corals.

As the MPs would potentially further magnify the effects of numerous other anthropogenic factors on the coral reefs, including overfishing, recreational activities, and water pollution, there is an urgent need to monitor the MPs in coral reef ecosystems. A recent United Nation Environment Program (UNEP) report also highlighted the critical need for monitoring MPs pollution patterns and ecological relevance in shallow water coral reefs (Sweet et al., 2019). With the MPs pollution in the South China Sea becoming an increasingly serious environmental problem, it is very important to understand the current status of MPs in coral reefs, especially in the fringing reefs. Fringing reefs, characterized by a long-term reef growth process from an attached shoreline, are always heavily impacted by human activities and natural causes.

The objective of this study was to investigate the abundance and characteristics of MPs in two reef-building corals (*Acropora millepora, Galaxea fascicularis*) and their living seawater environments in the Sanya Bay, Hainan Island. The coral *G. fascicularis* is one of the dominant species, while *A. millepora* is the common species within the study area (Sun et al., 2018). We sought to examine the difference and relationship of MPs contained in corals and seawater. This study would contribute to understand the potential impacts of MPs contamination on reef ecosystems and improve the strategies for local plastic waste management.

MATERIALS AND METHODS

Study Location

Sanya Bay is a typical tropical bay in China, located in the southern part (109°20′–109°30′E, 18°11′–18°18′N) of Hainan Island, with a sea area covers about 120 km^2 and an average depth of 16 m. Xidao Island, Dongdao Island located in the middle of the bay with narrow fringing reefs surrounded, and Xiaozhou Island and Luhuitou Peninsula possess the typical fringing reef. The Sanya River located in the eastern part of the bay, characterized by a length of 31.3 km, drainage area of 337 km^2 (Composed of Liuluo River, Shuijiao River, and Banling River. The mainstream Liuluo River originates from the southern foothill of the Zhongjian Mountain and flows from the north to the south.), and mean annual flow of 5.86 m^3s^{-1}. The annual mean seawater surface temperature (SST) and salinity in the bay are 26.9℃ and 32.7‰ respectively (Lian et al., 2010).

Sample Collection

The water and coral samples were collected from four sites in Sanya Bay, Hainan Island in November 2019, as showed in **Figure 1**. These sampling sites can be divided into two different regions. Sites Xidao (XD) and Dongdao (DD) were on the islets not far from the shore were treated as offshore sites (OS), while the sites Xiaozhoudao (XZD) and Luhuitou (LHT) were on the fringing reef along the shore were defined as inshore sites (IS). Both of the two types of sites suffered dense influence by human activities.

All tools and containers were dealt with Milli-Q water before sampling. A total of 30 L seawater was collected from each site with a 5 L plexiglass water sampler for this study. Two replicates of 15 L of seawater were then filtered using a 45 μm pore size stainless steel sieve with a glass fiber membrane of 0.45 μm. The filtered residue on the sieves and membranes was washed with Milli-Q water and transferred into a 50 mL glass bottle as one sample. Samples were stored at −20℃ before analysis.

Three coral colonies of *Acropora millepora*, *Galaxea fascicularis* in each sampling sites were collected using a hammer and a chisel by SCUBA diving, rinsed with pre-filtered seawater (filtered through a stainless sieve with 30 μm pore size with a glass fiber membrane of 0.45 μm), and preserved in a glass bottle with 95% ethanol immediately for transportation. All corals and seawater samples were collected at depths of 3–4 m at each sites.

Sample Preparation

The preparation of seawater and coral samples was performed with reference to previous studies (Hidalgo-Ruz et al., 2012; Catarino et al., 2017; Rotjan et al., 2019). In order to dissolve the organic matter in the seawater, samples were treated with 30 mL H_2O_2 (30%, V/V) for 24 h at room temperature (Nuelle et al., 2014; Yan et al., 2019). Then, the digested solution was filtered through 0.45 μm glass-fiber membrane (GF/F, 47 mm

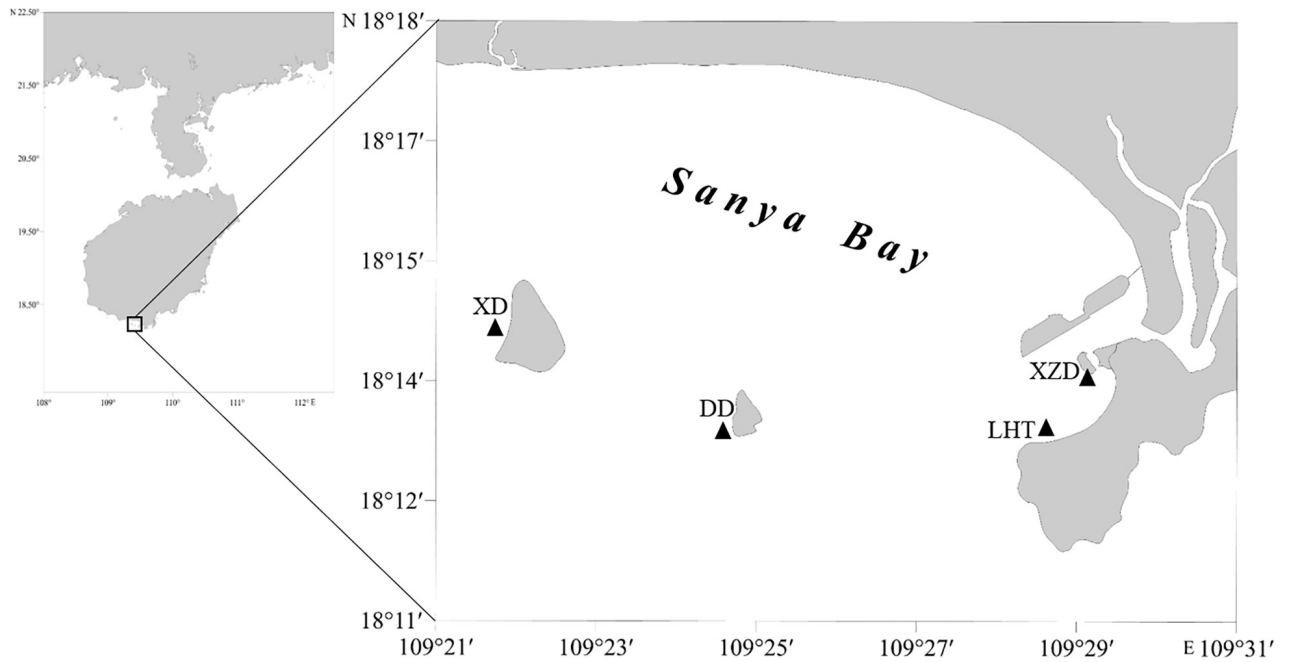

FIGURE 1 | Sample sites in Sanya Bay, China. XD, Xidao; DD, Dongdao; XZD, Xiaozhoudao; LHT, Luhuitou.

Ø, Whatman). The filters were transferred to covered glass petri dishes and air-dried for further analysis.

As the reef corals are colonial, meaning that the individuals called polyps are connected together by the coenosarc (a portion of continuous tissue that links polyps together). In the laboratory, fixed corals were removed from ethanol using metal forceps, cut into about 1 cm^2 rectangle pieces (4–33 polyps), rinsed with Milli-Q water to remove surface debris, air-dried in a covered glass petri dish and weighed. Polyp number was recorded. Corals were then decalcified with a 1.0% HCl solution for 12 h (Rotjan et al., 2019), filtered using a glass-fiber membrane of 0.45 μm, and then back washed into a sterile glass vial (Rotjan et al., 2019; Oldenburg et al., 2021). After that, 150 ml NaOH (10%, V/V) was added to the vial to digest any organic tissue residue, and then the vials were placed in a 60 ℃ drying oven for at least 24 h to allow for digestion of organic material (Catarino et al., 2017). Following this incubation, all samples were rinsed thoroughly with Milli-Q water onto a 0.45 μm glass-fiber membrane to remove NaOH residue. Each cleaned sample was washed back into a glass vial, and then the contents of the vial were pipetted onto a glass microscope slide and placed in the drying oven at 60 ℃ until the sample was completely dried onto the slide.

Blank control samples were prepared similarly to the sample preparation protocol. For the seawater blank control samples, 15 L Milli-Q water and 30 mL H_2O_2 (30%, V/V) were filtered onto a 0.45 μm glass-fiber membrane, then the filtered residue on the sieves and membranes was washed with Milli-Q water and transferred into a 50 mL glass container as blank control. For the coral blank control samples, the sieve and membrane were washed with 100 mL Milli-Q water, added 10 mL 1.0% HCl solution and 150 mL NaOH (10%, V/V), filtered through a 0.45 μm glass-fiber membrane, rinsed and backwashed with Milli-Q water into a clean glass container, and then pipetted onto a glass microscope slide.

Quantification and Identification of Microplastics

A stereomicroscope (M165 FC, Leica, Germany) was used for visually identifying and measuring the MPs according to their physical characteristics (Hidalgo-Ruz et al., 2012). The number, type (film, granule, fragment, fiber, fiber bundle), color (black, red, blue, green, transparent, other), and size of the plastics were recorded. According to the size, MPs are divided into five classifications: < 0.5, 0.5–1, 1–2, 2–3, and 3–5 mm.

For each sample and control, every MPs on the petri dish or slide was counted. Counts were conducted in triplicate for each sample. The mean value of controls was subtracted from the mean value of each sample. The unit of MPs abundance for seawater samples was reported as the number of particles per liter (items L^{-1}), while for the coral samples, the values were divided by the polyp number of the sample to calculate the number of MPs per polyp (items $polyp^{-1}$).

Additionally, a total of 121 representative particles from different types of samples were detected and identified by a micro-Raman spectrometer (Thermo Fisher Scientific DXR2, United States). Each measurement was performed with sixteen scans. All the suspected polymer types of the spectroscopy results were confirmed by comparison with the Raman polymer spectrum libraries that were applicable to the spectrometer. Only matches with the confidence levels of 70% at least was considered reliable and accepted (after visual inspection). Finally,

the visual identification data were adjusted according to the Raman identification results before analysis.

Quality Assurance and Control

In order to prevent potential pollution, all the containers were rinsed at least three times with Milli-Q water before being used. The microscope, lab bench, fume hood and drying oven were cleaned with 95% ethanol; meanwhile, the cotton lab coats and nitrile gloves were worn throughout the experiment. Prepared samples and the controls were stored in desiccator made of glass to reduce their exposure to the ambient environment. Furthermore, blank experiments without seawater, coral tissue were arranged simultaneously to correct and evaluate background MPs contamination during the experiment.

Data Analyses

Means, standard error (SE) were calculated for each site or coral species. Prior to analysis, the raw data were checked for normality and homogeneity of variances by the Shapiro-Wilk test and Brown-Forsythe test, respectively, and data were log(x + +1)-transformed when necessary. The difference between the abundance of the four sample sites was analyzed with the one-way analysis of variance (one-way ANOVA). A two-way ANOVA was used to assess the effects of site and coral species on MPs abundance (**Tables 1**, **2**). Tukey HSD *post hoc* tests were used to evaluate the significance of each pairwise comparison if factors were found to be significant ($p < 0.05$) in the ANOVA. Principal Coordinate analysis (PCO) was performed using Euclidean distance matrices to illustrate the clustering of the MPs characteristics between the seawater and coral samples. The MPs characteristics of the four sites in both seawater and corals were summarized using PCO combined with cluster analysis based on log(x + 1)-transformed/normalized of the raw data, including size, color and polymer type. Analyses were performed using Sigmaplot 14 and PRIMER 7 + PERMANOVA considering a 5% significance level (Anderson et al., 2008; Clarke and Gorley, 2015).

RESULTS

Abundance and Distribution of Microplastics

MPs were detected in all the seawater and coral samples from the four coral reef stations in the Sanya Bay of Hainan Island (**Figures 2A–D**). Items classified as potential plastics were identified in all of the 32 samples. A total of 121 particles were identified, 81% were less than 5 mm in size classifying them as MPs. MPs particles abundance in the seawater ranging from 15.50 ± 1.50 items L^{-1} at DD to 22.14 ± 0.90 items L^{-1} at XZD, with an average of 18.37 ± 2.60 items L^{-1}. The abundance at the XZD was significantly higher than that in the DD, and average MPs abundance in the seawater were higher in the IS (20.29 ± 1.16 items L^{-1}) than in the OS (16.45 ± 0.85 items L^{-1}) ($p < 0.05$) (**Figures 2A,B**).

The average MPs abundance in *A. millepora* was 0.27 ± 0.26 items $polyp^{-1}$ whereas that in *G. fascicularis* was 2.32 ± 0.86 items $polyp^{-1}$, and there was a significant difference between them ($p < 0.001$) (**Table 1** and **Figures 2C,D**). There was no statistical difference was measured in coral *A. millepora* among the sample sites, and similar result in the coral *G. fascicularis* except between XZD and DD (**Table 2**). Within the four sample sites, coral *G. fascicularis* contained significantly more MPs than that in coral *A. millepora*, and the MPs abundance in the two corals differed significantly between each other at the same site (**Figures 2C,D** and **Table 2**). In addition, coral *A. millepora* in the IS and OS contained no different abundance of MPs while coral *G. fascicularis* differed from each other significantly (**Figure 2D**).

TABLE 1 | Results of analysis of variance (ANOVA) to test the effect of coral species, site, and coral species: site on microfiber abundance in corals.

Variation	DF	SS	MS	*F*	*P*
Species	1	1.022	1.022	120.01	< 0.001
Site	3	0.0784	0.0261	3.072	0.058
Species × site	3	0.029	0.00967	1.136	0.364
Residual	16	0.136	0.00851		

TABLE 2 | Significant results of Tukey HSD test to assess the effect of coral species, site, and coral species: site on MPs abundance in corals.

Variation		Diff of means	*p*	*q*	*P*
Species	AM—GF	0.413	2	15.493	< 0.001
Site	XZD—DD	0.161	4	4.264	0.037
Species: Site	GF:XZD—GF:DD	0.258	4	4.844	0.017
	AM:XD—GF:XD	0.406	2	7.613	< 0.001
	AM:DD—GF:DD	0.311	2	5.833	< 0.001
	AM:XZD—GF:XZD	0.506	2	9.492	< 0.001
	AM:LHT—GF:LHT	0.429	2	8.047	< 0.001

AM, A. millepora; GF, G. fascicularis; XD, Xidao; DD, Dongdao; XZD, Xiaozhoudao; LHT, Luhuitou.

Characteristics and Composition of Microplastics

Both in the seawater and coral samples, more than 60 and 80% of the MPs were smaller than 1 and 2 mm, respectively, while those > 3 mm contributed the least to them (varied from 1.39 to 6.27%) (**Figure 3A** and **Supplementary Table 3**). MPs size of < 0.5 mm accounted for the largest proportion in seawater (42.83%), while the size of 0.5–1 mm accounted for the largest proportion in corals (*A. millepora*: 36.63%, *G. fascicularis*: 37.62%) (**Figure 3A**).

Five types of MPs shapes were detected in the seawater and coral samples, including fiber, granule, fiber bundle, fragment and film, but the vast majority was fiber both in the seawater (77.18%) and corals (*A. millepora*: 92.46%, *G. fascicularis*: 90.34%) (**Figure 3B**).

The most common color of MPs detected in seawater was black, accounting for 58.63%, however, the most frequent color of MPs detected in corals was transparent, accounting for 66.82%, 69.94% in *A. millepora*, *G. fascicularis*, respectively (**Figure 3C**).

The identified MPs compounds included polyethylene terephthalate (PET), cellophane (CP), polyethylene (PE),

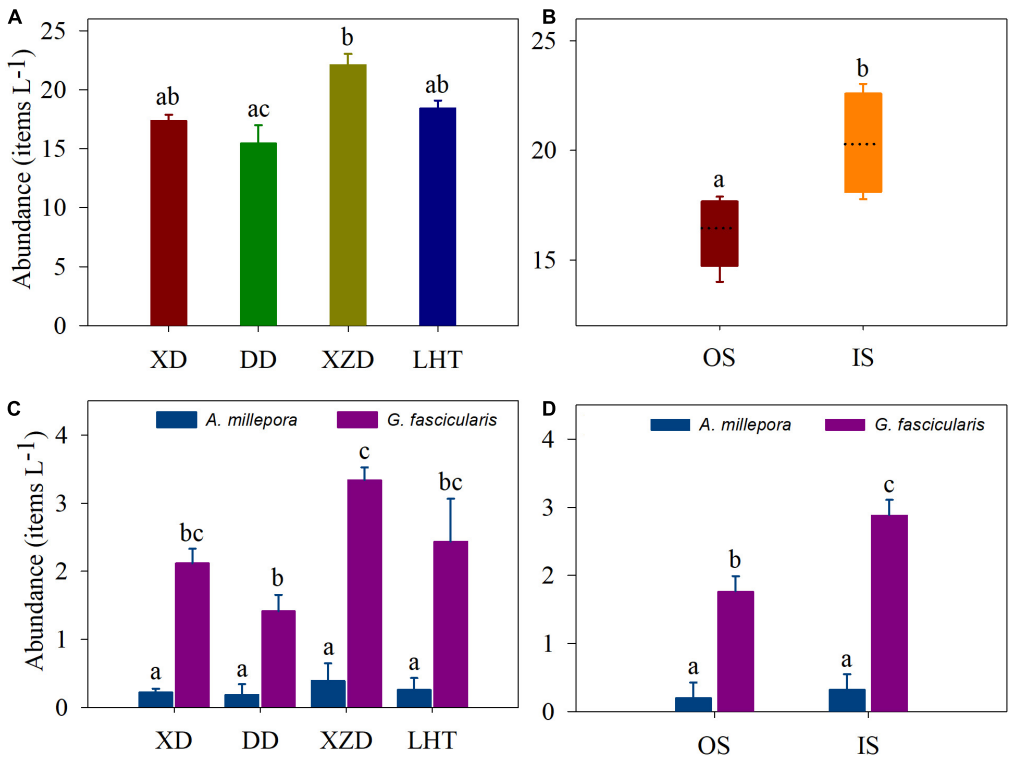

FIGURE 2 | MPs abundance in seawater **(A,B)** and corals **(C,D)**. XD, Xidao; DD, Dongdao; XZD, Xiaozhoudao; LHT, Luhuitou. Shared letters above the bars indicate there were not statistically different as determined by Tukey's HSD *post hoc* test.

polystyrene (PS), polyamide (PA), polypropylene (PP), and polypropylene–polyethylene (PP–PE). Results revealed that PET and CP were the dominant components of MPs both in the seawater and coral samples. In terms of the seawater samples, PET accounted for the highest proportion (47.02%), followed by CP (46.30%). As for the coral samples, CP component accounted for the majority (54.76%), followed by PET (35.12%) (**Figure 3D**).

Relationship of Microplastics in Seawater and Coral

The ordination biplot from PCO combined with cluster analysis clearly showed the separation between the characteristics of MPs contended in seawater and coral samples (**Figure 4**). The coral groups and seawater groups clustered separately first and then clustered with each other. The first two axes (PCO1 and PCO2) explained a total of 59.1% variance from the characteristics data of the seawater and coral samples. These findings implied that most of the tested seawater samples had similar MPs characteristics, and so did the corals. The characteristics of MPs in seawater had a close relationship except DD, whereas the features in the two coral species closed to each other within the same site.

DISCUSSION

The present study carried out the investigation of MPs abundance and distribution characteristics in both seawater and corals among the coral reef systems of Sanya Bay of Hainan Island. The results provided evidence that the coral reef region in Sanya Bay is extensively affected by MPs pollution, which indicates that reef organisms in surrounding seawater are suffering extensively from MPs.

Microplastics Features in Seawater

Our study observed the spatial differences in the extent of MPs contamination levels in the seawater of the Sanya Bay reef region. The average abundance of MPs in the four detected sites was 15.50 items L^{-1} which was greater in IS than in the OS. These variations could be linked to the sampling location and the impact degree of anthropogenic activities. The abundance of MPs in the XZD was significantly higher compared with the DD. This is because the XZD is located close to the Sanya River estuary and intensively affected by nearby human activities, while DD locates in relatively to the open-water site and under the control of the military. Another reason is that the rapid tourism industry development has driven the economic growth in Sanya since the late 1990s, and the increasing coastal development and urbanization have resulted in sewage discharge and increased levels of terrestrial runoff (Qiu, 2013). Additionally, due to the behavior of the visitors has not been effectively supervised (Haiying et al., 2018), visitors may discard plastics randomly or accidentally, such as bags, bottles and cutlery, directly into the sea.

The MPs abundance in the seawater were similar to that reported in the east coast of Hainan Island (14.9 items L^{-1})

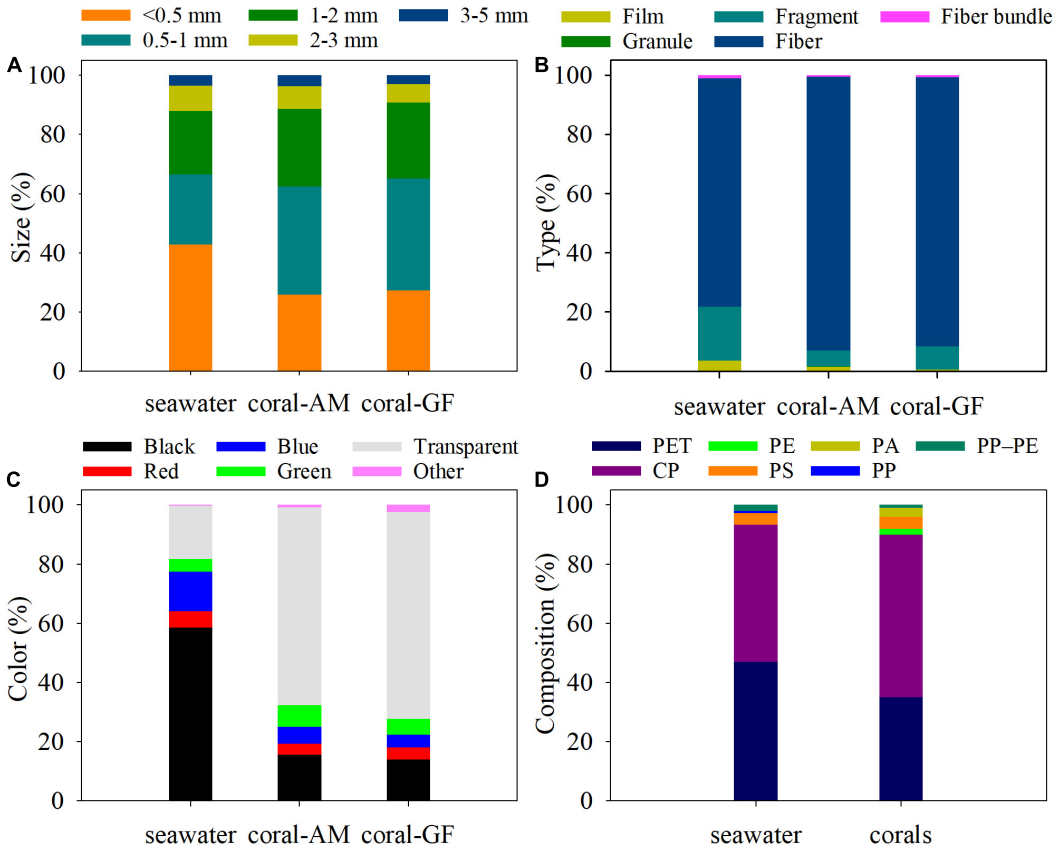

FIGURE 3 | Proportion of MPs size **(A)**, type **(B)**, color **(C)** and composition **(D)** in seawater and coral samples. AM, *A. millepora*; GF, *G. fascicularis*.

(Tang et al., 2021) and in the lagoon of the Xisha Islands (15.9 items L^{-1}) (Ding et al., 2019). However, this was much higher than the other observations in the South China Sea, such as the Hong Kong coast, Haikou Bay, Pearl River Estuary, the Xisha Islands, and the Nansha Islands (Cai et al., 2018; Ding et al., 2019; Huang et al., 2019; Nie et al., 2019; Wang et al., 2019; Yan et al., 2019; Qi et al., 2020; Tan et al., 2020; Tsang et al., 2020; Xie et al., 2021).

Additionally, the difference in MPs abundance might due to the different sampling methods. In our study, the seawater were sampled by plexiglass water sampler and all the particles above 45 μm were collected, while the other collected by plankton net (153 μm) (Tsang et al., 2020) or nylon Neuston nets (333 μm) (Cai et al., 2018; Qi et al., 2020; Tan et al., 2020). The MPs with the size range of 153–333 μm could be easily lost when sampling. Therefore, this suggests the need to establish standardized methods to evaluate the MPs pollution status more efficiently and make the data obtained more comparable.

Our results showed that the MPs of smaller size (<1 mm), fibrous types, black, and PET and CP accounted for the largest proportion in the reef region. Similar results were also observed in other coral reef environment (Cai et al., 2018; Ding et al., 2019; Huang et al., 2019; Tan et al., 2020; Tang et al., 2021). Many studies reported that smaller size of MPs (<1 mm) were the most dominant in the human activity-intense areas, such as the Pearl River Estuary (Yan et al., 2019), Haikou Bay (Qi et al., 2020), and the east coast of Hainan Island (Tang et al., 2021). The higher proportion of fibers was also observed in Arctic polar water (Lusher et al., 2015), the San Francisco Bay (Sutton et al., 2016), and the Xisha Islands (Ding et al., 2019). Studies showed that the main sources of fibers may be related to intensive ship transportation, fisheries, and domestic sewage discharges (Lusher et al., 2015; Sutton et al., 2016; Forero-Lopez et al., 2021).

Additionally, PET and CP are widely used in the daily life as the packaging materials (Tang et al., 2021). Besides, the dominant color of black in the seawater was also observed in the Haikou Bay, the Bahía Blanca Estuary, and estuary in the Gulf of Mexico (Qi et al., 2020; Forero-Lopez et al., 2021; Sanchez-Hernandez et al., 2021). MPs fibers were mostly black, blue, and transparent in general, and high proportions of black MPs are mainly sourced from tires, abrasives and plastic bags (Lassen et al., 2015). Moreover, mechanical damage in some fibers (e.g., fractures and color fading) can be associated with the weathering of polymers in seawater, while the digestion process of some animals could aggravate the physical damage in fibers (Forero-Lopez et al., 2021). For example, a recent study reported there were 90% black and blue fibers in the abdominal muscle and digestive tract of the shrimp *Pleoticus muelleri* (Fernandez Severini et al., 2020).

Overall, our results revealed that MPs were widely distributed in the coral reef ecosystems of Sanya Bay. Spatially, the highest

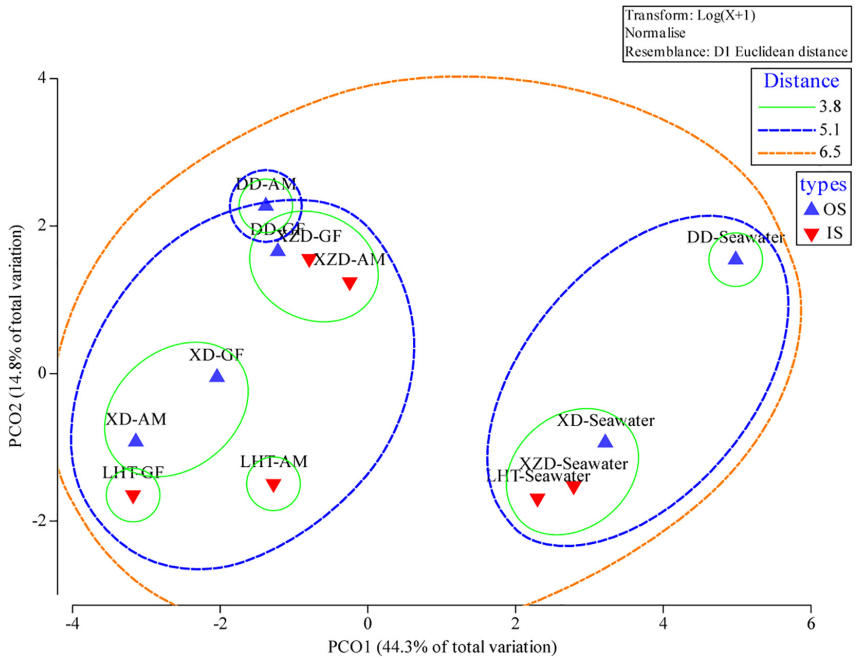

FIGURE 4 | PCO combined with cluster analysis showed the MPs distribution patterns in coral and seawater. XD, Xidao; DD, Dongdao; XZD, Xiaozhoudao; LHT, Luhuitou; AM, *A. millepora*; GF, *G. fascicularis*.

MPs abundance in seawater was found at XZD, and the high MPs concentrations may be associated with the local human activities, while the other reasons such as hydrological factors (water movement, etc.) require further assessment.

Microplastics Features in Corals

In the present investigation, the MPs abundance of the two corals differed significantly from each other among the sampling area. At each sampling site, the high MPs abundance in coral polyps corresponds to the high abundance in seawater, and the highest MPs concentration was found in *G. fascicularis* (3.34 items polyp^{-1}) in XZD, of which the majority were fibers, consistent with the results by Tang et al. (2021). The higher feeding rates of *G. fascicularis* (Hii et al., 2009) probably resulted in the higher concentration in the tissue than that in the coral *A. millepora*, and the high MPs concentration in the seawater could increase the probability of corals ingesting the MPs particles.

Unlike the MPs in the seawater were dominantly black, most of those in coral tissue were transparent. Transparent MPs, as well as the size (20-200 μm) and shape (slender), are similar to many phytoplankton and microalgae species (Ding et al., 2019; Nie et al., 2019; Keshavarzifard et al., 2021). A recent study found the transparent MPs were the most abundant (43%) in tissues of shrimp *Metapenaeus affinis*, which could pretend to be their food sources (Keshavarzifard et al., 2021). Ding et al. (2019) reported that transparent MPs were preferentially selective in capturing prey by fish due to their size was closer to the diatoms. Besides, the transparent fiber with a slender shape was similar to little jellyfish or zooplankton might result in being easily mistakenly ingested by marine animals, and then enriched in their organs (Nie et al., 2019), because some low-nutrient organisms were more readily available and easily exposed to suspended microplastics (reviewed in Yang et al., 2021). Thus, the high proportion of transparent particles in coral tissue may be due to their higher heterotrophic ability and therefore such MPs were ingested by mistake.

Martin et al. (2019) found *A. hemprichii* with small-size polyps (∼0.5 mm) preferably ingested and retained smaller MPs particles, while no preference was observed for *Goniastrea retiformis* with large polyps (2–3 mm), and this result was further confirmed by our present study as the major size in the coral tissue was smaller than 1 mm. In our study, the polyp size of *A. millepora* and *G. fascicularis* is 0.4–1.6 mm and 4.0–10.2 mm, respectively. The size of MPs particles ingested and retained in corals most likely relates to the size of the polyp (Martin et al., 2019). Besides, MPs attached frequently on the corals surfaces were detected (Reichert et al., 2018; Ding et al., 2019; Martin et al., 2019), indicating that this phenomenon would serve as a potential sink for marine MPs (Martin et al., 2019). However, MPs ingestion can inhibit food intake (Rotjan et al., 2019), which in turn induce a variety of negative impacts on the health of corals (Soares et al., 2020), as well as on the coral-Symbiodiniaceae symbiosis (Okubo et al., 2020; Su et al., 2020). All these results revealed that MPs are an emerging threat to coral reefs globally and thus have a long-term effect on population dynamics.

Relationship of Microplastics in Seawater and Coral

The PCO combined with cluster analysis clearly separated the characteristics of MPs contended in seawater and coral samples

implied that the characteristics of MPs in the two coral species differed from those in the seawater. An investigation along the east coast of Hainan Island revealed the characteristics of MPs enriched by two scleractinian coral differed from those in the environmental samples (Tang et al., 2021), and a study of Xisha Islands reported there was no apparent relationship between MPs distribution in seawater and corals (Ding et al., 2019).

The proportion of the MPs size of smaller than 2 mm, type of fragment, color of black, and the PET in the seawater samples were significant higher than those in coral samples, while the size of 0.5–1 mm, type of fiber, color of transparent, and the CP in the coral samples were significant higher than those in seawater samples. A previous study found MPs characteristics (size, shape and color) in reef-dwellers and the environments formed two distinct clusters, while variations were much smaller within the same group and mostly clustered together (Tang et al., 2021). Consistent with these previous studies, this study further revealed that MPs characteristics differed greatly in seawater and organisms, which was confirmed by the two distinct clusters between seawater and corals. DD was the outlier of the seawater cluster, and the MPs abundance in the seawater was the lowest among all the seawater sample sites due to the military control, while the proportion of the MPs size of smaller than 0.5 mm, type of fragment, and color of blue and green was the highest among all sites.

Although the MPs abundance was significantly different in the two corals, there were many overlaps within the coral cluster indicating that the MPs in the tissue of the two corals shared many similar characteristics, which highlights the conclusions that corals could selectively enrich MPs from the environment (Martin et al., 2019; Tang et al., 2021).

CONCLUSION

This is the first investigation to show the presence and distribution of MPs both in corals and seawater within the coral reef area of Sanya Bay, Hainan Island. The results showed widespread MPs contamination in the coral reef ecosystems in this research region. Difference in the spatial distribution of seawater may be related to the discharge from Sanya River and the intensive anthropogenic activities. The most frequently measured MPs we sampled were smaller than 2 mm, and shape of fiber, reiterating the strong presence of fiber as a contaminant in the ocean. Further analysis revealed that the MPs characteristics in the coral species were different from those in the seawater, indicating the potential selective enrichment in the corals. Furthermore, the size of MPs (0.5–1 mm) dominant in coral tissue suggests that the MPs particles ingested by corals most likely relates to the size of polyps. Corals are interacting with MPs in their natural habitats reflecting the coral communities to be potentially harmed by these contaminants. However, the origins and pathways bringing MPs to the Sanya Bay remain unclear. Further research is required to understand the effects of microplastic-coral interaction within this productive ecosystem. Ultimately, understanding the abundance, spatial distribution, and potential sources of MPs in coral reefs will help improve regional management of plastic waste in vital coastal ecosystems.

DATA AVAILABILITY STATEMENT

The original contributions presented in the study are included in the article/**Supplementary Material**, further inquiries can be directed to the corresponding author/s.

AUTHOR CONTRIBUTIONS

XL and HC collected the samples and analyzed the data. XL, HC, YL, YS, LJ, YZ, GZ, and HH wrote and revised the manuscript. All authors designed the experiment and collected the data.

FUNDING

This research was funded by the National Natural Science Foundation of China (Grant Nos. 41306144, 41876192, and 41976120), the Guangdong Basic and Applied Basic Research Foundation (Grant No. 2019A1515011532), the Key Research and Development Project of Hainan Province, China (Grant No. ZDYF2020200), the Science and Technology Planning Project of Guangdong Province, China (Grant No. 2020B1212060058), the Innovation Academy of South China Sea Ecology and Environmental Engineering, Chinese Academy of Sciences (Grant No. ISEE2021ZD03).

SUPPLEMENTARY MATERIAL

The Supplementary Material for this article can be found online at: https://www.frontiersin.org/articles/10.3389/fmars.2021.728745/full#supplementary-material

REFERENCES

Anderson, M. J., Gorley, R. N., and Clarke, K. R. (2008). *PERMANOVA+ for PRIMER Guide To Software And Statistical Methods*. Plymouth: PRIMER-E Ltd.

Andrady, A. L. (2011). Microplastics in the marine environment. *Mar. Pollut. Bull.* 62, 1596–1605. doi: 10.1016/j.marpolbul.2011.05.030

Cai, M. G., He, H. X., Liu, M. Y., Li, S. W., Tang, G. W., Wang, W. M., et al. (2018). Lost but can't be neglected: huge quantities of small microplastics hide in the South China Sea. *Sci. Total Envir.* 633, 1206–1216. doi: 10.1016/j.scitotenv.2018.03.197

Carpenter, E. J., Anderson, S. J., Harvey, G. R., Miklas, H. P., and Peck, B. B. (1972). Polystyrene spherules in coastal waters. *Science* 178, 749–750. doi: 10.1126/science.178.4062.749

Catarino, A. I., Thompson, R., Sanderson, W., and Henry, T. B. (2017). Development and optimization of a standard method for extraction of microplastics in mussels by enzyme digestion of soft tissues. *Environ. Toxicol. Chem.* 36, 947–951. doi: 10.1002/etc.3608

Clarke, K. R., and Gorley, R. N. (2015). *Primer v7: User Manual/Tutorial*. Plymouth: PRIMER-E Ltd.

Ding, J., Jiang, F., Li, J., Wang, Z., Sun, C., Wang, Z., et al. (2019). Microplastics in the coral reef systems from xisha islands of South China Sea. *Environ. Sci. Technol.* 53, 8036–8046. doi: 10.1021/acs.est.9b01452

Fernandez Severini, M. D., Buzzi, N. S., Forero Lopez, A. D., Colombo, C. V., Chatelain Sartor, G. L., Rimondino, G. N., et al. (2020). Chemical composition and abundance of microplastics in the muscle of commercial shrimp *Pleoticus muelleri* at an impacted coastal environment (Southwestern Atlantic). *Mar. Pollut. Bull.* 161(Pt A):111700. doi: 10.1016/j.marpolbul.2020.111700

Forero-Lopez, A. D., Rimondino, G. N., Truchet, D. M., Colombo, C. V., Buzzi, N. S., Malanca, F. E., et al. (2021). Occurrence, distribution, and characterization of suspended microplastics in a highly impacted estuarine wetland in Argentina. *Sci. Total Environ.* 785:147141. doi: 10.1016/j.scitotenv.2021.147141

Haiying, C., Linsi, H., Peng, L., Xiaohong, Z., and Changjiang, Y. (2018). Relationship of stakeholders in protected areas and tourism ecological compensation: a case study of sanya coral reef national nature reserve in China. *J. Resour. Ecol.* 9, 164–173. doi: 10.5814/j.issn.1674-764x.2018.02.006

Hidalgo-Ruz, V., Gutow, L., Thompson, R. C., and Thiel, M. (2012). Microplastics in the marine environment: a review of the methods used for identification and quantification. *Environ. Sci. Technol.* 46, 3060–3075. doi: 10.1021/es201505

Hii, Y. S., Soo, C. L., and Liew, H. C. (2009). Feeding of scleractinian coral, Galaxea fascicularis, on Artemia salina nauplii in captivity. *Aquac. Int.* 17, 363–376. doi: 10.1007/s10499-008-9208-4

Hoegh-Guldberg, O., Mumby, P. J., Hooten, A. J., Steneck, R. S., Greenfield, P., Gomez, E., et al. (2007). Coral reefs under rapid climate change and ocean acidification. *Science* 318, 1737–1742. doi: 10.1126/science.1152509

Huang, Y., Yan, M., Xu, K., Nie, H., Gong, H., and Wang, J. (2019). Distribution characteristics of microplastics in Zhubi Reef from South China Sea. *Environ. Pollut.* 255(Pt 1):113133. doi: 10.1016/j.envpol.2019.113133

Hughes, T. P., Barnes, M. L., Bellwood, D. R., Cinner, J. E., Cumming, G. S., Jackson, J. B. C., et al. (2017). Coral reefs in the Anthropocene. *Nature* 546, 82–90. doi: 10.1038/nature22901

Keshavarzifard, M., Vazirzadeh, A., and Sharifinia, M. (2021). Occurrence and characterization of microplastics in white shrimp, Metapenaeus affinis, living in a habitat highly affected by anthropogenic pressures, northwest Persian Gulf. *Mar. Pollut. Bull.* 169:112581. doi: 10.1016/j.marpolbul.2021.112581

Lamb, J. B., Willis, B. L., Fiorenza, E. A., Couch, C. S., Howard, R., Rader, D. N., et al. (2018). Plastic waste associated with disease on coral reefs. *Science* 359, 460–462. doi: 10.1126/science.aar3320

Lassen, C., Hansen, S. F., Magnusson, K., Norén, F., Hartmann, N. I. B., Jensen, P. R., et al. (2015). *Microplastics-Occurrence, Effects and Sources of Releases to the Environment in Denmark. Environmental Project No. 1793*. Copenhagen K: The Danish Environmental Protection Agency. Available online at: https://www.tilogaard.dk/Miljostyrelsens_rapport_om_mikroplast_978-87-93352-80-3.pdf

Lian, J. S., Huang, H., Huang, L. M., and Wang, D. R. (2010). *Coral Reef And Its Biodiversity Of Sanya*. Beijing: Marine Press.

Liao, B., Wang, J., Xiao, B., Yang, X., Xie, Z., Li, D., et al. (2021). Effects of acute microplastic exposure on physiological parameters in Tubastrea aurea corals. *Mar. Pollut. Bull.* 165:112173. doi: 10.1016/j.marpolbul.2021.112173

Lusher, A. L., Tirelli, V., O'Connor, I., and Officer, R. (2015). Microplastics in Arctic polar waters: the first reported values of particles in surface and sub-surface samples. *Sci. Rep.* 5:14947. doi: 10.1038/srep14947

Martin, C., Corona, E., Mahadik, G. A., and Duarte, C. M. (2019). Adhesion to coral surface as a potential sink for marine microplastics. *Environ. Pollut.* 255(Pt 2):113281. doi: 10.1016/j.envpol.2019.113281

Moore, C. J. (2008). Synthetic polymers in the marine environment: a rapidly increasing, long-term threat. *Environ. Res.* 108, 131–139. doi: 10.1016/j.envres.2008.07.025

Nie, H., Wang, J., Xu, K., Huang, Y., and Yan, M. (2019). Microplastic pollution in water and fish samples around Nanxun Reef in Nansha Islands, South China Sea. *Sci. Total Environ.* 696:134022. doi: 10.1016/j.scitotenv.2019.134022

Nuelle, M. T., Dekiff, J. H., Remy, D., and Fries, E. (2014). A new analytical approach for monitoring microplastics in marine sediments. *Environ. Pollut.* 184, 161–169. doi: 10.1016/j.envpol.2013.07.027

Okubo, N., Tamura-Nakano, M., and Watanabe, T. (2020). Experimental observation of microplastics invading the endoderm of *anthozoan polyps*. *Mar. Environ. Res.* 162:105125. doi: 10.1016/j.marenvres.2020.105125

Oldenburg, K. S., Urban-Rich, J., Castillo, K. D., and Baumann, J. H. (2021). Microfiber abundance associated with coral tissue varies geographically on the Belize Mesoamerican Barrier Reef System. *Mar. Pollut. Bull.* 163:111938. doi: 10.1016/j.marpolbul.2020.111938

Qi, H. Y., Fu, D. D., Wang, Z. Z., Gao, M. Y., and Peng, L. C. (2020). Microplastics occurrence and spatial distribution in seawater and sediment of Haikou Bay in the northern South China Sea. *Estuar. Coast. Shelf Sci.* 239:106757. doi: 10.1016/j.ecss.2020.106757

Qiu, W. (2013). The sanya coral reef national marine nature reserve, China: a governance analysis. *Mar. Policy* 41, 50–56. doi: 10.1016/j.marpol.2012.12.030

Reichert, J., Arnold, A. L., Hoogenboom, M. O., Schubert, P., and Wilke, T. (2019). Impacts of microplastics on growth and health of hermatypic corals are species-specific. *Environ. Pollut.* 254(Pt B):113074. doi: 10.1016/j.envpol.2019.113074

Reichert, J., Schellenberg, J., Schubert, P., and Wilke, T. (2018). Responses of reef building corals to microplastic exposure. *Environ. Pollut.* 237, 955–960. doi: 10.1016/j.envpol.2017.11.006

Rochman, C. M., Tahir, A., Williams, S. L., Baxa, D. V., Lam, R., Miller, J. T., et al. (2015). Anthropogenic debris in seafood: plastic debris and fibers from textiles in fish and bivalves sold for human consumption. *Sci. Rep.* 5:14340. doi: 10.1038/srep14340

Rotjan, R. D., Sharp, K. H., Gauthier, A. E., Yelton, R., Lopez, E. M. B., Carilli, J., et al. (2019). Patterns, dynamics and consequences of microplastic ingestion by the temperate coral, Astrangia poculata. *Proc. Biol. Sci.* 286:20190726. doi: 10.1098/rspb.2019.0726

Saliu, F., Montano, S., Leoni, B., Lasagni, M., and Galli, P. (2019). Microplastics as a threat to coral reef environments: detection of phthalate esters in neuston and *scleractinian* corals from the Faafu Atoll, Maldives. *Mar. Pollut. Bull.* 142, 234–241. doi: 10.1016/j.marpolbul.2019.03.043

Sanchez-Hernandez, L. J., Ramirez-Romero, P., Rodriguez-Gonzalez, F., Ramos-Sanchez, V. H., Marquez Montes, R. A., Romero-Paredes Rubio, H., et al. (2021). Seasonal evidences of microplastics in environmental matrices of a tourist dominated urban estuary in Gulf of Mexico, Mexico. *Chemosphere* 277:130261. doi: 10.1016/j.chemosphere.2021.130261

Setala, O., Fleming-Lehtinen, V., and Lehtiniemi, M. (2014). Ingestion and transfer of microplastics in the planktonic food web. *Environ. Pollut.* 185, 77–83. doi: 10.1016/j.envpol.2013.10.013

Soares, M. O., Matos, E., Lucas, C., Rizzo, L., Allcock, L., and Rossi, S. (2020). Microplastics in corals: an emergent threat. *Mar. Pollut. Bull.* 161(Pt A):111810. doi: 10.1016/j.marpolbul.2020.111810

Su, Y., Zhang, K., Zhou, Z., Wang, J., Yang, X., Tang, J., et al. (2020). Microplastic exposure represses the growth of endosymbiotic *dinoflagellate* Cladocopium goreaui in culture through affecting its apoptosis and metabolism. *Chemosphere* 244:125485. doi: 10.1016/j.chemosphere.2019.125485

Sun, Y., Lei, X., Lian, J., Yang, J., Wu, Y., and Huang, H. (2018). Ecosystem status and health assessment of sanya coral reef national nature reserve. *Biodivers. Sci.* 26, 258–265. doi: 10.17520/biods.2017312

Sutton, R., Mason, S. A., Stanek, S. K., Willis-Norton, E., Wren, I. F., and Box, C. (2016). Microplastic contamination in the San Francisco Bay, California, USA. *Mar. Pollut. Bull.* 109, 230–235. doi: 10.1016/j.marpolbul.2016.05.077

Sweet, M., Stelfox, M., and Lamb, J. (2019). *Plastics And Shallow Water Coral Reefs: Synthesis Of The Science For Policy-Makers*. Nairobi: United Nations Environment Program.

Tan, F., Yang, H., Xu, X., Fang, Z., Xu, H., Shi, Q., et al. (2020). Microplastic pollution around remote uninhabited coral reefs of Nansha Islands, South China Sea. *Sci. Total Environ.* 725:138383. doi: 10.1016/j.scitotenv.2020.138383

Tanaka, K., and Takada, H. (2016). Microplastic fragments and microbeads in digestive tracts of *planktivorous* fish from urban coastal waters. *Sci. Rep.* 6:34351. doi: 10.1038/srep34351

Tang, J., Wu, Z., Wan, L., Cai, W., Chen, S., Wang, X., et al. (2021). Differential enrichment and physiological impacts of ingested microplastics in *scleractinian* corals in situ. *J. Hazard. Mater.* 404(Pt B):124205. doi: 10.1016/j.jhazmat.2020.124205

Tsang, Y. Y., Mak, C. W., Liebich, C., Lam, S. W., Sze, E. T. P., and Chan, K. M. (2020). Spatial and temporal variations of coastal microplastic pollution in Hong Kong. *Mar. Pollut. Bull.* 161(Pt B):111765. doi: 10.1016/j.marpolbul.2020.111765

Wang, T., Zou, X., Li, B., Yao, Y., Zang, Z., Li, Y., et al. (2019). Preliminary study of the source apportionment and diversity of microplastics: taking floating microplastics in the South China Sea as an example. *Environ. Pollut.* 245, 965–974. doi: 10.1016/j.envpol.2018.10.110

Xiao, B., Li, D., Liao, B., Zheng, H., Yang, X., Xie, Y., et al. (2021). Effects of Microplastics Exposure on the *Acropora sp*. Antioxidant, immunization and energy metabolism enzyme activities. *Front. Microbiol.* 12:666100. doi: 10.3389/fmicb.2021.666100

Xie, Q., Li, H. X., Lin, L., Li, Z. L., Huang, J. S., and Xu, X. R. (2021). Characteristics of expanded polystyrene microplastics on island beaches in the Pearl River Estuary: abundance, size, surface texture and their metals-carrying capacity. *Ecotoxicology* 30, 1632–1643. doi: 10.1007/s10646-020-02329-7

Yan, M., Nie, H., Xu, K., He, Y., Hu, Y., Huang, Y., et al. (2019). Microplastic abundance, distribution and composition in the Pearl River along Guangzhou city and Pearl River estuary, China. *Chemosphere* 217, 879–886. doi: 10.1016/j.chemosphere.2018.11.093

Yang, H., Chen, G., and Wang, J. (2021). Microplastics in the marine environment: sources, fates, impacts and microbial degradation. *Toxics* 9:41. doi: 10.3390/toxics9020041

Conflict of Interest: The authors declare that the research was conducted in the absence of any commercial or financial relationships that could be construed as a potential conflict of interest.

Publisher's Note: All claims expressed in this article are solely those of the authors and do not necessarily represent those of their affiliated organizations, or those of the publisher, the editors and the reviewers. Any product that may be evaluated in this article, or claim that may be made by its manufacturer, is not guaranteed or endorsed by the publisher.

frontiers in Marine Science

METHODS
published: 14 October 2021
doi: 10.3389/fmars.2021.739683

In-situ Detection Method for Microplastics in Water by Polarized Light Scattering

Tong Liu[1,2], Shijun Yu[1,3], Xiaoshan Zhu[2], Ran Liao[1,2], Zepeng Zhuo[1,4], Yanping He[5] and Hui Ma[1,4]*

[1] Guangdong Research Center of Polarization Imaging and Measurement Engineering Technology, Shenzhen International Graduate School, Tsinghua University, Shenzhen, China, [2] Institute for Ocean Engineering, Shenzhen International Graduate School, Tsinghua University, Shenzhen, China, [3] Department of Biomedical Engineering, Tsinghua University, Beijing, China, [4] Department of Physics, Tsinghua University, Beijing, China, [5] Department of Environmental Engineering, Tsinghua University, Beijing, China

Microplastics (MPs) have become the widespread contaminants, which raises concerns on their ecological hazards. *In-situ* detection of MP in water bodies is essential for clear assessment of the ecological risks of MPs. The present study proposes a method based on polarized light scattering which measures the polarization parameters of the scattered light at 120° to detect MP in water. This method takes the advantage of *in-situ* measurement of the individual particles and the experimental setup in principle is used. By use of the measured polarization parameters equipped by machine learning, the standard polystyrene (PS) spheres, natural water sample, and lab-cultured microalgae are explicitly discriminated, and MP with different physical and chemical properties can be differentiated. It can also characterize the weathering of different MP and identify the specific type from multiple types of MP. This study explores the capability of the proposed method to detect the physical and chemical properties, weathering state and concentration of MP in water which promises the future application in water quality sensing and monitoring.

Keywords: *in-situ* detection, microplastics, polarization, scattering light, classification, machine learning

OPEN ACCESS

Edited by:
Youji Wang,
Shanghai Ocean University, China

Reviewed by:
Jinjia Guo,
Ocean University of China, China
Fuhong Cai,
Hainan University, China

***Correspondence:**
Ran Liao
liao.ran@sz.tsinghua.edu.cn

Specialty section:
This article was submitted to Marine Pollution, a section of the journal Frontiers in Marine Science

Received: *11 July 2021*
Accepted: *21 September 2021*
Published: *14 October 2021*

Citation:
Liu T, Yu S, Zhu X, Liao R, Zhuo Z, He Y and Ma H (2021) In-situ Detection Method for Microplastics in Water by Polarized Light Scattering. Front. Mar. Sci. 8:739683. doi: 10.3389/fmars.2021.739683

INTRODUCTION

Microplastics (MPs) are defined as plastic particles with size <5 mm (Amaral-Zettler et al., 2020), widely distribute in water environments including oceans (Saeed et al., 2020), lakes (Yu et al., 2020), and rivers (Auta et al., 2017). Once inside the body, microplastics can release toxins, additives, and monomers which have been found to trigger carcinogenic behavior. Moreover, the human intake of microplastics can cause lung damage and liver function changes. Thus, microplastics pollution should be understood and controlled to uphold human, animal, and aquatic health (Golwala et al., 2021). In order to assess the effects of MPs on aquatic ecosystem, the detection method of MPs in water has attracted the attention of researchers (Sadri and Thompson, 2014; Amaral-Zettler et al., 2020).

The current detection methods for MPs mainly include visual method (including naked eye visual method and microscope visual method), Fourier infrared spectroscopy, Raman spectroscopy, and thermal pyrolysis analysis (Mai et al., 2018). The analysis of MPs in water usually includes

sampling, filtering, cleaning, identification, and other steps (Song et al., 2015). The difficulty of MPs identification lies in the identification of MPs from many impurity particles. Visual method is widely used due to convenience and cheapness, and it can give the physical properties of MPs, such as size, color, and shape (Eriksen et al., 2013; Vianello et al., 2013). However, the visual method is low accuracy and subjected to the subjective influence, and often makes an overestimate of the abundance of MPs in samples (Lenz et al., 2015). Spectroscopic methods, including Fourier infrared spectroscopy and Raman spectroscopy, can determine the chemical composition of the sample, and the accuracy is relatively high, and the size resolution can approach 1 micron (Kappler et al., 2016). However, there is seldom reported about the *in-situ* detection of MPs using spectroscopic methods. The thermal pyrolysis analysis, such as Pyrolysis-GC/MS and TGA-MS have been used for the microplastic analysis. Samples are firstly thermally degraded and the resultant products are subsequently sent to the mass spectrometer for analysis. The collected data are compared with reference to obtain such sample information as identity and concentration. However, the method is less applicable for mixtures with high concentration of impurities (Zhang et al., 2019). Due to the needed sampling, these methods are not suitable to *in-situ* detect MPs in water. Nowadays, an *in-situ* detection method with high speed, convenience, non-destruction, and acceptable accuracy is still desired (Yin et al., 2021).

Polarization is a fundamental property of light. The polarization state is more sensitive to microstructure and can provide more information than conventional optical intensity (Sun et al., 2014). Polarized light scattering methods have been successfully used to characterize and classify biological tissues (Ghosh and Vitkin, 2011), marine microalgae (Chami, 2007), and nanoplastics (Yu et al., 2021). Measurement sensors based on polarized light scattering methods have been successfully integrated into *in-situ* underwater instruments (Liao et al., 2019).

The polarization state of light is usually represented by the Stokes vector S as shown in Eq. 1. I represents the light intensity; Q and U represent the linearly residual polarization of light; Q is the intensity difference between the horizontal and vertical components, and U is intensity difference between 45° and −45° linear components; V is the circularly residual polarization of light, and equals to the intensity difference between the right-hand and left-hand components. Usually, the Stokes vector is normalized as Eq. 2 to obtain the three polarization parameters of q, u, and v.

$$S = \begin{bmatrix} I \\ Q \\ U \\ V \end{bmatrix}, \tag{1}$$

$$q \equiv Q/I, u \equiv U/I, v \equiv V/I. \tag{2}$$

In this paper, we propose a polarized light scattering method to *in-situ* detect the MPs in water. This method takes the advantage of the different responses of the MPs and other particles in water to the incident polarized light. We record the polarization parameters (q, u, v) of the light scattered by the individual particles at 120° scattering angle, and then use machine learning algorithms, such as linear discrimination analysis (LDA) and support vector machine (SVM) to analyze the data. The samples consist of the mixture of the natural water, the microalgae, and the MPs with different size, shape and materials. Experiments have found that microplastic (MP) can be well-discriminated from the mixtures. We also did the experiments to discriminate the weathered MP from the natural water even for the complex compositions of MPs samples, and the results are encouraging. Additionally, we found that polarization parameters can be used to characterize MP size decreasing after weathering. The concentration calibration shows a linear relationship between the measured pulse number per unit time and the concentration of MP. The results promised the present method suitable *in-situ* detecting those suspended MPs from complex water environment, with no weathering disturbance while a lower detectable concentration limit of MPs (0.01 mg/L).

METHODS

Experimental Setup

The experimental setup designed by our lab is a backward 120° polarized light scattering measurement system for suspended particles. Its working principle and optical path design are similar with the previous work (Wang et al., 2018), and its reliability has been verified (Liao et al., 2019). Our previous works demonstrate that the polarization parameters at the 120° scattering angle can effectively characterize the microstructures of particles (Wang et al., 2018). The scattered intensity of the bulk water volume at 120° is almost not sensitive to the size distribution of particles (Boss and Pegau, 2001). Such that, we continue to use the 120° scattering angle in this work. The light source (S) emits vertically polarized light. The polarization state generator (PSG) changes the light into any polarization state we want, and in this work, PSG generate and fix at the 135° linearly polarized light. And the diaphragm (D) limits the size of the incident light spot. Lens 1 (L1) focuses the light beam to a small spot to illuminate the individual particles. The aquatic suspension is contained in a round beaker. During the experiment, the particles in the aquatic suspension are stirred to keep suspended by a magnetic stirrer at the speed of 100 rounds per minute. In the setup, the round beaker is embedded in a dodecagon pool with the central coaxial. The beaker is marked by a red arrow in **Figure 1A**. The distilled water is filled between the beaker and the dodecagon pool for the refractive index matching. The parallel beam is normally incident on a flat surface of dodecagon and the scattered light is received through the other flat surface at the 120° scattering angle. The flat surfaces and the distilled water are used to effectively reduce the light deformation when passing through the surfaces. The 120° backward scattered light is received by lens 2 (L2), filtered by pinhole (P), and changed by lens 3 (L3) to the parallel light and finally analyzed by the polarization state analyzer (PSA).

In **Figure 1**, the detection volume containing the particle and the pinhole is the object-image relationship by L2. Since the conjugate relation, the detected volume in water and its size is

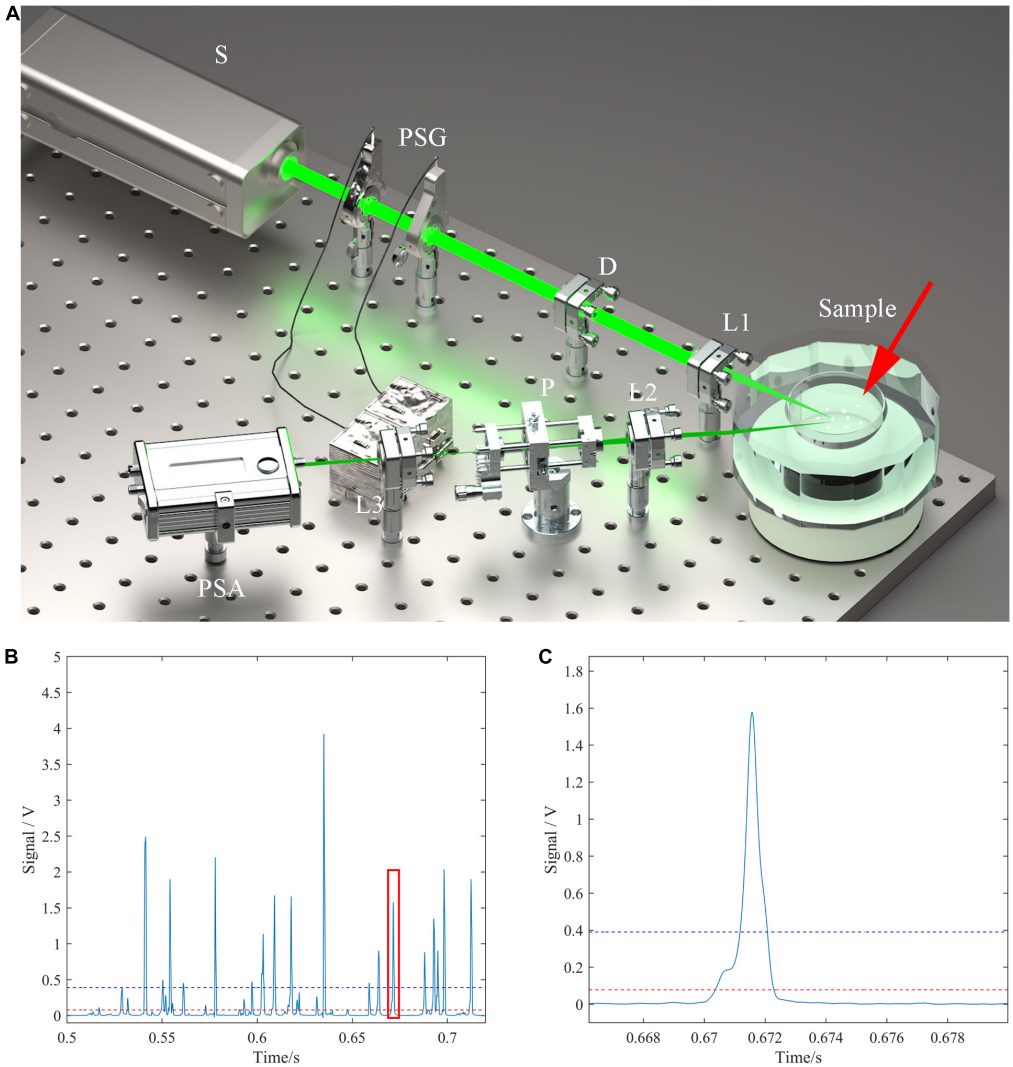

FIGURE 1 | (A) Backward 120° suspended particle measurement system based on polarized light scattering. S, light source; PSG, polarization state generator; D, diaphragm; L, lens; P, pinhole; PSA, polarization state analysis. **(B)** Received signals of the setup. **(C)** The magnification of the temporal pulse. Red line: the background noise; blue line: threshold voltage.

determined by the location of L2 in the optical path and the size of the pinhole. The pinhole size is 100 microns in the setup. The scattering volume is the conjunction volume of the light spot and the detected volume. Finally, we can limit the scattering volume to be <0.01 micro liter (L). If the volume concentration of the particles is $<10^5$ per milliliter, in statistics there is one particle at most in the scattering volume and only its scattered light is received each time. Such that the received signals of the setup are a series of temporal pulses, as shown in **Figure 1B**, which demonstrates the measurement of the individual particles. **Figure 1C** shows one of the temporal pulse, and one can see that the temporal duration of the pulse is around 1 ms.

PSA consists of non-polarization beam splitters to split the parallel light after L3 into four parts. Passing through a 135°-oriented quarter-wave plate with 90° polarizers, a single 0° polarizers, a single 90° polarizers and a single 45° polarizers respectively, the resulting four components of the polarized light are obtained to, respectively, get the left-handed circularly polarized component, horizontal component, vertical component, and 45° linearly polarized component. They are converted by photoelectric converters to voltages, simultaneously recorded by a data acquisition card working at 300,000 samplings per second and then calculated to the Stokes vector. And finally, the polarization parameters (q, u, v) of the light scattered by the individual particles are obtained. And for each sample, more than 3,000 pulses are recorded, and that is, more than 3,000 particles are measured.

Samples

The samples in this work include the river water, 10-micron spherical Polystyrene (PS), microalgae, and 300-mesh MP. The sampling point of the river water was in the Dasha

River, University Town, Shenzhen, Guangdong Province, China. The sampling time was January 13, 2021, with a 0-meter water layer. The 10-micron spherical PS was purchased from Suzhou Nanomicro Technology Co., Ltd., with a diameter of 10 microns. The microalgae include *Scenedesmus Obliquus* (SO), *Prymnesium Parvum* (PP), *Haematococcus Pluvialis* (HP), *Scrippsiella Trochoidea* (ST), *Phaeodactylum Tricornutum* (PT), *Chlorella Vulgaris* (CV), and *Cyanobacteria* (CB). The culture conditions are 2,000 lux light, light-dark cycle 12 h:12 h, medium BG11. 300-mesh MP are industrial plastic raw materials, granular, whose average size is <50 μm. There are six specific types, *Polystyrene* (PS), *Polyethylene* (PE), *Polyethylene Eerephthalate* (PET), *Polypropylene* (PP), *Nylon* (PA), and *Polyvinyl Chloride* (PVC). All of them are purchased from Guangdong Dongguan Huachuang Plastic Chemical Co., Ltd. Note that these types of MP are the most reported in literatures and the most common types in aquatic environments.

In this work, there are three types of samples used, namely microalgae, river water, and microplastics. All samples are stored in a constant temperature environment of 20 ± 2°C. The microalgae are stored in a closed test tube with 2,000 lux light. Each time the river water is sampled from the Dasha river and stored in glass tubes for <1 h before the measurements, the dry microplastics are stored in sealed glass cups and their aquatic suspensions are prepared and then are measured within 1 h. The preservation time of microalgae is around 4 h, the preservation time of river water is around 4 h, and the preservation time of microplastics is 2 days.

Data Processing

We firstly add the raw data of the four channels together to get the total temporal signals. And then we use the median filter to get rid of the random noise, and then get the histogram of the total temporal signals and consider the voltage where the peak value locates as the background. The dark noises of the detectors, the environmental light, scattering of the water, etc., may contribute to the background. We use a threshold which is 10 times of the background. Then we get the pulses whose temporal values are all larger than the threshold, such that the signal-noise-ratio of the pulse is larger than 10. Here each pulse is sampled for multiple times whose number is determined by the pulse's time interval. Till now, we get a series of pulses and then go to find the according data of the four channels. For each pulse in each channel, we average the multiple samplings in the pulse and get the mean value. And then we can use four mean values from the four channels to calculate the Stokes vector.

Linear discrimination analysis is widely used in the field of pattern recognition, such as facial recognition, ship recognition, and other graphics and image recognition (Li and Yuan, 2005). LDA is a dimensionality reduction technology of supervised learning. It projects data to one dimension, so that the projection points of the same type of data are as close as possible, and the distance between the projection center points of different types of data is as large as possible. For the two types of polarization data, the LDA algorithm will calculate an optimal projection function f, to project the three-dimensional polarization data $[q, u, v]$ to the one-dimensional projection parameter X, as shown in Eq. 3.

$$X = f\left(\left[q, u, v\right]\right). \tag{3}$$

Discriminant degree, D, is defined as Eq. 4:

$$D = \frac{2\left|X_1^p - X_2^p\right|}{FWHM_1 + FWHM_2}, \tag{4}$$

where X_1^p and X_2^p are the peak locations of the distribution 1 and distribution 2, respectively; $FWHM_1$ and $FWHM_2$, respectively are the full width at the half maximum (FWHM) of the distribution 1 and distribution 2. D represents the effect of discrimination. The larger is the D, the better is the discrimination effect. Generally, when $D = 2$, there is significant discrimination between these two distributions; when $1 = D < 2$, there is good discrimination between the two distributions; and when $D = 1$, these two distributions cannot be discriminated.

Support vector machine is a classification technique of supervised learning (Shan et al., 2019). The goal of SVM is to find a segmentation surface that can discriminate the two sets of data, while keeping the maximum distance from the sample points of the two sets of data that are closest to the segmentation surface.

RESULTS

River Water and Polystyrene

Experiments were performed on the river water and 10-micron spherical PS separately, and the experimental data of the two were processed by LDA. The projection parameter with the best discrimination between river water and 10-micron spherical PS data is $X = 0.41q - 0.56u - 0.71v$, and this projection parameter is used for LDA processing of other samples and 10-micron spherical PS unless otherwise specified below. As shown in **Figure 2A**, the river water is marked as RW, and the distribution of the river water is located on the left of the figure while that of the 10-micron spherical PS is located on the right, and both are normalized to the maxima of themselves. From **Figure 2A**, one can see that the discrimination is significant between RW and PS where $D = 3.1$.

Then the suspension of the 10-micron spherical PS was added gradually into the river water for mixing experiments, and then the different PS concentration in the mixture were got and each mixture was measured by the setup. The experimental results are shown in **Figure 2B**. All the distributions of X for mixtures are bimodal and each distribution is normalized to its left peak value. According to **Figure 2A**, the left peak of the distributions in **Figure 2B** represents the river water, and the right peak represents the spherical PS. The peak values represent the relative number of particles measured in each mixture. From **Figure 2B** one can see that the right peak value increases with the PS concentration, which is shown in **Figure 2C**. The linearity can be found in **Figure 2C**. These results show that the current method can effectively recognize the special PS (as a specific MP) and retrieve its concentration in the river water (as a type of the natural water body).

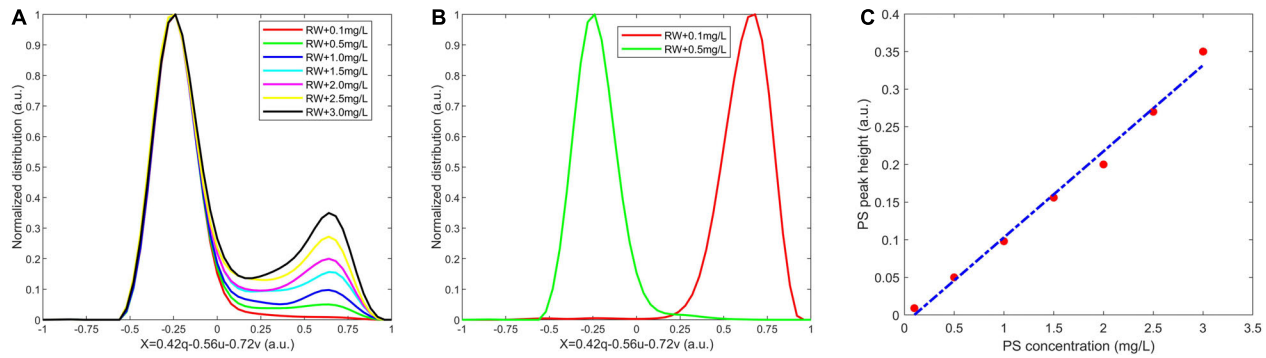

FIGURE 2 | Distribution of river water and 10-micron spherical polystyrene (PS). **(A)** Mixing experiment of river water and different concentrations of 10-micron spherical PS. **(B)** Individual experimental data. **(C)** Quantitative graph of PS with increasing concentration.

Microalgae and Polystyrene

Microalgae are one of the main compositions of suspended particles in water, and play the key role in the aquatic ecosystem. Recently, the interaction between the microalgae and MPs is an extensively discussed topic in current scientific community. In this work, to investigate the discrimination between microalgae and MP, experiments with the single composition samples and mixture were performed on SO and 10-micron spherical PS. The used projection parameter provided by LDA is same with that of river water and 10-micron spherical PS, and the results with the single composition samples are shown in **Figure 3A**. *D* equals to 2.8 which means the discrimination is still significant, and SO is distributed on the left of the figure, while the 10-micron spherical PS is distributed on the right.

Then the suspension of the 10-micron spherical PS was added gradually to SO suspension for mixing experiments as different PS concentrations. The experimental results are shown in **Figure 3B**. And the similar bimodal structure with those in **Figure 2B** can be found, and each distribution is normalized to its left peak value. From **Figure 3A**, the left peak of the distributions in **Figure 3B** represents SO, while the right peak represents the 10-micron spherical PS. The value of the right peak increases with the increase of the 10-micron spherical PS concentration which is shown in **Figure 3C**. And also, one can find the linearity relationship between the PS concentration with the relative amount of the PS in the mixtures. These experiments demonstrate that the current method can detect PS (as a specific MP) in suspended mixtures of microalgae and MP.

To test the discrimination of the microalgae with PS, we conducted more experiments with seven different species of microalgae. And the cultured suspension of each species of the microalgae was successionally added into the 10-micron spherical PS suspension with a concentration of 1 mg/L, and the order of addition was SO, PP, HP, ST, PT, CV, and CB. Distributions of the experimental results are shown in **Figure 3D**, and they are also bimodal. According to **Figures 3A,B**, the left peak of each distribution represents microalgae, the right peak represents 10-micron spherical PS, and each distribution is normalized to its right peak value. From **Figure 3D**, one can find that the seven microalgal species are all significantly discriminated from PS. And the values of the left peaks increase with the continuous addition of microalgae. Note that the location of the left peaks shifts which is quite different from that in **Figures 3A,B**. Since the polarization properties of the seven species are inherently different among them, the polarization parameters of the mixed microalgal group become diverse and the distributions correspondingly change. But still the difference of them with PS is dominant in the mixtures. These results show that our detection method can detect MP in complex scenes including a variety of microalgae.

Microplastic With Different Size, Shape, and Material

Due to the diverse types of MP in water, MP with different size, shape, and material are also investigated in this work. The 10-micron spherical PS and industrial PS plastic raw materials were tested separately. And still using the previous projection parameter, *X*, the experimental results are shown in **Figure 4A** and normalized to their own maxima. We found that the difference between 10-micron spherical PS and 300-mesh (around 45-micron) granular PS is significant, with $D = 2.4$. Because of the irregular shape of the 300-mesh PS, the distribution is relatively divergent while the curve is relatively wide. On the contrary, the distribution of 10-micron spherical PS is uniform while the curve is relatively narrow.

Then the suspension of MP with different materials were measured separately. **Figure 4B** shows the normalized distributions of 300-mesh PS and 300-mesh PP, with the different projection parameter *X*, as **Figure 4A**. And then, we compare the normalized distributions of PP and PET with the same sizes, as shown in **Figure 4C**. This time, the projection parameter is recalculated using LDA since the old one cannot work, which implies that the projection parameter in **Figure 4A** may be exclusively effective for MP with PS material. From **Figure 4C**, the 300-mesh granular PP and PET have a good discrimination, with $D = 1.6$. It shows that our method has the ability to characterize the shape, particle size, material and other properties of MP.

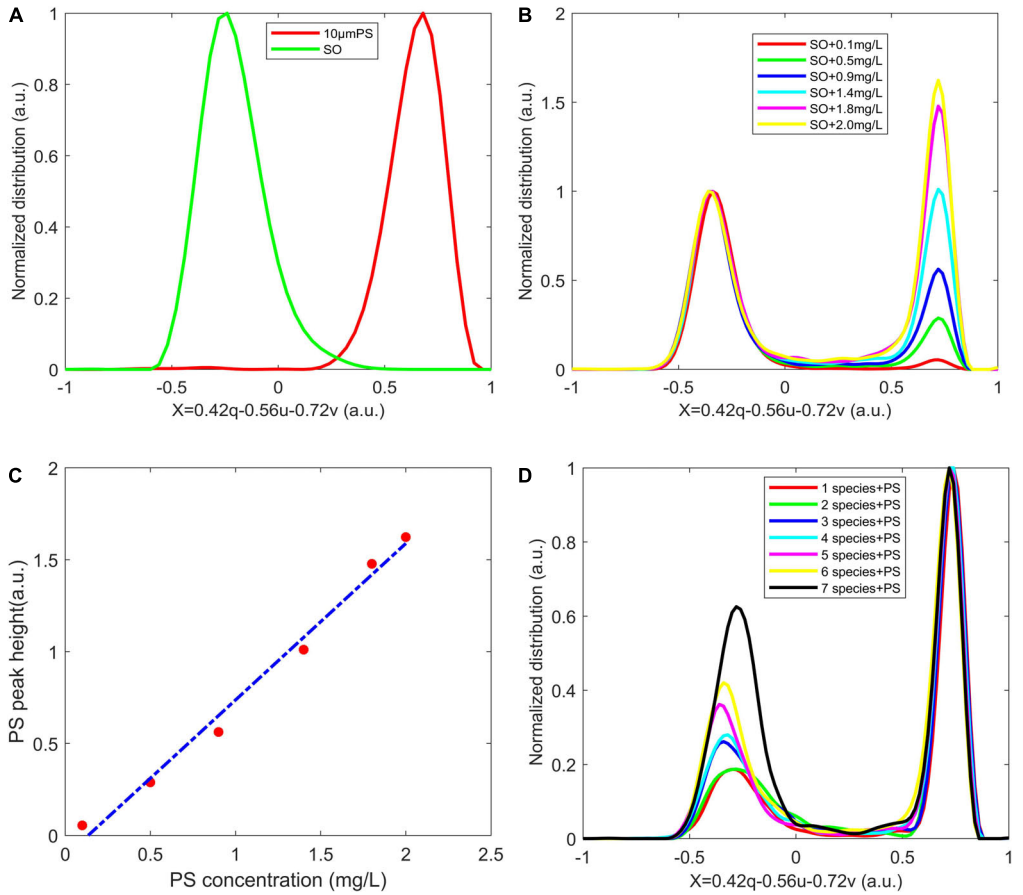

FIGURE 3 | Polarized linear discrimination analysis (LDA) distribution of microalgae and 10-micron spherical polystyrene (PS). **(A)** Separate experiment of *Scenedesmus Obliquus* (SO) and PS. **(B)** Mixed experiment of SO and different concentrations of PS. **(C)** Quantitative graph of PS with increasing concentration. **(D)** Adding SO, *Prymnesium Parvum* (PP), *Haematococcus Pluvialis* (HP), *Scrippsiella Trochoidea* (ST), *Phaeodactylum Tricornutum* (PT), *Chlorella Vulgaris* (CV), and *Cyanobacteria* (CB) in sequence to 1 mg/L PS.

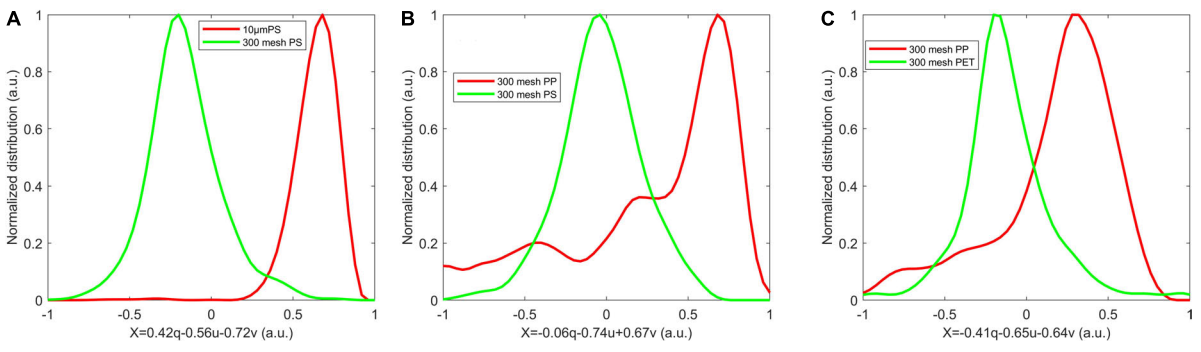

FIGURE 4 | Normalized distributions of different MP. **(A)** 10-micron spherical polystyrene (PS) and 300-mesh PS. **(B)** 300-mesh *Prymnesium Parvum* (PP) and 300-mesh PS. **(C)** 300-mesh PP and 300-mesh *Polyethylene Eerephthalate* (PET).

Microplastic Weathering in the Natural Environment

Microplastic will weather in the natural environment due to the ultra-violet radiation, physical force, chemical erosion and biological fouling (Wei et al., 2021). To detect the diverse types of MP in water, we mixed 6 kinds of 300-mesh MP of PS, PE, PET, PP, PA, PVC together as the mixed MP. We measured the river water (RW1) and the mixed MP separately. And then we soaked the mixed MP in river water for three months to simulate the weathering of MP in the natural environment. Three

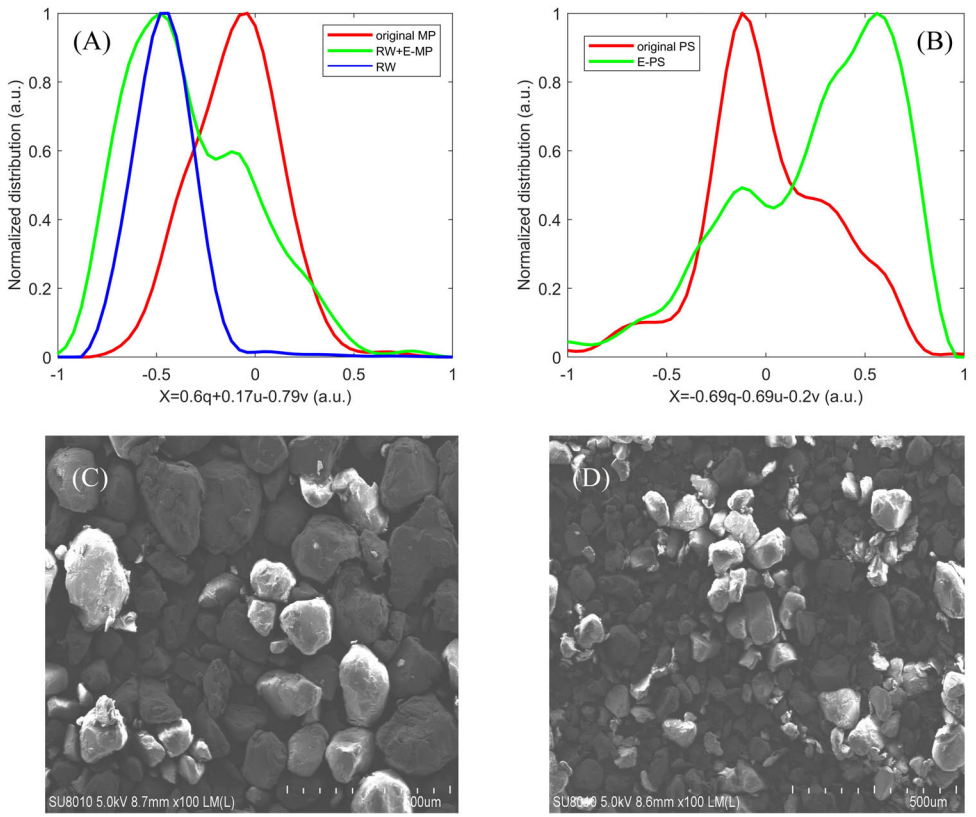

FIGURE 5 | (A) Distribution of Microplastic (MP) in the environment water, the mixed MP, river water (RW), and environmental MP (E-MP). **(B)** Distribution of PS before and after weathering, original polystyrene (PS), environmental PS (E-PS). **(C)** 300-mesh PS before weathering. **(D)** 300-mesh PS after weathering.

months later, experiments were performed on the suspension consisting of river water (RW2) and the environmental MP (E-MP). The experimental results are shown in **Figure 5A**, and each distribution is normalized to its own maximum. It can be found that the distribution of the final suspension (RW2 + E-MP) has a bimodal structure. The position of the left peak is close to the original river water data (RW1), and the position of the right peak is close to the mixed MP data. Based on this, the left peak can be considered as the suspended particulate matter contained in the river water itself while the right peak represents MP.

Note that there is difference between the river waters in **Figure 5A** due to the time interval of 3 months. But the difference between the river water and MP is dominant, and the changes of river waters are relatively trivial. This experiment shows that even if the composition of MP in natural water is complex and weathering may occur, our method can still effectively identify MP. After weathering in the natural environment, the composition of MP is complex and may be compounded with each other. The matching degree of the spectrum of Fourier infrared spectroscopy will be reduced, which lowers the detection accuracy (Shim et al., 2017), but our method is not affected by weathering.

More weathering experiments were conducted to investigate the polarization effects of the size changes of MP. And this time, we filtered the natural water by 0.45 μm filter membrane to remove the particulate matter, and then soaked 300-mesh PS into the water in reagent bottles, and illuminated them by the ultraviolet light. At the same time, we used a magnetic stirrer to stir the suspension with 150 rounds per minute to simulate weathering in the natural environment. Six months later, the environmental PS (E-PS) suspension was obtained, and the experiment of the weathered PS suspension was carried out. And the results are shown in **Figure 5B** and each distribution is normalized to its own maximum. Distributions of both the original PS and E-PS data show the bimodal structures, which indicates the multiple compositions in the samples. After 6 months of weathering, the left peak of the original PS decreases, but the right peak rises, which implies some physical properties of the MP (such as size, shape, etc.) have changed.

A scanning electron microscope was used to observe the PS before and after the weathering and the results are shown in **Figures 5C,D**, respectively. It is observed that in statistics, the particle size of the weathered MP is reduced and it seems that the physical breaking is majority in this kind of weathering (Duan et al., 2021). Based on this, it can be inferred that the left peak in **Figure 5B** represents the PS with large particle sizes, and the right peak represents the PS with small particle sizes. The particle size decreases after weathering corresponding to the decrease in the height of the left peak in **Figure 5B** and the increase in the height of the right peak in **Figure 5B**. It shows that our method can

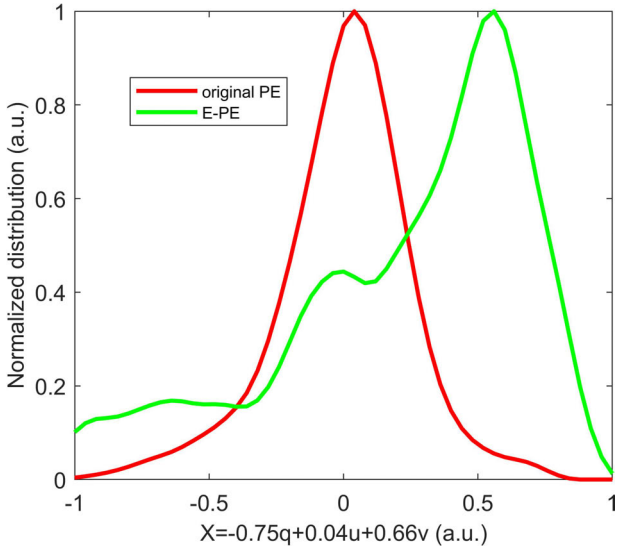

FIGURE 6 | *Polyethylene* (PE) before and after weathering.

characterize the weathering process of MP or provide relevant information about the degree of weathering.

As a common type of MP, we also study the polarization changes during the weathering of PE. The original suspension of the 300-mesh PE particles was measured first. And then it has been soaked in water for six months. After that, experiments were performed on the weathered PE in aquatic environment (E-PE). The results are shown in **Figure 6**. The projection parameter distribution of the original PE is relatively narrower than those of E-PE, which means that the particle size, shape, and surface texture of the original PE are more uniform than those of E-PE. Note that the distribution of E-PE has 2 peaks. The peak near $X_n = 0$ basically overlap with the original PE, indicating that the physical form of some PE remains unchanged or changes little. The two peaks around $X_n$equal to 0.5 and -0.7 are obviously not the original PE, which implies that these two types of particles are newly generated by the weathering. Notably the type of particles whose distribution is peaked around $X_n = 0.5$ is the majority in E-PE, which means the original PE is weathering toward this type of particles. Recalling the weathering of PS in **Figure 5**, PS is weathering toward reducing the sizes. The projection parameters in **Figures 5B**, **6** are different, since the polarization properties of PS and PE are quite different, and in the other wards, polarization parameters have the exclusively discriminant ability to different types of MP.

DISCUSSION

Concentration Calibration

The concentration of MPs in water is one of the most concerned information. To explore the ability of our method to retrieve the concentration of MP in water, we performed experiments on suspensions containing different concentrations of 10-micron spherical PS. For each concentration, we measured the samples for some time (larger than 10 min) which consisted of the succeeding time intervals, to evaluate the detected signals of MP per unit time. The so-called "unit time" is the fixed and minimal time interval in the data acquisition, and in this work, it's 10 s. The relationship between the number of detected pulses per unit time and MP concentration was are got and shown in **Figure 7**.

It can be found from **Figure 7A** that when the concentration is in the range of 1−10μg/L, the pulse number per unit time does not obviously change with the increase of the PS concentration. However, when the concentration is in the range of 0.01–8 mg/L, as shown in **Figures 7B,C**, the pulse number per unit time increases with the increase of the PS concentration. There is a linear relationship between the pulse number per unit time with the PS concentration. A linear regression algorithm is used to fit the data in **Figures 7B,C**. When the PS concentration is in the range of 0.01–0.1 mg/L, the determination coefficient is 0.87. When the concentration is in the range of 0.1–10 mg/L, the determination coefficient is larger than 0.99. This linear relationship between the pulse number per unit time with the PS concentration is the PS concentration calibration relationship, shown as the dashed line in **Figures 7B,C**.

Recalling that the proposed method in this work measures the individual suspended particles, each particle passing through the scattering volume will generate a corresponding scattering pulse. Therefore, the pulse number per unit time should increase with the particle concentration. However, the linearity indicates the more direct and deep relationship between them than the expectation, which implies the possibility to retrieve the PS concentration by measuring the pulse number per unit time. At the same time, from the error bar of **Figure 7C**, we can find that the relative error of each measurement is small, and the data measurement is relatively stable.

These results show that our method can effectively detect the concentration of MP. The pulse number per unit time has a linear relationship with the concentration of MP, and the lower limit of detection concentration is about 0.01 mg/L.

Polystyrene Concentration in Mixture and the Pulse Number Per Unit Time

To further testify the ability of our method to detect the concentration of MP in natural water, we investigate the data in **Figures 2B**, **3B**. Since LDA can give the optimal projection of the multiple dimensions data to one dimension, it is used to visually present the difference of the physical features between two samples in above results. However, SVM is more convenient to build the classifier to classify the specific particles from the suspensions. Firstly, the SVM processing is used to build a classifier to classify the river water and 10-micron spherical PS. The dataset is the experimental data of separate experiments of them. Seventy percentage of the dataset is used for the classifier training, and thirty percentage of the dataset is used for the classifier testing. The accuracy obtained by the test is 98.55%, which indicates the classifier is accurate and effective. Secondly, we use this classifier to classify the experimental data of the quantitative mixing experiment of river water and 10-micron

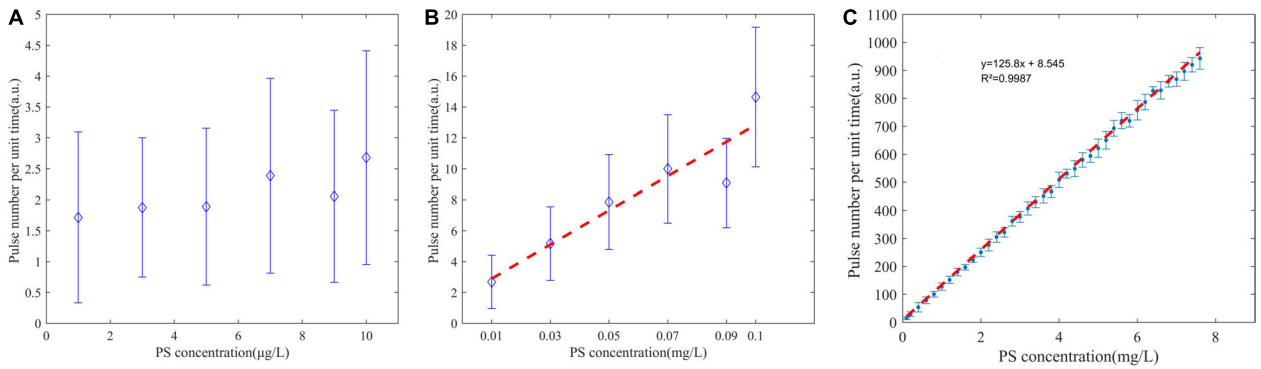

FIGURE 7 | The relationship between the concentration of 10-micron spherical polystyrene (PS) and the pulse number per unit time. **(A)** The pulse number per unit time when the concentration is in the range of 1–10 μg/L. **(B)** The pulse number per unit time when the concentration is in the range of 0.01–0.1 mg/L. **(C)** The pulse number per unit time when the concentration is in the range of 0.1–8 mg/L.

spherical PS to get the PS number, and then we divide the PS number by time duration to obtain the PS number per unit time. The relationship between the PS number per unit time and PS concentration is shown in **Figure 8A**. It can be found that there is a linear relationship between them, and the determination coefficient is larger than 0.99.

We repeat the above operation for the experimental data of SO and spherical PS, the accuracy of the testing is 98.74%, and finally the new SVM classifier works excellently. The PS pulse number per unit time and the PS concentration are shown in **Figure 8B**, which also has a linear relationship between them and the determination coefficient is larger than 0.99. It showed that the proposed method can not only detect the presence of PS but also the concentration of PS in the suspension with complex compositions. However, we note that the linear relationship in **Figures 8A,B** are slightly different, and both of them are different from the PS concentration calibration relationship. It is necessary to investigate the generalization of the linear relationship between the PS number per unit time and the PS concentration. So, we merge the data of **Figures 8A,B** together and draw them with the PS concentration calibration relationship in **Figure 8C**. It can be found that the PS number per unit time vs. the PS concentration, in two experimental data of the mixed samples are distributed near the PS concentration calibration relationship. The determination coefficient is 0.89 for the data of mixtures of river water and PS, and the determination coefficient is 0.98 for the data of mixtures of microalgae and PS. **Figure 8C** demonstrates that the PS concentration calibration relationship has good generalization in predicting the PS concentration in suspensions with the complex compositions.

Identification of Specific Microplastic

Since PP and PET are two of the most reported MP in related literatures (Li et al., 2019), we explore the ability of the proposed method to identify them from the mixture of multiple types of MP. We firstly adjust the polarization state of the incident light to the right-handed circular polarization state. And then we do experiments on 6 types of 300-mesh MP (i.e., PS, PET, PP, PE, PVC, PA). Comparing the measured polarization parameters of PP with the other 5 MP by LDA, the result is shown in **Figure 9A**. D = 1.38, which is a good discrimination. If we transform the incident polarization state to the vertically linear polarization. The experimental result of PET and the other five types of MP is shown in **Figure 9B**. D = 1.01, which is also a good discrimination. Note that there are some fluctuations in the distributions in **Figure 9**. Considering the number of the measured particles are at least 3,000 which is enough for the analysis, then these fluctuations may originate from the multiple compositions in the mixed MP samples.

Figure 9 tells that the polarization parameters can identify PP and PET from the set of multiple types of MP. However, the incident polarization state changes for the identification of the different MP. Note that the measured polarization parameters are originated from the Stokes vector, and only include the partial polarization properties of the particles. This means that under the illumination of the incident light with the different polarization states, we measure the different parts of the polarization properties, and some of them can be effective to discriminate PP or PET from the multiple types of MP. This makes it possible that we just need to illuminate the sample with the specified polarized light and measure the polarization parameters, and then we can identify the concerned type of MP.

Polarization theory says that the scattering of the individual particle changes the polarization state of the incident light, S_{in}, to the polarization state of the scattered light S_{out}, which carries the physical polarization property of the particle. Traditionally, the relationship between the polarization states of the incident light and the scattered light is Mueller matrix, M, which is a 4 × 4 matrix to describe the polarization property of the particle, as shown in Eqs. 5, 6.

$$M = \begin{bmatrix} m_{11}, m_{12}, m_{13}, m_{14} \\ m_{21}, m_{22}, m_{23}, m_{24} \\ m_{31}, m_{32}, m_{33}, m_{34} \\ m_{41}, m_{42}, m_{43}, m_{44} \end{bmatrix}, \tag{5}$$

$$S_{out} = M \times S_{in}. \tag{6}$$

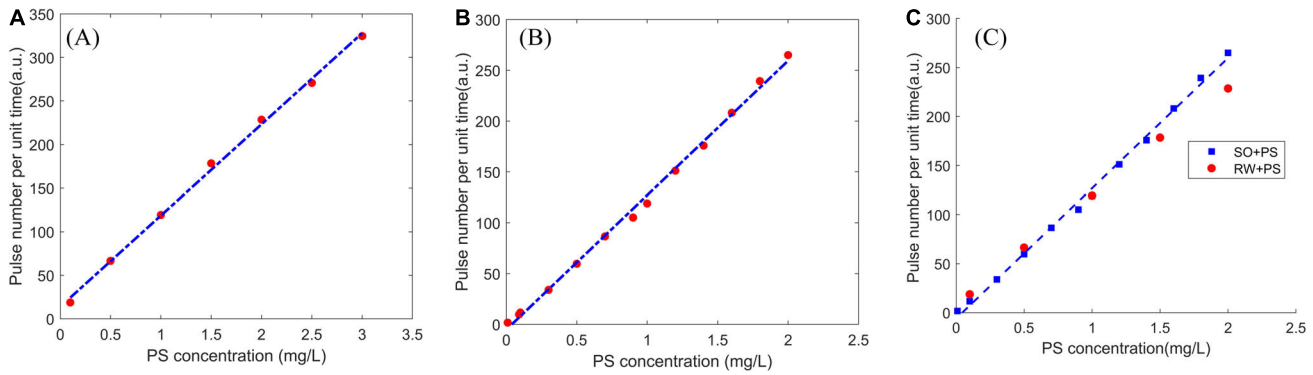

FIGURE 8 | The relationship between the polystyrene (PS) concentration and the pulse number per unit time in panel **(A)** the data of the mixtures of the river water and different concentrations of PS, and in panel **(B)** the data of the mixtures of *Scenedesmus Obliquus* (SO) and different concentrations of PS. **(C)** The PS concentration calibration relationship and the experimental data in panels **(A,B)**.

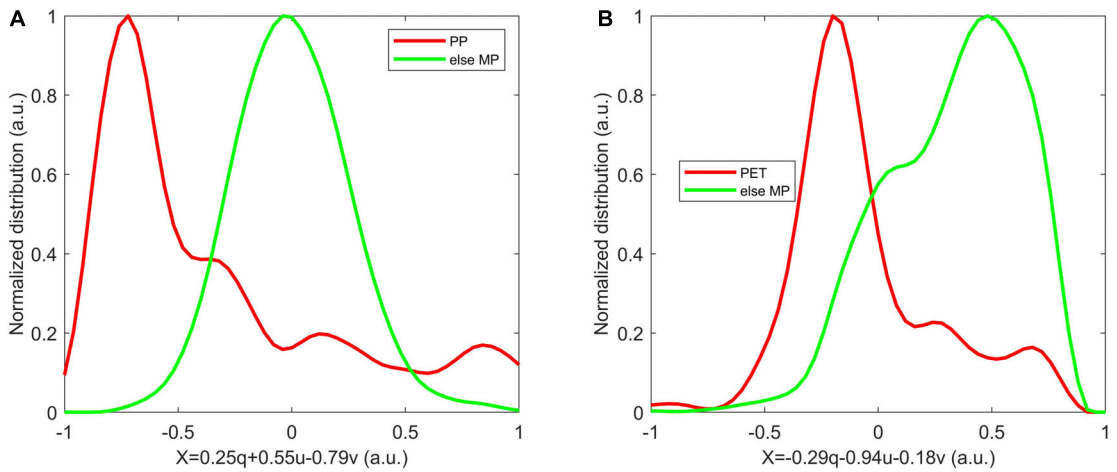

FIGURE 9 | (A) *Prymnesium Parvum* (PP) and other five types of microplastics (MPs). **(B)** *Polyethylene Eerephthalate* (PET) and other five types of MPs.

In this work, since the incident light is 135° linearly polarized, $S_{in} = [1, 0, -1, 0]^{\mathrm{T}}$. Then from Eqs. 5, 6, we get,

$$S_{out} = \begin{bmatrix} m_{11} - m_{13} \\ m_{21} - m_{23} \\ m_{31} - m_{33} \\ m_{41} - m_{43} \end{bmatrix}. \quad (7)$$

So, the polarization parameters, q, u, v calculated from Eqs. 1, 2, and their derivatives are determined by the element differences of the first and third columns of Mueller matrix.

Basically, LDA gives the optimal linear combination of q, u, v, that is, $X = a * q + b * u + c * v$, under which the distributions of the two samples differ each other most. The coefficients, a, b, c, are just the weight of q, u, v, and are also the weight of the elements of S_{out} in Eq. 7. In principle, the different X in **Figures 2–6** are selected to enhance the difference between the two samples and suppress the similar parts by adjusting a, b, c.

Alternatively, we can also find the way to discriminate the two samples by changing the incident polarization S_{in} and fixing a, b, c. In this case, we require PSG can generate the wanted polarization state of light, which needs the sophisticated design of PSG but has the advantage of the fixed X. According to Eq. 6, this way is basically different from the above one and it optimally combines the different elements of Mueller matrix to select out X.

Here we know that the difference between the samples is originated from their Mueller matrix which is fundamentally determined by the physical polarization properties, such as size, shape, structures, materials, etc. Previous researchers have reported some findings about the Mueller matrix elements and their combination which can effectively characterize the physical properties of the particles. For example, Volten et al. (1998) have shownm_{12}/m_{11} is sensitive to the material and gas vacuole structure. Van De Merwe et al. (2004) find m_{34}/m_{11} can determine a large size parameter range for spherical or randomly oriented rod-shaped particles. The m_{22}/m_{11} is always related to the sphericity of the particles (Ossikovski and Arteaga, 2019). Svensen et al. (2011) have found that the combined elements, $m_{12}m_{11}$, $m_{33}m_{44}$ have noticeable differences between different algae species, because of their different inner structures and

refractive indices. Li et al. (2021) recently have reported the combined elements of Mueller matrix are able to discriminate the particles with the different materials and microstructures.

These results and analysis encourage us that if we measure the Mueller matrix of the polarization properties of MP, we can much easily to achieve the discrimination of the different types of MP. Generally, Mueller matrix polarimetry needs multiple measurements with different incident polarization states. For the suspended MP particles in water, they are instantaneously changing and passing through the scattering volume in very short time interval. So, it's still challenging to the community to measure the Mueller matrix of the suspended MP but it deserves to be considered in future.

In this work, we firstly use the 10-micro spherical PS to show the excellent discrimination between it with the river water and the microalgae by using our method. And then we present the ability of the method to discriminate the MPs (including PS) with different size and materials, and to characterize the MP changes originated from the weathering in the environments. Also, during the concentration calibration, we use the PS samples. However, the PS particles is just used as the standard MP to show the ability and feasibility of the proposed method to *in-situ* detect them in water. The potential of the method should not be limited to PS particles. It should be noted that by using the polarization parameters, the mixed MP can effectively be discriminated from the river water before and after the environmental weathering, and especially the compositions of PE sample can be also characterized during the weathering. Indeed, it is challenging to identify all types of MP in water by the current method, but the effort and expectation are still deserved to pay for its realization in future by some sophisticated methods or Mueller matrix polarimetry.

CONCLUSION

An *in-situ* method based on polarized light scattering is proposed to detect the microplastics (MP) in water. The scattered polarization parameters of individual particles are *in-situ* measured in aquatic suspensions. The illumination polarization state of the incident light can be adjusted to achieve the best discrimination of the different MPs. The polarization parameters of microalgae, natural water bodies and 10-micron spherical PS have a significant discrimination. MP in the mixture of a variety of microalgae and natural water samples therefor can be effectively identified. Moreover, the present method could be used in distinguishing MP samples with different size, shape and material. For example, 300-mesh granular PS obtained by grinding has a remarkable discrimination from the 10-micron spherical PS; and the 300-mesh granular PP has a good discrimination from PET. It is interesting that the weathering of MP is observed and the polarization parameters can still detect MP from the river water after several months' soaking. The different compositions of the weathered MP can be characterized by the polarization parameters which is confirmed by PS and PP samples. Finally, we successfully identify the PP and PET from the multiple types of MP, which is encouraging to identify the specific MP with well-designed illumination polarization state of light. The concentration is calibrated by the 10-micron spherical PS samples. The low limit of the detected concentration can lower to 0.01 mg/L. The linear relationship of the concentration with the pulse number per unit time is well-generalized and works effectively for the former experiments. These results demonstrate the capability of the proposed method to *in-situ* detect the MP in water, which promises the application in water quality sensing and monitoring.

DATA AVAILABILITY STATEMENT

The original contributions presented in the study are included in the article/supplementary material, further inquiries can be directed to the corresponding author.

AUTHOR CONTRIBUTIONS

RL conceived the project aim. TL, SY, and RL designed the methodology. YH collected and obtained the samples. TL and SY carried out the sample processing work and the analysis. TL led the manuscript writing. XZ, RL, and HM revised the analyses and manuscript. All the authors contributed critically to the drafts and gave final approval for publication.

FUNDING

This work was supported by the Key-Area Research and Development Program of Guangdong Province (2020B1111040001), the National Key Project of Research and Development Program of China (2018YFC1406600), the National Natural Science Foundation of China (NSFC) (41527901 and 61975088), and the Science and Technology Project of Shenzhen Grant (JCYJ20160818143050110).

ACKNOWLEDGMENTS

We thank the staff at the Guangdong Research Center of Polarization Imaging and Measurement Engineering Technology as well as Yihan Shi, Jincai Dai, and Yong Wang for excellent assistance during the work.

REFERENCES

Amaral-Zettler, L. A., Zettler, E. R., and Mincer, T. J. (2020). Ecology of the plastisphere. *Nat. Rev. Microbiol.* 18, 139–151. doi: 10.1038/s41579-019-0308-0

Auta, H. S., Emenike, C. U., and Fauziah, S. H. (2017). Distribution and importance of microplastics in the marine environment: a review of the sources, fate, effects, and potential solutions. *Environ. Int.* 102, 165–176. doi: 10.1016/j.envint.2017.02.013

Boss, E., and Pegau, W. S. (2001). Relationship of light scattering at an angle in the backward direction to the backscattering coefficient. *Appl. Opt.* 40, 5503–5507. doi: 10.1364/AO.40.005503

Chami, M. (2007). Importance of the polarization in the retrieval of oceanic constituents from the remote sensing reflectance. *J. Geophys. Res.* 112:C05026. doi: 10.1029/2006JC003843

Duan, J., Bolan, N., Li, Y., Ding, S., Atugoda, T., Vithanage, M., et al. (2021). Weathering of microplastics and interaction with other coexisting constituents in terrestrial and aquatic environments. *Water Res.* 196:117011. doi: 10.1016/j.watres.2021.117011

Eriksen, M., Mason, S., Wilson, S., Box, C., Zellers, A., Edwards, W., et al. (2013). Microplastic pollution in the surface waters of the Laurentian Great Lakes. *Mar. Pollut. Bull.* 77, 177–182. doi: 10.1016/j.marpolbul.2013.10.007

Ghosh, N., and Vitkin, I. A. (2011). Tissue polarimetry: concepts, challenges, applications, and outlook. *J. Biomed. Opt.* 16:110801. doi: 10.1117/1.3652896

Golwala, H., Zhang, X., Iskander, S. M., and Smith, A. L. (2021). Solid waste: an overlooked source of microplastics to the environment. *Sci. Total Environ.* 769, 144581. doi: 10.1016/j.scitotenv.2020.144581

Kappler, A., Fischer, D., Oberbeckmann, S., Schernewski, G., Labrenz, M., Eichhorn, K. J., et al. (2016). Analysis of environmental microplastics by vibrational microspectroscopy: FTIR, Raman or both? *Anal. Bioanal. Chem.* 408, 8377–8391. doi: 10.1007/s00216-016-9956-3

Lenz, R., Enders, K., Stedmon, C. A., Mackenzie, D. M. A., and Nielsen, T. G. (2015). A critical assessment of visual identification of marine microplastic using Raman spectroscopy for analysis improvement. *Mar. Pollut. Bull.* 100, 82–91. doi: 10.1016/j.marpolbul.2015.09.026

Li, J., Lusher, A. L., Rotchell, J. M., Deudero, S., Turra, A. I, Brate, L. N., et al. (2019). Using mussel as a global bioindicator of coastal microplastic pollution. *Environ. Pollut.* 244, 522–533. doi: 10.1016/j.envpol.2018.10.032

Li, J. J., Wang, H. J., Liao, R., Wang, Y., Liu, Z. D., Zhuo, Z. P., et al. (2021). Statistical Mueller matrix driven discrimination of suspended particles. *Opt. Lett.* 46, 3645–3648. doi10.1364/OL.433870

Li, M., and Yuan, B. (2005). 2D-LDA: a statistical linear discriminant analysis for image matrix. *Pattern Recognit. Lett.* 26, 527–532. doi: 10.1016/j.patrec.2004.09.007

Liao, R., Li, Q., and Mao, X. (2019). "A prototype for detection of particles in sea water by using polarize-light scattering," in *Proccedings of the OCEANS 2019–Marseille*, (Marseill), 1–4. doi: 10.1109/OCEANSE.2019.8867414

Mai, L., Bao, L. J., Shi, L., Wong, C. S., and Zeng, E. Y. (2018). A review of methods for measuring microplastics in aquatic environments. *Environ. Sci. Pollut. Res. Int.* 25, 11319–11332. doi: 10.1007/s11356-018-1692-0

Ossikovski, R., and Arteaga, O. (2019). Complete Mueller matrix from a partial polarimetry experiment: the nine-element case. *J. Opt. Soc. Am.Opt. Image Sci. Vision* 36, 403–415. doi: 10.1364/JOSAA.36.000403

Sadri, S. S., and Thompson, R. C. (2014). On the quantity and composition of floating plastic debris entering and leaving the Tamar Estuary. *South. Engl. Mar. Pollut. Bull.* 81, 55–60. doi: 10.1016/j.marpolbul.2014.02.020

Saeed, T., Al-Jandal, N., Al-Mutairi, A., and Taqi, H. (2020). Microplastics in Kuwait marine environment: results of first survey. *Mar. Pollut. Bull.* 152:110880. doi: 10.1016/j.marpolbul.2019.110880

Shan, J., Zhao, J., Zhang, Y., Liu, L., Wu, F., and Wang, X. (2019). Simple and rapid detection of microplastics in seawater using hyperspectral imaging technology. *Anal. Chim. Acta* 1050, 161–168. doi: 10.1016/j.aca.2018.11.008

Shim, W. J., Hong, S. H., and Eo, S. E. (2017). Identification methods in microplastic analysis: a review. *Anal. Methods* 9, 1384–1391. doi: 10.1039/C6AY02558G

Song, Y. K., Hong, S. H., Jang, M., Han, G. M., Rani, M., Lee, J., et al. (2015). A comparison of microscopic and spectroscopic identification methods for analysis of microplastics in environmental samples. *Mar. Pollut. Bull.* 93, 202–209. doi: 10.1016/j.marpolbul.2015.01.015

Sun, M., He, H., Zeng, N., Du, E., Guo, Y., Liu, S., et al. (2014). Characterizing the microstructures of biological tissues using Mueller matrix and transformed polarization parameters. *Biomed. Opt. Express* 5, 4223–4234. doi: 10.1364/BOE.5.004223

Svensen, O., Stamnes, J. J., Kildemo, M., Aas, L. M. S., Erga, S. R., and Frette, O. (2011). Mueller matrix measurements of algae with different shape and size distributions. *Appl. Opt.* 50, 5149–5157. doi: 10.1364/AO.50.005149

Van De Merwe, W. P., Czégé, J., Milham, M. E., and Bronk, B. V. (2004). Rapid optically based measurements of diameter and length for spherical or rod-shaped bacteria in vivo. *Appl. Opt.* 43, 5295–5302. doi: 10.1364/AO.43.005295

Vianello, A., Boldrin, A., Guerriero, P., Moschino, V., Rella, R., Sturaro, A., et al. (2013). Microplastic particles in sediments of Lagoon of Venice, Italy: first observations on occurrence, spatial patterns and identification. *Estuar. Coast. Shelf Sci.* 130, 54–61. doi: 10.1016/j.ecss.2013.03.022

Volten, H., De Haan, J., Hovenier, J. W., Schreurs, R., Vassen, W., Dekker, A. G., et al. (1998). Laboratory measurements of angular distributions of light scattered by phytoplankton and silt. *Limnol. Oceanogr.* 43, 1180–1197. doi: 10.4319/lo.1998.43.6.1180

Wang, Y., Liao, R., Dai, J., Liu, Z., Xiong, Z., Zhang, T., et al. (2018). Differentiation of suspended particles by polarized light scattering at 120 degrees. *Opt. Express* 26, 22419–22431. doi: 10.1364/OE.26.022419

Wei, X. F., Bohlen, M., Lindblad, C., Hedenqvist, M., and Hakonen, A. (2021). Microplastics generated from a biodegradable plastic in freshwater and seawater. *Water Res.* 198:117123. doi: 10.1016/j.watres.2021.117123

Yin, K., Wang, D., Zhao, H., Wang, Y., Guo, M., Liu, Y., et al. (2021). Microplastics pollution and risk assessment in water bodies of two nature reserves in Jilin Province: correlation analysis with the degree of human activity. *Sci. Total Environ.* 799:149390. doi: 10.1016/j.scitotenv.2021.149390

Yu, Q., Hu, X., Yang, B., Zhang, G., Wang, J., and Ling, W. (2020). Distribution, abundance and risks of microplastics in the environment. *Chemosphere* 249:126059. doi: 10.1016/j.chemosphere.2020.126059

Yu, S., Dai, J., Liao, R., Chen, L., Zhong, W., Wang, H., et al. (2021). Probing the nanoplastics adsorbed by microalgae in water using polarized light scattering. *Optik* 231:166407. doi: 10.1016/j.ijleo.2021.166407

Zhang, S., Wang, J., Liu, X., Qu, F., Wang, X., Wang, X., et al. (2019). Microplastics in the environment: a review of analytical methods, distribution, and biological effects. *TrAC Trends Anal. Chem.* 111, 62–72. doi: 10.1016/j.trac.2018.12.002

Conflict of Interest: The authors declare that the research was conducted in the absence of any commercial or financial relationships that could be construed as a potential conflict of interest.

Publisher's Note: All claims expressed in this article are solely those of the authors and do not necessarily represent those of their affiliated organizations, or those of the publisher, the editors and the reviewers. Any product that may be evaluated in this article, or claim that may be made by its manufacturer, is not guaranteed or endorsed by the publisher.

frontiers in Marine Science

ORIGINAL RESEARCH
published: 26 October 2021
doi: 10.3389/fmars.2021.770606

Increased Cu(II) Adsorption Onto UV-Aged Polyethylene, Polypropylene, and Polyethylene Terephthalate Microplastic Particles in Seawater

*Xiaoxin Han[1,2], Rolf D. Vogt[3], Jiaying Zhou[1], Boyang Zheng[1], Xue Yu[1], Jianfeng Feng[1] and Xueqiang Lu[1]**

[1] Tianjin Key Laboratory of Environmental Technology for Complex Trans-Media Pollution, Tianjin International Joint Research Center for Environmental Biogeochemical Technology, College of Environmental Science and Engineering, Nankai University, Tianjin, China, [2] Changchun Bureau of Ecology and Environment, Changchun, China, [3] Centre for Biogeochemistry in the Anthropocene, Department of Chemistry, University of Oslo, Oslo, Norway

OPEN ACCESS

Edited by:
Xiaoshan Zhu, Tsinghua University, China

Reviewed by:
Chun Ciara Chen, Shenzhen University, China
Zhenghua Duan, Tianjin University of Technology, China

***Correspondence:**
Xueqiang Lu
luxq@nankai.edu.cn

Specialty section:
This article was submitted to Marine Pollution, a section of the journal Frontiers in Marine Science

Received: *04 September 2021*
Accepted: *24 September 2021*
Published: *26 October 2021*

Citation:
Han X, Vogt RD, Zhou J, Zheng B, Yu X, Feng J and Lu X (2021) Increased Cu(II) Adsorption Onto UV-Aged Polyethylene, Polypropylene, and Polyethylene Terephthalate Microplastic Particles in Seawater. Front. Mar. Sci. 8:770606. doi: 10.3389/fmars.2021.770606

Environmental effects of microplastic are rather due to their adsorption capacity of contaminants than themselves. Aging is a key factor influencing adsorption properties of environmental microplastics. In order to clarify this influence, polyethylene (PE), polypropylene (PP), and polyethylene terephthalate (PET) microplastics with particle sizes of <0.9 mm, 0.9–2 mm, and 2–5 mm were artificially aged in seawater for 12 months. This enabled an assessment of the change in Cu(II) adsorption capacity to the microplastics particles under aging. According to the FTIR spectra, fresh microplastics were oxidized during the UV induced aging process. The adsorption capacities of microplastic were positively correlated with their aging time. After 12-months aging, the amount of Cu(II) adsorbed to the aged microplastics was 1.45–2.92 times higher than on the fresh microplastic particles. For PP and PET, the aging effect increased with decreasing size of the microplastic particles. In the case of PE, particles with the medium particle size (0.9–2 mm) had the strongest aging effect.

Keywords: microplastics, aging effect, adsorption, Cu(II), particle sizes

INTRODUCTION

Plastics bring great convenience to daily life, but poses also potential risks to the environment. Annual global production of plastic in 2018 was 360 million tons (Plastic Europe, 2019). Only 9% of the plastic waste is recycled. Most of it is thus dumped into landfills or just disposed of. Since plastic can take between 50 to more than 200 years to decompose, it eventually accumulates in the environment (Barnes et al., 2009; Jambeck et al., 2015; Geyer et al., 2017). It was estimated that about 4.8–12.7 million tons of plastic waste flows into the marine environment each year (Jambeck et al., 2015). If the current practice continues the weight of plastics in the ocean will be greater than

the weight of fish by 2050 (World Economic Forum, 2020). Plastic waste accounts for 60–80% of all marine debris (Wang et al., 2018), and about 92% of all plastic fragments in the marine environment are in the form of microparticles (Wang et al., 2019).

Microplastics may adsorb pollutants due to their small size, large specific surface area and high hydrophobicity. Although microplastics are likely not toxic in themselves, this adsorption of contaminants to the microplastic particles may cause them to serve as a carrier or transport vector of toxic compounds in the environment. Considering the magnitude of microplastic particles in the marine environment this may significantly alter the fate and effect of pollutants in the environment (Wang et al., 2017). Heavy metals on microplastics collected from river sediments are found to have originated from the surrounding environment (Deheyn and Latz, 2006). Adsorption properties of microplastics will change over time in the environmental mainly due to exposure to solar radiation and physical weathering by e.g., wind or wave chopping. This aging causes modifications to the physicochemical properties of microplastic surfaces. Aged microplastics are found to adsorb more heavy metals than fresh microplastics (Deheyn and Latz, 2006; DeForest et al., 2007; Holmes et al., 2014; Turner and Holmes, 2015). For example, Holmes et al. (2014) reported that the adsorption capacity of beached plastic pellets was at least an order of magnitude greater than that of virgin pellets (Holmes et al., 2014). Photo-oxidation through UV exposure changes the physical morphology as well as the functional groups on the plastic polymer surfaces. Despite the potentially important role of microplastics in governing fate and effect of contaminants in the environment, there are few detailed studies on the photolytic aging process and how this aging affects metal adsorption capacity of microplastics with time in seawater.

In this article the UV aging effect on polyethylene (PE), polypropylene (PP), and polyethylene terephthalate (PET), the three most consumed types of plastics in the world[1,2,3], are studied in laboratory experiments. Copper (Cu), which may cause toxic effects on humans and represent an ecological risk (Fu et al., 2017), is selected as target contaminant to explore the heavy metal adsorption capacity of microplastics with different degree of aging. The effect of particle size of the microplastics on the Cu adsorption capacity is also assessed.

MATERIALS AND METHODS

Chemicals and Microplastic Materials

$Cu(NO_3)_2$ was obtained from Shanghai Aladdin Bio-Chem Technology Corporation (Shanghai, China). HNO_3 was purchased from Bohua Chemical Reagent Corporation (Tianjin, China). NaCl, Na_2SO_4, KCl, $NaHCO_3$, KBr, H_3BO_3, NaF, $MgCl_2{\cdot}6H_2O$, $CaCl_2{\cdot}2H_2O$, and $SrCl_2{\cdot}6H_2O$, which are all used to prepare artificial seawater, were acquired from Macklin Bio-Chem Technology Corporation (Shanghai, China). All chemicals were analytical grade or higher purity. PE, PP, and PET pellets were procured from Yousuo Chemical Technology Corporation (Shandong, China).

Microplastic Aging Experiment

The aging experiment of microplastics was carried out in the laboratory using UV radiation and artificial seawater. PE, PP, and PET microplastics with particle sizes of 5 mm were crushed using a high-speed crusher. The crushed microplastic particles were then sequentially sieved through 20-, 10-, and 4- mesh screens in order to separate the particle sizes <0.9 mm, 0.9–2 mm, and 2–5 mm. The prepared size fractions of microplastics were submerged by artificial seawater in petri dishes with a diameter of 20 cm. The petri dishes were placed about 3 cm under two parallel placed UV-340 mm lamps with irradiation intensity of 29.80 J $s^{-1}{\cdot}m^{-2}$. Artificial seawater was prepared according to the method by Kester et al. (1967). The simulated aging time was estimated by the following equation:

$$n = (E_0 \times 365\ \mathrm{d} \times 24\ \mathrm{h} \times 3600\ \mathrm{s})/E_1 \quad (1)$$

In which n is the ratio of radiation intensity between the experiment and ambient conditions, E_0 ($J{\cdot}s^{-1}{\cdot}m^{-2}$) is irradiation intensity of UV lamps, and E_1 (J m^{-2}) is annual outdoor ultraviolet (UV) radiation. In the Tianjin area, which is the location of the experiment, the yearly UV radiation is 178.85 × 106 J m^{-2} (Li, 1999), yielding an n value of 5.2545. The microplastics were taken out after being exposed to UV radiation for 556, 1,112, and 1,668 h, which are equivalent to 4, 8, and 12 months of natural aging, respectively. The artificially aged microplastics were rinsed several times with distilled water and dried before storage in the dark until characterized or used for the adsorption experiments.

Characterization by Fourier Transformed Infrared

Functional groups on the surface of PE, PP, and PET microplastics before and after aging were characterized by attenuated total reflection Fourier transformed infrared spectroscopy (ATR-FTIR, Bruker Tensor II, Germany). The ATR-FTIR is a single beam, percent transmission technique that runs 40 scans per sample at a resolution of 0.4 cm^{-1} over the wavelength range from 4,000 to 350 cm^{-1}.

Adsorption Experiments

The fresh and aged PP, PE, and PET microplastics with particle size of <0.9 mm, 0.9–2 mm, and 2–5 mm were used to conduct the Cu(II) adsorption experiments. The experiments were carried out at room temperature in centrifuge tubes, each containing 0.5 g microplastics and 50 mL solutions of Cu(II) with concentration of 5 mg L^{-1}. The adsorption time was 240 h, which was the time required to assure equilibrium based on a pre-experiment. All experiments were conducted in duplicate. After

[1]The Essential Chemical Industry (ECI): Poly(ethene) (Polyethylene) [OL]. [2018-09-06]. http://www.essentialchemicalindustry.org/polymers/polyethene.html.

[2]The Essential Chemical Industry (ECI): Poly(propene) (Polypropylene) [OL]. [2018-09-06]. http://www.essentialchemicalindustry.org/polymers/polypropene.html.

[3]The Essential Chemical Industry (ECI): Polyesters [OL]. [2018-09-06]. http://www.essentialchemicalindustry.org/polymers/polyesters.html.

adsorption, the microplastics were separated from the solution by filtration using filter paper with a pore size of 15–20 μm. The microplastics on the filter were dried and transferred to 10 mL centrifuge tubes. Then, 5 mL 2% HNO_3 was added to the tube and sonicated using ultrasound for 10 min to desorb the Cu(II) metal ions from the microplastic surfaces. The sonicated mixtures were subsequently filtered through 0.45 μm syringe filters transferring the filtered solutions to clean PP centrifuge tubes for measuring the Cu(II) concentration using an inductively coupled plasma mass spectrometry (ICP-MS, Elan drc-e, United States).

RESULTS AND DISCUSSION

Fourier Transformed Infrared Characterization of Microplastics With Different Degree of Aging

Attenuated total reflection Fourier transformed infrared spectra of the PE, PP, and PET microplastics surfaces with different exposure times to UV irradiation are shown in **Figure 1**. The spectra show that new functional groups are generated on the surface of PE and PP microplastic particles. For PE, characteristic peaks for –OH, –COOH, and –C–O– were evolved at wave numbers of 3,360 cm^{-1} (**Figure 1A-1**), 1,610 cm^{-1} (**Figure 1A-2**), and 1,150 cm^{-1} (**Figure 1A-3**), indicating that alcohol, carboxylic acid and fatty ether functional groups were formed by the photolytic oxidation of the surfaces. The peak observed at 850 cm^{-1} is due to the adsorption by $–CCl_3$. This indicates that a substitution reaction occurred during the aging process, in which the hydrogen in the carbon polymer was replaced by chlorine in the artificial seawater. For aged PP, only a peak at 3,360 cm^{-1} appeared (**Figure 1B**), indicating that PP microplastics were oxidized to less extent than PE during the aging process by UV irradiation in seawater environment. The peak is attributed to the adsorption of –OH, implying that alcohol functional groups were produced. For PET, there was no significant change in the surface functional groups based on the FTIR spectra (**Figure 1C**). Its greater resistance toward degradation is also documented by other studies (Chamas et al., 2020). It was worthy to note that no obvious peaks detected for 12-month-aged 2∼5 mm PE and 12-month-aged 0.9∼2 mm PP. Because ATR-FTIR has a rigorous demand for sample surface flatness, the uneven protrusions found on the surface of two particles might lead to the peak lack.

Aging Effect of Microplastics on Cu(II) Adsorption

As shown in **Figure 2**, the sequence of Cu(II) adsorption capacity for the three virgin microplastic materials is PE > PET > PP. Smaller microplastic particle sizes have, as could be expected due to greater surface area, higher Cu(II) adsorption capacity. For PE the capacity increases from 0.3 μg/g, for particle sizes between 0.9 and 5 mm, to 0.6 μg/g in particles smaller than 0.9 mm. This is less than expected considering that the surface area of a sphere increases by a factor of 25 when its size increases from 0.5 to 2.5 mm. The adsorbed Cu(II) increased with increasing aging time on all plastic materials and particle sizes. After 12 months aging, the amount of adsorbed Cu(II) on the aged microplastic particles were between 1.45 and 2.92 times greater than that on

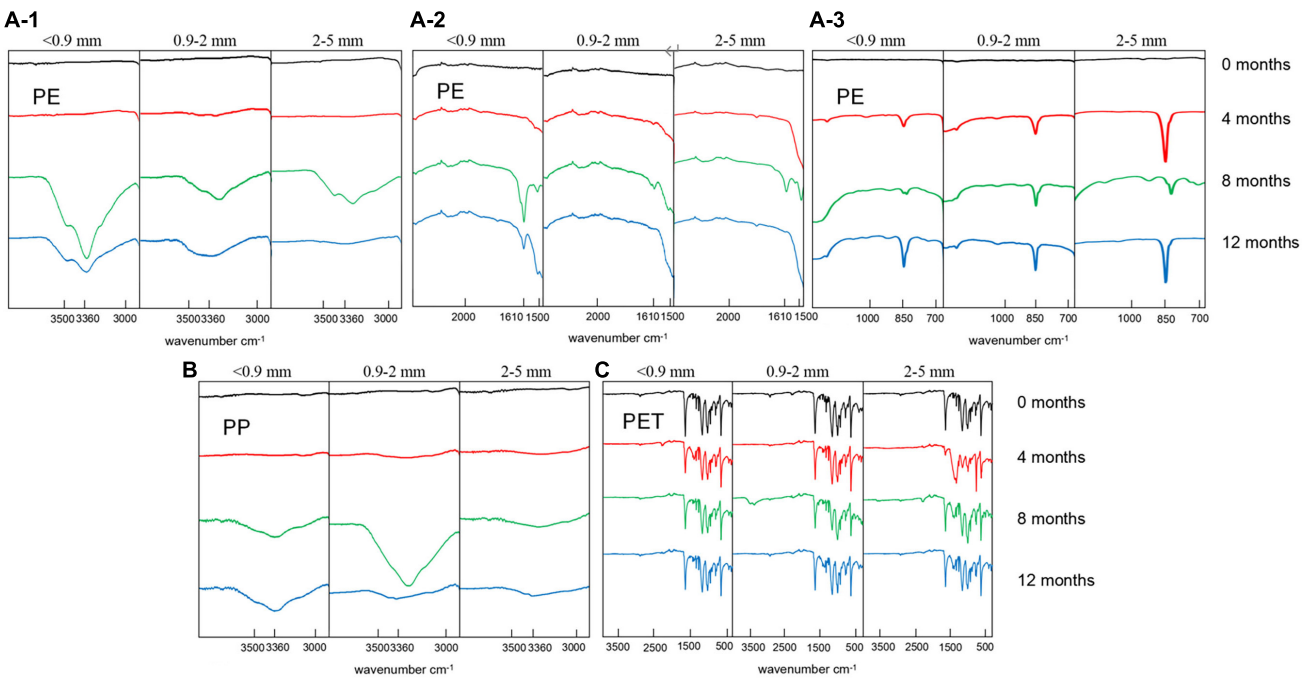

FIGURE 1 | Selection of FTIR spectra of PE, PP, and PET microplastics surfaces with different aging time.

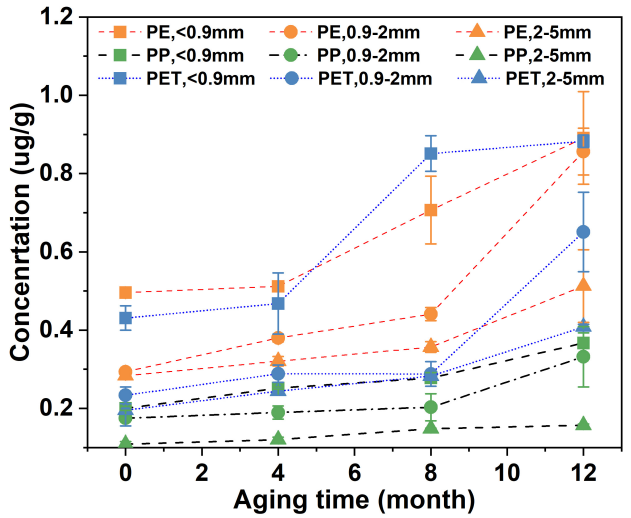

FIGURE 2 | Adsorbed Cu(II) on aged PE, PP, and PET microplastics.

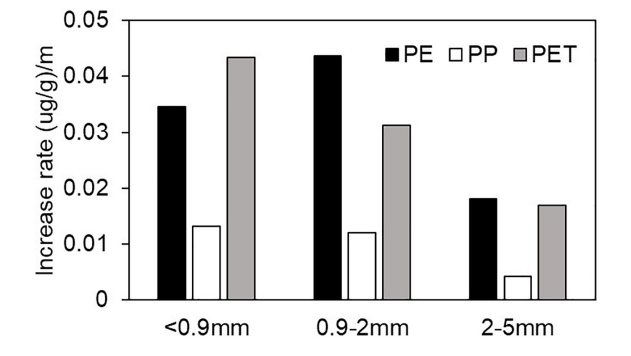

FIGURE 3 | Aging-derived increase rate [(μg/g)/m] of adsorbed Cu(II) on aged microplastic.

the fresh microplastic particles. Such increased Cu (II) adsorption in this study was also observed for aged beach plastic pellets (Holmes et al., 2014). However, the aging time was unclear in the study of Holmes et al. (2014).

Increased Cu(II) adsorption on aged microplastic particles can be attributed to that the surface of the microplastic materials are oxidized during the aging process. The oxygen-containing functional groups that are produced, provide sorption sites and thus enhanced adsorption capacity of metal ions. Moreover, the UV light alter the surface morphology of microplastics by generating a rougher surface, which increase the specific surface area and thereby the adsorption capacity of metal ions (Wang et al., 2020). The increase in metal adsorption by aged PE and PP microplastics may thus be due to both the chemical reaction and morphological change taking place in the aging process. However, for PET microplastics, due to the lack of chemical changes, the increased adsorption capacity can only be explained by the physical morphological change caused by the aging process.

The aging-derived increased adsorption capacity for Cu(II) on microplastics (**Figure 3**) is quantitatively evaluated by the linear regression slopes of adsorbed Cu(II) on microplastics against aging time (**Figure 2**). Generally, the aging-derived increases in adsorption capacity for PE and PET were much higher than that for PP. This implies that PE and PET microplastics have higher potential to act as vectors for heavy metal transport than PP. Moreover, for PP and PET, the increase rate in Cu(II) adsorption capacity exhibited an increasing trend with the decrease of microplastic particle size. In case of PE, the increase in capacity for smaller size particles (<0.9 mm and 0.9–2 mm) are similarly higher than that for the large size fraction (2–5 mm). This implies that the aging of smaller microplastics might have greater potential for impacting the fate and effect of heavy metals in the environment than the larger microplastic particles.

CONCLUSION

Microplastic particles of PE, PP, and PET polymers in a seawater environment were aged to different degrees by UV irradiation in order to explore the effect of aging on their adsorption capacity of Cu(II).

The adsorption capacity of Cu(II) differs between microplastic polymer types. PE has the highest adsorption capacity to Cu(II), while PP has the lowest. The adsorption capacity of Cu(II) increased with the degree of aging. Microplastics with smaller particle size have a higher adsorption capacity. The adsorption capacity of microplastics with particle size less than 0.9 mm is about twice as large as for particle size between 2 and 5 mm. From this we can deduce that microplastics with smaller particle size have higher potential to have a significant effect on the fate and effect of heavy metals in the marine environment.

DATA AVAILABILITY STATEMENT

The original contributions presented in the study are included in the article/supplementary material, further inquiries can be directed to the corresponding author/s.

AUTHOR CONTRIBUTIONS

XH: experiment, data curation, and writing-original draft preparation. RV: conceptualization and writing-review and editing. JZ, BZ, and XY: experiment. JF: supervision, writing-review and editing, and resources. XL: conceptualization, supervision, writing-review and editing, and resources. All authors contributed to the article and approved the submitted version.

FUNDING

This work was financially supported by the projects from the National Key Research and Development Program of China (2018YFC1406403 and 2020YFC1909500).

REFERENCES

Barnes, D. K. A., Galgani, F., Thompson, R. C., and Barlaz, M. (2009). Accumulation and fragmentation of plastic debris in global environments. *Philos. Trans. R. Soc. Lond. B Biol. Sci.* 364, 1985–1998. doi: 10.1098/rstb.2008.0205

Chamas, A., Moon, H., Zheng, J., Qiu, Y., Tabassum, T., Jang, J. H., et al. (2020). Degradation rates of plastics in the Environment. *ACS Sustainable Chem. Eng.* 8, 3494–3511. doi: 10.1021/acssuschemeng.9b06635

DeForest, D. K., Brix, K. V., and Adams, W. J. (2007). Assessing metal bioaccumulation in aquatic environments: the inverse relationship between bioaccumulation factors, trophic transfer factors and exposure concentration. *Aquat. Toxicol.* 84, 236–246. doi: 10.1016/j.aquatox.2007.02.022

Deheyn, D. D., and Latz, M. I. (2006). Bioavailability of metals along a contamination gradient in San Diego Bay (California, USA). *Chemosphere* 63, 818–834. doi: 10.1016/j.chemosphere.2005.07.066

Fu, Z., Guo, W., Dang, Z., Hu, Q., Wu, F., Feng, C., et al. (2017). Refocusing on nonpriority toxic metals in the aquatic environment in China. *Environ. Sci. Technol.* 51, 3117–3118. doi: 10.1021/acs.est.7b00223

Geyer, R., Jambeck, J. R., and Law, K. L. (2017). Production, use, and fate of all plastics ever made. *Sci. Adv.* 3:e1700782. doi: 10.1126/sciadv.1700782

Holmes, L. A., Turner, A., and Thompson, R. C. (2014). Interactions between trace metals and plastic production pellets under estuarine conditions. *Mar. Chem.* 167, 25–32. doi: 10.1016/j.marchem.2014.06.001

Jambeck, J. R., Geyer, R., Wilcox, C., Siegler, T. R., Perryman, M., Andrady, A., et al. (2015). Plastic waste inputs from land into the ocean. *Science* 347, 768–771. doi: 10.1126/science.1260352

Kester, D. R., Duedall, I. W., Connors, D. N., and Pytkowicz, R. M. (1967). Preparation of Artificial Seawater. *Limnol. Oceanogr.* 12, 176–179.

Li, C. (1999). Observation of the intensity of solar UV rradiation in tianjin area. *J. Clin. Dermatol.* 28, 29–30.

Plastic Europe (2019). *An Analysis of European Plastics Production, Demand and Waste. Data. Plastics – The Facts 2019*. Brussels: Plastic Europe.

Turner, A., and Holmes, L. A. (2015). Adsorption of trace metals by microplastic pellets in fresh water. *Environ. Chem.* 12:600. doi: 10.1071/EN14143

Wang, F., Wong, C. S., Chen, D., Lu, X., Wang, F., and Zeng, E. Y. (2018). Interaction of toxic chemicals with microplastics: a critical review. *Water Res.* 139, 208–219. doi: 10.1016/j.watres.2018.04.003

Wang, J., Peng, J., Tan, Z., Gao, Y., Zhan, Z., Chen, Q., et al. (2017). Microplastics in the surface sediments from the Beijiang River littoral zone: composition, abundance, surface textures and interaction with heavy metals. *Chemosphere* 171, 248–258. doi: 10.1016/j.chemosphere.2016.12.074

Wang, Q., Zhang, Y., Wangjin, X., Wang, Y., Meng, G., and Chen, Y. (2020). The adsorption behavior of metals in aqueous solution by microplastics effected by UV radiation. *J. Environ. Sci.* 87, 272–280. doi: 10.1016/j.jes.2019.07.006

Wang, W., Gao, H., Jin, S., Li, R., and Na, G. (2019). The ecotoxicological effects of microplastics on aquatic food web, from primary producer to human: a review. *Ecotoxicol. Environ. Saf.* 173, 110–117. doi: 10.1016/j.ecoenv.2019.01.113

World Economic Forum (2020). *The New Plastics Economy - Rethinking the Future of Plastics*. Cologny: World Economic Forum.

Conflict of Interest: The authors declare that the research was conducted in the absence of any commercial or financial relationships that could be construed as a potential conflict of interest.

frontiers in Marine Science

BRIEF RESEARCH REPORT
published: 24 December 2021
doi: 10.3389/fmars.2021.785146

Kinetics and Size Effects on Adsorption of Cu(II), Cr(III), and Pb(II) Onto Polyethylene, Polypropylene, and Polyethylene Terephthalate Microplastic Particles

Xiaoxin Han[1,2†], Shiyu Wang[1†], Xue Yu[1], Rolf D. Vogt[3,4], Jianfeng Feng[1], Lifang Zhai[1], Weiqi Ma[1], Lin Zhu[1] and Xueqiang Lu[1]**

[1] Tianjin Key Laboratory of Environmental Technology for Complex Trans-Media Pollution, Tianjin International Joint Research Center for Environmental Biogeochemical Technology, College of Environmental Science and Engineering, Nankai University, Tianjin, China, [2] Changchun Bureau of Ecology and Environment, Changchun, China, [3] Department of Chemistry, Center for Biogeochemistry in the Anthropocene, University of Oslo, Oslo, Norway, [4] Norwegian Institute for Water Research (NIVA), Oslo, Norway

Due to its small size, large specific surface area and hydrophobicity, microplastics, and the adsorbed contaminants may together cause potential negative effects on ecosystems and human beings. In this study, kinetics and size effects on adsorption of Cu(II), Cr(III), and Pb(II) onto PE, PP and PET microplastic particles were explored. Results indicated that the PE and PET microplastics have the higher adsorption capacity for Cu(II), Cr(III), and Pb(II) than that for PP microplastic. The adsorption capacity was affected by microplastic types and metal species. Among the three metals, Pb(II) had the largest adsorption amount on microplastic particles, especially on PET particles. Moreover, the adsorption capacities of microplastics increase with the decrease of particle size. The metal adsorption capacity of <0.9 mm microplastics is greater than that of 0.9–2 mm and 2–5 mm microplastics. The size effect on metal adsorption was largest for PE microplastic. More attention should be paid in case of the coexistence of heavy metals and tiny PE and PET microplastics in the environment.

Keywords: microplastics, kinetics, metal, adsorption, size effect

OPEN ACCESS

Edited by:
Lincoln Fok, The Education University of Hong Kong, Hong Kong SAR, China

Reviewed by:
Xuegang Li, Institute of Oceanology, Chinese Academy of Sciences (CAS), China
Muhammad Reza Cordova, Center for Oceanographic Research, Indonesian Institute of Sciences, Indonesia

***Correspondence:**
Lifang Zhai
zhailifang01@163.com
Xueqiang Lu
luxq@nankai.edu.cn

† These authors have contributed equally to this work and share first authorship

Specialty section:
This article was submitted to Marine Pollution, a section of the journal Frontiers in Marine Science

Received: *28 September 2021*
Accepted: *09 December 2021*
Published: *24 December 2021*

Citation:
Han X, Wang S, Yu X, Vogt RD, Feng J, Zhai L, Ma W, Zhu L and Lu X (2021) Kinetics and Size Effects on Adsorption of Cu(II), Cr(III), and Pb(II) Onto Polyethylene, Polypropylene, and Polyethylene Terephthalate Microplastic Particles. Front. Mar. Sci. 8:785146. doi: 10.3389/fmars.2021.785146

INTRODUCTION

Microplastics have already posed potentially risk for human health through transmission and accumulation in food chain (Yang et al., 2015; Xu et al., 2019) as they have already been widely detected in food (Liebezeit and Liebezeit, 2013, 2014; Yang et al., 2015). In the future, the environmental exposure risk of microplastic may be elevated as the plastic production is expected to increase to 318 million tons annually in 2050 (Neufeld et al., 2016). Furthermore, environmental microplastics could be a carrier for heavy metals transport from river to sea due to its small size, large specific surface area and hydrophobicity (Wang et al., 2017). As commonly detected pollutants in the environment (Zhang et al., 2018), heavy metals such as Cu, Cr, and Pb were also frequently detected in environmental microplastics (Selvam et al., 2021), and the metal concentration of microplastics was even similar or higher than that of the sediment phase (Ashton et al., 2010). It indicated that microplastics were able to enhance the mobility of heavy metal along river-coast-sea system. Once the metal-contained microplastics are ingested by aquatic organisms, these metals

may be released in the organism, causing further damage to the function of the organism. Then threaten human health via gradual accumulation in food chain (Fries et al., 2013). Therefore, the potential risk of microplastics and the heavy metal to freshwater-marine ecosystems would be both intensified. Therefore, to investigate the affinity of heavy metals to microplastics is essential to estimate the coexisting toxicity of heavy metals and microplastics in aqueous environments (Xu et al., 2018).

Although microplastics have ability to adsorb heavy metals (Koelmans et al., 2016; Wang et al., 2019; Fu et al., 2021), the adsorption capacity varies with the type of microplastics and heavy metals because of the difference in physicochemical properties of various microplastics and heavy metals. For example, polystyrene and film microplastic have greater adsorption capacity for Cu(II) than polyvinyl chloride, polyethylene, fishing line fibers and bottle cap particles, due to the conducive physicochemical properties of film microplastic (Almeida et al., 2020; Gao et al., 2021a). Compared with Cu and Cd, Pb showed the higher affinity to microplastics, because it is more likely to efficiently bind to function group on microplastics to promote the adsorption (Gao et al., 2019, 2021b). In addition, particle size is the generally essential factor influencing adsorption. In the environments, microplastics will be further fragmented into smaller part due to environmental dynamics, thereby affecting the adsorption capacity of heavy metals on microplastics (Gao et al., 2019; Zhang et al., 2020).

Therefore, it is important to investigate how microplastic size and type affect the interaction with heavy metals, which heavy metal has the most potential to be absorbed onto microplastics, and how the interaction will change with time. Adsorption kinetics are a conventional method to identify the temporal change of adsorption process, and the model parameters would attribute to reveal the possible adsorption mechanism (Almeida et al., 2020; Purwiyanto et al., 2020). Here, polyethylene (PE), polypropylene (PP) and polyethylene terephthalate (PET), which are three mostly used and typical types of plastics in the world (The Essential Chemical Industry (ECI), 2016a,b, 2017), are selected to study the adsorption kinetics and size effect for the three typical metal ions of Cu(II), Cr(III), and Pb(II) to test the hypotheses: (a) different temporal change in metal adsorption for different microplastics; and (b) larger metal adsorption for smaller microplastic particles.

MATERIALS AND METHODS

Chemicals and Materials

$Cu(NO_3)_2$, $Cr(NO_3)_3$, and $Pb(NO_3)_2$ were purchased from Aladdin Bio-Chem Technology Corporation (Shanghai, China). HNO_3 was purchased from Bohua Chemical Reagent Corporation (Tianjin, China). All chemicals were analytical grade or higher purity. PE, PP, and PET pellets with particle size of 5mm were purchased from Yousuo Chemical Technology Corporation (Shandong, China). Before use, the PE, PP, and PET pellets were crushed using a high-speed crusher. The crushed microplastic particles were then sequentially sieved through 20-, 10-, and 4- mesh screens in order to separate the particle sizes 2–5, 0.9–2, and <0.9 mm. The morphology of PE, PP, and PET microplastics were observed with a scanning electron microscope (Tescan Mira 4). To prevent contamination, all the lab materials were soaked in 10% (v/v) HCl solution for at least 48h, rinsed at least three times with deionized water (conductivity < 0.1 mS cm^{-1}) and dried in an oven at 50^{o}C.

Adsorption Experiments

The first experiment was to investigate temporal change of metal adsorption onto microplastics. Three microplastics (PE, PP, and PET) with same particle size < 0.9 mm were mixed with 50 mL solutions of Cu(II) with concentration of 5 mg L^{-1} in centrifuge tubes. The adsorption of Cr(III) and Pb(II) were also conducted simultaneously at the same condition. The medium is the deionized water. Samples were shaken at 150 r/min in a constant temperature water bath shaker at room temperature (∼25^{o}C). Sub-samples after 1, 2, 4, 8, 24, 72, 120, 168, 240, 312, and 384 h were taken, respectively.

The second experiment was to investigate the influence of microplastic particle size on adsorption. PE, PP, and PET microplastics with particle size 2–5, 0.9–2, and <0.9 mm were used. A series of centrifuge tubes, respectively containing 0.5 g microplastic with different size and 50 mL solutions of Cu(II) with concentration of 5 mg L^{-1}, were shaken for 240 h at 150 r/min in a constant temperature water bath shaker at room temperature (∼25^{o}C). At the same time, the adsorption of Cr(III) and Pb(II) were also conducted at the same condition. The medium is the deionized water.

At the terminal of shaking step, the mixture was immediately filtered with filter paper with a pore size of 15 to 20 μm. The trapped microplastics were collected, then were dried and transferred to a series of 10 mL centrifuge tubes. Then, 5 mL 2% HNO_3 was added to these tubes and ultrasound for 10 min to extract metal ions from microplastics. Finally, the mixture after ultrasonic was filtered with a syringe filter and the filtered solution was transferred to a clean PP centrifuge tube for quantification analysis. An inductively coupled plasma mass spectrometry (ICP-MS, Elan DRC-e, PerkinElmer) was used to analyze the heavy metal contents using the certified reference material (CRM). The detection limits for the three metals are 1 ppt and the recoveries for all are above 90%. All the treatments were in duplicate. The amount of heavy metal adsorbed by per unit mass of microplastic (q) could be calculated by Eq. (1).

$$q = \frac{VC}{m} \quad (1)$$

where, m (g) was the mass of microplastics used in adsorption, V (L) was the volume of the added solution with 2% HNO_3, C (μg L^{-1}) was the concentration of heavy metals after ultrasonic, respectively.

Kinetic Models

Four kinetic models were used to describe the kinetic adsorption of Cu(II), Cr(III), Pb(II) onto PE, PP, and PET microplastics.

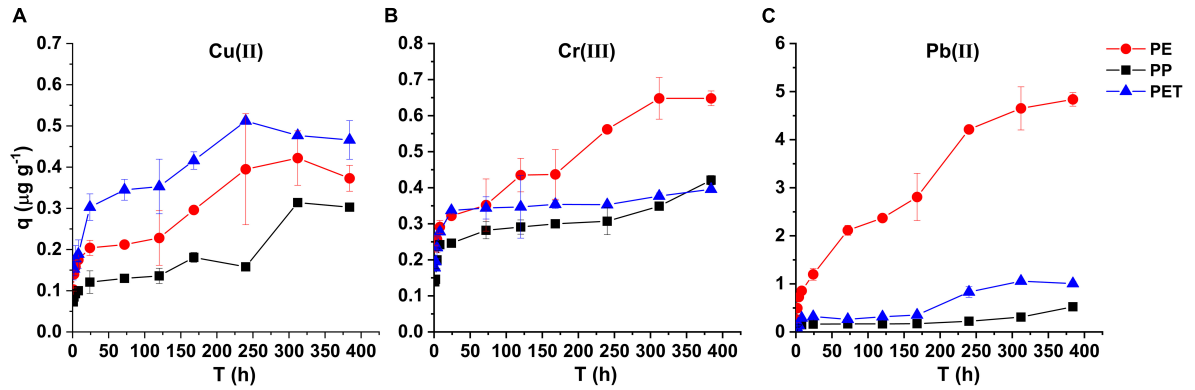

FIGURE 1 | (A) The Cu(II), **(B)** Cr(III), and **(C)** Pb(II) adsorption of PE, PP, and PET microplastics with a particle size of <0.9 mm at different adsorption time.

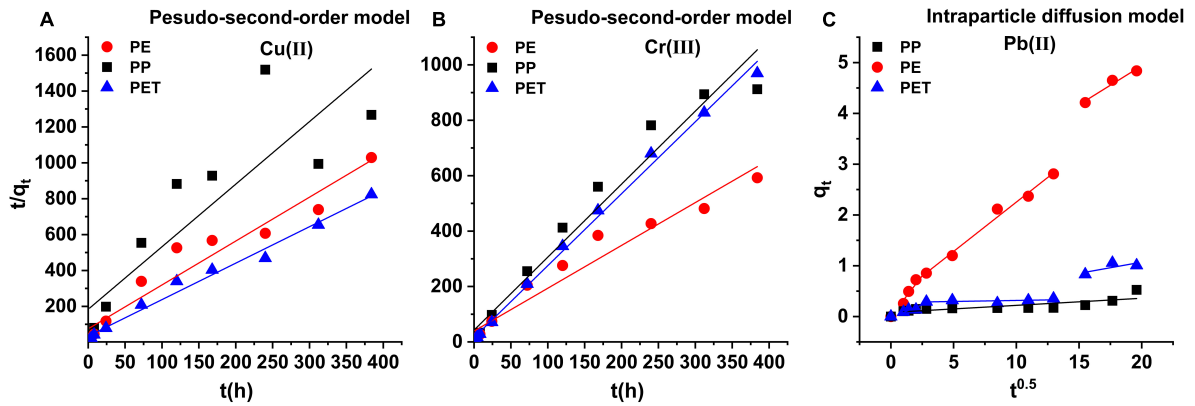

FIGURE 2 | (A) The pseudo-second-order kinetic model for Cu(II), **(B)** Cr(III) adsorption on PE, PP, and PET microplastics, and **(C)** the intra-particle diffusion model for Pb(II) adsorption on PE, PP and PET microplastics.

TABLE 1 | The fitting parameters of different models of Cu(II), Cr(III), and Pb(II) adsorbed onto PE, PP, and PET microplastics, respectively.

		Cu(II)			Cr(III)			Pb(II)		
		PE	PP	PET	PE	PP	PET	PE	PP	PET
Pesudo-second-order model	q_e (μg g^{-1})	0.402	0.278	0.488	0.649	0.380	0.385	5.128	0.370	1.04
	k_2 (g/(μg·h)$^{-1}$)	0.0025	0.0005	0.0081	0.0107	0.0034	0.0094	2.217	0.0009	0.0123
	R^2	0.94	0.78	0.98	0.95	0.96	0.99	0.88	0.67	0.52
Pesudo-first-order model	q_e (μg g^{-1})	0.303	0.287	0.147	1.71	0.267	0.151	6.97	0.542	1.21
	k_1 (h^{-1})	0.0072	0.0076	0.007	0.014	0.006	0.0076	0.015	0.0066	0.104
	R^2	0.69	0.67	0.61	0.82	0.71	0.82	0.76	0.48	0.60
Elovich model	a (μg g^{-1})	21.8	32.3	16.5	15.7	27.4	29.8	1.09	26.7	7.63
	B (μg g^{-1} h^{-1})	0.046	0.031	0.061	0.065	0.037	0.034	0.73	0.038	0.131
	R^2	0.80	0.60	0.93	0.79	0.88	0.94	0.84	0.39	0.59
Intraparticle diffusion model	$k_{p,1}$ (μg g^{-1} h$^{-0.5}$)	0.111	0.015	0.019	0.022	0.0602	0.056	0.320	0.0464	0.014
	C_1 (μg g^{-1})	0.112	0.058	0.154	0.209	0.0727	0.120	0.0042	0.0252	0.078
	R^2	0.90	0.79	0.92	0.96	0.95	0.99	0.89	0.80	0.76
	$k_{p,2}$ (μg g^{-1} h$^{-0.5}$)					0.0062	0.002	0.194		0.0018
	C_2 (μg g^{-1})					0.222	0.327	0.311		0.149
	R^2					0.95	0.95	0.98		0.83
	$k_{p,3}$ (μg g^{-1} h$^{-0.5}$)					0.0276	0.0105	0.153		0.0727
	C_3 (μg g^{-1})					−0.126	0.191	1.87		−0.925
	R^2					0.93	0.99	0.93		0.85

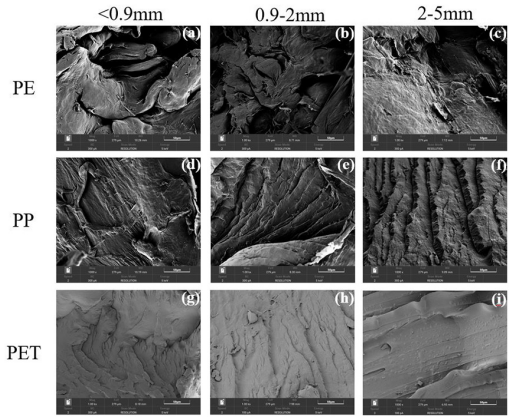

FIGURE 3 | (a–i) The morphology of PE, PP and PET microplastics.

The pseudo-second-order kinetic model:

$$\frac{t}{q_t} = \left(\frac{1}{k_2 q_e^2}\right)\frac{t}{+}q_e \quad (2)$$

The pseudo-first-order kinetic model:

$$\ln(q_e - q_t) = k_1 t + lnq_e \quad (3)$$

The Elovich kinetic model:

$$q_t = blnt + \frac{ln(ab)}{b} \quad (4)$$

The intra-particle diffusion model:

$$q_t = k_p t^{0.5} + C \quad (5)$$

where, q_t ($\mu g\ g^{-1}$) is the adsorption amount at the time of t (h); q_e ($\mu g\ g^{-1}$) is the saturated adsorption capacity of heavy metals at equilibrium; k_1 (h^{-1}) is the reaction rate constant of pseudo-first-order equation at equilibrium; k_2 ($g\ \mu g^{-1}\ h^{-1}$) is the reaction rate constant of the pseudo-second-order equation at equilibrium; a ($\mu g\ g^{-1}$) and b ($\mu g\ g^{-1}\ h^{-1}$) are the parameters of the Elovich equation; k_p ($\mu g\ g^{-1}\ h^{-0.5}$) is the constant of intra-particle diffusion model, C ($\mu g\ g^{-1}$) represents a conception about the thickness of boundary layer, describing the influence of thickness of boundary layer on adsorption.

RESULTS AND DISCUSSION

Metal Adsorption Kinetics

The kinetics experiments results were shown in **Figure 1**. The maximum of Cu(II) and Cr(III), Pb(II) adsorption were 0.51, 0.64, and 4.78 mg g^{-1} for PET, PE and PE, respectively. For all the three metals, the adsorption capacity on PP particles was the lowest. The adsorption of PE, PP, and PET particles increased rapidly in the initial 24 h, and then changed slowly. In general, the adsorption rates and adsorption capacities followed the orders of PET > PE > PP for Cu(II), and PE > PET > PP for Cr(III) and Pb(II).

As shown in **Figure 2**, the kinetics of Cu(II) and Cr(III) adsorption onto the PE, PP, and PET microplastics were well regressed by the pseudo-second-order model (**Table 1**). The derived equilibrium adsorption capacities (q_e) of Cu(II) and Cr(III) for PP microplastic were the lowest, which was the same with the experimental results in **Figure 1**. It may be attributed to no functional group on PP microplastic compared with PET microplastic and the smoother surface of PP microplastic than PE microplastic (**Figure 3**). The adsorption capacity of Cu(II) for PET microplastic is greater than that for PE microplastic, while the adsorption capacities of Cr(III) for PET microplastic is smaller than that for PE microplastic. However, other researchers found that sequence of adsorption capacity was PE > PP > PET for both Cu(II) and Cr(III) (Godoy et al., 2019). The differences may be because the microplastics they used were from daily objects and may be aged. This may suggest that the adsorption capacity of heavy metals on microplastic greatly varies with the change of microplastics surface. In **Table 1**, the values of k_2 were lower than 0.01 g (μgh) $^{-1}$ for Cu(II) and Cr(III) adsorption. It did not only indicate that the adsorption rate was proportional to the number of unoccupied sites (Fan et al., 2021), but also revealed the adsorption of Cu(II) and Cr(III) onto the microplastics were a slow process, especially for the virgin microplastics with relatively homogeneous smooth surface (Li et al., 2019; Oz et al., 2019; Wang et al., 2020).

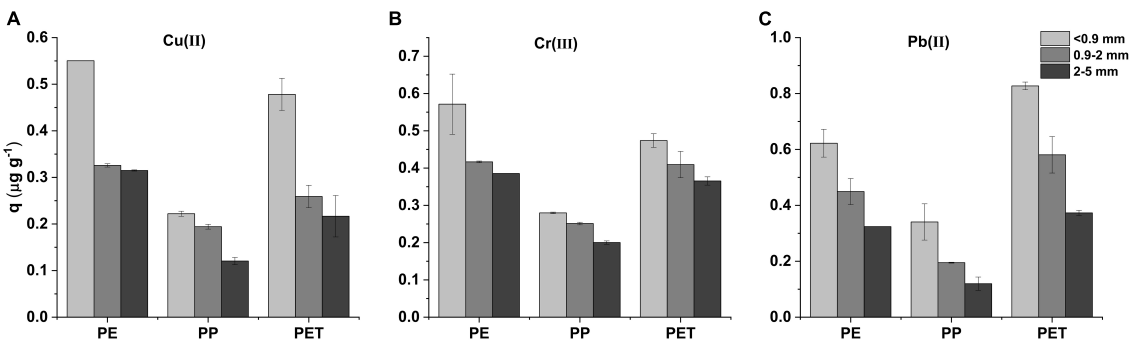

FIGURE 4 | (A) The Cu(II), **(B)** Cr(III), and **(C)** Pb(II) adsorption capacities of PP, PE, and PET microplastics with different particle sizes in 240 h.

Turner and Holmes (2015) and Wang et al. (2020) also found that the interaction between metals and microplastics was a long-term process even for the aged microplastics. It indicated that the microplastics might continue to accumulate heavy metals when the interaction time is long. However, further evidence is needed.

There was obvious discrepancy in Pb(II) adsorbed on PE, PP, and PET microplastics (**Figures 1**, **2**). The adsorption amount of Pb(II) on PE microplastic was the highest, which may attribute to the higher crystallinity, high pore volume and rough surfaces of PE microplastic (Wang and Wang, 2018; Zou et al., 2020). It indicated that the crystallinity of microplastic may be one of the essential factors influencing Pb(II) adsorption, even more important than function group for the virgin microplastics. The kinetics of Pb(II) adsorption on PE, PP, and PET microplastics were well fitted by the intra-particle diffusion model ($R^2 \geq 0.76$ in **Table 1**), implying the inter-particle diffusion process was the rate-controlling step. The negative influence of the boundary layer on adsorption over time decreased to the lowest ($C_3 < 0$) explained the keep growing in amount of adsorbed Pb(II) on PET microplastic. Although the order of C on PE microplastic was $C_1 > C_2 > C_3$, the adsorption amount continuously increased with time. Turner and Holmes (2015) also found the same trend when the added Pb(II) concentration was 5 mg L^{-1}. It implied that Pb(II) had strong prosperity of affinity and temporal accumulation on PE microplastic. However, the adsorption can quickly achieve the equilibrium at about 48h in the seawater medium (Holmes et al., 2012), because the ions existence would fasten the adsorption process and change the temporal procedure of adsorption.

Size Effect on Metal Adsorption

The results shown in **Figure 4** validated the heavy metal absorption on microplastics decreased with increasing particle size. With the decrease of microplastic size from 2–5 mm to <0.9 mm, the adsorption amount increased about 1.8–2.2, 1.3–1.5, and 1.94–2.83 times for Cu(II), Cr(III), and Pb(II), respectively. In addition, the amount of adsorbed Cr(III) varied more slightly with the particle size. Namely, the effect of particle size of PP microplastic on metal adsorption was relatively low.

The phenomenon may attribute to the more complex morphology and higher specific area with decrease of particle size (**Figure 3**), which can lead more unoccupied site for adsorption. For Cu(II) and Pb(II), the observed adsorption variations with particle size implied that the adsorption on microplastic was considerably related to the porosity. Compared with Cu(II) and Pb(II), the influence of particle size on Cr(III) adsorption was relatively small, which is similar to the tendency observed in other studies (e.g., Zhang et al., 2021). It may be attributable to the insensitive response of Cr(III) adsorption to the stratification variation of the microplastic surface. The relatively low influence of particle size on PP microplastic adsorption profitably emphasized the significance of crystallinity and function group.

According to the experimental results above, it may be inferred that the adsorption amount of microplastics to other metals may also possibly increase with decrease of particle size. Namely, microplastics with a smaller particle size in the environment may cause higher environmental risks as a carrier of heavy metals (Thompson et al., 2004; Zhang et al., 2020). With the aging process of microplastics in natural environment, such as UV-irradiation, acid and alkali corrosion, particle crushing, biofouling, it would become more toxic to the environment. This means the results in this study may be regarded as the lowest metal amounts absorbed by microplastics in the natural environment.

All the three heavy metals can be accumulated increasingly with time onto the three microplastics. The PET microplastic has the relatively rapid and strong ability to adsorb Cu(II) and PE microplastic has the relatively rapid and strong ability to adsorb Cr(III) and Pb(II). It means that the virgin microplastic PE and PET can be a conducive carrier for heavy metal transport in the environment and their environmental toxicity would be magnified, especially for the combination of Pb(II) and PE. The risk to environmental security would be further elevated due to the aging process of PP and PET in the environment (Han et al., 2021). Therefore, more attention should be paid to PE and PET microplastics if metal contaminants exist in the aqueous system.

DATA AVAILABILITY STATEMENT

The raw data supporting the conclusions of this article will be made available by the authors, without undue reservation.

AUTHOR CONTRIBUTIONS

XH and SW: investigation, data curation, validation, and writing-original draft preparation. XY: writing, reviewing, and editing. RV: conceptualization, writing, reviewing, and editing. JF, LZha, WM, and LZhu: resources, writing, reviewing, and editing. XL: conceptualization, supervision, writing, reviewing, and editing. All authors contributed to the article and approved the submitted version.

FUNDING

This work was financially supported by the projects from the National Key Research and Development Program of China (2018YFC1406403 and 2020YFC1909500).

REFERENCES

Almeida, C. M. R., Manjate, E., and Ramos, S. (2020). Adsorption of Cd and Cu to different types of microplastics in estuarine salt marsh medium. *Mar. Pollut. Bull.* 151:110797. doi: 10.1016/j.marpolbul.2019.110797

Ashton, K., Holmes, L., and Turner, A. (2010). Association of metals with plastic production pellets in the marine environment. *Mar. Pollut. Bull.* 60, 2050–2055. doi: 10.1016/j.marpolbul.2010.07.014

Fan, X. L., Ma, Z. X., Zou, Y. F., Liu, J. Q., and Hou, J. (2021). Investigation on the adsorption and desorption behaviors of heavy metals by tire wear particles

with or without UV ageing processes. *Environ. Res.* 195:110858. doi: 10.1016/j.envres.2021.110858

Fries, E., Dekiff, J. H., Willmeyer, J., Nuelle, M. T., Ebert, M., and Remy, D. (2013). Identification of polymer types and additives in marine microplastic particles using pyrolysis-GC/MS and scanning electron microscopy. *Environ. Sci. Process. Impacts* 15, 1949–1956. doi: 10.1039/c3em00214d

Fu, Q. M., Tan, X. F., Ye, S. J., Ma, L. L., Gu, Y. L., Zhang, P., et al. (2021). Mechanism analysis of heavy metal lead captured by natural-aged microplastics. *Chemosphere* 270:128624. doi: 10.1016/j.chemosphere.2020.128624

Gao, F. L., Li, J. X., Sun, C. J., Zhang, L. T., Jiang, F. H., Cao, W., et al. (2019). Study on the capability and characteristics of heavy metals enriched on microplastics in marine environment. *Mar. Pollut. Bull.* 144, 61–67. doi: 10.1016/j.marpolbul.2019.04.039

Gao, L., Fu, D., Zhao, J., Wu, W., Wang, Z., Su, Y., et al. (2021a). Microplastics aged in various environmental media exhibited strong sorption to heavy metals in seawater. *Mar. Pollut. Bull.* 169:112480. doi: 10.1016/j.marpolbul.2021.112480

Gao, X., Hassan, I., Peng, Y. T., Huo, S. L., and Ling, L. (2021b). Behaviors and influencing factors of the heavy metals adsorption onto microplastics: a review. *J. Clean. Prod.* 319:128777. doi: 10.1016/j.jclepro.2021.128777

Godoy, V., Blazquez, G., Calero, M., Quesada, L., and Martin-Lara, M. A. (2019). The potential of microplastics as carriers of metals. *Environ. Pollut.* 255(Pt 3):113363.

Han, X., Vogt, R. D., Zhou, J., Zheng, B., Yu, X., Feng, J., et al. (2021). Increased Cu(II) adsorption onto UV-aged polyethylene, polypropylene, and polyethylene terephthalate microplastic particles in seawater. *Front. Mar. Sci.* 8:770606. doi: 10.3389/fmars.2021.770606

Holmes, L. A., Turner, A., and Thompson, R. C. (2012). Adsorption of trace metals to plastic resin pellets in the marine environment. *Environ. Pollut.* 160, 42–48. doi: 10.1016/j.envpol.2011.08.052

Koelmans, A. A., Bakir, A., Burton, G. A., and Janssen, C. R. (2016). Microplastic as a vector for chemicals in the aquatic environment: critical review and model-supported re-interpretation of empirical studies. *Environ. Sci. Technol.* 50, 3315–3326. doi: 10.1021/acs.est.5b06069

Li, X., Mei, Q., Chen, L., Zhang, H., Dong, B., Dai, X., et al. (2019). Enhancement in adsorption potential of microplastics in sewage sludge for metal pollutants after the wastewater treatment process. *Water Res.* 157, 228–237. doi: 10.1016/j.watres.2019.03.069

Liebezeit, G., and Liebezeit, E. (2013). Non-pollen particulates in honey and sugar. *Food Addit. Contam.* 30, 2136–2140. doi: 10.1080/19440049.2013.843025

Liebezeit, G., and Liebezeit, E. (2014). Synthetic particles as contaminants in German beers. *Food Addit. Contam.* 31, 1574–1578. doi: 10.1080/19440049.2014.945099

Neufeld, L., Stassen, F., Sheppard, R., and Gilman, T. (2016). *In the New Plastics Economy: Rethinking the Future of Plastics*. Cologny: World Economic Forum.

Oz, N., Kadizade, G., and Yurtsever, M. (2019). Investigation of heavy metal adsorption on microplastics. *Appl. Ecol. Environ. Res.* 17:4. doi: 10.15666/aeer/1704_73017310

Purwiyanto, A. I. S., Suteja, Y., Trisno, N. P., Putri, W., Rozirwan, R., Agustriani, F., et al. (2020). Concentration and adsorption of Pb and Cu in microplastics: case study in aquatic environment. *Mar. Pollut. Bull.* 158:111380. doi: 10.1016/j.marpolbul.2020.111380

Selvam, S., Jesuraja, K., Venkatramanan, S., Roy, P. D., and Jeyanthi Kumari, V. (2021). Hazardous microplastic characteristics and its role as a vector of heavy metal I groundwater and surface water of coastal south India. *J. Hazard. Mater.* 402:123786. doi: 10.1016/j.jhazmat.2020.123786

The Essential Chemical Industry (ECI) (2016a). *Poly(propene)(Polypropylene)[OL]*. Available online at: http://www.essentialchemicalindustry.org/polymers/polypropene.html. (accessed August 21, 2016).

The Essential Chemical Industry (ECI) (2016b). *Polyesters[OL]. [2018-09-06]*. Available online at: http://www.essentialchemicalindustry.org/polymers/polyesters.html. (accessed August 25, 2016).

The Essential Chemical Industry (ECI) (2017). *Poly(ethene)(Polyethylene)[OL]*. Available online at: http://www.essentialchemicalindustry.org/polymers/polyethene.html. (accessed April 27, 2017).

Thompson, R. C., Ylva, O., Mitchell, R. P., Anthony, D., Rowland, S. J., John, A. W. G., et al. (2004). Lost at sea: where is all the plastic? *Science* 304:838.

Turner, A., and Holmes, L. A. (2015). Adsorption of trace metals by microplastic pellets in fresh water. *Environ. Chem.* 12, 600–610.

Wang, F., Yang, W., Cheng, P., Zhang, S., Zhang, S., Jiao, W., et al. (2019). Adsorption characteristics of cadmium onto microplastics from aqueous solutions. *Chemosphere* 235, 1073–1080. doi: 10.1016/j.chemosphere.2019.06.196

Wang, J., Peng, J., Tan, Z., Gao, Y., Zhan, Z., Chen, Q., et al. (2017). Microplastics in the surface sediments from the Beijiang River littoral zone: composition, abundance, surface textures and interaction with heavy metals. *Chemosphere* 171, 248–258. doi: 10.1016/j.chemosphere.2016.12.074

Wang, Q., Zhang, Y., Wangjin, X., Wang, Y., Meng, G., and Chen, Y. (2020). The adsorption behavior of metals in aqueous solution by microplastics effected by UV radiation. *J. Environ. Sci. (China)* 87, 272–280. doi: 10.1016/j.jes.2019.07.006

Wang, W., and Wang, J. (2018). Comparative evaluation of sorption kinetics and isotherms of pyrene onto microplastics. *Chemosphere* 193, 567–573. doi: 10.1016/j.chemosphere.2017.11.078

Xu, P., Peng, G. Y., Su, L., Gao, Y. Q., Gao, L., and Li, D. J. (2018). Microplastic risk assessment in surface waters: a case study in the Changjiang Estuary. *China. Mar. Pollut. Bull.* 133, 647–654. doi: 10.1016/j.marpolbul.2018.06.020

Xu, S., Ma, J., Ji, R., Pan, K., and Miao, A. J. (2019). Microplastics in aquatic environments: occurrence, accumulation, and biological effects. *Sci. Total Environ.* 703:134699. doi: 10.1016/j.scitotenv.2019.134699

Yang, D., Shi, H., and Li, L. (2015). Microplastic pollution in table salts from China. *Environ. Sci. Technol.* 49:13622. doi: 10.1021/acs.est.5b03163

Zhang, J., Zhou, F., Chen, C., Sun, X., Shi, Y., Zhao, H., et al. (2018). Spatial distribution and correlation characteristics of heavy metals in the seawater, suspended particulate matter and sediments in Zhanjiang Bay, China. *PLoS One* 13:e0201414. doi: 10.1371/journal.pone.0201414

Zhang, L., Li, Y., Wang, W., Zhang, W., Zuo, Q., Abdelkader, A., et al. (2021). Heynderickx PM, Kim KH. The potential of microplastics as adsorbents of sodium dodecyl benzene sulfonate and chromium in an aqueous environment. *Environ. Res.* 197:111057. doi: 10.1016/j.envres.2021.111057

Zhang, S. W., Han, B., Sun, Y. H., and Wang, F. Y. (2020). Microplastics influence the adsorption and desorption characteristics of Cd in an agricultural soil. *J. Hazard. Mater.* 388:121775. doi: 10.1016/j.jhazmat.2019.121775

Zou, J., Liu, X., Zhang, D., and Yuan, X. (2020). Adsorption of three bivalent metals by four chemical distinct microplastics. *Chemosphere* 248:126064. doi: 10.1016/j.chemosphere.2020.126064

Conflict of Interest: The authors declare that the research was conducted in the absence of any commercial or financial relationships that could be construed as a potential conflict of interest.

Publisher's Note: All claims expressed in this article are solely those of the authors and do not necessarily represent those of their affiliated organizations, or those of the publisher, the editors and the reviewers. Any product that may be evaluated in this article, or claim that may be made by its manufacturer, is not guaranteed or endorsed by the publisher.

frontiers in Marine Science

REVIEW
published: 11 January 2022
doi: 10.3389/fmars.2021.800782

Influence of Functional Group Modification on the Toxicity of Nanoplastics

Haihong Zhang[1], Haodong Cheng[1], Yudi Wang[1], Zhenghua Duan[1], Wenjie Cui[1], Yansong Shi[1] and Li Qin[2]**

[1] Tianjin Key Laboratory of Hazardous Waste Safety Disposal and Recycling Technology, School of Environmental Science and Safety Engineering, Tianjin University of Technology, Tianjin, China, [2] Agro-Environmental Protection Institute, Ministry of Agriculture and Rural Affairs, Tianjin, China

OPEN ACCESS

Edited by:
Xiangrong Xu,
South China Sea Institute of Oceanology, Chinese Academy of Sciences (CAS), China

Reviewed by:
Mingkai Xu,
University of Chinese Academy of Sciences (UCAS), China
Chun Ciara Chen,
Shenzhen University, China

***Correspondence:**
Zhenghua Duan
duanzhenghua@mail.nankai.edu.cn
Li Qin
ql-tj@163.com

Specialty section:
This article was submitted to Marine Pollution, a section of the journal Frontiers in Marine Science

Received: *24 October 2021*
Accepted: *10 December 2021*
Published: *11 January 2022*

Citation:
Zhang H, Cheng H, Wang Y, Duan Z, Cui W, Shi Y and Qin L (2022) Influence of Functional Group Modification on the Toxicity of Nanoplastics. Front. Mar. Sci. 8:800782. doi: 10.3389/fmars.2021.800782

Nanoplastics (NPs) are ubiquitous in harvested organisms at various trophic levels, and more concerns on their diverse responses and wide species-dependent sensitivity are continuously increasing. However, systematic study on the toxic effects of NPs with different functional group modifications is still limited. In this review, we gathered and analyzed the toxic effects of NPs with different functional groups on microorganisms, plants, animals, and mammalian/human cells *in vitro*. The corresponding toxic mechanisms were also described. In general, most up-to-date relevant studies focus on amino ($-NH_2$) or carboxyl ($-COOH$)-modified polystyrene (PS) NPs, while research on other materials and functional groups is lacking. Positively charged PS-NH_2 NPs induced stronger toxicity than negatively charged PS-COOH. Plausible toxicity mechanisms mainly include membrane interaction and disruption, reactive oxygen species generation, and protein corona and eco-corona formations, and they were influenced by surface charges of NPs. The effects of NPs in the long-term exposure and in the real environment world also warrant further study.

Keywords: nanoplastic, functional group modification, surface charge, toxic effect, mechanism

INTRODUCTION

Plastics discarded into the environment has become a global concerned pollution (Alak et al., 2021; Zhang et al., 2021). Microplastics, especially nanoplastics (NPs, smaller than 1 μm), could more likely to penetrate the cell membranes and impose adverse impacts on living organisms (Shen et al., 2019). However, due to limitations in quantitative detection, the varying effects of their environmental concentrations are still unclear, although Schirinzi et al. (2019) reported traces of nano-sized polystyrene (PS) in estuarine and surface waters of the West Mediterranean Sea. Toxicities of NPs on development, behavioral alterations, and oxidative stress have attached great importance in various organisms (Duan et al., 2020). Ultimately, they may cause hazards to human health (Sun M. et al., 2021).

The aged plastics through photo-degradation, biodegradation, hydrolysis, and mechanical abrasion in the environment, will result in different surface modifications in NPs. Negatively charged NPs, such as the carbonyl groups (−COOH), are expected to be the most common ones due to surface oxidation and acquisition of functionalities during the weathering (Luan et al., 2019). Positively charged NPs, such as amino modification ($-NH_2$), may also consider as an important counterpart due to the hydrolyzation of polyamides (Wang et al., 2019). However, compared with morphology and size (Aznar et al., 2019; Cheng et al., 2020), the presence of functional groups on the surface modifications of plastic polymers working on their toxicological effects remains to be systematically studied.

Thus, the toxic effects of NPs, with different functional groups or without modification (bare NPs), were reviewed and compared on microorganisms, plants, animals, and mammalian/human cells *in vitro* in the present study. We aim to provide some new information concerning on the health risk of NPs in the environment.

BIBLIOMETRIC ANALYSIS

The keywords used in the bibliographic search were as follows: "nanoplastics, toxic mechanism, toxic effects, surface modification, and functional group" or "nanoplastics, toxic mechanism, toxic effects, and amino-modified" or "nanoplastics, toxic mechanism, toxic effects, and carboxyl-modified" in Science Direct database and Web of Science database from January 2012 to December 2021. A total of 477 references were obtained, including review articles and research articles. Abstracts of the retrieved publications were reviewed separately to screen the relevant literature. Only studies that involved the toxic effects and/or toxic mechanisms of NPs researched on organisms were selected for further analysis. Literature that did not specify whether NPs were modified, or the information of NPs was incomplete, or the toxic mechanisms were not assessed based on organisms, were excluded. In addition, a manual review of the reference lists of the selected publications was conducted to recover articles not included in the bibliographic search. Eventually, 6 review articles and 59 research articles (summarized in **Table 1**) were screened, accounting for approximately 13.6% of the total. The numbers of manuscripts talked about the functional groups including: $-NH_2$ (48), −COOH (40), −COC (1), $-SO_3H$ (3), $-CNH_2NH_2{}^+$(1), and bare NPs (19).

Cite Space software (5.8.R2, 64 bit) and Origin Pro 9.0 (Origin Lab Corp., Northampton, MA, United States) were used to perform visualization and bibliometric analysis, mainly for the number of annual publications and keyword co-occurrence analysis. As shown in **Figure 1**, the number of published articles on NPs increased from 2 in 2012 to 272 in 2021, which indicated that the toxicity of NPs played important roles in relevant studies. However, only 11 studies compared the toxicities of NPs with different functional groups in 2021. The co-occurrence network (**Figure 2**) showed that *Caenorhabditis elegan*, *Artemia franciscana*, *Daphnia magna*, mussel, oyster, and algae were the main species used in the previous studies. The main toxic effects included growth, behavior, apoptosis, and cytotoxicity. The main toxic mechanisms discussed involved oxidative stress, accumulation, activation, adsorption, ingestion, surface charge, size, aggregation, and extracellular polymeric substance.

TOXIC EFFECTS OF NPS WITH DIFFERENT FUNCTIONAL GROUP MODIFICATIONS

Microorganisms

Microorganisms play important roles in the biological chain as decomposers for the ecosystem (Liu et al., 2020). NPs can penetrate into cells through microbial cell membranes and destroy cell functions (Ning et al., 2021). The toxicity is greater when the particle size is smaller (Miao et al., 2019). For example, PS NPs of 100 and 200 nm had no effect on the growth of *Escherichia coli*, whereas PS NPs of 30 nm had an increased inhibition on bacterial growth (Ning et al., 2021).

Amino-modified NPs are usually positively charged, which make it easier for them to get into the negatively charged bio-membrane due to the electrostatic interaction (González-Fernández et al., 2018; Tallec et al., 2018). Therefore, the toxicity of amino-modified NPs was supposed to be higher than that of carboxyl-modified NPs and bare NPs. However, to our knowledge, only five manuscripts compared the toxicity of NPs with different functional groups in microorganisms to date. PS-NH_2 NPs more strongly inhibited the growth of *Synechococcus* and damaged the membrane integrity of *Synechococcus* than PS-SO_3H NPs (Feng et al., 2019). PS-NH_2 NPs of 50 nm produced a higher reactive oxygen species (ROS) level in *Halomonas Alkaliphila*than that bare PS NPs of 55 nm, and the generated ROS may cross extracellular polymers (EPS) and cause great damages (Sun et al., 2018). PS-NH_2, bare PS, and PS-COOH NPs caused cell membrane damage and induced oxidative stress in activated sludge and biofilms, and PS-NH_2 NPs induced the highest effect among them (Miao et al., 2019; Qian et al., 2021). NPs inhibited the bacterial growth of *Escherichia coli* in the order of PS-NH_2 > PS-COC > PS-COOH (Ning et al., 2021).

Algae and Plants

Algae-adsorbed NPs might be ingested by aquatic animals and transmitted through the food chains, and ultimately result in health risk to human beings (Heddagaard and Møller, 2019; Huang et al., 2020; Mateos-Cárdenas et al., 2021). The potential risks of NPs to the algae in freshwater and seawater have been well documented recently. The toxicity of NPs to the algae was affected by exposure doses, particle sizes, and types of functional groups (González-Fernández et al., 2019). Exposure to carboxyl-modified NPs inhibited the growth of *Raphidocelis subcapitata*, diatom, *Chlorella Vulgaris*, *Phaeodactylum tricornutum*, and *Rhodomonas baltica*, which was manifested in morphological changes, interference

TABLE 1 | Summary of toxicity assessment of NPs with different functional groups.

Species	NPs type	Particle size	Exposure concentration	Toxic effects	References
Microorganisms					
Biofilms	PS-bare	100 and 500 nm	5–100 mg/L	Oxidative stress	Miao et al., 2019
	PS-NH_2				
	PS-COOH				
Activated sludge	PS-bare	100 nm	100 mg /L	Cell membrane damage and oxidative stress	Qian et al., 2021
	PS-NH_2				
	PS-COOH				
Halomonas alkaliphila	PS-bare	55 nm	20–320 mg/L	Inhibit growth and oxidative stress	Sun et al., 2018
	PS-NH_2	50 nm			
Synechococcus	PS-NH_2	50 nm	2–9 μg/mL	Inhibit growth; damage the membrane integrity; changes in metabolic; and oxidative stress	Feng et al., 2019
	PS-SO_3H	52.03 nm			
Escherichia coli	PS-bare	30–200 nm	4–32 mg/L	Inhibit growth; oxidative stress; and DNA damage	Ning et al., 2021
	PS-NH_2	200 nm			
	PS-COC				
	PS-COOH				
Algae in freshwater					
Pseudokirchneriella subcapitata	PS-NH_2	20 nm	10 mg/L	Inhibition of photosynthesis and/or cell wall disruption	Nolte et al., 2017
	PS-COOH	110 nm			
Raphidocelis subcapitata	PS-COOH	88 nm	0.5–50 mg/L	Interfere with mitosis and cell metabolism	Bellingeri et al., 2019
Microcystis aeruginosa	PS-NH_2	50 nm	3.4 and 6.8 μg/mL	Inhibit photosystem II efficiency; reduce organic substance synthesis; induce oxidative stress; and enhance the synthesis of microcystin	Feng et al., 2020
	PS-SO_3H	–	100 μg/mL		
Algae in seawater					
Diatom	PS-NH_2	50 nm	0.05 and 5 μg/mL	Inhibit photosynthesis and destroy lipid structure	González-Fernández et al., 2020
	PS-NH_2	500 nm	2.5 μg/mL	Decrease in esterase activity and diminished neutral lipid content	Seoane et al., 2019
Dunaliella tertiolecta	PS-NH_2	50 nm	5–50 μg/mL	Inhibit growth and photosynthesis	Bergami et al., 2017
	PS-COOH	40 nm			
Phaeodactylum tricornutum	PS-COOH	60 nm	1–100 mg/L	No toxic effects	Grassi et al., 2020
Chlorella vulgaris	PS-NH_2	90, 200, and 300 nm	25–200 mg/L	Inhibit photosynthesis and algal growth	Khoshnamvand et al., 2021
Rhodomonas baltica	PMMA	50 nm	0.5–100 μg/mL	Cell cycle injury; loss of membrane integrity; inhibition of photosynthesis; and decrease cell viability	Gomes et al., 2020
	PMMA-COOH	50 nm			
Chlorella sp.	PS-bare	217 nm	1 mg/L	Eco-corona formation and decline the oxidative stress	Natarajan et al., 2020
	PS-NH_2	217 nm			
	PS-COOH	220 nm			
	PS-NH_2	200 nm	5 mg/L	Reduced bioavailability of TiO_2 and decrease oxidative stress and enhance photosynthetic yield	Natarajan et al., 2021
	PS-COOH				
Terrestrial plants					
Arabidopsis thaliana	PS-NH_2	200 nm	10, 50, and 100 μg/mL	Induced a higher accumulation of ROS and inhibit plant growth and seedling development	Sun X. D. et al., 2020
	PS-SO_3H				
	PS-COOH	40 nm	0.029 g/L	Accumulation of plastics at root surface and cap cells	Taylor et al., 2020
			8.3×10^{11} n/mL		
Maize	PS-NH_2	22 nm	10–500 ng/spot	Inhibit photosynthesis; inhibit growth; oxidative damage; and upset metabolic balance	Sun H. et al., 2021
	PS-COOH	24 nm			
Wheat	PS-COOH	40 nm	0.029 g/L	Accumulation of plastics at root surface and cap cells	Taylor et al., 2020
			8.3×10^{11} n/mL		
Aquatic animals in freshwater					
Daphnia magna-Zooplankton	PS-bare	100 nm	75 mg/L	Stimulate the antioxidant system	Lin et al., 2019
	PS-n-NH_2	50 and 100 nm	40 mg/L		

(Continued)

TABLE 1 | (Continued)

Species	NPs type	Particle size	Exposure concentration	Toxic effects	References
	PS-COOH	300 nm	70 mg/L		
	PS-p-NH_2	110 nm	100 mg/L		
	PS(-CNH_2NH_2 $^+$)	200 nm	50 and 150 mg/L	Acute toxicity	Saavedra et al., 2019
	PS(-COO-)				
Caenorhabditis elegans-Zooplankton	PS-bare	35 nm	1–1000 μg/L	Reproductive and gonadal developmental toxicity and genotoxicity	Qu et al., 2019
	PS-NH_2				
	PS-bare	35 nm	1–100 μg/L	Reproductive and gonadal developmental toxicity and genotoxicity	Sun L. et al., 2020
	PS-NH_2				
	PS-COOH	200 and 500 nm	100 nm/L	Reduce survival rate	Yilimulati et al., 2020
	PS-bare	50 and 60 nm	1–50 mg/L	Effects on survival, growth, and reproduction	Schultz et al., 2021
	PS-NH_2				
	PS-COOH				
	PS-bare	116.2 nm	1 and 10 μg/mL	Change cellular behavior	Kim et al., 2020
	PS-COOH	110.6 nm			
	PS-NH_2	120.2 nm			
Brachionus calyciflorus-Zooplankton	PS(-CNH_2NH_2 $^+$)	200 nm	50 and 150 mg/L	Acute toxicity	Saavedra et al., 2019
	PS(-COO-)				
Coregonus lavaretus	PS-COOH	50 nm	100 and 10000 pcs	Decrease sperm motility and reduce offspring body mass and impair swimming ability	Yaripour et al., 2021
Aquatic animals in seawater					
Brachionus plicatilis-Zooplankton	PS-NH_2	50 nm	0.5–50 μg/mL	Increase mortality rate	Manfra et al., 2017
	PS-COOH	40 nm			
Ciona robusta-Zooplankton	PS-NH_2	50 nm	2–15 μg/mL	Developmental toxicity and induced oxidative stress	Eliso et al., 2020
	PS-COOH	60 nm	5–100 μg/mL		
Artemia franciscana-Zooplankton	PS-NH_2	50 nm	1 and 10 μg/mL	Exfoliation; increase mortality rates; inhibit growth; inhibit activity; and regulate *clap* and *cstb* gene expressions	Bergami et al., 2017
	PS-COOH	40 nm			
	PS-NH_2	50 nm	0.1–10 μg /mL	Inhibit growth; inhibit gene expression; neurotoxicity; and higher mortality rate	Varó et al., 2019
	PS-NH_2	50 nm	5–100 μg/mL	Impair feeding, motility and multiple molting	Bergami et al., 2016
	PS-COOH	40 nm			
Mytilus galloprovincialis Lam.	PS-NH_2	50 nm	1–50 μg/mL	Stimulate increase in extracellular ROS and NO and induce lysosomal damage and a dramatic decrease in phagocytosis	Canesi et al., 2015
			0.001–20 mg/L	Induce malformations and a delay in development dysregulation of transcription of genes and decrease in shell length	Balbi et al., 2017
			0.15 mg/L		
			1–50 μg/mL	Increase cellular damage and ROS production and induce lysosomal damage and a dramatic decrease in phagocytosis	Canesi et al., 2016
			10 μg/L	Induce lysosomal release and a dramatic decrease in phagocytosis	Auguste et al., 2020a
			10 μg/L	Dysregulation of transcription of genes and affect immune function	Auguste et al., 2020b
Meretrix	PS-NH_2	100 nm	0.02–2 mg/L	Inhibit growth; disrupt energy homeostasis; Digestive tubule atrophy and necrosis; induce lysosomal damage; and inhibit phagocytic activity	Liu et al., 2021
Sea urchin	PS-NH_2	50 nm	1–50 μg/mL	Increase the appearance of malformations and undeveloped embryos and effects on gene expression	Della Torre et al., 2014
	PS-COOH	40 nm	2.5–50 μg/mL		
	PS-NH_2	50 nm	1 and 5 μg/mL	Induce lysosomal damage and a dramatic decrease in phagocytosis	Bergami et al., 2019
	PS-COOH	40 nm			
	PS-NH_2	50 nm	5–25 μg/mL	Induce lysosomal damage	Marques-Santos et al., 2018
Euphausia superba	PS-NH_2	50 nm	2.5 mg/L	Increase molting and inhibit swimming activity	Bergami et al., 2020

(Continued)

TABLE 1 | (Continued)

Species	NPs type	Particle size	Exposure concentration	Toxic effects	References
	PS-COOH	60 nm			
	PS-COOH	40 nm			
Crassostrea gigas	PS-bare	50 and 500 nm	0.1–25 μmg/L	Developmental toxicity and cytotoxicity	Tallec et al., 2018
	$PS-NH_2$	50 nm			
	PS-COOH	50 nm			
	$PS-NH_2$	100 nm	0.1–100 mg/L	ROS generation	González-Fernández et al., 2018
	PS-COOH	100 nm			
Mammalian animal					
Mice	PS-bare	100 nm	10 mg/mL	Weight loss induce cell apoptosis; inflammation; structural disorder; damage to the blood system; and lipid metabolism disorders	Xu et al., 2021
	$PS-NH_2$				
	PS-COOH				
	PS@Bap	192 nm	0.5 mg/mL	Protein corona and inhibit cell viability	Ji et al., 2020
	PS-bare	188 nm			
Mammalian cells *in vitro*					
Neonatal rat ventricular myocytes	$PS-NH_2$	50 nm	25 μg/mL	Damage contractility, glycolytic homeostasis and the mitochondrial activity of neonatal cardiomyocytes	Roshanzadeh et al., 2021
	PS-COOH				
Human cells *in vitro*					
HepG2	PS-bare	50 nm	10, 50, and 100 μg/mL	Inhibit cell viability; destroy cell morphology; and damage the antioxidant structure	He et al., 2020
	$PS-NH_2$				
	PS-COOH				
Caco-2/HT29-MTX-E12/THP-1	PS-bare	50 nm	1–50 $\mu g/cm^2$	Reduce cell viability; cytotoxicity; and decrease metabolic activity	Busch et al., 2020
	$PS-NH_2$				
	PS-COOH	50 and 500 nm	0.01–100 μg/mL	No effect on cell viability	Hesler et al., 2019
BEAS-2B	PS-bare	60 nm	1–40 μg/mL	Inhibit cell viability; increase ROS production; lead endoplasmic reticulum stress; and induce Lysosomal, autophagic cell death, and protein misfolding	Chiu et al., 2015
	$PS-NH_2$				
	PS-COOH				
Calu-3	PS-bare	50 nm	0.3–32.3 μg cm^{-2}	Decrease cell viability; induce genotoxicity; and increase ROS production	Paget et al., 2015
	$PS-NH_2$				
	PS-COOH				
Caco-2, HT29-MTX-E1, RajiB co-culture	PS-bare	50 and 100 nm	250 μg/mL	Shift the translocation rates; protein corona; and membrane integrity	Walczak et al., 2015
	$PS-NH_2$				
	PS-COOH				
Caco-2, HT29 and LS174T monocultures	PS-bare	60 nm	20–100 μg/mL	Inhibit cell viability; induce apoptosis; and induce mucin interaction and cell apoptosis	Inkielewicz-Stepniak et al., 2018
	$PS-NH_2$				
	PS-COOH				
THP-1	$PS-NH_2$	120 nm	1–100 μg/mL	Inhibit cell viability and polarization and induce inflammation	Fuchs et al., 2016
	PS-COOH				
THP-1	PS-bare	50 nm	0.3–32.3 μg cm^{-2}	Decrease cell viability; induce genotoxicity; and increase ROS production	Paget et al., 2015
	$PS-NH_2$				
	PS-COOH				
Human erythrocytes	PS-COOH	200 nm	50–2000 particles $cell^{-1}$	Sensitivity to osmotic, mechanical, oxidative and complement lysis	Pan et al., 2016
Astrocyte 131N	$PS-NH_2$	50 nm	100 μg/mL	Induce apoptosis and lysosomal cell death; cell membrane damage	Wang et al., 2013
	PS-COOH	40 nm			
Brain capillary endothelial cells	PS-COOH	40, 100, and 200 nm	25–100 μg/ mL	Affect cell viability; particle uptake; induce inflammation; and no cell death	Raghnaill et al., 2014
Human endothelial	PS-COOH	20, 40, 100, 200, and 500 nm	10–100 μg/mL	Cell viability, particle localization, lysosome function and integrity	Fröhlich et al., 2012
Alveolar cells	PS-NH2	50 nm	100 μg/mL	Interfere the mechanoadaptive capacity of alveolar cells; cyclic stretch induces higher ROS levels in alveolar cells treated with PS-NPs; and upregulate pro-apoptotic gene expressions	Roshanzadeh et al., 2020
	PS-COOH				

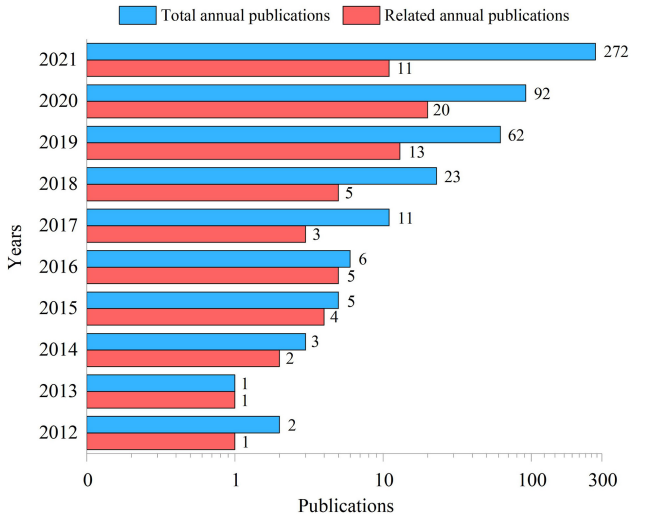

FIGURE 1 | Total annual publications and publications from 2012 to 2021 related to this manuscript indexed in Science Direct and Web of Science.

with mitotic cycle, reduction in chlorophyll content, and photosynthetic efficiency (Bellingeri et al., 2019). PS-NH_2 NPs with diameters of 90 and 200 nm decreased the biomass and the content of chlorophyll a in *Chlorella Vulgaris*, and mall-sized PS-NH_2 NPs were more toxic than large-sized ones (Khoshnamvand et al., 2021).

Positively charged NPs induced higher toxicology on the algae than negatively charged NPs, which was also due to the electrostatic interaction with bio-membrane. For example, PS-NH_2 NPs had higher adsorption ratios on the cell surface of the algae than bare PS and PS-COOH NPs, which limited the material transfer, gas exchange, and energy transfer in diatom (Seoane et al., 2019; González-Fernández et al., 2020). PS-NH_2 NPs more significantly inhibited the photo-system efficiency than PS-COOH NPs in *Pseudokirchneriella subcapitata* (Nolte et al., 2017) and PS-SO_3H NPs in *Microcystis aeruginosa* (Feng et al., 2020). Poly methyl methacrylate (PMMA) caused a higher impact on cellular and physiological parameters than PMMA-COOH (Gomes et al., 2020).

Land-based sources have been considered an important long-term sink for NPs (Rochman, 2018). NPs could accumulate and aggregate on the leaves of land-based plants, transfer from leaves to stems, and finally to roots (Yu et al., 2021). However, the toxicity of NPs to land-based plants was poorly understood although three relevant studies were reported recently. PS-COOH NPs mainly accumulated on the root surface and cap cells of *Arabidopsis thaliana* and wheat, rather than in roots (Taylor et al., 2020). Compared with PS-COOH NPs, PS-NH_2 NPs were more present in roots, which resulted in a stronger inhibitory effect on photosynthesis and growth of maize leaves; they also activated a more obvious oxidative defense mechanism (Sun H. et al., 2021). PS-NH_2 NPs induced a higher accumulation of ROS in *Arabidopsis thaliana*, and they inhibited the plant growth and the seedling development more strongly than PS-SO_3H NPs (Sun X. D. et al., 2020).

Animals and Mammalian/Human Cells *in vitro*

The functional groups of NPs influenced their toxicities to zooplankton in fresh water and seawater (Saavedra et al., 2019; Kim et al., 2020; Gola et al., 2021). PS-NH_2 NPs enhanced the gonad development, the reproductive capacity, and the genotoxicity to nematode (*Caenorhabditis elegan*) compared with bare PS NPs and PS-COOH NPs (Qu et al., 2019; Kim et al., 2020; Sun L. et al., 2020; Yilimulati et al., 2020; Schultz et al., 2021). Compared with PS-COOH NPs, PS-NH_2 NPs induced higher mortality in rotifers (*Brachionus plicatilis*) (Manfra et al., 2017); PS-NH_2 NPs caused more effects on the molting amount, the developmental toxicity on larval *Artemia franciscana* (Bergami et al., 2016, 2017; Varó et al., 2019), larval *Ciona robusta* (Eliso et al., 2020), and *Daphnia magna* (Lin et al., 2019); they also more significantly reduced the swimming activity of *Euphausia superba* (Bergami et al., 2020).

As for other aquatic animals, pre-fertilization exposure of sperm to PS-NH_2 NPs decreased offspring size and swimming performance in the European whitefish (*Coregonus lavaretus*) (Yaripour et al., 2021). PS-NH_2 NPs stimulated the increase in extracellular ROS, induced lysosomal damage, and decreased shell length in two kinds of mussels, *Mytilus galloprovincialis* (Canesi et al., 2015, 2016; Balbi et al., 2017; Auguste et al., 2020a,b) and *Meretrix* (Liu et al., 2021). Compared with PS-COOH NPs, PS-NH_2 NPs induced severe developmental defects and genetic regulations in the development of sea urchin (*Paracentrotus Lividus*) embryos (Della Torre et al., 2014). Nevertheless, the controversial joint effects were obtained in some cases. PS-COOH NPs had a significant increase in ROS production in sperm cells of *Crassostrea gigas*, whereas PS-NH_2 NPs did not (González-Fernández et al., 2018). In contrast to PS-COOH, positively charged PS-NH_2 seemed to affect the antioxidant and immune genetic responses differently and to a lesser extent in coelomocytes of the Antarctic sea urchin (Bergami et al., 2019).

Few studies have been conducted on their toxic effects on mammals except Xu et al. (2021) reported that PS-NH_2 NPs significantly affected the body weight of mice compared with PS-COOH NPs. Several *in vitro* studies on mammalian and human cells have also confirmed the high toxicity of positively charged NPs. PS-NH_2 NPs were more highly internalized in neonatal rat ventricular myocytes when compared with PS-COOH NPs, which resulted in decreased myocardial contractility (Roshanzadeh et al., 2021). PS-NH_2 NPs accumulated more than bare PS NPs in human hepatocellular carcinoma (*HepG2*) cells, and caused greater oxidative damage than PS-COOH NPs in *HepG2* cells (He et al., 2020). PS-NH_2 NPs increased the cytotoxicity and induced cell apoptosis of human *BEAS-2B* (Chiu et al., 2015), *Calu-3* (Paget et al., 2015), *Caco-2* (Walczak et al., 2015; Busch et al., 2020), *HT29-MTX-E12* (Inkielewicz-Stepniak et al., 2018), *THP-1* cell lines (Fuchs et al., 2016; Hesler et al., 2019), and human alveolar cells (Roshanzadeh et al., 2020). On

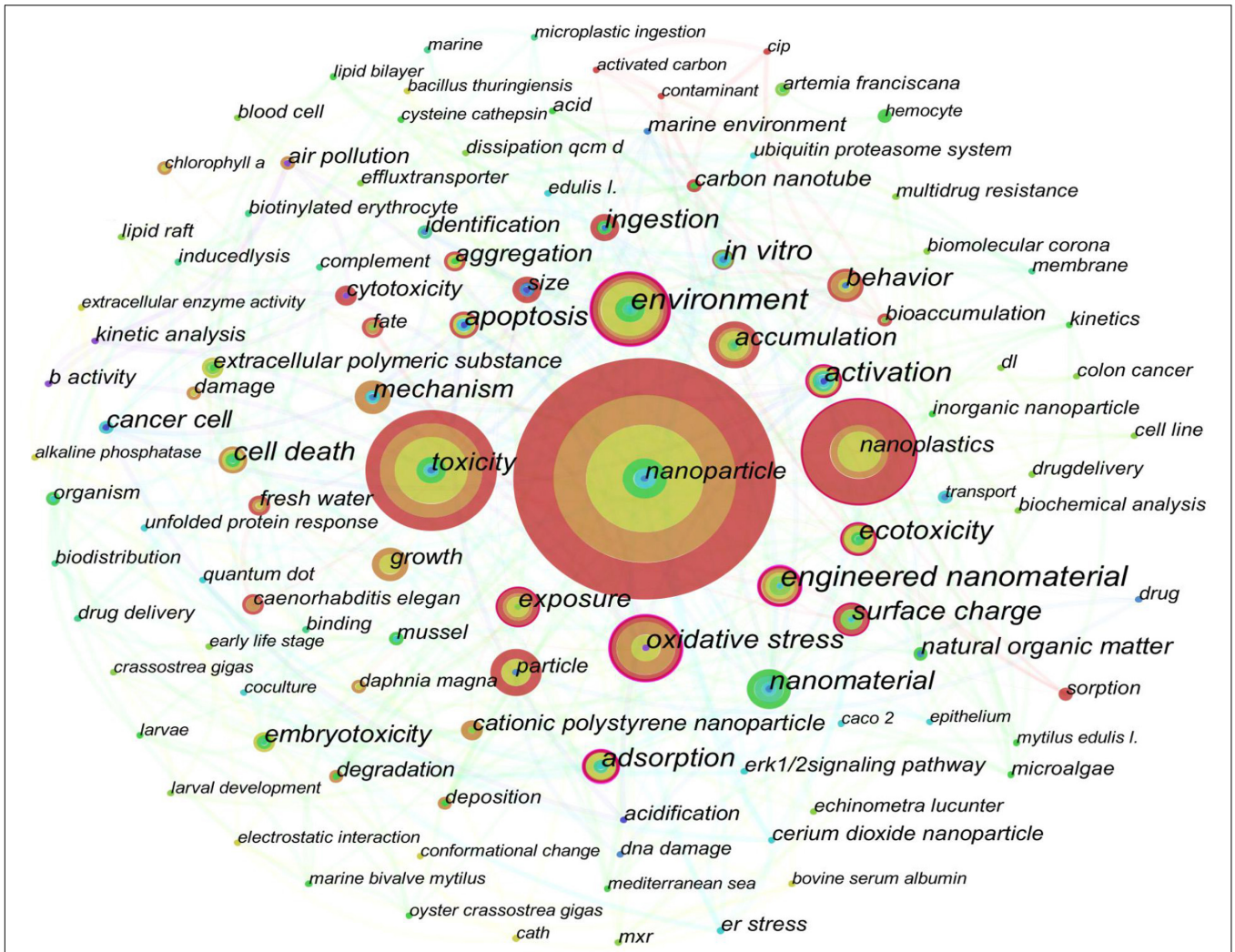

FIGURE 2 | Co-occurrence network of keywords extracted from the obtained literature. The size of each node represents the occurrence frequency of the corresponding keyword.

the contrary, bare PS NPs and PS-COOH NPs did not or were in a lesser extent.

TOXIC MECHANISM OF NANOPLASTICS WITH DIFFERENT FUNCTIONAL GROUP MODIFICATIONS

This manuscript summarizes the toxic effects of NPs with different functional groups in various organisms. Most studies focus on PS NPs, while research on other materials of NPs is lacking. The above mentioned studies show that NPs with different functional groups greatly impact on the toxicity of NPs, but most groups are concentrated in amino ($-NH_2$) and carboxyl ($-COOH$) groups. Only a few studies have been performed on the toxic effects of other functional groups. The surface charge of NPs considerably contribute to the toxic mechanisms of NPs (Banerjee and Shelver, 2020; Zhao et al., 2020). Positively charged NPs ($PS\text{-}NH_2$) usually induce stronger toxicity than bare NPs and negatively charged NPs (PS-COOH, $PS\text{-}SO_3H$ NPs, and PS-COC).

In general, the stimulatory effect of exogenous particles causes granulocytosis to generate ROS in organisms (Qin et al., 2021). Significant decreases in the cell viability and the changed membrane integrity due to the generation of ROS and other cellular parameters are common toxic mechanisms in the microorganisms, algae, plants, animals, and mammalian/human cells *in vitro* we reviewed above. Positively charged NPs are more likely to interact with the cell membranes due to the negative charges of cell surfaces and cell walls; thus, they will generate more ROS (Sun X. D. et al., 2020), which will result in more effects on oxidative stresses, changes in membrane permeability, and destruction of cell function; they even induce cell apoptosis (Pan et al., 2016; Ning et al., 2021).

Nevertheless, the differences of toxicity mechanisms affected by charged groups of NPs still exist among different species. For

microorganisms, the toxic mechanism is limited to the membrane disruption via the generated ROS (Sun et al., 2018), because larger particles cannot be internalized. Algae and plant cells are affected mainly by the adsorption of NPs to the surface through disrupted/damaged membrane, aquaporins, and cell pores, and further cause ROS generation and sequentially damage to the photosynthesis system (Sun H. et al., 2021). As for animal/human cells, the cellular processes of NPs internalized into lysosomesis are also related to their different surface charges (Fröhlich et al., 2012; Raghnaill et al., 2014). Negative NPs can escape from lysosomes and interact with cellular components to trigger cellular stress (Wang et al., 2013; Marques-Santos et al., 2018; Matthews et al., 2021), whereas Positive NPs destabilize lysosomes and initiate a cascade of cellular damage via ROS generation due to the proton sponge hypothesis (Nel et al., 2009). Thus, the cellular process of NPs in animals and human beings might be more complicatedly affected by their charged groups.

The eco-corona on the surface of NPs will be stimulated through coating different components of natural organic matters (NOMs; Grassi et al., 2020). The eco-corona formation enhances the aggregation of the NPs and accompanied with the decreased effective surface area, which will reduce the toxic impact of NPs (Bergami et al., 2017). The formation of the eco-corona is also influenced by the surface charge of NPs (Saavedra et al., 2019). Negatively charged NPs are more effective to form the eco-corona in the presence of EPS than positively charged NPs, which helps them in more significantly lessening the oxidative stress and cytotoxic impact on biological cells (Natarajan et al., 2020, 2021). However, the characteristics of the surrounding environment will significantly influence the biological effects of eco-corona on NPs. For example, PS-NH_2 NPs are usually better dispersed than PS-COOH NPs in nature seawater (Della Torre et al., 2014; Bergami et al., 2019). Yet the abundance and composition of NOMs vary significantly across different seawater bodies. Humic acids (HA), one of the main compositions of NOMs in seawater, was found to stabilize negatively charged NPs due to electrostatic repulsion between negative charges and steric effect, whereas it induced PS-NH_2 NPs to agglomerate (Wu et al., 2019). Thus, the controversial joint effects might be obtained in marine organisms in some cases (González-Fernández et al., 2018; Bergami et al., 2019).

In addition, the types and charges of surface chemical modification will affect the formation of the protein corona on NPs (Ji et al., 2020). The protein corona might be formed on the surface of NPs when they enter the physiological environment (Li et al., 2020). The formation of the protein corona in the serum is considered as a general protective effect from the potential cytotoxicity of NPs (Coglitore et al., 2019), because they reduce NP surface energy by non-specific adsorption, which leads to the lowered membrane adhesion and uptake efficiency (Lesniak et al., 2013). Positively charged NPs usually adsorb more plasma proteins than negatively charged NPs, which cause more opportunities for them to form the protein corona (Liu et al., 2019). Thus, positively charged NPs are hypothesized to weaken their toxicity more than negatively charged NPs. However, the formation of a PS-NH_2-protein corona in hemolymph serum (HS) increased the short term cellular damage and ROS production of PS-NH_2 toward immunocytes (Canesi et al., 2016), because NP-protein complexes were hypothesized to function as recognizable molecular patterns to be cleared by phagocytic cells (Hayashi et al., 2013). In addition, the enhanced formation of the protein corona on positively charged NPs will promote their "Trojan-horse effect" on other pollutants (Matthews et al., 2021). The studies on the biological effects of NPs with the protein corona are still in the initial stage. Most of recent results obtained were *in vitro*, which do not entirely reflect a realistic exposure scenario *in vivo*. More efforts should be contributed on the specific cell biological behavior of various NPs in the real environment, not limited to their effects on cell uptake efficiency and biocompatibility (Qin et al., 2021).

CONCLUSION AND RESEARCH PROSPECTS

In sum, amino-modified polystyrene nanoparticles (PS-NH_2) usually induce stronger toxicity than modified NPs, due to their positively charge characteristics. Positively charged NPs are more likely to interact with the cell membranes and generate more ROS than negatively charged NPs, which is mainly due to the negative charges of cell surfaces and cell walls. Nevertheless, there are still some differences existed among different species in the toxicity mechanisms of NPs affected by charged groups. The biological effects of NPs with the eco-corona and protein corona also contribute a lot to their differentiate toxic mechanisms. The exact environmental distributions of these functional group-modified NPs are unclear to date due to the limitations of quantitative detection. The mass balance of NPs between intake and excretion in organisms is also far from being established. Thus, the transmission of these modified NPs on organisms needs to be further researched. Reducing the inherent toxicity of NPs will be an urgent topic due to the substantial environmental problems they induced. The effect of NPs in the long-term exposure and in reality should also be explored.

AUTHOR CONTRIBUTIONS

HZ: data curation and writing—original draft preparation. YW and HC: data curation. YS and WC: data collection. ZD: supervision, writing, reviewing, editing, and resources. LQ: conceptualization, writing, reviewing, and editing. All authors contributed to the article and approved the submitted version.

FUNDING

This work was financially supported by the National Natural Science Foundation of China (41807487) and National College Students Innovation and Entrepreneurship Training Program of China (202010060009).

REFERENCES

Alak, G., Köktürk, M., and Atamanalp, M. (2021). Evaluation of different packaging methods and storage temperature on MPs abundance and fillet quality of rainbow trout. *J. Hazard. Mater.* 420:126573. doi: 10.1016/j.jhazmat.2021.126573

Auguste, M., Lasa, A., Balbi, T., Pallavicini, A., Vezzulli, L., et al. (2020a). Impact of nanoplastics on hemolymph immune parameters and microbiota composition in *Mytilus galloprovincialis*. *Mar. Environ. Res.* 159:105017. doi: 10.1016/j.marenvres.2020.105017

Auguste, M., Balbi, T., Ciacci, C., Canonico, B., Papa, S., Borello, A., et al. (2020b). Shift in immune parameters after repeated exposure to nanoplastics in the marine bivalve *Mytilus*. *Front. Immunol.* 11:426. doi: 10.3389/fimmu.2020.00426

Aznar, M., Ubeda, S., Dreolin, N., and Nerín, C. (2019). Determination of non-volatile components of a biodegradable food packaging material based on polyester and polylactic acid (PLA) and its migration to food simulants. *J. Chromatogr. A* 583, 1–8. doi: 10.1016/j.chroma.2018.10.055

Balbi, T., Camisassi, G., Montagna, M., Fabbri, R., Franzellitti, S., Carbone, C., et al. (2017). Impact of cationic polystyrene nanoparticles (PS-NH2) on early embryo development of *Mytilus galloprovincialis*: effects on shell formation. *Chemosphere* 186, 1–9. doi: 10.1016/j.chemosphere.2017.07.120

Banerjee, A., and Shelver, W. L. (2020). Micro- and nanoplastic induced cellular toxicity in mammals: a review. *Sci. Total Environ.* 755(Pt. 2):142518. doi: 10.1016/j.scitotenv.2020.142518

Bellingeri, A., Bergami, E., Grassi, G., Faleri, C., Redondo-Hasselerharm, P., Koelmans, A. A., et al. (2019). Combined effects of nanoplastics and copper on the freshwater alga *Raphidocelis subcapitata*. *Aquat. Toxicol.* 210, 179–187. doi: 10.1016/j.aquatox.2019.02.022

Bergami, E., Bocci, E., Vannuccini, M. L., Monopoli, M., Salvati, A., Dawson, K. A., et al. (2016). Nano-sized polystyrene affects feeding, behavior and physiology of brine shrimp *Artemia franciscana* larvae. *Ecotoxicol. Environm. Saf.* 123, 18–25. doi: 10.1016/j.ecoenv.2015.09.021

Bergami, E., Krupinski Emerenciano, A., González-Aravena, M., Cárdenas, C. A., Hernández, P., Silva, J., et al. (2019). Polystyrene nanoparticles affect the innate immune system of the Antarctic sea urchin *Sterechinus neumayeri*. *Polar Biol.* 42, 743–757. doi: 10.1007/s00300-019-02468-6

Bergami, E., Manno, C., Cappello, S., Vannuccini, M. L., and Corsi, I. (2020). Nanoplastics affect moulting and faecal pellet sinking in Antarctic krill (*Euphausia superba*) juveniles. *Environ. Int.* 143:105999. doi: 10.1016/j.envint.2020.105999

Bergami, E., Pugnalini, S., Vannuccini, M. L., Manfra, L., Faleri, C., Savorelli, F., et al. (2017). Long-term toxicity of surface-charged polystyrene nanoplastics to marine planktonic species *Dunaliella tertiolecta* and *Artemia franciscana*. *Aquat. Toxicol.* 189, 159–169. doi: 10.1016/j.aquatox.2017.06.008

Busch, M., Bredeck, G., Kämpfer, A. A. M., and Schins, R. P. F. (2020). Investigations of acute effects of polystyrene and polyvinyl chloride micro- and nanoplastics in an advanced in vitro triple culture model of the healthy and inflamed intestine. *Environ. Res.* 193:110536. doi: 10.1016/j.envres.2020.110536

Canesi, L., Ciacci, C., Bergami, E., Monopoli, M. P., Dawson, K. A., Papa, S., et al. (2015). Evidence for immunomodulation and apoptotic processes induced by cationic polystyrene nanoparticles in the hemocytes of the marine bivalve *Mytilus*. *Mar. Environ. Res.* 111, 34–40. doi: 10.1016/j.marenvres.2015.06.008

Canesi, L., Ciacci, C., Fabbri, R., Balbi, T., Salis, A., Damonte, G., et al. (2016). Interactions of cationic polystyrene nanoparticles with marine bivalve hemocytes in a physiological environment: role of soluble hemolymph proteins. *Environ. Res.* 150, 73–81. doi: 10.1016/j.envres.2016.05.045

Cheng, H., Feng, Y., Duan, Z., Duan, X., Zhao, S., Wang, Y., et al. (2020). Toxicities of microplastic fibers and granules on the development of zebrafish embryos and their combined effects with cadmium. *Chemosphere* 269:128677. doi: 10.1016/j.chemosphere.2020.128677

Chiu, H. W., Xia, T., Lee, Y. H., Chen, C. W., Tsai, J. C., and Wang, Y. J. (2015). Cationic polystyrene nanospheres induce autophagic cell death through the induction of endoplasmic reticulum stress. *Nanoscale* 7, 736–746. doi: 10.1039/c4nr05509h

Coglitore, D., Janot, J. M., and Balme, S. (2019). Protein at liquid solid interfaces: toward a new paradigm to change the approach to design hybrid protein/solid-state materials. *Adv. Coll. Interface Sci.* 270, 278–292. doi: 10.1016/j.cis.2019.07.004

Della Torre, C., Bergami, E., Salvati, A., Faleri, C., Cirino, P., Dawson, K. A., et al. (2014). Accumulation and embryotoxicity of polystyrene nanoparticles at early stage of development of sea urchin embryos *Paracentrotus lividus*. *Environ. Sci. Technol.* 48, 12302–12311. doi: 10.1021/es502569w

Duan, Z., Duan, X., Zhao, S., Wang, X., Wang, J., Liu, Y., et al. (2020). Barrier function of zebrafish embryonic chorions against microplastics and nanoplastics and its impact on embryo development. *J. Hazard. Mater.* 395:122621. doi: 10.1016/j.jhazmat.2020.122621

Eliso, M. C., Bergami, E., Manfra, L., Spagnuolo, A., and Corsi, I. (2020). Toxicity of nanoplastics during the embryogenesis of the ascidian *Ciona robusta* (Phylum Chordata). *Nanotoxicology* 14, 1415–1431. doi: 10.1080/17435390.2020.1838650

Feng, L., Li, J., Xu, E. G., Sun, X., Zhu, F., Ding, Z., et al. (2019). Short-term exposure of positively charged polystyrene nanoparticles causes oxidative stress and membrane destruction in cyanobacteria. *Environ. Sci. Nano* 6, 3072–3079. doi: 10.1039/c9en00807a

Feng, L., Sun, X., Zhu, F., Feng, Y., Duan, J., Xiao, F., et al. (2020). Nanoplastics promote microcystin synthesis and release from cyanobacterial *Microcystis aeruginosa*. *Environ. Sci. Technol.* 54, 3386–3394. doi: 10.1021/acs.est.9b06085

Fröhlich, E., Meindl, C., Roblegg, E., Ebner, B., Absenger, M., and Pieber, T. R. (2012). Action of polystyrene nanoparticles of different sizes on lysosomal function and integrity. *Part. Fibre Toxicol.* 9:26. doi: 10.1186/1743-8977-9-26

Fuchs, A. K., Syrovets, T., Haas, K. A., Loos, C., Musyanovych, A., Mailänder, V., et al. (2016). Carboxyl- and amino-functionalized polystyrene nanoparticles differentially affect the polarization profile of M1 and M2 macrophage subsets. *Biomaterials* 85, 78–87. doi: 10.1016/j.biomaterials.2016.01.064

Gola, D., Kumar Tyagi, P., Arya, A., Chauhan, N., Agarwal, M., Singh, S. K., et al. (2021). The impact of microplastics on marine environment: a review. *Environ. Nanotechnol. Monit. Manag.* 16:100552. doi: 10.1016/j.enmm.2021.100552

Gomes, T., Almeida, A. C., and Georgantzopoulou, A. (2020). Characterization of cell responses in *Rhodomonas baltica* exposed to Pmma nanoplastics. *Sci. Total Environ.* 726:138547. doi: 10.1016/j.scitotenv.2020.138547

González-Fernández, C., Le Grand, F., Bideau, A., Huvet, A., Paul-Pont, I., and Soudant, P. (2020). Nanoplastics exposure modulate lipid and pigment compositions in diatoms. *Environ. Pollut.* 262:114274.

González-Fernández, C., Tallec, K., Le Goïc, N., Lambert, C., Soudant, P., Huvet, A., et al. (2018). Cellular responses of Pacific oyster (*Crassostrea gigas*) gametes exposed in vitro to polystyrene nanoparticles. *Chemosphere* 208, 764–772. doi: 10.1016/j.chemosphere.2018.06.039

González-Fernández, C., Toullec, J., Lambert, C., Goic, N. L., Seoane, M., Moriceau, B., et al. (2019). Do transparent exopolymeric particles (tep) affect the toxicity of nanoplastics on chaetoceros neogracile? *Environ. Pollut.* 250, 873–882. doi: 10.1016/j.envpol.2019.04.093

Grassi, G., Gabellieri, E., Cioni, P., Paccagnini, E., Faleri, C., Lupetti, P., et al. (2020). Interplay between extracellular polymeric substances (EPS) from a marine diatom and model nanoplastic through eco-corona formation. *Sci. Total Environ.* 725:138457. doi: 10.1016/j.scitotenv.2020.138457

Hayashi, Y., Miclaus, T., Scavenius, C., Kwiatkowska, K., Sobota, A., Engelmann, P., et al. (2013). Species differences take shape at nanoparticles: protein corona made of the native repertoireassists cellular interaction. *Environ. Sci. Technol.* 47, 14367–14375.

He, Y., Li, J., Chen, J., Miao, X., Li, G., He, Q., et al. (2020). Cytotoxic effects of polystyrene nanoplastics with different surface functionalization on human HepG2 cells. *Sci. Total Environ.* 723:138180. doi: 10.1016/j.scitotenv.2020.138180

Heddagaard, F. E., and Møller, P. (2019). Hazard assessment of small-size plastic particles: is the conceptual framework of particle toxicology useful? *Food Chem. Toxicol.* 136:111106. doi: 10.1016/j.fct.2019.111106

Hesler, M., Aengenheister, L., Ellinger, B., Drexel, R., Straskraba, S., Jost, C., et al. (2019). Multi-endpoint toxicological assessment of polystyrene nano- and microparticles in different biological models in vitro. *Toxicol. In Vitro* 61:104610. doi: 10.1016/j.tiv.2019.104610

Huang, D., Tao, J., Cheng, M., Deng, R., Chen, S., Yin, L., et al. (2020). Microplastics and nanoplastics in the environment: macroscopic transport and effects on creatures. *J. Hazard. Mater.* 407:124399. doi: 10.1016/j.jhazmat.2020.124399

Inkielewicz-Stepniak, I., Tajber, L., Behan, G., Zhang, H., Radomski, M., Medina, C., et al. (2018). The role of mucin in the toxicological impact of polystyrene nanoparticles. *Materials* 11:724. doi: 10.3390/ma11050724

Ji, Y., Wang, Y., Shen, D., Kang, Q., and Chen, L. (2020). Mucin corona delays intracellular trafficking and alleviates cytotoxicity of nanoplastic-benzopyrene combined contaminant. *J. Hazard. Mater.* 406:124306. doi: 10.1016/j.jhazmat.2020.124306

Khoshnamvand, M., Hanachi, P., Ashtiani, S., and Walker, T. R. (2021). Toxic effects of polystyrene nanoplastics on microalgae *Chlorella vulgaris*: changes in biomass, photosynthetic pigments and morphology. *Chemosphere* 280:130725. doi: 10.1016/j.chemosphere.2021.130725

Kim, H. M., Long, N. P., Min, J. E., Anh, N. H., Kim, S. J., Yoon, S. J., et al. (2020). Comprehensive phenotyping and multi-omic profiling in the toxicity assessment of nanopolystyrene with different surface properties. *J. Hazard. Mater.* 399:123005. doi: 10.1016/j.jhazmat.2020.123005

Lesniak, A., Salvati, A., Santos-Martinez, M. J., Radomski, M. W., Dawson, K. A., and Aberg, C. (2013). Nanoparticle adhesion to the cell membrane and its effect on nano-particle uptake efficiency. *J. Am. Chem. Soc.* 135, 1438–1444. doi: 10.1021/ja309812z

Li, X., He, E., Jiang, K., Peijnenburg, W. J. G. M., and Qiu, H. (2020). The crucial role of a protein corona in determining the aggregation kinetics and colloidal stability of polystyrene nanoplastics. *Water Res.* 190:116742. doi: 10.1016/j.watres.2020.116742

Lin, W., Jiang, R., Hu, S., Xiao, X., Wu, J., Wei, S., et al. (2019). Investigating the toxicities of different functionalized polystyrene nanoplastics on *Daphnia magna*. *Ecotoxicol. Environ. Saf.* 180, 509–516. doi: 10.1016/j.ecoenv.2019.05.036

Liu, L., Zheng, H., Luan, L., Luo, X., Wang, X., Lu, H., et al. (2021). Functionalized polystyrene nanoplastic-induced energy homeostasis imbalance and the immunomodulation dysfunction of marine clams (*Meretrix meretrix*) at environmentally relevant concentrations. *Environ. Sci. Nano* 8, 2030–2048. doi: 10.1039/d1en00212k

Liu, N., Tang, M., and Ding, J. (2019). The interaction between nanoparticles-protein corona complex and cells and its toxic effect on cells. *Chemosphere* 245:125624. doi: 10.1016/j.chemosphere.2019.125624

Liu, X., Ma, J., Yang, C., Wang, L., and Tang, J. (2020). The toxicity effects of nano/microplastics on an antibiotic producing strain – *Streptomyces coelicolor* M145. *Sci. Total Environ.* 764:142804. doi: 10.1016/j.scitotenv.2020.142804

Luan, L., Wang, X., Zheng, H., Liu, L., Luo, X., and Li, F. (2019). Differential toxicity of functionalized polystyrene microplastics to clams (*Meretrix meretrix*) at three key development stages of life history. *Mar. Pollut. Bull.* 139, 346–354. doi: 10.1016/j.marpolbul.2019.01.003

Manfra, L., Rotini, A., Bergami, E., Grassi, G., Faleri, C., and Corsi, I. (2017). Comparative ecotoxicity of polystyrene nanoparticles in natural seawater and reconstituted seawater using the rotifer *Brachionus plicatilis*. *Ecotoxicol. Environ. Saf.* 145, 557–563. doi: 10.1016/j.ecoenv.2017.07.068

Marques-Santos, L. F., Grassi, G., Bergami, E., Faleri, C., Balbi, T., Salis, A., et al. (2018). Cationic polystyrene nanoparticle and the sea urchin immune system: biocorona formation, cell toxicity, and multixenobiotic resistance phenotype. *Nanotoxicology* 12, 1–21. doi: 10.1080/17435390.2018.1482378

Mateos-Cárdenas, A., van Pelt, F. N. A. M., O'Halloran, J., and Jansen, M. A. K. (2021). Adsorption, uptake and toxicity of micro- and nanoplastics: effects on terrestrial plants and aquatic macrophytes. *Environ. Pollut.* 284:117183. doi: 10.1016/j.envpol.2021.117183

Matthews, S., Mai, L., Jeong, C. B., Lee, J. S., Zeng, E. Y., and Xu, E. G. (2021). Key mechanisms of micro- and nanoplastic (MNP) toxicity across taxonomic groups. *Comp. Biochem. Physiol. Part C Toxicol. Pharmacol.* 247:109056. doi: 10.1016/j.cbpc.2021.109056

Miao, L., Hou, J., You, G., Liu, Z., Liu, S., Li, T., et al. (2019). Acute effects of nanoplastics and microplastics on periphytic biofilms depending on particle size, concentration and surface modification. *Environ. Pollut.* 255(Pt. 2):113300. doi: 10.1016/j.envpol.2019.113300

Natarajan, L., Jenifer, M. A., Chandrasekaran, N., Suraishkumar, G. K., and Mukherjee, A. (2021). Polystyrene nanoplastics diminish the toxic effects of Nano-TiO2 in marine algae *Chlorella* sp. *Environ. Res.* 204:112400. doi: 10.1016/j.envres.2021.1

Natarajan, L., Omer, S., Jetly, N., Jenifer, M. A., Chandrasekaran, N., Suraishkumar, G. K., et al. (2020). Eco-corona formation lessens the toxic effects of polystyrene nanoplastics towards marine microalgae *Chlorella* sp. *Environ. Res.* 188:109842. doi: 10.1016/j.envres.2020.109842

Nel, A. E., Mädler, L., Velegol, D., Xia, T., Hoek, E. M. V., Somasundaran, P., et al. (2009). Understanding biophysicochemical interactions at the nano–bio interface. *Nat. Mater.* 8, 543–557. doi: 10.1038/nmat2442

Ning, Q., Wang, D., An, J., Ding, Q., Huang, Z., Zou, Y., et al. (2021). Combined effects of nanosized polystyrene and erythromycin on bacterial growth and resistance mutations in *Escherichia coli*. *J. Hazard. Mater.* 422:126858. doi: 10.1016/j.jhazmat.2021.126858

Nolte, T. M., Hartmann, N. B., Kleijn, J. M., Garnæs, J., van de Meent, D., Jan Hendriks, A., et al. (2017). The toxicity of plastic nanoparticles to green algae as influenced by surface modification, medium hardness and cellular adsorption. *Aquat. Toxicol.* 183, 11–20. doi: 10.1016/j.aquatox.2016.12.005

Paget, V., Dekali, S., Kortulewski, T., Grall, R., Gamez, C., Blazy, K., et al. (2015). Specific uptake and genotoxicity induced by polystyrene nanobeads with distinct surface chemistry on human lung epithelial cells and macrophages. *PLoS One* 10:e0123297. doi: 10.1371/journal.pone.0123297

Pan, D., Vargas-Morales, O., Zern, B., Anselmo, A. C., Gupta, V., Zakrewsky, M., et al. (2016). The effect of polymeric nanoparticles on biocompatibility of carrier red blood cells. *PLoS One* 11:e0152074. doi: 10.1371/journal.pone.0152074

Qian, J., He, X., Wang, P., Xu, B., Li, K., Lu, B., et al. (2021). Effects of polystyrene nanoplastics on extracellular polymeric substance composition of activated sludge: the role of surface functional groups. *Environ. Pollut.* 279:116904. doi: 10.1016/j.envpol.2021.116904

Qin, L., Duan, Z., Cheng, H., Wang, Y., Zhang, H., Zhu, Z., et al. (2021). Size-dependent impact of polystyrene microplastics on the toxicity of cadmium through altering neutrophil expression and metabolic regulation in zebrafish larvae. *Environ. Pollut.* 291:118169. doi: 10.1016/j.envpol.2021.118169

Qu, M., Qiu, Y., Kong, Y., and Wang, D. (2019). Amino modification enhances reproductive toxicity of nanopolystyrene on gonad development and reproductive capacity in nematode *Caenorhabditis elegans*. *Environ. Pollut.* 254(Pt. A):112978. doi: 10.1016/j.envpol.2019.112978

Raghnaill, M. N., Bramini, M., Ye, D., Couraud, P. O., Romero, I. A., Weksler, B., et al. (2014). Paracrine signaling of inflammatory cytokines from an in vitro blood brain barrier model upon exposure to polymeric nanoparticles. *Analyst* 139, 923–930. doi: 10.1039/C3AN01621H

Rochman, C. M. (2018). Microplastics research-from sink to source. *Science* 360, 28–29. doi: 10.1126/science.aar7734

Roshanzadeh, A., Oyunbaatar, N. E., Ganjbakhsh, S. E., Park, S., Kim, D. S., Kanade, P. P., et al. (2021). Exposure to nanoplastics impairs collective contractility of neonatal cardiomyocytes under electrical synchronizatio. *Biomaterials* 278:121175. doi: 10.1016/j.biomaterials.2021.121175

Roshanzadeh, A., Park, S., Ehteshamzadeh Ganjbakhsh, S., Park, J., Lee, D. H., Lee, S., et al. (2020). Surface Charge-dependent cytotoxicity of plastic nanoparticles in alveolar cells under cyclic stretches. *Nano Lett.* 20, 7168–7176. doi: 10.1021/acs.nanolett.0c02463

Saavedra, J., Stoll, S., and Slaveykova, V. I. (2019). Influence of nanoplastic surface charge on eco-corona formation, aggregation and toxicity to freshwater zooplankton. *Environ. Pollut.* 252, 715–722. doi: 10.1016/j.envpol.2019.05.135

Schirinzi, G. F., Llorca, M., Seró, R., Moyano, E., Barceló, D., Abad, E., et al. (2019). Trace analysis of polystyrene microplastics in natural waters. *Chemosphere* 236:124321. doi: 10.1016/j.chemosphere.2019.07.052

Schultz, C. L., Bart, S., Lahive, E., and Spurgeon, D. J. (2021). What is on the outside matters—surface charge and dissolve organic matter association affect the toxicity and physiological mode of action of polystyrene nanoplastics to C. *elegans*. *Environ. Sci. Technol.* 55, 6065–6075. doi: 10.1021/acs.est.0c07121

Seoane, M., González-Fernández, C., Soudant, P., Huvet, A., Esperanza, M., Cid, Á, et al. (2019). Polystyrene microbeads modulate the energy metabolism of the marine diatom *Chaetoceros neogracile*. *Environ. Pollut.* 251, 363–371. doi: 10.1016/j.envpol.2019.04.142

Shen, M., Zhang, Y., Zhu, Y., Song, B., Zeng, G., Hu, D., et al. (2019). Recent advances in toxicological research of nanoplastics in the environment: a review. *Environ. Pollut.* 252(Pt. A), 511–521. doi: 10.1016/j.envpol.2019.05.102

Sun, H., Lei, C., Xu, J., and Li, R. (2021). Foliar uptake and leaf-to-root translocation of nanoplastics with different coating charge in maize plants. *J. Hazard. Mater.* 416:125854. doi: 10.1016/j.jhazmat.2021.125854

Sun, L., Liao, K., and Wang, D. (2020). Comparison of transgenerational reproductive toxicity induced by pristine and amino modified nanoplastics in *Caenorhabditis elegans*. *Sci. Total Environ.* 768:144362. doi: 10.1016/j.scitotenv.2020.144362

Sun, M., Ding, R., Ma, Y., Sun, Q., Ren, X., Sun, Z., et al. (2021). Cardiovascular toxicity assessment of polyethylene nanoplastics on developing zebrafish embryos. *Chemosphere* 282:131124. doi: 10.1016/j.chemosphere.2021.131124

Sun, X. D., Yuan, X. Z., Jia, Y., Feng, L. J., Zhu, F. P., Dong, S. S., et al. (2020). Differentially charged nanoplastics demonstrate distinct accumulation in *Arabidopsis thaliana*. *Nat. Nanotechnol.* 15, 755–760. doi: 10.1038/s41565-020-0707-4

Sun, X., Chen, B., Li, Q., Liu, N., Xia, B., Zhu, L., et al. (2018). Toxicities of polystyrene nano- and microplastics toward marine bacterium *Halomonas alkaliphila*. *Sci. Total Environ.* 642, 1378–1385. doi: 10.1016/j.scitotenv.2018.06.141

Tallec, K., Huvet, A., Di Poi, C., González-Fernández, C., Lambert, C., Petton, B., et al. (2018). Nanoplastics impaired oyster free living stages, gametes and embryos. *Environ. Pollut.* 242, 1226–1235.

Taylor, S. E., Pearce, C. I., Sanguinet, K. A., Hu, D., Chrisler, W. B., Kim, Y. M., et al. (2020). Polystyrene nano- and microplastic accumulation at *Arabidopsis* and wheat root cap cells, but no evidence for uptake into roots. *Environ. Sci. Nano* 7, 1942–1953. doi: 10.1039/d0en00309c

Varó, I., Perini, A., Torreblanca, A., Garcia, Y., Bergami, E., Vannuccini, M. L., et al. (2019). Time-dependent effects of polystyrene nanoparticles in brine shrimp *Artemia franciscana* at physiological, biochemical and molecular levels. *Sci. Total Environ.* 675, 570–580. doi: 10.1016/j.scitotenv.2019.04.157

Walczak, A. P., Kramer, E., Hendriksen, P. J. M., Tromp, P., Helsper, J. P. F. G., van der Zande, M., et al. (2015). Translocation of differently sized and charged polystyrene nanoparticles in vitro intestinal cell models of increasing complexity. *Nanotoxicology* 9, 453–461. doi: 10.3109/17435390.2014.944599

Wang, F., Yu, L., Monopoli, M. P., Sandin, P., Mahon, E., Salvati, A., et al. (2013). The biomolecular corona is retained during nanoparticle uptake and protects the cells from the damage induced by cationic nanoparticles until degraded in the lysosomes. *Nanomedicine* 9, 1159–1168. doi: 10.1016/j.nano.2013.04.010

Wang, X., Liu, L., Zheng, H., Wang, M., Fu, Y., Luo, X., et al. (2019). Polystyrene microplastics impaired the feeding and swimming behavior of mysid shrimp *Neomysis japonica*. *Mar. Pollut. Bull.* 50:110660. doi: 10.1016/j.marpolbul.2019.110660

Wu, J., Jiang, R., Lin, W., and Ouyang, G. (2019). Effect of salinity and humic acid on the aggregation and toxicity of polystyrene nanoplastics with different functional groups and charges. *Environ. Pollut.* 245, 836–843.

Xu, D., Ma, Y., Han, X., and Chen, Y. (2021). Systematic toxicity evaluation of polystyrene nanoplastics on mice and molecular mechanism investigation about their internalization into Caco-2 cells. *J. Hazard. Mater.* 417:126092. doi: 10.1016/j.jhazmat.2021.126092

Yaripour, S., Huuskonen, H., Rahman, T., Keklinen, J., Akkanen, J., Magris, M., et al. (2021). Pre-fertilization exposure of sperm to nano-sized plastic particles decreases offspring size and swimming performance in the European whitefish (*Coregonus lavaretus*). *Environ. Pollut.* 291:118196. doi: 10.1016/j.envpol.2021.118196

Yilimulati, M., Wang, L., Ma, X., Yang, C., and Habibul, N. (2020). Adsorption of ciprofloxacin to functionalized nano-sized polystyrene plastic: kinetics, thermochemistry and toxicity. *Sci. Total Environ.* 750:142370. doi: 10.1016/j.scitotenv.2020.142370

Yu, Z., Song, S., Xu, X., Ma, Q., and Lu, Y. (2021). Sources, migration, accumulation and influence of microplastics in terrestrial plant communities. *Environ. Exp. Bot.* 192:104635. doi: 10.1016/j.envexpbot.2021.104635

Zhang, K., Hamidian, A. H., Tubić, A., Zhang, Y., Fang, J. K. H., Wu, C., et al. (2021). Understanding plastic degradation and microplastic formation in the environment: a review. *Environ. Pollut.* 274:116554. doi: 10.1016/j.envpol.2021.116554

Zhao, T., Tan, L., Zhu, X., Huang, W., and Wang, J. (2020). Size-dependent oxidative stress effect of nano/micro-scaled polystyrene on *Karenia mikimotoi*. *Mar. Pollut. Bull.* 154:111074. doi: 10.1016/j.marpolbul.2020.111074

Conflict of Interest: The authors declare that the research was conducted in the absence of any commercial or financial relationships that could be construed as a potential conflict of interest.

frontiers in Marine Science

ORIGINAL RESEARCH
published: 13 January 2022
doi: 10.3389/fmars.2021.789615

Distribution and Characteristics of Microplastics in Barnacles and Wild Bivalves on the Coast of the Yellow Sea, China

Tao Zhang[1,2,3,4†], Kexin Song[1†], Liting Meng[1], Ruikai Tang[1], Tongtong Song[1], Wei Huang[5] and Zhihua Feng[1,2,3,4]*

[1] Jiangsu Key Laboratory of Marine Bioresources and Environment, Jiangsu Ocean University, Lianyungang, China, [2] Co-Innovation Center of Jiangsu Marine Bio-Industry Technology, Jiangsu Ocean University, Lianyungang, China, [3] Jiangsu Key Laboratory of Marine Biotechnology, Jiangsu Ocean University, Lianyungang, China, [4] Jiangsu Institute of Marine Resources Development, Jiangsu Ocean University, Lianyungang, China, [5] Key Laboratory of Marine Ecosystem and Biogeochemistry, Second Institute of Oceanography, Ministry of Natural Resources, Hangzhou, China

OPEN ACCESS

Edited by:
Xiaoshan Zhu,
Tsinghua University, China

Reviewed by:
Ke Pan,
Shenzhen University, China
Daniel Rittschof,
Duke University, United States

***Correspondence:**
Zhihua Feng
fengzhihua@jou.edu.cn

[†] These authors have contributed equally to this work and share first authorship

Specialty section:
This article was submitted to Marine Pollution, a section of the journal Frontiers in Marine Science

Received: 05 October 2021
Accepted: 09 December 2021
Published: 13 January 2022

Citation:
Zhang T, Song K, Meng L, Tang R, Song T, Huang W and Feng Z (2022) Distribution and Characteristics of Microplastics in Barnacles and Wild Bivalves on the Coast of the Yellow Sea, China. Front. Mar. Sci. 8:789615. doi: 10.3389/fmars.2021.789615

Barnacles and bivalves are two well-known sessile invertebrates that play important roles in marine ecosystems. Microplastic (MP) pollution has attracted widespread attention. Barnacles and wild bivalves are smaller than farmed individuals; thus, they may be more sensitive to MPs. However, less is known about the abundance and spatial distribution of MPs in wild bivalves along with the coastal areas of China. This study evaluates MP pollution in the most abundant bivalves and barnacles (*Crassostrea gigas*, *Ostrea cucullata*, *Mytilus edulis*, and *Balanus albicostatus*) at five stations in the intertidal zone of the Yellow Sea. *B. albicostatus* was divided into ecotype A and ecotype B. The abundance of MPs in barnacles, wild bivalves barnacles, and wild bivalves varied from 0 to 2.25 items/individual and 0 to 118.21 items/g. *O. cucullata* and *B. albicostatus* (ecotype A) had the highest abundance of MPs, with average abundances of 0.56 ± 0.36 items/individual and 21.59 ± 27.26 items/g, respectively. The types of MPs found in bivalves and barnacles include fibers, fragments, films, and microbeads. The most abundant size was less than 1,000 μm, which accounted for 53% of the total MPs. Cellophane (CP), polypropylene (PP), polyethylene (PE), and polyethylene terephthalate (PET) were the main polymer types in bivalves and barnacles. This study suggests that the abundance of MPs in wild bivalves is close to that of farmed bivalves with commercial specifications, despite their smaller size. The MP abundance of barnacles in the Yellow Sea is higher than that in other areas in terms of items per gram. In addition, the ecological type may affect the ability of barnacles to accumulate MPs. Ingestion of MPs by barnacles and wild bivalves should be of concern because they may enter the human body through the food web and may pose a potential threat to human health.

Keywords: microplastic, native oysters, mussels and barnacles, pollution, ecosystem

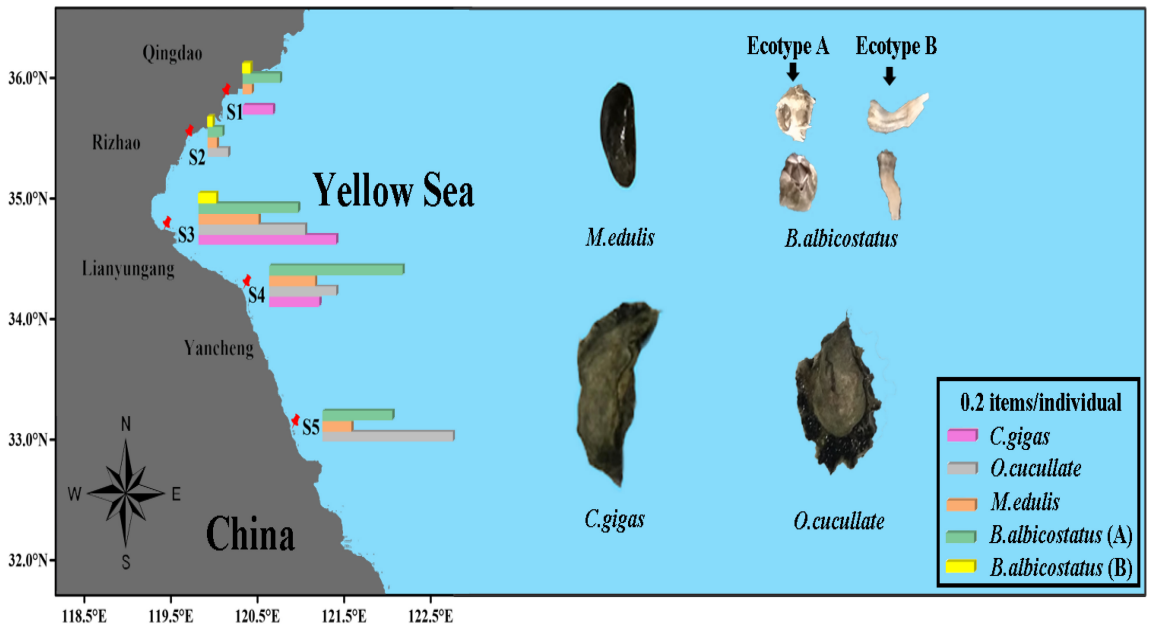

GRAPHICAL ABSTRACT | Microplastics in wild bivalves and wild bivalves on the coast of the Yellow Sea.

INTRODUCTION

Since plastic was invented in the middle of the last century, it has changed our life due to its multiple advantages, resulting in the massive replacement of traditional materials with plastic (Thompson et al., 2004; Barnes et al., 2009). Actually, the annual production of plastic in the world exceeded an estimate of 335 million tons in 2016 (Plastics Europe, 2018). A considerable amount of plastic waste is discharged into the ocean due to ineffective disposal by humans. As a result, plastic materials account for 60–80% of all marine debris in the ocean (Gregory and Ryan, 1997). It has become a potentially important menace to the marine environment on this planet (Zalasiewicz et al., 2016).

Microplastics (MPs) are defined as any plastic particles smaller than 5 mm in diameter (Thompson et al., 2004), including primary MPs and secondary MPs. Primary MPs are usually derived from industrial production (Costa et al., 2010), while secondary MPs are produced from mesoplastics and macroplastics by physical damage, photodegradation, oxidation, and biodegradation (Thompson et al., 2004; Auta et al., 2017; Isobe et al., 2019). Due to the small size of MPs, they are more easily dispersed in the ocean than large plastics. Consequently, MPs are ubiquitous in ocean environmental media (Rachel, 2018; Zhao et al., 2018; Zhu et al., 2018; Deanna and Mona, 2019). This leads to the ingestion of MPs by many marine organisms, including plankton (Lima et al., 2014), marine worms (Besseling et al., 2013), sea cucumber (Mohsen et al., 2019), bivalves (Von Moos et al., 2012; Li et al., 2018; Qu et al., 2018; Teng et al., 2019), crab (Zhang et al., 2021), fish (Foekema et al., 2013; Feng et al., 2019; Su et al., 2019), and even sea birds (Provencher et al., 2018). Moreover, MPs have the ability to carry out more toxic matters due to their large specific surface area and are more difficult to remove (Zhu et al., 2019). Therefore, MPs not only pose a threat to wildlife but are also potentially harmful to the global marine environment (Lebreton et al., 2017; Haward, 2018).

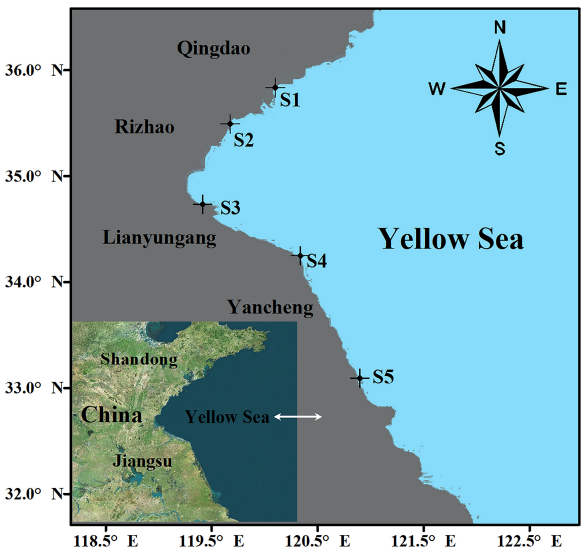

FIGURE 1 | Geographic position of five sampling sites along with coastal areas in the Yellow Sea.

Seafood provides approximately 20% of the animal protein intake of nearly 3 billion people worldwide, and the annual consumption of mollusks per person in China is 9.98 kg (FAO, 2017). During bivalve and barnacle feeding, a large amount of seawater is filtered, consequently accumulating MPs from the seawater. Moreover, previous studies have shown that MPs are

TABLE 1 | Sampling station information summary.

	Sampling sites	Longitude (°E)	Latitude (°N)	Sample weight (g)	Sample number	MPs number
	S1	120.05182	35.86453	0.01–2.94	814	71
	S2	119.62457	35.52201	0.01–1.49	990	67
	S3	119.36516	34.7613	0.01–1.69	755	259
	S4	120.28931	34.27538	0.01–2.38	354	151
	S5	120.85261	33.11599	0.09–3.17	154	52
Total					3067	600

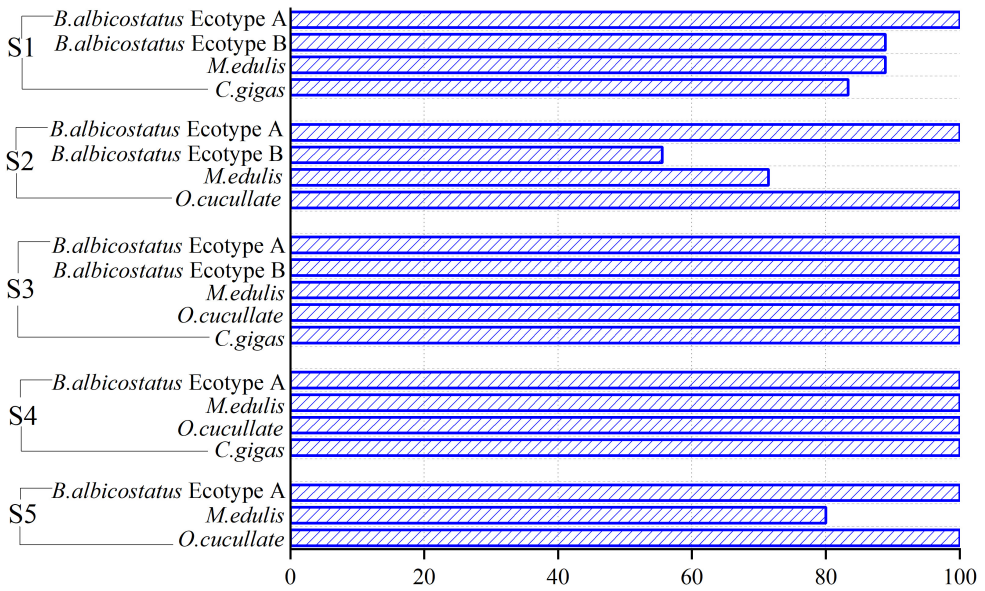

FIGURE 2 | Microplastic (MP) detection rates at five sampling sites; 100% of the sessile organism groups from S3 to S4 were detected.

present in cultured bivalves around the world (Lisbeth and Colin, 2014; Dannielle, 2016; Li et al., 2018; Qu et al., 2018 Teng et al., 2019; Feng et al., 2020c). However, there are few studies on MP pollution in wild bivalves, especially those attached to rocks in the intertidal zone as easily accessible seafood. In addition, bivalves and barnacles play a vital role in coastal ecosystems as an important part of the food chain. Some barnacles and wild bivalves are even thought to be ideal biological indicators in monitoring MP pollution (Li et al., 2018; Qu et al., 2018; Xu et al., 2020). Therefore, it is necessary to conduct more investigations on MP pollution in bivalves and barnacles. Moreover, wild individuals are often small, while cultured individuals are large, which may affect their MP levels. Breeding individuals often use breeding appliances, such as net cages, which are considered to be a source of marine MPs (Feng et al., 2020b). In addition, the difference in density per unit area of wild and cultured individuals is also an important factor affecting the abundance of biological MPs (Sfriso et al., 2020).

This study aims to increase our knowledge about the distribution of MPs in different barnacles and wild bivalves and to quantify MP variability between four species widely distributed in the Yellow Sea, China. The abundance and characteristics of MPs ingested by barnacles and wild bivalves collected from intertidal reefs along the Yellow Sea were investigated. In addition, two different ecotypes of barnacles were of particular concern. This study provides evidence for future evaluation of the selection of indicator organisms and the ecological and health risks caused by MP pollution of wild seafood in the marine environment.

MATERIALS AND METHODS

Sampling Collection

Wild bivalve and barnacle samples were collected at five locations (S1–S5) in the intertidal zone of the Yellow Sea in November 2018 using new stainless steel tools and knives (**Figure 1**). The collected barnacles and wild bivalves were held in aluminum foil bags. After the collection was completed, they were temporarily stored in a cooler (−5°C) and then stored in a refrigerator at −20°C in the laboratory for further analysis. Prior to dissection and digestion, all wild bivalve and barnacle samples were kept for not more than 3 weeks. *Balanus albicostatus* specimens were divided into two ecotypes based on whether there was a tube at their base (ecotype A without tube and ecotype B with tube).

Quality Assurance and Control

New tools made of stainless steel were used to collect wild bivalve and barnacle samples. When sampling, researchers in

TABLE 2 | MPs ingestion reported in the literature for sessile invertebrates.

Species	Location	Digestion method	Quantity	References
Mussels	Coast of China	30% H_2O_2	2.2 items/g	Li et al., 2016
Mussels	East China Sea	30% H_2O_2	9.2 items/g	Kolandhasamy et al., 2018
Mussels	Coast of China	30% H_2O_2	1.52–5.36 items/g	Qu et al., 2018
Oysters	Pearl River Estuary, China	10% KOH	1.5–7.2 items/g 1.4–7.0 items/individual	Li et al., 2018
Oysters	Coast of China	10% KOH, 30% H_2O_2	0.11–2.35 items/g	Teng et al., 2019
Oysters	the upper Gulf, Thailand	69% HNO_3	0.37 ± 0.03–0.57 ± 0.22 items/g	Gajahin et al., 2017
Barnacles	the upper Gulf, Thailand	69% HNO_3	0.23 ± 0.10–0.43 ± 0.33 items/g	Gajahin et al., 2017
Barnacles	Coast of Hong Kong, China	10% KOH	0–8.63 items/g 0–1.90 items/individual	Xu et al., 2020
Oysters	The Yellow Sea, China	10% KOH	0.44–1.31 items/g A = 0.87 items/g 0.07–0.85 items/individual A = 0.57 items/individual	This study
Mussels	The Yellow Sea, China	10% KOH	1.20–17.31 items/g A = 7.95 items/g 0.07–0.43 items/individual A = 0.21 items/individual	This study
Barnacles	The Yellow Sea, China	10% KOH	1.88–41.50 items/g A = 17.09 items/g 0.04–0.95 items/individual A = 0.42 items/individual	This study

this study used aluminum foil bags and quickly packed the collected stemless invertebrates separately to reduce atmospheric pollution. Laboratory processing was performed in a laminar flow cabinet (SW-CJ-2F, SUJING, China). Operators in the laboratory were kept to a minimum, and outdoor air circulation was minimized. All liquids were filtered with glass microfibers (Φ = 8 μm, d = 47 mm) before use. Clothing and instrument cleaning procedures of the operator were consistent with those in our previous studies (Feng et al., 2020b). The MP pollution status in the laboratory passed the program blank (without wild bivalve and barnacle samples) detection, and five program blanks were set for each batch of sample processing.

Sampling Dissection and Digestion

Samples were selected to remove damaged individuals before digestion. The shells of stemless invertebrates were thoroughly rinsed with deionized water after defrosting. Due to their small size and large numbers, the digestion of barnacles and wild bivalves was not suitable for single sample digestion from the perspective of economy and operability. Therefore, this study uses 30–50 sessile organisms to be digested and processed in groups. The wet weight of soft tissues and total individuals was determined by a precision electronic balance (BS124S, Sartorius Electronic Balance, Beijing). The digestion process was based on previous studies (Foekema et al., 2013; Karami et al., 2017; Feng et al., 2020a). After complete digestion, the clear yellow light digestion solution was transferred and filtered through 8-μm pore size glass microfiber filter membranes (Haining Jinzheng, China) using a filtration unit with one Büchner funnel (AP-01P, Autoscience, Tianjin). The filter membranes were placed in clean Petri dishes with lids and dried at room temperature.

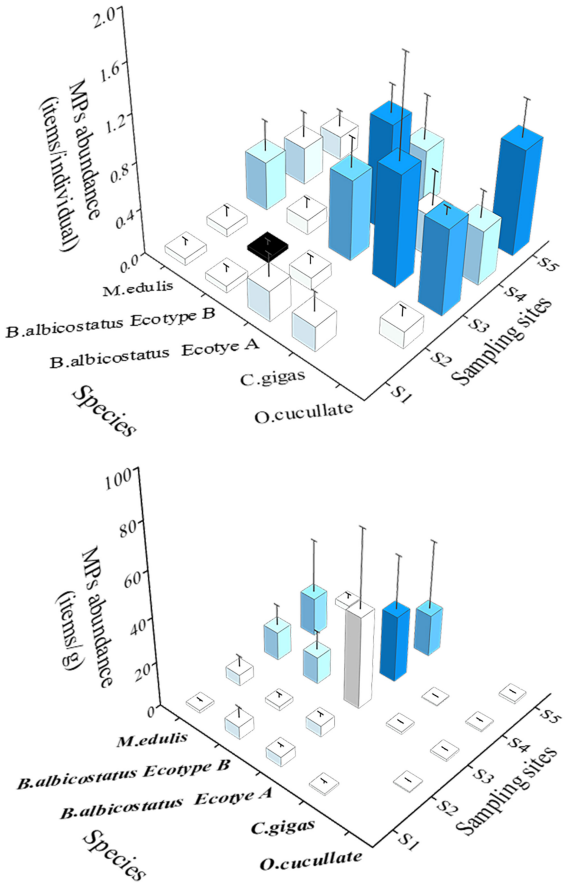

FIGURE 3 | Abundance of MPs (mean ± SD) in four species of barnacles and wild bivalves from different sites in the Yellow Sea.

Microplastic Identification and Data Analysis

The observation and identification of MPs were consistent with previous studies (Zhao et al., 2016; Cai et al., 2019; Feng et al., 2019; Zhang et al., 2021). The data were analyzed using SPSS version 23 (IBM, New York, NY, United States) and visualized using Origin 2021 (Originlab, Northampton, Massachusetts, United States). The MP size data conformed to a normal distribution (Shapiro–Wilk, $P > 0.05$), and the

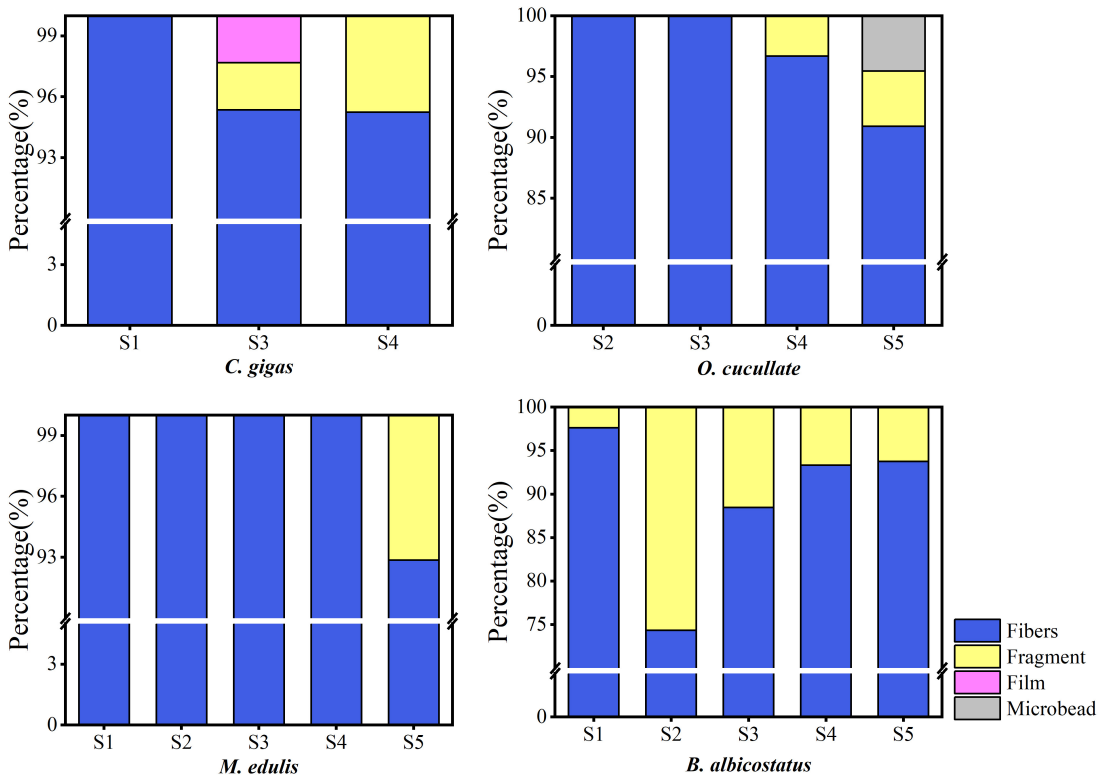

FIGURE 4 | Shape distribution of MPs in four species of barnacles and wild bivalves from different sites in the Yellow Sea.

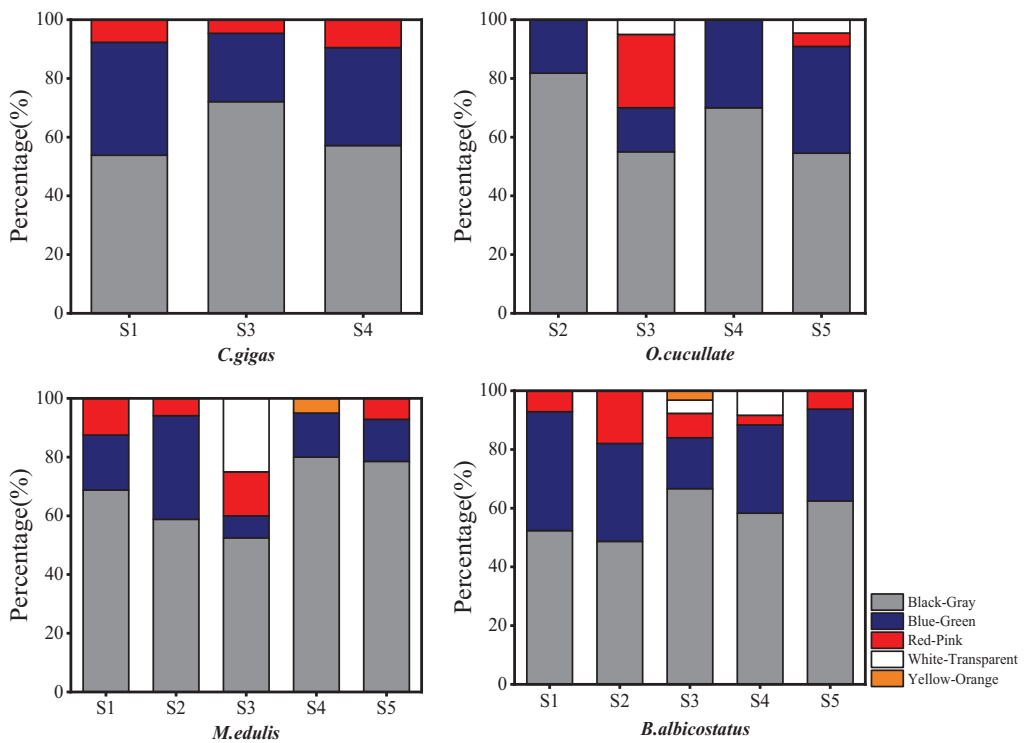

FIGURE 5 | Color distribution of MPs in four species of barnacles and wild bivalves from different sites in the Yellow Sea.

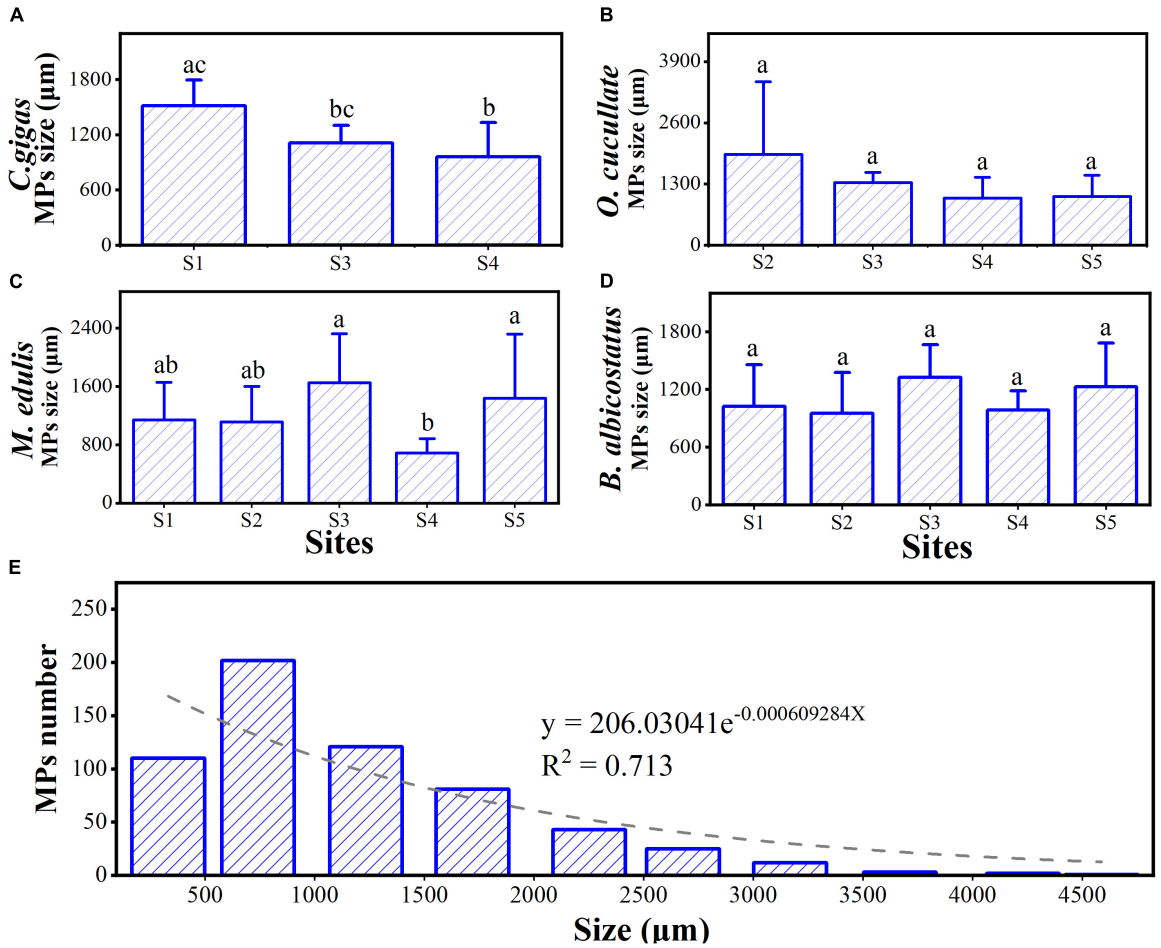

FIGURE 6 | Mean MP size (± SD) in four species of barnacles and wild bivalves from different sites **(A–D)** in the Yellow Sea and the size distribution of the MPs in all wild bivalves and barnacle samples **(E)**. Different letters above the bars indicate significant differences among species (one-way ANOVA, $P < 0.05$). The gray dashed represents the fit between the number and the particle size of MPs.

variances could be considered equal (Levene's test, $P > 0.05$). One-way ANOVA was conducted to assess differences in MP size among different stations. The least significant difference was determined by ANOVA *post hoc* investigation. Kruskal–Wallis ANOVA was used to determine whether there was a significant difference in MP abundance for different species and various sampling stations. A CI of 95% was set for all tests. A linear regression analysis was applied to determine the significant correlation between MP abundance and wild bivalve and barnacle soft tissue weight.

RESULTS

Characteristics of Barnacles and Wild Bivalves

A total of 3,067 barnacles and wild bivalves were collected from five sites along the Yellow Sea (**Table 1**). These barnacles and wild bivalves were identified as four species, namely, *Crassostrea gigas* (*C. gigas*), *Ostrea cucullata* (*O. cucullata*), *Mytilus edulis* (*M. edulis*), and *B. albicostatus*. *B. albicostatus* was found in two different ecotypes, one of which had bases without tubes (ecotype A), while the other had bases with tubes (ecotype B), as shown in the Graphical Abstract. The numbers of *C. gigas*, *O. cucullata*, *M. edulis, B. albicostatus* (ecotype A), and *B. albicostatus* (ecotype B) were 200, 233, 940, 660, and 1,034, respectively.

Microplastic Abundance in Barnacles and Wild Bivalves in Different Areas

Microplastics were detected visually in more than 91% of the groups, with a total number of 600 items among all barnacles and wild bivalves. MPs were found in all barnacles and wild bivalves at sites S3 and S4. The lowest detection rate was from S2, which also reached 77.78% (**Figure 2**).

The MP abundance in barnacles and wild bivalves from five areas was revealed (**Figure 3**). MP abundance in barnacles and wild bivalves from different areas was significantly different for items per individual (Kruskal–Wallis, $P = 0.000$) and items per gram (Kruskal–Wallis, $P = 0.000$). When both normalized to individual or mass, barnacles and wild bivalves from S3 had

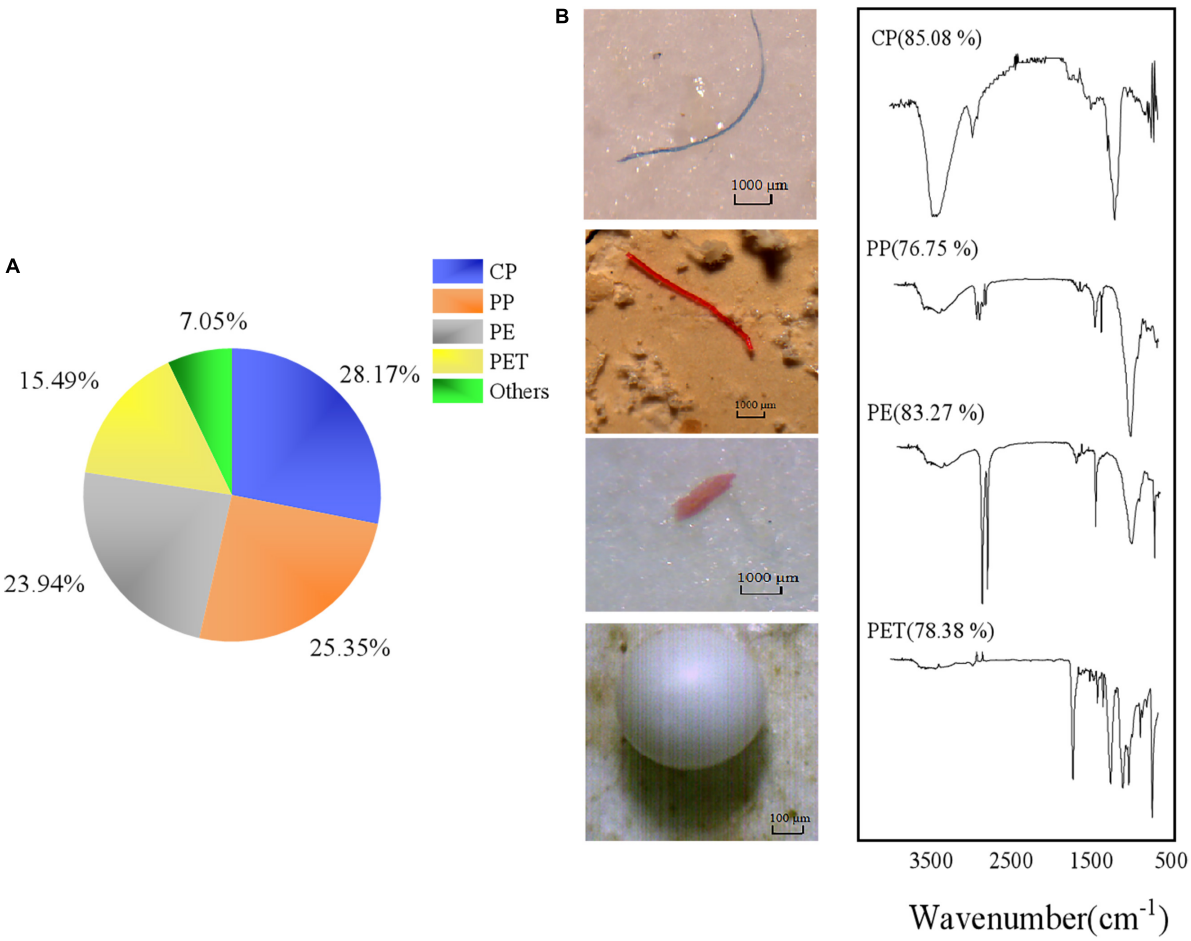

FIGURE 7 | Type distribution **(A)** and material spectra **(B)** identified by μ-FT-IR microscopy of the MPs observed in barnacles and wild bivalves. Proportions less than 5% were classified as others, including polymethacrylates (PMA, 4.23%), polyacrylonitrile (PAN, 1.41%), and poly(urethane:ethylene terephthalate) (PU-PET, 1.41%).

the highest MP abundance (0.52 ± 0.45 items/individual and 16.85 ± 23.42 items/g), while in terms of items per individual, MP abundance in S2 samples had the lowest level, at 0.08 ± 0.08 items/individual and 3.13 ± 3.50 items/g.

The abundance of MPs of barnacles and wild bivalves for different species was further studied (**Figure 3**). Kruskal–Wallis ANOVA showed that the MP abundance of various barnacles and wild bivalves was significantly different for both items per individual (P = 0.002) and items per gram (P = 0.000). The highest MP abundance in items per individual was *O. cucullata* (0.56 ± 0.36), while *M. edulis* was the lowest (0.21 ± 0.21). *B. albicostatus* had the highest value (14.09 ± 21.31), and *C. gigas* was 0.77 ± 0.81 when it was normalized to items per gram.

Characteristics of Microplastics in Barnacles and Wild Bivalves

Multiple types of MPs, including fibers, fragments, films, and microbeads, occurred in the tissues of the barnacles and wild bivalves (**Figure 4**). The most diverse types were observed as fibers, followed by fragments. The most popular colors were black, blue, green, and red, which were over 90% (**Figure 5**). The size of MPs varied from 135.12 to 2,917.69 μm, 86.55 to 4,867.23 μm, 137.85 to 3,331.06 μm, 69.83 to 3,743.20 μm, and 194.66 to 2,885.65 μm in *C. gigas*, *O. cucullata*, *M. edulis*, and *B. albicostatus* ecotype A and ecotype B, respectively. MPs less than 1 mm in size were the most common. As the size of MPs increased, the abundance trend of MPs decreased exponentially (R^2 = 0.713, P < 0.01) (**Figure 6**). The materials of suspected MPs in the barnacles and wild bivalves were also confirmed (**Figure 7**). Most of them were cellophane (CP, 28.17%), followed by polypropylene (PP, 25.35%) and polyethylene (PE, 23.94%).

Microplastic Pollution Features of Various Ecotypes

The abundance of MPs of different ecotypes and habitats of *B. albicostatus* was also analyzed (**Figure 8**). Ecotype A barnacles had a higher MP pollution level than ecotype B in terms of both items per individual and items per gram. An average of 0.52 ± 0.38 MPs was found in ecotype A, while 0.08 ± 0.08 MPs were found in ecotype B. In terms of items per gram,

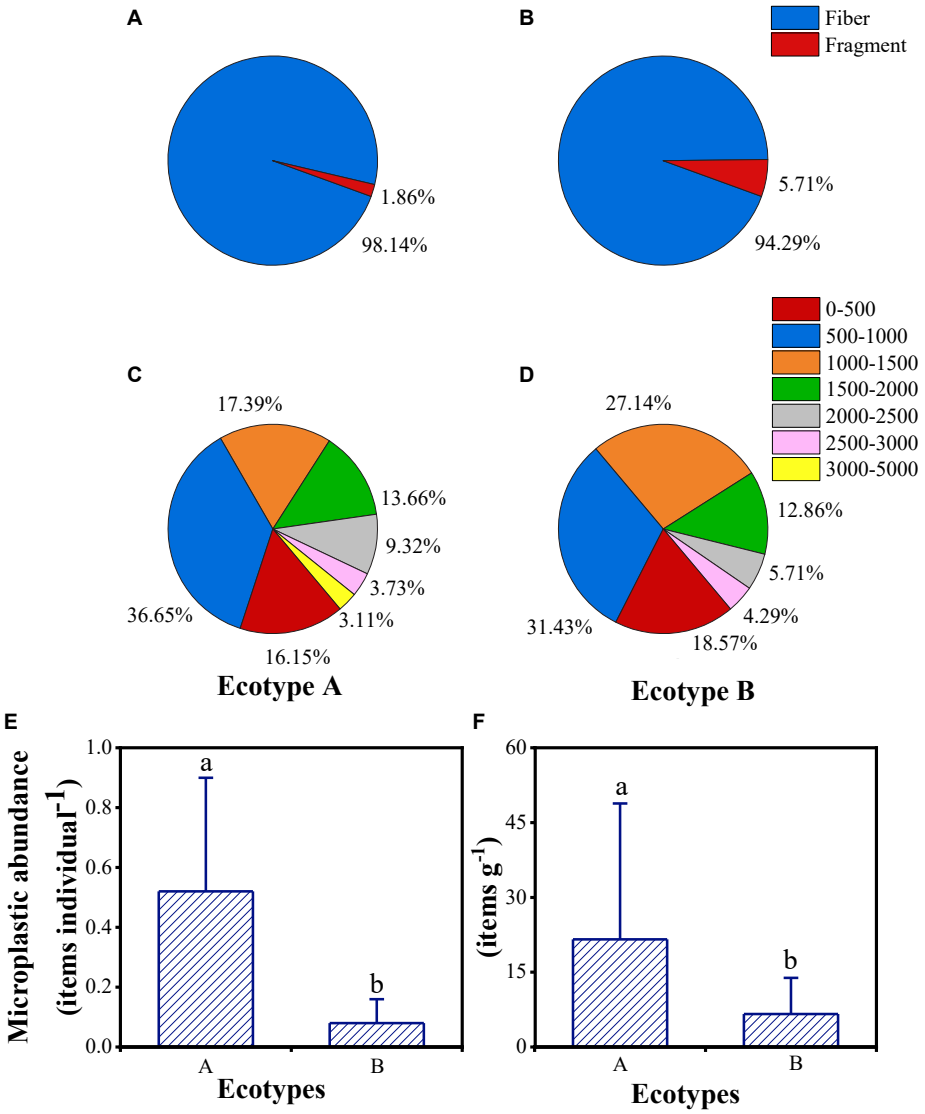

FIGURE 8 | The shape, size and abundance of MPs in ecotypes A **(A,C,E)** and B **(B,D,F)** of barnacles. Different letters above the bars indicate significant differences among ecotypes (one-way ANOVA, $P < 0.05$). Different letters above the bars indicate significant differences among ecotypes (one-way ANOVA, $P < 0.05$).

21.59 ± 27.26 existed in ecotype A compared with 6.60 ± 7.25 in ecotype B. Both fibers and fragments were found in different *B. albicostatus* ecotypes, but slight differences in proportion existed (fibers occupied 98.14% in ecotype A and 94.29% in ecotype B). There was no significant difference in the particle size distribution of MPs below 3,000 μm. However, MPs with a particle size larger than 3,000 μm were only found in ecotype A barnacles.

Relationship Between Microplastic Abundance and Soft Tissue Weight of Barnacles and Wild Bivalves

To further explore the relationship between the biological characteristics of sessile organisms and MP pollution levels, the relationship between MP abundance and soft tissue weight was analyzed (**Figure 9**). The results suggested that the MP value was highly positively related to the tissue weight of *O. cucullata* ($r = 0.680$, $P < 0.01$) and *B. albicostatus* ecotype B ($r = 0.684$, $P < 0.01$) normalized to items per individual.

DISCUSSION

Microplastic Pollution Level in Barnacles and Wild Bivalves of the Yellow Sea

In this study, MP abundance in four species of barnacles and wild bivalves in the Yellow Sea was investigated. The high MP detection rate (91.85%) indicates that MPs are widespread in barnacles and wild bivalves, suggesting that barnacles and wild bivalves can accumulate MPs. These results indicate that the

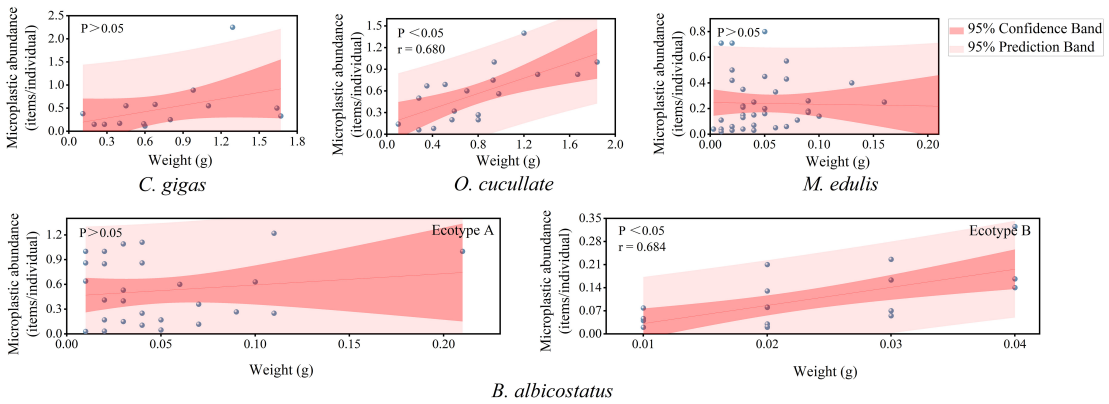

FIGURE 9 | Correlation analysis between MP abundance and wet weight of the total tissues of barnacles and wild bivalves. The red line is the fitted trend line, gray ball represents the abundance value of MPs in different weights of organisms.

intertidal zone of the Yellow Sea has been contaminated by MPs (Teng et al., 2019; Feng et al., 2020c). Therefore, barnacles and wild bivalves can be exposed to MPs in natural environments. However, the abundance of MPs in the barnacles and wild bivalves was significantly different, indicating significant spatial variability (**Figure 8**). The highest abundance of MPs and 100% MP detection rate were found in the barnacles and wild bivalves from the S3 region, whether calculated by an individual or by items per gram. The results were also consistent with previous studies on MPs in marine invertebrates (Carney and Eggert, 2019; Teng et al., 2019; Feng et al., 2020a,b), showing that the S3 area is more seriously affected by human activities, such as shipping and mariculture.

In contrast, the abundance of MPs showed great variation between the species of barnacles and wild bivalves, with range values of 0–2.25 items/individual and 0–118.21 items/g. The ability to ingest or eliminate MPs may lead to interspecific differences in MP abundance (Xu et al., 2020). Compared with previous studies (**Table 2**), the values of MP abundance in mussels showed a higher level by items per gram (Li et al., 2016; Qu et al., 2018), which was only lower than the results of Kolandhasamy et al. (2018). However, it was much lower when expressed by individuals (Li et al., 2016; Kolandhasamy et al., 2018; Qu et al., 2018). For the oysters in this study, both items per gram and items per individual showed intermediate levels of contamination compared with traditional studies (Gajahin et al., 2017; Li et al., 2018; Teng et al., 2019). Few studies have been conducted on MPs in barnacles, and our results show that the pollution level of barnacles in the Yellow Sea is much higher than that in the upper gulf in Thailand and the coast of Hong Kong in terms of items per gram (Gajahin et al., 2017; Xu et al., 2020). When calculated for individuals, the abundance of MPs in barnacles along the coast of Hong Kong was higher than that in this study (Xu et al., 2020). According to the current research results, the uptake of MPs by barnacles and wild bivalves is ubiquitous, and the degree of habitat pollution and the size of individuals are the main influencing factors. In particular, MPs are found in oysters and mussels, although they are not cultured on ropes or cages. In addition, it is worth noting that due to different methods, there may be differences in comparing the levels and abundance of MP pollution between different studies (**Table 2**).

Characteristics of Microplastic Pollution in Barnacles and Wild Bivalves

In this study, MPs with a size of <1,000 μm were the most abundant, which has also been found in many previous studies (Peng et al., 2017; Teng et al., 2019; Feng et al., 2020a). Browne et al. (2011) reported that MPs with small particle sizes may be more likely to be ingested and to accumulate in tissues, and MPs with small particle sizes may show extremely high toxic effects on copepod adults and offspring. In terms of the shape of particles in barnacles and wild bivalves, most MPs were fibrous, which was consistent with the results from seawater samples from the Yellow Sea (Sun et al., 2018). In the South Yellow Sea, the high-frequency use of plastic fishing tools (such as fishing gear, ropes, and fishing nets) has led to fibers becoming the most common shape in this area (Feng et al., 2019). In addition, fibers may also be the most abundant shape of MPs in the ocean (Frias et al., 2016; Andrés and Ruth, 2017). For materials, CP, PP, PE, and polyethylene terephthalate (PET) were the main polymer types in the barnacles and wild bivalves. These four material types are also the most abundant materials for MPs in coastal environments and organisms (Jabeen et al., 2017; Zhu et al., 2018; Feng et al., 2019; Mohsen et al., 2019; Teng et al., 2019; Zhang et al., 2019).

Microplastic Pollution in Different Ecotypes of Barnacles

In our study, the distribution of barnacles was found at Stations S1–S5. Among them, two types of barnacles with different ecotypes (ecotype A without tubes and ecotype B with tubes) were found at Stations S1–S3. The abundance of MPs in these two different ecotypes of barnacles was different, and the abundance of MPs in barnacles with tubes was significantly lower than that of tubeless barnacles. In addition, the characteristics of MPs of different ecotypes of barnacles are manifested only in the significant differences in the abundance of MPs, and there was no significant difference in type. These results may indicate

that differences in ecotypes affect the accumulation of MPs in marine organisms (**Figure 8**). In this study, during the sampling process, we found that barnacles with ecotype B had a higher population density than those with ecotype A. We speculate that when the environment has a certain number of MPs, the larger the number of individuals is, the smaller the number of MPs that can be obtained. There were similar inferences in a study of MP pollution of the benthos (Sfriso et al., 2020). However, the mechanism of MP accumulation in individuals caused by different ecological types still needs further confirmation. In previous studies, the abundance of MPs in two different ecotypes of *Ulva prolifera* (drifting and attached) showed significant differences, which provides evidence supporting our conclusion (Feng et al., 2020b). We speculate that ecotypes may play an important role in the accumulation of MPs, not only in plants but also in animals. Thus, we suggested that the selection of MP indicator organisms should consider in-depth their ecological type (**Figure 9**).

Characteristics of Microplastic Pollution in Barnacles and Wild Bivalves

A large number of studies have confirmed that MPs can cause damage to marine invertebrates, including mechanical damage caused by abrasion or obstruction of the digestive tract, reduction in a filter-feeding rate and growth rate, energy consumption, and oxidative stress (Von et al., 2012; Rochman et al., 2013; Wright et al., 2013). In addition, the large specific surface area of MPs allows MPs to interact with pollutants in the environment. In particular, MPs have a strong adsorption capacity for persistent organic pollutants (POPs, Rochman et al., 2013; Wright et al., 2013). This adsorption behavior allows MPs to act as carriers for contaminants to enter the organism through the food chain (Derraik, 2002; Cole et al., 2011). In addition, barnacles and wild bivalves play an important ecological function in the intertidal zone. They are not only important feeders of phytoplankton and zooplankton but also serve as prey for various marine animals. This bioaccumulation effect of MPs may gradually have a negative impact on the diversity of coastal organisms and the functionality of ecosystems.

Mussels, oysters, and some species of barnacles are important sources of seafood along the coast of China. Barnacles and wild bivalves distributed in the intertidal zone are also easy to obtain for consumption. Furthermore, they are consumed whole, without gut removal. As a result, the consumption of this contaminated seafood may increase the potential risk to human health (Hussain et al., 2001). However, detailed investigations should be conducted to understand the mutual transmission and accumulation of MPs through the food webs of coastal and marine ecosystems and the harmful effects for marine life in regard to MP ingestion.

CONCLUSION

Our study found that MP pollution in barnacles and wild bivalves is widespread in the intertidal zone of the Yellow Sea. Barnacles and wild bivalves can be used as ecological indicators of MPs. Different ecotypes may lead to differences in the accumulation of MPs in barnacles. However, the mechanism of MP accumulation in different ecotypes of barnacles remains to be studied. In addition, our study indicates that MPs are widespread in seafood, such as shellfish, representing a potential risk to human health.

DATA AVAILABILITY STATEMENT

The original contributions presented in the study are included in the article/supplementary material, further inquiries can be directed to the corresponding author.

AUTHOR CONTRIBUTIONS

TZ: conceptualization, methodology, writing original draft – reviewing and editing, supervision, and funding acquisition. KS: investigation, methodology, formal analysis, and visualization. LM: conceptualization, methodology, and writing, reviewing, and editing. RT and TS: investigation. WH: methodology. ZF: conceptualization, formal analysis, writing original draft, reviewing and editing, supervision, and funding acquisition. All authors contributed to the article and approved the submitted version.

FUNDING

This work was supported by Jiangsu Industry-University-Research Cooperation Project (BY2020428), Open-end Funds of Jiangsu Key Laboratory of Marine Bioresources and Environment (SH20201210), Provincial Policy Guidance Program (North Jiangsu Science and Technology Special Project) (SZ-LYG202131), College Student Innovation and Entrepreneurship Training Program of Jiangsu Province (202111641155Y), Universities Natural Science Research Project of Jiangsu Province (20KJB170029), Jiangsu Province Postdoctoral Research Foundation (2021K212B), and Postdoctoral Research Foundation of Lianyungang (LYG2021002).

REFERENCES

Andrés, R. S., and Ruth, P. (2017). Morphological and physical characterization of microplastics. *Compr. Anal. Chem.* 7, 49–66. doi: 10.1016/bs.coac.2016.10.007

Auta, H. S., Emenike, C. U., and Fauziah, S. H. (2017). Distribution and importance of microplastics in the marine environment: a review of the sources, fate, effects, and potential solutions. *Environ. Int.* 102, 165–176. doi: 10.1016/j.envint.2017.02.013

Barnes, D. K. A., Galgani, F., Thompson, R. C., and Barlaz, M. (2009). Accumulation and fragmentation of plastic debris in global environments. *Philos. Trans. R. Soc. B Biol. Sci.* 364, 1985–1998. doi: 10.1098/rstb.2008.0205

Besseling, E., Wegner, A., Foekema, E. M., Van Den Heuvel-Greve, M. J., and Koelmans, A. A. (2013). Effects of microplastic on fifitness and PCB bioaccumulation by the lugworm *Arenicola marina* (L.). *Environ. Sci. Technol.* 47, 593–600. doi: 10.1021/es302763x

Browne, M. A., Crump, P., Niven, S. J., Teuten, E., Tonkin, A., Galloway, T., et al. (2011). Accumulation of Microplastic on shorelines woldwide: sources and sinks. *Environ. Sci. Technol.* 45, 9175–9179. doi: 10.1021/es201811s

Cai, H. W., Du, F. N., Li, L. Y., Li, B. W., Li, J. N., and Shi, H. H. (2019). A practical approach based on FT-IR spectroscopy for identification of semi-synthetic and natural celluloses in microplastic investigation. *Sci. Environ.* 669, 692–701. doi: 10.1016/j.scitotenv.2019.03.124

Carney, A. B., and Eggert, H. (2019). Marine plastic pollution: sources, impacts, and policy tissues. *Rev. Environ. Econ. Policy* 13, 317–326. doi: 10.1093/reep/rez012

Cole, M., Lindeque, P., Halsband, C., and Galloway, T. S. (2011). Microplastics as contaminants in the marine environment: a review. *Mar. Pollut. Bull.* 62, 2588–2597. doi: 10.1016/j.marpolbul.2011.09.025

Costa, M. F., Ivar do, S. J. A., Silva-Cavalcanti, J. S., Araújo, M. C. B., Spengler, A., and Tourinho, P. S. (2010). On the importance of size of plastic fragments and pellets on the strandline: a snapshot of a Brazilian beach. *Environ. Monit. Assess.* 168, 299–304. doi: 10.1007/s10661-009-1113-4

Dannielle, S. G. (2016). Effects of microplastics on European flat oysters, *Ostrea edulis* and their associated benthic communities. *Environ. Pollut.* 216, 95–103. doi: 10.1016/j.envpol.2016.05.043

Deanna, R., and Mona, W. (2019). Characterization of microplastics in the surface waters of Kingston Harbour. *Sci. Total Environ.* 664, 753–760. doi: 10.1016/j.scitotenv.2019.01.319

Derraik, J. G. B. (2002). The pollution of the marine environment by plastic debris: a review. *Mar. Pollut. Bull.* 44, 842–852. doi: 10.1016/S0025-326X(02)00220-5

FAO (2017). *Food and Agriculture Organization of the United Nations; The State of World Fisheries and Aquaculture*. Rome: FAO, 230.

Feng, Z. H., Zhang, T., Li, Y., He, X. R., Wang, R., Xu, J. T., et al. (2019). The accumulation of microplastics in fish from an important fish farm and mariculture area, Haizhou Bay, China. *Sci. Total Environ.* 696:133948. doi: 10.1016/j.scitotenv.2019.133948

Feng, Z. H., Zhang, T., Wang, J. X., Huang, W., Wang, R., Xu, J. T., et al. (2020c). Spatio-temporal features of microplastics pollution in macroalgae growing in an important mariculture area, China. *Sci. Total Environ.* 719:137490. doi: 10.1016/j.scitotenv.2020.137490

Feng, Z. H., Zhang, T., Shi, H. H., Gao, K. S., Huang, W., Xu, J. T., et al. (2020b). Microplastics in bloom-forming macroalgae: distribution, characteristics and impacts. *J. Hazard. Mater.* 397:122752. doi: 10.1016/j.jhazmat.122752

Feng, Z. H., Wang, R., Zhang, T., Wang, J. X., Huang, W., Li, J., et al. (2020a). Microplastics in specific tissues of wild sea urchins along the coastal areas of northern China. *Sci. Total Environ.* 728:138660. doi: 10.1016/j.scitotenv.2020.138660

Foekema, E. M., De Gruijter, C., Mergia, M. T., Van Franeker, J. A., Murk, A. T. J., and Koelmans, A. A. (2013). Plastic in North Sea fish. *Environ. Sci. Technol.* 47, 8818–8824. doi: 10.1021/es400931b

Frias, J. P. G. L., Gago, J., Otero, V., and Sobral, P. (2016). Microplastics in coastal sediments from Southern Portuguese shelf waters. *Mar. Environ. Res.* 114, 24–30. doi: 10.1016/j.marenvres.2015.12.006

Gajahin, G. N. T., Jayan, D. M. S., Amararatne, Y., and Suchana, C. (2017). Effects of Microplastics on barnacles and wild bivalves in the eastern coast of Thailand: an approach to coastal zone conservation. *Mar. Pollut. Bull.* 124, 349–355. doi: 10.1016/j.marpolbul.2017.06.010

Gregory, M. R., and Ryan, P. G. (1997). "Pelagic plastics and other seaborne persistent synthetic debris: a review of Southern Hemisphere perspectives," in *Marine Debris–Sources, Impacts and Solutions*, eds J. M. Coe and D. B. Rogers (New York, NY: Springer), 49–66. doi: 10.1007/978-1-4613-8486-1-6

Haward, M. (2018). Plastic pollution of the world's seas and oceans as a contemporary challenge in ocean governance. *Nat. Commun.* 9:667. doi: 10.1038/s41467-018-03104-3

Hussain, N., Jaitley, V., and Florence, A. T. (2001). Recent advances in the understanding of uptake of microparticulates across the gastrointestinal lymphatics. *Adv. Drug Deliv. Rev.* 50, 107–142. doi: 10.1016/S0169-409X(01)00152-1

Isobe, A., Iwasaki, S., Uchida, K., and Tokai, T. (2019). Abundance of non-conservative microplastics in the upper ocean from 1957 to 2066. *Nat. Commun.* 10:417. doi: 10.1038/s41467-019-08316-9

Jabeen, K., Su, L., Li, J., Yang, D., Tong, C., Mu, J., et al. (2017). Microplastics and mesoplastics in fish from coastal and fresh waters of China. *Environ. Pollut.* 221, 141–149. doi: 10.1016/j.envpol.2016.11.055

Karami, A., Golieskardi, A., Choo, C. K., Romanoc, N., Yu, B. H., and Salamatinia, B. (2017). A high-performance protocol for extraction of microplastics in fish. *Sci. Total Environ.* 578, 485–494. doi: 10.1016/j.scitotenv.2016.10.213

Kolandhasamy, P., Su, L., Li, J., Qu, X., Jabeen, K., and Shi, H. H. (2018). Adherence of microplastics to soft tissue of mussels: a novel way to uptake microplastics beyond ingestion. *Sci. Total Environ.* 610–611, 635–640. doi: 10.1016/j.scitotenv.2017.08.053

Lebreton, L. C. M., Joost, V. D. Z., Damsteeg, J. W., Slat, B., Andrady, A., and Reisser, J. (2017). River plastic emissions to the world's oceans. *Nat. Commun.* 8:15611. doi: 10.1038/ncomms15611

Li, H. X., Ma, L. S., Lin, L., Ni, Z. X., Xu, X. R., Shi, H. H., et al. (2018). Microplastics in oysters Saccostrea Cucullata, along the Pearl River Estuary, China. *Environ. Pollut.* 236, 619–625. doi: 10.1016/j.envpol.2018.01.083

Li, J. N., Qu, X. Y., Su, L., Zhang, W. W., Yang, D. Q., Kolandhasamy, P., et al. (2016). Microplastics in mussels along the coastal waters of China. *Environ. Pollut.* 214, 177–184. doi: 10.1016/j.envpol.2016.04.012

Lima, A. R. A., Costa, M. F., and Barletta, M. (2014). Distribution patterns of microplastics within the plankton of a tropical estuary. *Environ. Res.* 132, 146–155. doi: 10.1016/j.envres.2014.03.031

Lisbeth, V. C., and Colin, R. J. (2014). Microplastics in bivalves cultured for human consumption. *Environ. Pollut.* 193, 65–70. doi: 10.1016/j.envpol.2014.06.010

Mohsen, M., Wang, Q., Zhang, L. B., Sun, L. N., Lin, C. G., and Yang, H. S. (2019). Microplastic ingestion by the farmed sea cucumber *Apostichopus japonicus* in China. *Environ. Pollut.* 245, 1071–1078. doi: 10.1016/j.envpol.2018.11.083

Peng, G. Y., Zhu, B. S., Yang, D. Q., Su, L., Shi, H. H., and Li, D. D. (2017). Microplastics in sediments of the Changjiang Estuary, China. *Environ. Pollut.* 225, 283–290. doi: 10.1016/j.envpol.2016.12.064

Plastics Europe (2018). *Plastics–The Facts 2017-An Analysis of European Plastics Production, Demand and Waste Data*. Frankfurt: Plastics Europe.

Provencher, J. F., Vermaire, J. C., Avery-Gomm, S., Braune, B. M., and Mallory, M. L. (2018). Garbage in guano? Microplastic debris found in faecal precursors of seabirds known to ingest plastics. *Sci. Total Environ.* 644, 1477–1484. doi: 10.1016/j.scitotenv.2018.07.101

Qu, X. Y., Su, L., Li, H. X., Liang, M. Z., and Shi, H. H. (2018). Assessing the relationship between the abundance and properties of microplastics in water and in mussels. *Sci. Total Environ.* 621, 679–686. doi: 10.1016/j.scitotenv.2017.11.284

Rachel, W. O. (2018). Microplastics in Polar Regions: the role of long range transport. *Curr. Opin. Environ. Sci. Health* 1, 24–29. doi: 10.1016/j.coesh.2017.10.004

Rochman, C. M., Hoh, E., Kurobe, T., and The, S. J. (2013). Ingested plastic transfers hazardous chemicals to fish and induces hepatic stress. *Sci. Rep.* 3:3263. doi: 10.1038/srep03263

Sfriso, A. A., Tomio, Y., Rosso, B., Gambaro, A., Sfriso, A., Corami, F., et al. (2020). Microplastic accumulation in benthic invertebrates in Terra Nova Bay (Ross Sea, Antarctica). *Environ. Int.* 137:105587. doi: 10.1016/j.envint.2020.105587

Su, L., Deng, H., Li, B., Chen, Q., Pettigrove, V., Wu, C., et al. (2019). The occurrence of microplastic in specific organs in commercially caught fishes from coast and estuary area of East China. *J. Hazard. Mater.* 365, 716–724. doi: 10.1016/j.jhazmat.2018.11.024

Sun, X. X., Liang, J. H., Zhu, M. L., Zhao, Y. F., and Zhang, B. (2018). Microplastics in seawater and zooplankton from the Yellow Sea. *Environ. Pollut.* 242, 585–595. doi: 10.1016/j.envpol.2018.07.014

Teng, J., Wang, Q., Ran, W., Wu, D., Liu, Y. F., Sun, S., et al. (2019). Microplastic in cultured oysters from different coastal areas of China. *Sci. Total Environ.* 653, 1282–1292. doi: 10.1016/j.scitotenv.2018.11.057

Thompson, R., Olsen, Y., Mitchell, R., Davis, A., Rowland, S. J., John, A. W. G., et al. (2004). Lost at sea: where is all the plastic? *Science* 304:838. doi: 10.1126/science.1094559

Von Moos, N., Burkhardt-Holm, P., and Kohler, A. (2012). Uptake and effects of microplastics on cells and tissue of the blue mussel *Mytilus edulis* L. after an experimental exposure. *Environ. Sci. Technol.* 46, 11327–11335. doi: 10.1021/es302332w

Wright, S. L., Thompson, R. C., and Galloway, T. S. (2013). The physical impacts of microplastics on marine organisms: a review. *Environ. Pollut.* 178, 483–492. doi: 10.1016/j.envpol.2013.02.031

Xu, X. Y., Wong, C. Y., Tam, N. F. Y., Liu, H. M., and Cheung, S. G. (2020). Barnacles as potential bioindicator of microplastic pollution in

Hong Kong. *Mar. Pollut. Bull.* 154:111081. doi: 10.1016/j.marpolbul.2020.111081

Zalasiewicz, J., Waters, C. N., Sul, J. I. D., Corcoran, P. L., and Yonan, Y. (2016). The geological cycle of plastics and their use as a stratigraphic indicator of the Anthropocene. *Anthropocene* 13, 4–17. doi: 10.1016/j.ancene.2016.01.002

Zhang, F., Wang, X. H., Xu, J. Y., Zhu, L. X., Peng, G. Y., Xu, P., et al. (2019). Food-web transfer of microplastics between wild caught fish and crustaceans in East China Sea. *Mar. Pollut. Bull.* 146, 173–182.

Zhang, T., Sun, Y. X., Song, K. X., Du, W. G., Huang, W., Gu, Z. Q., et al. (2021). Microplastics in different tissues of wild crabs at three important fishing grounds in China. *Chemosphere* 271:129479. doi: 10.1016/j.chemosphere.2020.129479

Zhao, J. M., Ran, W., Teng, J., Liu, Y. L., Liu, H., Yin, X. N., et al. (2018). Microplastic pollution in sediments from the Bohai Sea and the Yellow Sea, China. *Sci. Total Environ.* 64, 637–645. doi: 10.1016/j.scitotenv.2018.05.346

Zhao, S. Y., Danley, M., Ward, J. E., Li, D., and Mincer, T. J. (2016). An approach for extraction, characterization and quantitation of microplastic in natural marine snow using Raman microscopy. *Anal. Methods* 9, 1470–1478. doi: 10.1039/C6AY02302A

Zhu, L., Bai, H., Chen, B., Sun, X., Qu, K., and Xia, B. (2018). Microplastic pollution in North Yellow Sea, China: observations on occurrence, distribution and identification. *Sci. Total Environ.* 636, 20–29.

Zhu, Z. L., Wang, S. C., Zhao, F. F., Wang, S. G., Liu, F. F., and Liu, G. Z. (2019). Joint toxicity of microplastics with triclosan to marine microalgae *Skeletonema costatum*. *Environ. Pollut.* 246, 509–517. doi: 10.1016/j.envpol.2018.12.044

Conflict of Interest: The authors declare that the research was conducted in the absence of any commercial or financial relationships that could be construed as a potential conflict of interest.

Publisher's Note: All claims expressed in this article are solely those of the authors and do not necessarily represent those of their affiliated organizations, or those of the publisher, the editors and the reviewers. Any product that may be evaluated in this article, or claim that may be made by its manufacturer, is not guaranteed or endorsed by the publisher.

frontiers in Marine Science

ORIGINAL RESEARCH
published: 13 January 2022
doi: 10.3389/fmars.2021.806952

Plastic After an Extreme Storm: The Typhoon-Induced Response of Micro- and Mesoplastics in Coastal Waters

Ryota Nakajima[1], Toru Miyama[1], Tomo Kitahashi[1], Noriyuki Isobe[1], Yuriko Nagano[1], Tetsuro Ikuta[1], Kazumasa Oguri[1,2], Masashi Tsuchiya[1], Takao Yoshida[1], Kunihiro Aoki[1], Yosaku Maeda[1], Kiichiro Kawamura[3], Maki Suzukawa[3], Takuya Yamauchi[4], Heather Ritchie[1,5], Katsunori Fujikura[1] and Akinori Yabuki[1]*

[1] Japan Agency for Marine-Earth Science and Technology (JAMSTEC), Yokosuka, Japan, [2] Department of Biology, Nordcee and Danish Center for Hadal Research, University of Southern Denmark, Odense, Denmark, [3] Graduate School of Science and Technology for Innovation, Yamaguchi University, Yamaguchi, Japan, [4] Faculty of Advanced Science and Technology, Kumamoto University, Kumamoto, Japan, [5] RZSS WildGenes, Royal Zoological Society of Scotland, Edinburgh, United Kingdom

OPEN ACCESS

Edited by:
Xiaoshan Zhu, Tsinghua University, China

Reviewed by:
Atsuhiko Isobe, Kyushu University, Japan
Muhammad Reza Cordova, Indonesian Institute of Sciences, Indonesia

***Correspondence:**
Ryota Nakajima
nakajimar@jamstec.go.jp

Specialty section:
This article was submitted to Marine Pollution, a section of the journal Frontiers in Marine Science

Received: *01 November 2021*
Accepted: *01 December 2021*
Published: *13 January 2022*

Citation:
Nakajima R, Miyama T, Kitahashi T, Isobe N, Nagano Y, Ikuta T, Oguri K, Tsuchiya M, Yoshida T, Aoki K, Maeda Y, Kawamura K, Suzukawa M, Yamauchi T, Ritchie H, Fujikura K and Yabuki A (2022) Plastic After an Extreme Storm: The Typhoon-Induced Response of Micro- and Mesoplastics in Coastal Waters. Front. Mar. Sci. 8:806952. doi: 10.3389/fmars.2021.806952

Extreme storms, such as tropical cyclones, are responsible for a significant portion of the plastic debris transported from land to sea yet little is known about the storm response of microplastics and other debris in offshore and open waters. To investigate this, we conducted floating plastic surveys in the center of Sagami Bay, Japan approximately 30 km from the coastline, before and after the passage of a typhoon. The concentrations (number of particles/km^2) of micro- and mesoplastics were two orders of magnitude higher 1-day after the typhoon than the values recorded pre-typhoon and the mass (g/km^2) of plastic particles (sum of micro- and mesoplastics) increased 1,300 times immediately after the storm. However, the remarkably high abundance of micro- and mesoplastics found at 1-day after the typhoon returned to the pre-typhoon levels in just 2 days. Model simulations also suggested that during an extreme storm a significant amount of micro- and mesoplastics can be rapidly swept away from coastal to open waters over a short period of time. To better estimate the annual load of plastics from land to sea it is important to consider the increase in leakages of plastic debris into the ocean associated with extreme storm events.

Keywords: hurricanes, macroplastics, mesoplastics, microplastics, Sagami Bay, tropical cyclones, typhoon

INTRODUCTION

Each year, approximately 20 million metric tons of land-based plastic debris makes its way into aquatic systems, including oceans and freshwater networks, and this figure is only likely to rise (Borrelle et al., 2020). Once they end up in the sea, plastic debris eventually accumulates in the marine environment as most plastics are believed to take several hundred years, or even longer, to break down completely (Derraik, 2002; Turner et al., 2020).

One of the main sources of plastic debris that ends up in the sea is mismanaged plastic waste that is leaked directly from shorelines or indirectly through riverine waterways (Lebreton et al., 2017), urban runoff (Weideman et al., 2020), sewage discharge (Browne et al., 2011) and wind dispersal (Schmidt et al., 2017). Particularly, flood events caused by heavy rainfall enhance the movement of plastic debris of land-based origin into the marine environments from multiple source points (Moore et al., 2002; Axelsson and van Sebille, 2017; Kataoka et al., 2019; Nihei et al., 2020). Therefore, extreme weather events that cause strong winds, heavy rainfall, and associated flooding can greatly enhance the leakage of plastic and other debris into the sea (Veerasingam et al., 2016; Gündoğdu et al., 2018; Hitchcock, 2020; Ockelford et al., 2020).

Tropical cyclones, including typhoons and hurricanes, are the most extreme episodic weather events occurring at low- and mid-latitudes. They bring heavy precipitation resulting in increased river flow and terrestrial runoff (Tsuchiya et al., 2015), and when coupled with the powerful winds they generate tropical cyclones can be a significant event that enhances the loading of plastic debris from land to the marine environment (Pelamatti et al., 2019; Wang et al., 2019; Hitchcock, 2020; Lo et al., 2020; Garcés-Ordóñez et al., 2021). For example, a single typhoon can contribute to more than 80% of the annual transport of microplastics that flow in the Edo River in Japan (Kudo et al., 2018). As such, an important focus of recent plastic research has been to establish the role of extreme storm events on plastic pollution and to determine how plastic debris varies in space and time after such events (Wang et al., 2019). Studies of past tropical cyclones have suggested that global warming may lead to increasing intensities of these episodic events (Kunkel et al., 2013; Tu and Chou, 2013) and therefore the impacts of tropical cyclones on the transport of marine debris will also be augmented. Understanding the leakage patterns of marine plastic debris by tropical cyclones and other storm events is essential for determining strategies to mitigate further pollution, especially in regions where there are frequent typhoon or hurricane events.

At present, most studies investigating how microplastics and other debris respond to storm disturbances are based on observing succession patterns by revisiting rivers (Hitchcock, 2020), beaches (Lo et al., 2020), shores (Zhao et al., 2015) or nearshore waters (<10 km) (Gündoğdu et al., 2018; Chen et al., 2019) after storm events. Although these studies provide valuable information on the storm response of microplastics and other debris in rivers, coasts and shallow waters, studies investigating the responses offshore or in open waters are scarce. Debris flowing into the coastal waters through rivers and shores *via* storm events will experience rougher sea conditions, such as higher waves and rapid currents, which may cause; an increase in transportation of debris out to the open waters, debris to be re-deposited into coastlines, or debris to sink to the sea bottom (Kukulka et al., 2012). As a result, the abundance of debris flowing into coastal waters may vary significantly over time after extreme storms. Yet, the true extent of plastic debris that is flowing into coastal waters and offshore through extreme weather events remains unclear.

In September 2019, Typhoon *Faxai*, equivalent to a Category 4 typhoon made landfall near Tokyo, Japan (Suzuki et al., 2020; Tamura et al., 2021). The destructive winds and storm surged with a maximum wind gust speed of 210 km h^{-1} which caused landslides, damage to buildings and homes, knocking out power and uprooting trees across central Japan, resulting in 25 billion USD economic loss (Eckstein et al., 2021). However, this typhoon event provided unique research opportunities for estimating the influence of extreme storm events on plastic debris in the marine environment.

Here we present the study of floating micro- and mesoplastics debris in the center of Sagami Bay, some 30 km away from the Japanese coastline, at 3-days before, 1-day after and 3-days the typhoon *Faxai*'s passage. Specifically, our study addressed two key topics regarding typhoon derived debris through observations and model simulations: (1) how much does the concentration of floating plastic debris offshore change before and after a typhoon passage? and (2) where does the debris that is carried from the land to coastal waters by the typhoon go? This will significantly contribute to our understanding of the fate of plastic debris after an extreme storm.

MATERIALS AND METHODS

Typhoon *Faxai*

Faxai (T1915) occurred east of the International Dateline presenting as a tropical depression on 2nd September 2019 before being upgraded to a typhoon on 5th September near Minami-Torishima Island as it moved across the Pacific Ocean (Japan Meteorological Agency, 2020; **Figure 1A**). The lowest central pressure of *Faxai* was 955 hPa with maximum sustained winds of 157 km h^{-1}. Shortly before 03:00 JST (Japan Standard time, + 9 GMT) on 9th September 2019, *Faxai* passed through Sagami Bay in central Japan with the largest diameter of storm wind determined to be 180 km (**Figure 1B**). The storm caused heavy precipitation with a maximum of 109 mm of rain in 1 h, resulting in urban flooding in Tokyo metropolitan area (Tokyo Regional Headquarters, 2019). This was one of the strongest typhoons to ever hit the region on record (Tamura et al., 2021). After *Faxai* passed through the Tokyo area, it was downgraded to an extra-tropical cyclone on 10th September 2019 off the east coast of Japan.

Plastic Sampling

Sampling was conducted at a location in the center of Sagami Bay (35°1.25′N; 139°22.65′E) over a water depth of 1,400 m (**Figure 1B**). This site was located near the center of the anticyclonic eddy of the bay (Iwata and Matsuyama, 1989) and thus an accumulation of debris was expected. We conducted sampling 3-days before *Faxai* reached the bay (September 7th), and revisited the same survey site at 1-day after (September 10th) and 3-days after (September 12th) the typhoon passed during a cruise on the R/V *Yokosuka* (YK19-11).

Floating micro- and mesoplastic particles were collected during the day (6:00–13:00) using a neuston net (mesh size, 333-μm; mouth opening size, 1.0 m width and 0.75 m height)

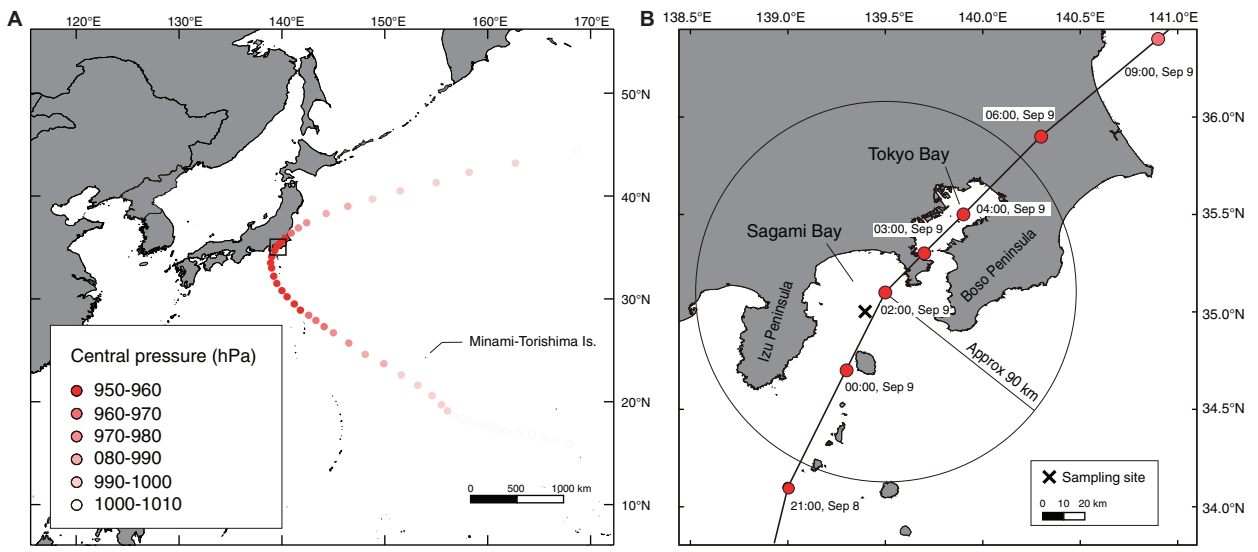

FIGURE 1 | Track of typhoon *Faxai* off **(A)** the east coast of Japan and **(B)** over Sagami Bay. The colors of circles on **(A,B)** donate the central pressure (hPa) of *Faxai*. Large circle on **(B)** represents the area of the storm with the wind speed of > 25 m/s (02:00 September 9th). Cross on **(B)** donates sampling site.

equipped with a pre-calibrated flow-meter (Rigo). Prior to towing, the net without cod-end was rinsed from the outside with running seawater in order to remove any contaminants in the net. The neuston net was deployed 4 m from the ship's starboard side using a crane and dragged for 20 min at a speed of 1–2 knots in the upper 0.4 m of the sea surface, where samples were collected in the cod-end of the net (Michida et al., 2019). Triplicate samples were collected at each sampling period by repeating the net towing. Once onboard, the net was thoroughly rinsed from the outside of net with running seawater to concentrate all particles into the cod-end. Samples were then transferred to 450 ml glass jars, fixed with 5% formalin and stored for laboratory analysis. The formalin was filtered before usage applying a 30 μm stainless mesh screen to avoid external contamination.

In addition to the neuston net sampling, floating macroplastic debris was visually counted 3-days before and 1-day after the storm. No visual observation was conducted 3-days after the storm. Three to four researchers were stationed on both the port and starboard side of the ship to observe floating debris for 70–90 min while the ship was running at a speed of 1 knot. All debris > 25 mm within 4 m from the side of the ship was visually counted. The lids of standard plastic bottles (ca. 28 mm in diameter), which were often observed during the observation, were used as a nominal calibration measure during the enumeration of debris > 25 mm.

Laboratory Analysis

Plastic-fiber free lab coats were worn in the laboratory and work surfaces were precleaned and dust-free prior to working. Sample processing was conducted in a laminar flow cabinet where possible. The neuston net samples were purified using 30% H_2O_2 at room temperature for 7 days (Hurley et al., 2018) and then visually inspected using a dissecting stereo microscope (Olympus, SZX16). All potential plastic particles were sorted out by hand using forceps and transferred to glass multiwell plates with glass lids. Particles were then dried at room temperature for 3 days, photographed with a connected camera (Olympus, DP74) to the microscope, and categorized according to their shape: fragments (mixture of hard fragments and films), line, foam, and pellet (Michida et al., 2019). Length and width of each particle were measured using an image software (Olympus, cellSens Dimension 2.1). Textile microfibers were excluded from the analysis due to the large mesh size of the net and to minimize the inclusion of external contamination. For the samples collected at the 1-day after the storm with many particles, large (>5 mm) or prominent plastic particles were sorted first where possible, then the remaining sample was split (1/8) using a stainless-steel splitter. All potential plastic particles, except for foamed particles, were then sorted from the split samples. As foamed particles were numerous in the split samples these samples were split further (1/8) and all foamed particles were sorted.

Polymer types for each of the sorted plastic-like particles were identified using Fourier Transform Infrared spectroscopy (FT-IR) with a single reflection diamond Attenuated Total Reflection (ATR) (Nicolet iS5, Thermo Fisher Scientific). The samples were positioned onto the ATR crystal and then compressed using the instrument clamp to achieve optical contact, allowing at 4 cm^{-1} spectral resolution by co-adding 16 scans per sample, and a background in air was collected every 60 min during measurement. Each collected spectrum was compared to multiple spectral database libraries containing both synthetic polymers and non-synthetic materials (Omnic 9, Thermo Fisher Scientific). A hit quality > 60% was used as the threshold for polymer types (Galgani et al., 2013). In total, 1,821 particles were identified as plastic polymers with FT-IR in this study.

Particles identified as plastic were pooled by each net tow sample and transferred to a pre-weighed glass vial, then the

weights of the plastic particles were measured. The plastic particles collected from the neuston nets were characterized into three size-categories: microplastic (<5 mm), mesoplastic (5–25 mm), and macroplastic (>25 mm) based on the lengths of each particle (GESAMP, 2019). After the counting of individual plastic particles in each sample, densities (number of particles per square kilometer) were calculated from the towed distance measured by the flow-meter and the frequency of sample split.

Wooden and plant debris from the neuston net samples were sorted out using forceps prior to the plastic analysis and pooled by net tow sample. These pooled samples were dried for 24 h at 60°C and then weighed. In addition, prominent insects were also counted and sorted out, and identified to family level wherever possible.

Particle Tracking Simulations After Storm

We conducted particle tracking simulations at the surface of Sagami Bay before and after the typhoon passage using the surface current reproduced from a tide-resolution general circulation model with the horizontal resolution of 1/36 (JCOPE-T DA) (Miyazawa et al., 2021). See **Supplementary Material** for the details of the model configuration. We aligned 100 model particles on the coast of Sagami Bay 2, 7, 9, and 12 h after the storm, and 1 week before the storm to see how many particles could be flushed out of the Sagami Bay across different time scales. We defined the extent of the bay as the inner side of the line connecting the edge of Boso Peninsula and the edge of Izu Peninsula (**Figure 1B**), and the particles which moved out of this line were considered to have been transported out of the bay. Finally, we compared the relative abundance of residual particles in the bay between the different time set ups.

Statistical Analysis

The difference in the density, mass, and length of microplastics and mesoplastics between different sampling periods (3-days before, and 1- and 3-days after the storm passage) was determined using a one-way ANOVA and differences among means were then analyzed using Tukey-Kramer multiple comparison tests. A difference at $p < 0.05$ was considered significant.

RESULTS

Changes in the Density and Mass of Plastic and Other Debris

At 3-days before the typhoon passed (September 7th), the densities of micro- and mesoplastics were on average (± SD) 101,762 ± 13,213 pieces km^{-2} and 11,340 ± 7,198 pieces km^{-2}, respectively (**Figures 2A,B**). At 1-day after the typhoon passage (September 10th), the concentrations of micro- and mesoplastics significantly increased by two orders of magnitude ($p < 0.01$ for both micro- and mesoplastics, Tukey-Kramer), being 226 times and 274 times greater than those at the pre-typhoon period, respectively. Mean concentration of micro- and mesoplastics 1-day after the typhoon passage reached 23,032,769 ± 8,372,347 pieces km^{-2} and 3,104,930 ± 1,847,652 pieces km^{-2}, respectively. At 3-days after the typhoon passage, the concentration of micro- and mesoplastics significantly ($p < 0.05$ for both micro- and mesoplastics, Tukey-Kramer) dropped to concentrations similar to pre-typhoon levels (microplastic, 77,698 ± 10,863 pieces km^{-2}; mesoplastics, 12,143 ± 10,244 pieces km^{-2}). There were no significant differences in the density of microplastics ($p > 0.05$) and mesoplastics ($p > 0.05$) between the samples taken pre-typhoon and 3-days after the typhoon passed.

The mass (g km^{-2}) of plastic particles collected by the net (sum of micro- and mesoplastics) showed the same trend as the density data (**Figure 2C**). The mass was on average 0.070 ± 0.035 kg km^{-2} before the typhoon passage, which significantly ($p < 0.01$, Tueky-Kramer) increased 1,309 times immediately after the storm to 91.6 ± 30.9 kg km^{-2}. Then, it significantly ($p < 0.01$, Tueky-Kramer) decreased to the pre-typhoon level at 3-days after the storm (0.11 ± 0.062 kg km^{-2}). There was no significant difference in the mass between pre- and 3-days post typhoon ($p > 0.05$, Tueky-Kramer).

In addition to plastic debris, a markedly large amount of fine wooden debris and plant debris was collected from the net 1-day after typhoon, reaching 415.3 ± 243.8 kg km^{-2} (**Figure 2D**). Wood and other plant debris were not collected before the typhoon or 3-days after the typhoon. Some insects, including wingless insects such as ants (Formicidae), were also only collected at 1-day after the storm (**Supplementary Figure 1**).

Large plastic debris was also prominent on the sea-surface 1-day after the storm. At 3-days before the typhoon passed, the density of visually counted macroplastic (> 25 mm) ranged from 1,824 to 2,183 pieces km^{-2} with a mean of 2004 pieces km^{-2} (**Supplementary Figure 2A**). At 1-day after the typhoon passed the mean density was 5.2 times greater than the pre-typhoon period, ranging from 10,092 to 10,698 pieces km^{-2} with a mean of 10,392 pieces km^{-2}. The mean density of visually counted macroplastic was lower than that obtained from the net sampling at 1-day after the storm (29,269 ± 26,713 pieces km^{-2}), though no macroplastics were collected by the net 3-days before or 3-days after the typhoon (**Supplementary Figure 2B**).

Changes in the Polymer Type, Shape and Size of Micro- and Mesoplastics

Polyethylene (PE) and polypropylene (PP) were dominant in microplastics and mesoplastics before the typhoon passed (PE 59.7 ± 10.3% and PP 30.2 ± 6.3% in microplastics; PE 80.0 ± 20.0% and PP 13.3 ± 11.5% in mesoplastics) (**Figures 3A,B**). At 1-day after the typhoon, microplastics consisted mostly of polystyrene (PS) (76.5 ± 14.1%) while mesoplastics were comprised mainly of PE (38.4 ± 24.9%) and PS (37.2 ± 18.3%). At 3-days after the storm, PS was still the highest proportion of polymer seen in microplastics (63.4 ± 3.3%) while mesoplastics were comprised mainly of PE (58.3 ± 52.0%) and PS (33.3 ± 57.7%).

The morphological shapes of microplastics and mesoplastics collected before the typhoon passed were predominantly fragments including hard fragments and films (93.4 ± 5.9% in

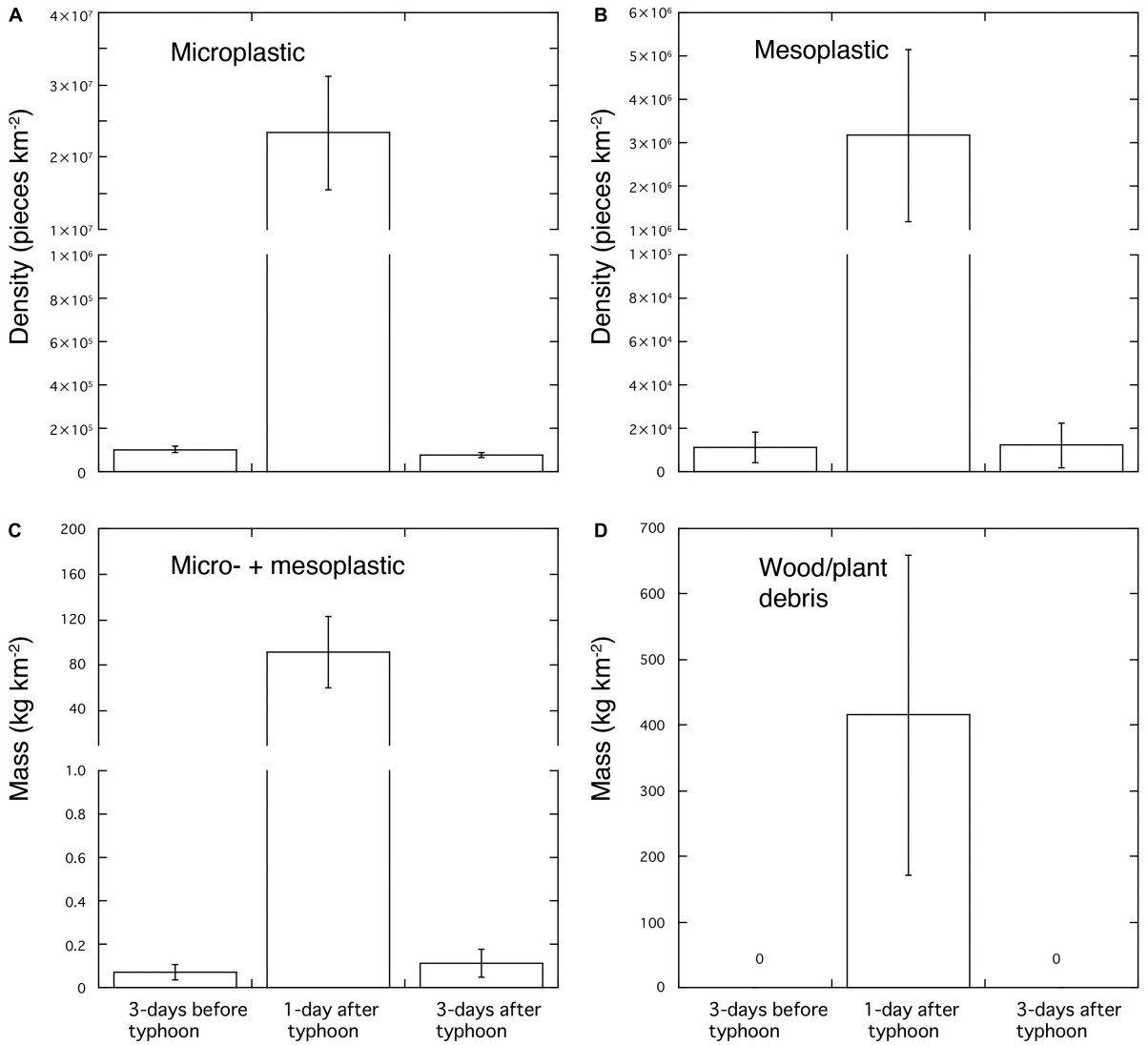

FIGURE 2 | Changes in the density and mass of plastic and other debris 3-days before, and 1- and 3-days after typhoon passage: density (pieces km^{-2}) of **(A)** microplastic and **(B)** mesoplastics, and mass (kg km^{-2}) of **(C)** micro− + mesoplastics and **(D)** wood and plant debris. Error bars indicate standard deviation of mean.

microplastics; 80.0 ± 20.0% in mesoplastics) followed by lines (6.6 ± 5.9% in microplastics; 13.3 ± 11.5% in mesoplastics) (**Figures 3C,D**). At 1-day after the typhoon, foamed particles, namely particles of expanded PS (EPS), were dominant in microplastics (81.7 ± 9.9%). Foamed particles were also an important component in mesoplastics (37.1 ± 17.9%) 1 day after the storm but the most dominant shapes seen were fragments (59.8 ± 15.1%). At 3-days after the storm, both microplastics and mesoplastics consisted mostly or entirely of fragments (97.8 ± 3.8 and 100.0 ± 0.0%, respectively).

Boxplots of particle length (μm) of microplastics and mesoplastics before and after the typhoon showed a presence of larger particles in microplastics 1-day after the storm (**Figure 4**). The mean size of microplastic particles at 1-day after the storm was significantly higher ($p < 0.01$, Tueky-Kramer) than before and 3-days after the storm, yet no significant difference was observed between before and 3-days after the storm (**Figure 4A**). For mesoplastics, no significant difference was found in particle size across the study periods ($p > 0.05$, Tueky-Kramer) (**Figure 4B**).

Particle-Tracking Simulations

Particle model analysis showed that plastic particles entering the bay immediately after the passage of the typhoon were highly likely to be transported out of the bay to the open ocean. In contrast, plastic particles that entered the bay before the typhoon, or more than 12 h after the passage of the typhoon, were less likely to be transported from the bay to the open ocean (**Figure 5**, see also movies in **Supplementary Material**). Most particles released from the coastline at 2 and 7 h after the typhoon passed (i.e., 04:00 and 09:00 September 9th) remained in the bay for the first 24 h (>90%), but only < 50% (45.7–49.3%) continued to persist in the

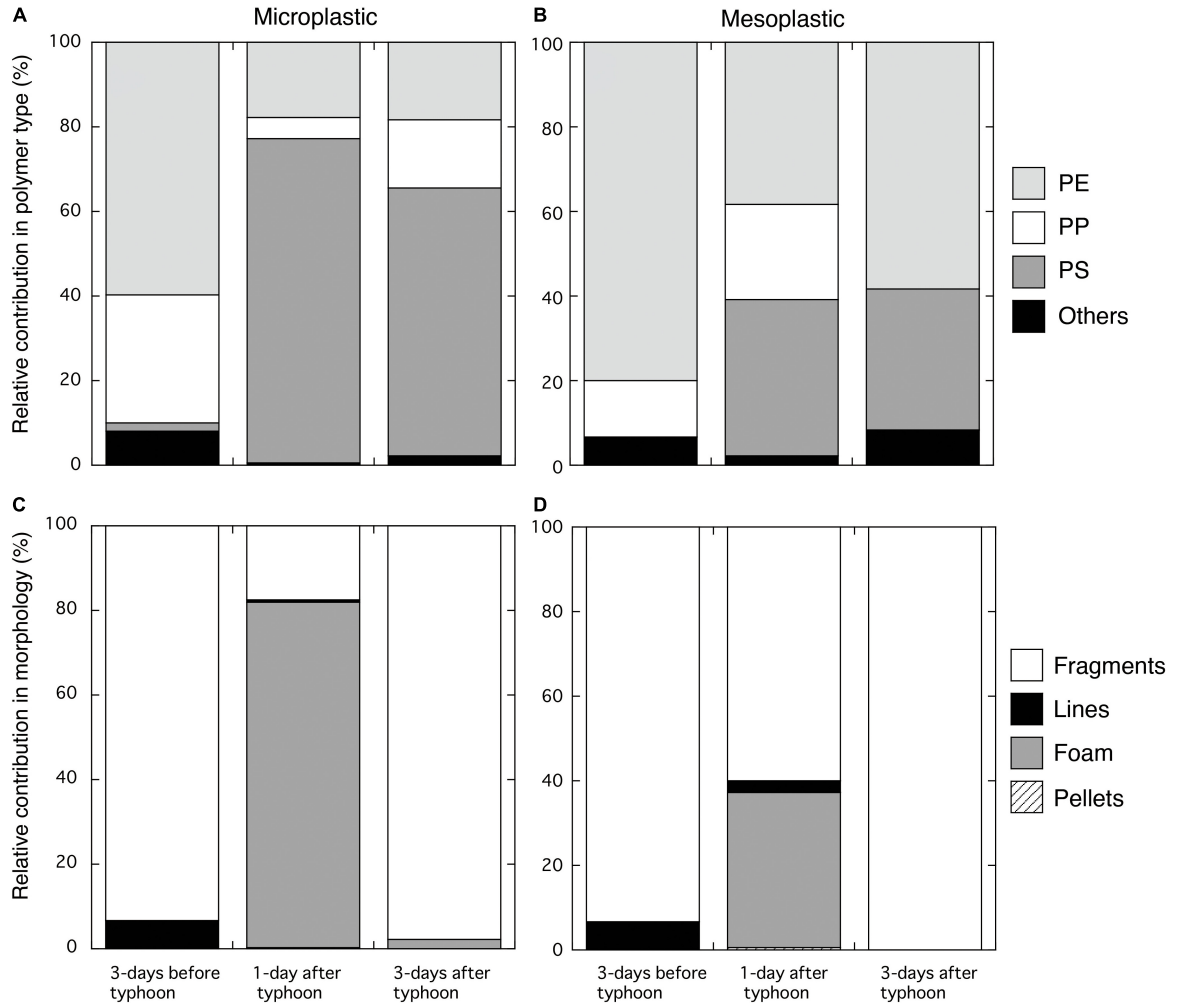

FIGURE 3 | Changes in the composition of **(A,B)** polymer type and **(C,D)** shape of microplastics and mesoplastics 1-day before and 1- and 3-days after the typhoon passage. PE, polyethylene; PP, polypropylene; PS, polystyrene. Fragments on **(C,D)** include hard fragments and films.

bay after 120 h due to leakage into the open waters (**Figure 5**). Similarly, particles released 9 h after the typhoon passage (11:00 September 9th) showed persistence of ca. 60% in the bay after 120 h. In contrast, particles released 12 h after the typhoon, or 1 week before the typhoon, showed relatively higher persistence in the bay with 78–82% still residing after 120 h.

DISCUSSION

Here we provide evidence that extreme weather events are one of the major driving forces responsible for transporting large amounts of plastic debris from the land to the sea. Although earlier studies have documented debris succession patterns before and after storm events in rivers, coasts, and shallow nearshore waters, our results highlight the degree of debris found offshore far from the coast (> 30 km) after an extreme storm event.

Flood events caused by heavy precipitation enhance the movement of plastic debris of terrestrial origin into the marine environments from multiple points, of which rivers are considered one of the major pathways (Kudo et al., 2018; Nihei et al., 2020). One typical debris that is abundant in rivers during heavy rainfalls is wooden debris (Doong et al., 2011). Considering the large amount of wooden debris found in this study, as well as the presence of wingless insects (ants), the plastic debris collected 1-day after the storm may be of river-based origin. This hypothesis is further supported by satellite image data taken at 1-day after the storm by Sentinel-2 showing muddy water flowing from the coastlines to the center of Sagami Bay which are occurrences of river runoff (Sentinel, 2019). In addition, the surface chlorophyll data provided by the satellite Shikisai (GCOM-C) showed that the bay at 1-day after the storm the bay experienced very little influx of oceanic seawater that could be a source of microplastics (Japan Aerospace Exploration Agency, 2019). Microplastics on the seafloor can be resuspended after storms that cause sufficient turbulence in the water column (Lattin et al., 2004). However, the study site has a total water depth of 1,400 m making resuspension of plastic debris from

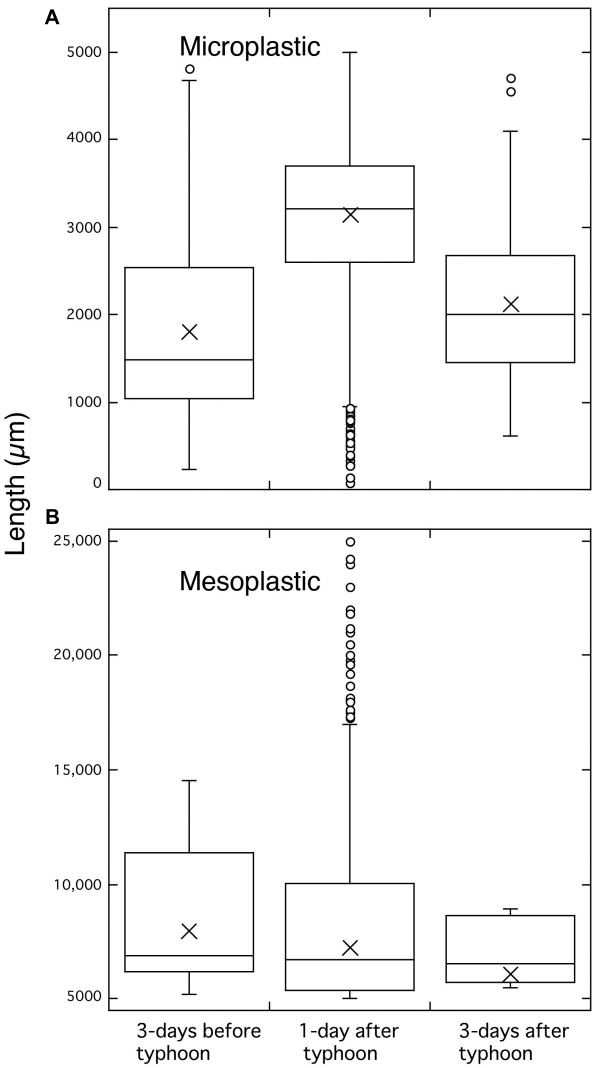

FIGURE 4 | Changes in the length (μm) of **(A)** microplastics and **(B)** mesoplastics 1-day before and 1-day and 3-days after typhoon passage. The line in the middle of the boxes represents the median values; the tops and bottoms of the boxes denote the 75 and 25% quartiles, respectively, and the top and bottom of the errors show the maximum and minimum value, excluding outliers (circles). Crosses denote the mean data.

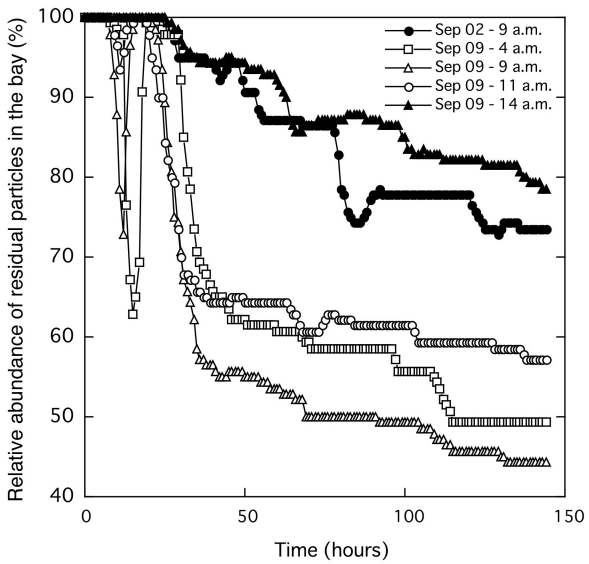

FIGURE 5 | Relative abundance (%) of residual particles in Sagami Bay after releasing particles from the shoreline at different time intervals based on the typhoon passage: 1 week before (09:00 September 2nd), 2 h after (04:00 September 9th), 7 h after (09:00 September 9th), 9 h after (11:00 September 9th) and 12 h after (14:00 September 9th).

sediments at this depth is unlikely. As such, we can infer that the majority of the debris observed in the center of Sagami Bay after the typhoon most likely originated from river sources.

Although comparatively fewer studies exist on plastic debris before and after tropical cyclones, it is apparent that extreme storms are responsible for a significant portion of the plastic debris transported from land to aquatic ecosystems. Previous investigations examining plastic debris before and after tropical cyclones, and other storm events have revealed that an increase in the abundance of microplastics and macroplastics is typically observed after storms (**Table 1**). For example, measurements of macroplastic debris densities in Hong Kong beaches during typhoon *Mangkhut* in 2018 showed a 12-fold increase compared with measurements taken before the typhoon passage (Lo et al., 2020). Similarly, typhoon *Meranti* in 2016 caused a 10 times increase in floating macroplastics in Xiamen Bay, China (Chen et al., 2019). Our results show that macroplastics (> 50 mm) yielded a 5-fold increase in abundance immediately after the storm, which is comparable to previous studies.

In studies of microplastics, previous investigations revealed that storm events caused 1.1–43.5-fold increase in the density of microplastics from rivers, beaches, estuary and nearshore waters (**Table 1**). However, in our study, microplastics (<5 mm) from offshore sites showed a 280-fold increase in density, which is the highest recorded value to date. Unlike microplastics found in rivers and shores, where microplastics continue to be transited from the land to the sea, the offshore study site is located near the center of an eddy in the bay and, as such, microplastics are likely to be accumulated. This propensity for accumulation at the offshore site compared to rivers and shores may explain the higher enrichment factor in microplastic density seen there. It is interesting to note that the study of the beaches in Hong Kong (Lo et al., 2020) showed a higher enrichment factor in the density of macroplastics than that of microplastics (11.5 vs. 1.8, respectively), which contradicts our offshore results that showed a higher enrichment factor for microplastics. This suggests that smaller plastic particles may be more likely to be transported offshore by storm events. Previous studies showed that microplastics have a much shorter residence time in shore waters than macroplastics so microplastics may be more easily transported to offshore waters *via* backwash waves (Hinata et al., 2017). This may also explain the higher microplastics enrichment factor seen for our offshore site. Additionally, the breakage

TABLE 1 | Comparative summary of the enrichment factors of macro- and microplastics in several bodies of water after storm events.

Study site	Specific sampling site/distance from shore (km)	Typhoon	Date	Collection method/mesh size	Collection media	Days after storm	Density after storm	Unit	Enrichment factor	Source
Macroplastics										
Hong Kong, China	Beach	Typhoon *Mangkhut*	16/09/2018	Hand picking	Beach	2–3	0.54	Items/km^2	11.5	Lo et al., 2020
Xiamen Bay, China	Nearshore/ < 5 km	Typhoon *Nepartak*	09/07/2016	Net/333 μm	Surface water	1	24[a]	Items/km^2	0.4	Chen et al., 2019
		Typhoon *Meranti*	15/09/2016				312[a]	Items/km^2	10.4	
Sagami Bay, Japan	Offshore/30 km	Typhoon *Faxai*		Visual	Surface water	1		Items/km^2		Present study
Microplastics										
Saitama, Japan	River	Typhoon *Talim*	17/09/2017	Net/350 μm	Surface water	1–2	11 billion	Transported items/year	2.9[b]	Kudo et al., 2018
NSW, Australia	River	Storm	05/10/2019	Bucket/37 μm	Surface waer	0	17,383	Items/m^3	43.5	Hitchcock, 2020
Hong Kong, China	Beach	Typhoon *Mangkhut*	16/09/2018	Quadrat	Beach	2–3	335	Items/kg	1.8	Lo et al., 2020
Fuzhou, China	Estuary	Typhoon *Soulik*	13/07/2013	Pump/333 μm	Surface water	1	1,246	Items/m^3	1.1	Zhao et al., 2015
Mersin Bay, Turkey	Nearshore/ < 10 km	Storm	Dec 2016–Jan 2017	Net/333 μm	Surface water	3 months	7,699,716	Items/km^2	14.3	Gündoğdu et al., 2018
California, US	Nearshore/ < 5 km	Storm	12/01/2001	Net/333 μm	Surface water	0	63	Items/m^3	6.3	Moore et al., 2002
Banderas Bay, Mexico	Nearshore/ < 3 km	Hurrican season		Net/333 μm	Surface water	–	0.044	Items/m^3	3.4	Pelamatti et al., 2019
Sanggou Bay, China	Neashore/ < 10 km	Typhoon *Haitang*, *Noru*	30/07/2017, 06/08/2017	Bucket/50 μm	Surface water	3	89,500	Items/m^3	1.4	Wang et al., 2019
				Grab	Sediment	3	3,035	Items/kg	1.4	
Sagami Bay, Japan	Offshore/30 km	Typhoon *Faxai*		Net/333 μm	Surface water	1	23,016,841	Items/km^2	226.2	Present study

[a]*Density was obtained from figures.* [b]*Result from a comparison with the annual cumulative transported microplastics.*

of fragile debris by rougher seas could also contribute to the increased number of small plastic particles recorded.

The most significant contributor to the increase in densities of micro- and macroplastics after the typhoon passed was polystyrene foam or expanded PS (EPS) particles. Polystyrene foams are extensively used as disposable take-way food boxes, heat-insulated containers and buoys, where polystyrene foam litter has been widely reported in the Asian-Pacific region (Yamashita and Tanimura, 2007; Kim et al., 2015; Fok et al., 2017). Most EPS particles found in this study were 2–3 mm in length, which largely contributed to the size shift of microplastics toward larger particles. Although the source of the EPS particles is unclear in our study, one possible source could be insulated containers such as the type used for transporting seafood products amongst other things as many EPS insulated containers are made of ca. 1–3 mm diameter of spherical EPS beads bonded together (Subhan, 2006). EPS made containers are fragile and are easily fragmented by external energy releasing small EPS particles (Majanga et al., 2015; Song et al., 2020). High physical energy associated with strong winds and rough ocean waves during typhoons could encourage the breakdown of exposed EPS containers into parts which could be further fragmented into smaller pieces that drift into offshore waters (Lee et al., 2013). As such, it is important to devise measures to prevent EPS containers from leaking into the environment in order to reduce microplastic leakage into the ocean.

The remarkably high abundance of micro- and mesoplastics found 1-day after the typhoon (91 kg/km^2) returned to the pre-typhoon level in just 2 days (0.1 kg/km^2). Essentially, ca. 90 kg/km^2 of plastic particles moved on from the survey site within a few days and it is not immediately clear where they have relocated to. It is unlikely that most plastic particles sank in just 2 days given that the predominant polymers were PP, PE and EPS, which have lower specific gravity than seawater. In fact, it would normally take several months to several years for buoyant plastic debris to move from the surface to the deeper water *via* events such as biofouling (Isobe et al., 2019; Nakajima et al., 2021). As such, the plastic particles may have been pushed back to the shore or swept away from the bay over a relatively short time scale. Our model shows that particles remain in the bay for a relatively longer period when they are not under the influence of a storm (i.e., 1 week before and 12 h after typhoon passage) probably due to the anticyclonic eddy in the Sagami Bay (Iwata and Matsuyama, 1989). On the contrary, half of the particles that moved into the bay right after the typhoon passed were shown to have been swept away from the bay in a few days probably due to the higher outflow from Tokyo Bay, next to Sagami Bay. The higher outflow from the mouth of Tokyo Bay, resulting from the typhoon which rotated counterclockwise and increased water volume in the bay due to increased precipitation (Okada et al., 2011), could have been responsible for the higher leakage of particles from the mouth of the Sagami Bay to the open waters. These results suggest that a significant amount of micro- and mesoplastics can be swept away rapidly from coastal waters to open waters by extreme storms. As such, it is important to consider the enhanced leakages of plastic debris into the ocean associated with extreme storm events to better estimate the annual plastic load from land to sea. This will be further emphasized in low- and mid-latitudes regions with frequent occurrences of tropical cyclones including typhoons and hurricanes. Notably East and Southeast Asia, the regions with frequent typhoons, account for approximately half of the plastic that ends up in the ocean (Jambeck et al., 2015), which could be upwardly revised considering the effect of typhoons. As the intensity of storm events is expected to increase with a changing climate (Knutson et al., 2010; Kossin et al., 2020), this study highlights the significance of the understanding the leakage patterns of marine plastic debris caused by extreme weather events. This will allow for the development of better strategies to mitigate plastic pollution, especially in regions where there are frequent typhoon or hurricane events.

It is important to note that while the effect of only a single typhoon was analyzed in this study, we believe that this adequately covers the significance of the debris leakage from land to sea. This is evidenced by the highest enrichment factor being recorded as a result of the typhoon *Faxai*. It should also be noted that, unlike rivers or coasts which are relatively easily accessible when typhoons occur, it is difficult to immediately investigate the changes in debris abundances at such an offshore site, some 30 km away from the coastline.

CONCLUSION

We provide insights into the fate of floating plastic debris transported offshore when a typhoon passed over Sagami Bay, Japan. Our investigation confirms the view that a tremendous amount of waste can be transported from the land to sea by an extreme storm event. This can result in two or three orders of magnitude higher abundance of micro- and macroplastics being recorded immediately after the typhoon compared to the values recorded pre-typhoon. However, the remarkably high abundance of micro- and mesoplastics found 1-day after the typhoon returned to the pre-typhoon levels in just 2 days, because the majority of the debris was swept away from the bay to the open ocean over a short period of time. The annual load of plastic debris being transported from land to sea will be underestimated if episodic storm events are not fully considered. In order to halt the leakage of plastic debris from land to sea, it is important to take measures that consider unexpected natural disasters such as typhoons.

DATA AVAILABILITY STATEMENT

The original contributions presented in the study are included in the article/**Supplementary Material**, further inquiries can be directed to the corresponding author/s.

AUTHOR CONTRIBUTIONS

RN: conceptualization, methodology, formal analysis, investigation, writing—original draft, and visualization. TM:

methodology, formal analysis, and visualization. TK, NI, YN, TI, KO, TYo, YM, KK, MS, TYa, and HR: investigation and writing—review and editing. MT and KF: supervision and writing—review and editing. AY: conceptualization, methodology, investigation, and writing—review and editing. All authors contributed to the article and approved the submitted version.

FUNDING

This study was partially funded by the New Energy and Industrial Technology Development Organization (NEDO) project (JPNP18016) to RN, NI, YN and JSPS KAKENHI grant (19H04262) awarded to RN.

ACKNOWLEDGMENTS

We thank the captain and the crew of R/V *Yokosuka* for their efforts to make the sampling possible, and Tomoko Morotomi, Rie Matsui and Nozomi Noha for their help in sample analysis. We also thank M. Morioka, Nippon Marine Enterprises, Ltd. for her technical help during the cruise.

SUPPLEMENTARY MATERIAL

The Supplementary Material for this article can be found online at: https://www.frontiersin.org/articles/10.3389/fmars.2021.806952/full#supplementary-material

REFERENCES

Axelsson, C., and van Sebille, E. (2017). Prevention through policy: urban macroplastic leakages to the marine environment during extreme rainfall events. *Mar. Pollut. Bull.* 124, 211–227. doi: 10.1016/j.marpolbul.2017.07.024

Borrelle, S. B., Ringma, J., Law, K. L., Monnahan, C. C., Lebreton, L., McGivern, A., et al. (2020). Predicted growth in plastic waste exceeds efforts to mitigate plastic pollution. *Science* 369, 1515–1518. doi: 10.1126/science.aba3656

Browne, M. A., Crump, P., Niven, S. J., Teuten, E., Tonkin, A., Galloway, T., et al. (2011). Accumulation of microplastic on shorelines woldwide: sources and sinks. *Environ. Sci. Technol.* 45, 9175–9179. doi: 10.1021/es201811s

Chen, H., Wang, S., Guo, H., Lin, H., Zhang, Y., Long, Z., et al. (2019). Study of marine debris around a tourist city in East China: implication for waste management. *Sci. Total Environ.* 676, 278–289. doi: 10.1016/j.scitotenv.2019.04.335

Derraik, J. G. B. (2002). The pollution of the marine environment by plastic debris: a review. *Mar. Pollut. Bull.* 44, 842–852. doi: 10.1016/s0025-326x(02)00220-5

Doong, D.-J., Chuang, H.-C., Shieh, C.-L., and Hu, J.-H. (2011). Quantity, distribution, and impacts of coastal driftwood triggered by a typhoon. *Mar. Pollut. Bull.* 62, 1446–1454. doi: 10.1016/j.marpolbul.2011.04.021

Eckstein, D., Künzel, V., and Schäfer, L. (2021). *Global Climate Risk Index 2021*. Who Suffers Most from Extreme Weather Events? Weather-Related Loss Events in 2019 and 2000-2019. Berlin: Germanwatch e.V.

Fok, L., Cheung, P. K., Tang, G., and Li, W. C. (2017). Size distribution of stranded small plastic debris on the coast of Guangdong. South China. *Environ. Pollut.* 220, 407–412. doi: 10.1016/j.envpol.2016.09.079

Galgani, F., Hanke, G., Werner, S., Oosterbaan, L., Nilsson, P., Fleet, D., et al. (2013). *Guidance on Monitoring of Marine Litter in European Seas*. Luxembourg: Publications Office of the European Union, doi: 10.2788/99475

Garcés-Ordóñez, O., Saldarriaga-Vélez, J. F., and Espinosa-Díaz, L. F. (2021). Marine litter pollution in mangrove forests from Providencia and Santa Catalina islands, after Hurricane IOTA path in the Colombian Caribbean. *Mar. Pollut. Bull.* 168:112471. doi: 10.1016/j.marpolbul.2021.112471

GESAMP (2019). *Guidelines for the Monitoring and Assessment of Plastic Litter in the Ocean-GESAMP*. Reports and Studies No. 99. Nairobi: United Nations Environment Programme, 130.

Gündoğdu, S., Çevik, C., Ayat, B., Aydoğan, B., and Karaca, S. (2018). How microplastics quantities increase with flood events? An example from Mersin Bay NE Levantine coast of Turkey. *Environ. Pollut.* 239, 342–350. doi: 10.1016/j.envpol.2018.04.042

Hinata, H., Mori, K., Ohno, K., Miyao, Y., and Kataoka, T. (2017). An estimation of the average residence times and onshore-offshore diffusivities of beached microplastics based on the population decay of tagged meso-and macrolitter. *Mar. Pollut. Bull.* 122, 17–26. doi: 10.1016/j.marpolbul.2017.05.012

Hitchcock, J. N. (2020). Storm events as key moments of microplastic contamination in aquatic ecosystems. *Sci. Total Environ.* 734:139436. doi: 10.1016/j.scitotenv.2020.139436

Hurley, R. R., Lusher, A. L., Olsen, M., and Nizzetto, L. (2018). Validation of a method for extracting microplastics from complex, organic-rich, environmental matrices. *Environ. Sci. Technol.* 52, 7409–7417. doi: 10.1021/acs.est.8b01517

Isobe, A., Iwasaki, S., Uchida, K., and Tokai, T. (2019). Abundance of non-conservative microplastics in the upper ocean from 1957 to 2066. *Nat. Commun.* 10:417. doi: 10.1038/s41467-019-08316-9

Iwata, S., and Matsuyama, M. (1989). Surface circulation in Sagami bay: the response to variations of the Kuroshio axis. *J. Oceanogr.* 45, 310–320.

Jambeck, J. R., Geyer, R., Wilcox, C., Siegler, T. R., Perryman, M., Andrady, A., et al. (2015). Plastic waste inputs from land into the ocean. *Science* 347, 768–771. doi: 10.1126/science.1260352

Japan Aerospace Exploration Agency (2019). *Shikisai GCOM-C Surface Chlorophyll*. Available online at: https://www.eorc.jaxa.jp/JASMES/SGLI_NRT/data/CHLA/2019/09/10/GC1SG1_20190910012000 4900_L2MG_IWPRQ_2000_CHLA_11.png (accessed November 27, 2021).

Japan Meteorological Agency (2020). *Annual Report on the Activities of the RSMC Tokyo-Typhoon Center 2019*. Available online at: https://www.jma.go.jp/jma/jma-eng/jma-center/rsmc-hp-pub-eg/AnnualReport/2019/Text/Text2019.pdf (accessed November 27, 2021).

Kataoka, T., Nihei, Y., Kudou, K., and Hinata, H. (2019). Assessment of the sources and inflow processes of microplastics in the river environments of Japan. *Environ. Pollut.* 244, 958–965. doi: 10.1016/j.envpol.2018.10.111

Kim, I.-S., Chae, D.-H., Kim, S.-K., Choi, S., and Woo, S.-B. (2015). Factors influencing the spatial variation of microplastics on high-tidal coastal beaches in Korea. *Arch. Environ. Contam. Toxicol.* 69, 299–309. doi: 10.1007/s00244-015-0155-6

Knutson, T. R., McBride, J. L., Chan, J., Emanuel, K., Holland, G., Landsea, C., et al. (2010). Tropical cyclones and climate change. *Nat. Geosci.* 3, 157–163.

Kossin, J. P., Knapp, K. R., Olander, T. L., and Velden, C. S. (2020). Global increase in major tropical cyclone exceedance probability over the past four decades. *Proc. Natl. Acad. Sci. U.S.A.* 117, 11975–11980.

Kudo, K., Kataoka, T., Nihei, Y., and Kitaura, F. (2018). Estimation of temporal variations and annual flux of microplastics in rivers under-and high-flow conditions. . *J. Jpn. Soc. Civ. Eng. Ser. B1 (Hydraul. Eng.).* 74, 529–534.

Kukulka, T., Proskurowski, G., Morét-Ferguson, S., Meyer, D. W., and Law, K. L. (2012). The effect of wind mixing on the vertical distribution of buoyant plastic debris. *Geophys. Res. Lett.* 39:L07601.

Kunkel, K. E., Karl, T. R., Brooks, H., Kossin, J., Lawrimore, J. H., Arndt, D., et al. (2013). Monitoring and understanding trends in extreme storms: state of knowledge. *Bull. Am. Meteorol. Soc.* 94, 499–514.

Lattin, G. L., Moore, C. J., Zellers, A. F., Moore, S. L., and Weisberg, S. B. (2004). A comparison of neustonic plastic and zooplankton at different depths near the southern California shore. *Mar. Pollut. Bull.* 49, 291–294. doi: 10.1016/j.marpolbul.2004.01.020

Lebreton, L. C. M., Van der Zwet, J., Damsteeg, J.-W., Slat, B., Andrady, A., and Reisser, J. (2017). River plastic emissions to the world's oceans. *Nat. Commun.* 8:15611.

Lee, J., Hong, S., Song, Y. K., Hong, S. H., Jang, Y. C., Jang, M., et al. (2013). Relationships among the abundances of plastic debris in different size classes

on beaches in South Korea. *Mar. Pollut. Bull.* 77, 349–354. doi: 10.1016/j.marpolbul.2013.08.013

Lo, H.-S., Lee, Y.-K., Po, B. H.-K., Wong, L.-C., Xu, X., Wong, C.-F., et al. (2020). Impacts of Typhoon Mangkhut in 2018 on the deposition of marine debris and microplastics on beaches in Hong Kong. *Sci. Total Environ.* 716:137172. doi: 10.1016/j.scitotenv.2020.137172

Majanga, B. D., Fujieda, S., Nishi, R., and Hosotani, K. (2015). Marine debris distribution, variation and pattern/seasonal changes along the coast and on sea surface of the Kagoshima Bay. *J. Jpn. Soc. Civ. Eng. Ser. B3 (Ocean Eng.).* 71, I_503–I_508.

Michida, Y., Chavanich, S., Cabañas, A. C., Hagmann, P., Hinata, H., Isobe, A., et al. (2019). *Guidelines for Harmonizing Ocean Surface Microplastic Monitoring Methods*. Tokyo: Ministry of the Environment Japan.

Miyazawa, Y., Varlamov, S. M., Miyama, T., Kurihara, Y., Murakami, H., and Kachi, M. (2021). A nowcast/forecast system for Japan's coasts using daily assimilation of remote sensing and *in situ* data. *Remote Sens.* 13:2431. doi: 10.3390/rs13132431

Moore, C. J., Moore, S. L., Weisberg, S. B., Lattin, G. L., and Zellers, A. F. (2002). A comparison of neustonic plastic and zooplankton abundance in southern California's coastal waters. *Mar. Pollut. Bull.* 44, 1035–1038. doi: 10.1016/s0025-326x(02)00150-9

Nakajima, R., Tsuchiya, M., Yabuki, A., Masuda, S., Kitahashi, T., Nagano, Y., et al. (2021). Massive occurrence of benthic plastic debris at the abyssal seafloor beneath the Kuroshio Extension, the North West Pacific. *Mar. Pollut. Bull.* 166:112188. doi: 10.1016/j.marpolbul.2021.112188

Nihei, Y., Yoshida, T., Kataoka, T., and Ogata, R. (2020). High-resolution mapping of Japanese microplastic and macroplastic emissions from the land into the sea. *Water* 12:951.

Ockelford, A., Cundy, A., and Ebdon, J. E. (2020). Storm response of fluvial sedimentary microplastics. *Sci. Rep.* 10:1865. doi: 10.1038/s41598-020-58765-2

Okada, T., Nakayama, K., Takao, T., and Furukawa, K. (2011). Influence of freshwater input and bay reclamation on long-term changes in seawater residence times in Tokyo Bay, Japan. *Hydrol. Process.* 25, 2694–2702. doi: 10.1002/hyp.8010

Pelamatti, T., Fonseca-Ponce, I. A., Rios-Mendoza, L. M., Stewart, J. D., Marín-Enríquez, E., Marmolejo-Rodriguez, A. J., et al. (2019). Seasonal variation in the abundance of marine plastic debris in Banderas Bay, Mexico. *Mar. Pollut. Bull.* 145, 604–610. doi: 10.1016/j.marpolbul.2019.06.062

Schmidt, C., Krauth, T., and Wagner, S. (2017). Export of plastic debris by rivers into the sea. *Environ. Sci. Technol.* 51, 12246–12253. doi: 10.1021/acs.est.7b02368

Sentinel (2019). *Sentinel-1 L2C True Color*. Available online at: https://apps.sentinel-hub.com/eo-browser/?zoom=10&lat=35.10755&lng=139.34647&themeId=DEFAULT-THEME&visualizationUrl=https%3A%2F%2Fservices.sentinel-hub.com%2Fogc%2Fwms%2F42924c6c-257a-4d04-9b8e-36387513a99c&datasetId=S2L1C&fromTime=2019-09-10T00%3A00%3A00 (accessed November 27, 2021).

Song, Y. K., Hong, S. H., Eo, S., Han, G. M., and Shim, W. J. (2020). Rapid production of micro-and nanoplastics by fragmentation of expanded polystyrene exposed to sunlight. *Environ. Sci. Technol.* 54, 11191–11200. doi: 10.1021/acs.est.0c02288

Subhan, T. F. L. (2006). Lightweight high strength concrete with expanded polystyrene beads. *Mektek* 8, 9–15.

Suzuki, T., Tajima, Y., Watanabe, M., Tsuruta, N., Takagi, H., Takabatake, T., et al. (2020). Post-event survey of locally concentrated disaster due to 2019 Typhoon Faxai along the western shore of Tokyo Bay, Japan. *Coast. Eng. J.* 62, 146–158. doi: 10.1080/21664250.2020.1738620

Tamura, H., Kawaguchi, K., Iwamoto, T., and Fujiki, T. (2021). Coastal destruction and unusual wave spectra induced by Typhoon Faxai in 2019. *Coast. Eng. J.* 63, 92–105. doi: 10.1080/21664250.2021.1877944

Tokyo Regional Headquarters. (2019). *Preliminary Weather Report of Typhoon Faxai 2019*. Tokyo: Tokyo Regional Headquarters.

Tsuchiya, K., Kuwahara, V. S., Hamasaki, K., Tada, Y., Ichikawa, T., Yoshiki, T., et al. (2015). Typhoon-induced response of phytoplankton and bacteria in temperate coastal waters. *Estuar. Coast. Shelf Sci.* 167, 458–465. doi: 10.1016/j.ecss.2015.10.026

Tu, J.-Y., and Chou, C. (2013). Changes in precipitation frequency and intensity in the vicinity of Taiwan: typhoon versus non-typhoon events. *Environ. Res. Lett.* 8:14023.

Turner, A., Arnold, R., and Williams, T. (2020). Weathering and persistence of plastic in the marine environment: lessons from LEGO. *Environ. Pollut.* 262:114299. doi: 10.1016/j.envpol.2020.114299

Veerasingam, S., Saha, M., Suneel, V., Vethamony, P., Rodrigues, A. C., Bhattacharyya, S., et al. (2016). Characteristics, seasonal distribution and surface degradation features of microplastic pellets along the Goa coast, India. *Chemosphere* 159, 496–505. doi: 10.1016/j.chemosphere.2016.06.056

Wang, J., Lu, L., Wang, M., Jiang, T., Liu, X., and Ru, S. (2019). Typhoons increase the abundance of microplastics in the marine environment and cultured organisms: a case study in Sanggou Bay, China. *Sci. Total Environ.* 667, 1–8. doi: 10.1016/j.scitotenv.2019.02.367

Weideman, E. A., Perold, V., Arnold, G., and Ryan, P. G. (2020). Quantifying changes in litter loads in urban stormwater run-off from Cape Town, South Africa, over the last two decades. *Sci. Total Environ.* 724:138310. doi: 10.1016/j.scitotenv.2020.138310

Yamashita, R., and Tanimura, A. (2007). Floating plastic in the Kuroshio current area, western North Pacific Ocean. *Mar. Pollut. Bull.* 4, 485–488. doi: 10.1016/j.marpolbul.2006.11.012

Zhao, S., Zhu, L., and Li, D. (2015). Microplastic in three urban estuaries, China. *Environ. Pollut.* 206, 597–604. doi: 10.1016/j.envpol.2015.08.027

Conflict of Interest: The authors declare that the research was conducted in the absence of any commercial or financial relationships that could be construed as a potential conflict of interest.

frontiers in Marine Science

ORIGINAL RESEARCH
published: 03 February 2022
doi: 10.3389/fmars.2021.779321

Combined Effects of Microplastics and Benzo[a]pyrene on the Marine Diatom *Chaetoceros muelleri*

Yuanyuan Su[1,2†], Huaiyuan Qi[1,2†], Yipeng Hou[1,2], Mengyi Gao[1,2], Jie Li[1,2], Minggang Cai[3], Xiaoshan Zhu[4], Miao Chen[2,5,6], Chengjun Ge[1,2], Dongdong Fu[1,2], Zezheng Wang[1,2] and Licheng Peng[1,2]*

[1] Key Laboratory of Agro-Forestry Environmental Processes and Ecological Regulation of Hainan Province, Hainan University, Haikou, China, [2] College of Ecology and Environment, Hainan University, Haikou, China, [3] State Key Laboratory of Marine Environmental Science, Xiamen University, Xiamen, China, [4] Institute of Ocean Engineering, Tsinghua Shenzhen International Graduate School, Tsinghua University, Shenzhen, China, [5] Hainan Key Laboratory of Tropical Eco-Circular Agriculture, Environment and Plant Protection Institute, Chinese Academy of Tropical Agricultural Sciences, Haikou, China, [6] Hainan Danzhou Tropical Agro-Ecosystem National Observation and Research Station, Danzhou, China

OPEN ACCESS

Edited by:
Jian Zhao,
Ocean University of China, China

Reviewed by:
Bin Xia,
Yellow Sea Fisheries Research Institute, Chinese Academy of Fishery Sciences (CAFS), China
Fei-fei Liu,
Shandong University, China

***Correspondence:**
Licheng Peng
lcpeng@hainanu.edu.cn

[†]These authors have contributed equally to this work and share first authorship

Specialty section:
This article was submitted to Marine Pollution, a section of the journal Frontiers in Marine Science

Received: *18 September 2021*
Accepted: *30 December 2021*
Published: *03 February 2022*

Citation:
Su Y, Qi H, Hou Y, Gao M, Li J, Cai M, Zhu X, Chen M, Ge C, Fu D, Wang Z and Peng L (2022) Combined Effects of Microplastics and Benzo[a]pyrene on the Marine Diatom Chaetoceros muelleri. Front. Mar. Sci. 8:779321. doi: 10.3389/fmars.2021.779321

Microplastics are regarded as ubiquitous pollutants in the ocean and have attracted worldwide concerns. Benzo[a]pyrene (B[a]P), one of typical polycyclic aromatic hydrocarbons (PAHs), is commonly detected in marine environment. Once coexisted, the microplastics and B[a]P may interact with each other and result in combined toxicity to organisms, and these remain to be systematically elucidated. Thus, this study aims to investigate (i) the effects of single micro-sized polystyrene (mPS), polyethylene terephthalate (mPET), and B[a]P on cell growth of *Chaetoceros muelleri*; and (ii) the interaction of microplastics and B[a]P, and their combined effects on *C. muelleri*. The results showed that both single microplastics and B[a]P at a high concentration of 150 μg/L inhibited the growth of *C. muelleri*. For single treatment of microplastics, stronger inhibition effects on microalgae was caused by mPET than that of mPS, with the highest IR of 25.23 and 11.17%, respectively. This may be attributed to the obvious surface roughness of mPET. By comparison, the combined effects of microplastics and B[a]P significantly inhibited the growth of *C. muelleri* as compared with the single treatment of B[a]P ($P < 0.05$). Synergistic effect was found in the combination of microplastics with B[a]P at high concentrations of 150 μg/L. Interestingly, the antagonistic effect on *C. muelleri* was observed in the combined treatment of microplastics and B[a]P at low concentrations of 10 μg/L. In addition, the pollutants reduced the content of photosynthetic pigments in microalgal cells. The SOD and MDA content of microalgae increased in the early stage of exposure to pollutants (e.g., Days 1 and 5), but decreased in the later stage (Day 15) compared with the control group. The decreased superoxide dismutase (SOD) and catalase (CAT) activity in single and composite systems may indicate that the antioxidative enzymatic system of microalgae has been inhibited or destroyed. This study will be helpful to further explore the ecological threats of microplastics and PAHs to the marine ecosystem.

Keywords: microplastics, benzo[a]pyrene, *Chaetoceros muelleri*, combined toxicity, oxidative stress

INTRODUCTION

Large quantities production (3.59 trillion tons in 2018) of plastics (EuropePlastics, 2019) would result in the accumulation of ubiquitous microplastics (<5 mm) in the environment (Jambeck et al., 2015; Fu et al., 2020). Microplastics are characterized as small size, large surface-to-volume ratio, mostly porous, rough surface, and abundant functional groups, and these features enable them to easily adsorb other contaminants such as polycyclic aromatic hydrocarbons (PAHs), heavy metals, pathogens, and others (Wright et al., 2013; Fu et al., 2019). The interaction of microplastics and other pollutants may alter their environmental behavior, toxicity, bioavailability, and may pose threats to the ecosystem and even human beings (Zhang et al., 2018; Yang et al., 2020).

Recently, more and more attention has been paid on the combination of microplastics and coexisting pollutants and their toxicological effects on marine organisms. For instance, some previous studies pointed out that microplastics (e.g., micro-sized polystyrene, polyethylene and polyamide) can strongly adsorb nonylphenol and therefore alleviate its toxicity to *Chlorella pyrenoidosa* (Yang et al., 2020). Moreover, a low level of mPS (10 μm, 2 μg/L) could decrease the toxicity of phenanthrene on the marine medaka *Oryzias melastigma* at its early developmental stage (Li Y. et al., 2020). Similarly, polystyrene divinylbenzene microspheres at a size of 97 μm did not magnify the acute effect of pyrene on the tropical fish *Lates calcarifer* (Guven et al., 2018). However, some contrary results were reported in other studies, for example, it was found that mPS significantly enhanced the bioaccumulation and toxicity of phenanthrene on *Daphnia magna* (Ma et al., 2016). Meanwhile, synergistic toxicities on microalgae were demonstrated in the combination of microplastics (red fluorescent polymer microspheres), procainamide, and doxycycline mixtures (Prata et al., 2018). Various factors may contribute to the difference, for example, the physical and chemical properties of microplastics, the tolerance of model organisms to pollutants, and the octanol water distribution coefficient and concentration of other pollutants (Zhu et al., 2018; Li et al., 2019; Yi et al., 2019; Yang et al., 2020). Under such circumstances, more systematic studies are required to elucidate the different combined toxicity of microplastics and coexisting pollutants on aquatic organisms.

B[a]P has a strong ability to enter and accumulate in the cells of aquatic organisms and causing various abnormalities and disorders due to its aromatic fused ring and lipophilicity (Derakhshesh et al., 2019). Previous studies showed that B[a]P is capable of influencing cell growth, effective quantum yield, and photosynthesis of phytoplankton (Li et al., 2021). For example, after 72 h of exposure to B[a]P (1–10 μg/L), the growth of *Skeletonema costatum* decreased significantly. However, *Akashiwo sanguinea* is more sensitive to B[a]P, and its growth decreased significantly at a quite lower concentration of 0.1 μg/L (Kim et al., 2004). Moreover, the interaction of coexisted B[a]P and microplastics would occur, especially the lipophilic B[a]P has strong affinity to suspended materials and sediments in the aquatic environment (Yu et al., 2018). Therefore, the microplastics in the environment are likely to become perfect carriers of B[a]P, increasing the bioavailability of B[a]P and enrichment in organisms along the food chain (Wang et al., 2021). However, further research on their combined toxicity to aquatic organisms is needed.

Microalgae are widely applied in ecotoxicological analytical tests due to their short generation time, easy operation and sensitivity to pollutants (Prata et al., 2019). Marine diatom *Chaetoceros muelleri*, as one of the most diverse phytoplanktons, was selected as the model organism to elucidate the single and combined effects of B[a]P, microplastics polystyrene (mPS) and polyethylene terephthalate (mPET). The parameters such as cell number, growth inhibition rate, scanning electron microscope (SEM), superoxide dismutase (SOD) and catalase (CAT) of *C. muelleri* were measured to clarify the toxic effects of microplastics, B[a]P and their combined effects on microalgae.

MATERIALS AND METHODS

Preparation of Microplastics

The microplastics (i.e., mPS and mPET) were purchased from Aladdin industrial corporation (Shanghai, China) and No. 8863 Huarun (Changzhou, China). The surface structure of mPS and mPET were observed using scanning electron microscopy (SEM, S3000). The functional groups of mPS and mPET were determined by using a Fourier Transform Infrared Spectrometer (FTIR, TENSOR27), respectively. The size of microplastics was measured by using a laser particle size analyzer (Masterizer 3000, Malvern Instruments Ltd., United Kingdom).

Microalgal Strain and Medium

Microalgae *C. muelleri* was obtained from the College of Oceanography, Hainan University. The *f/2* Guillard medium (Guillard, 1975) was prepared with natural seawater (filtered by 0.45 μm membrane) that was collected from the Xinbu Island in Hainan. The medium and flasks used in this study were sterilized at 121°C using an autoclave for 30 min (LDZM-60L-II, Shanghai Shenan Medical Instrument Factory). The initial microalgal concentration was maintained at approximately 1×10^5 cells/mL. Microalgae were cultivated in an Erlenmeyer flask (250 mL) under cool continuous white fluorescent lights (5,000 lx) with a light/dark cycle of 12 h/12 h. All the cultures were randomly placed in an incubator to achieve equal illumination. The temperature was kept at 25 ± 1°C, and all cultures were shaken every 12 h to prevent the aggregation and sedimentation of cells.

Toxicity Test of Pollutants on Microalgae

The concentration range of B[a]P was based on the pollution in the partial sea area of China, for example, an average concentration of B[a]P was 663 ng/L in Daya Bay (Shenzhen, China) while the total PAHs could reach up to 10, 984 ng/L (Qiu et al., 2004). Therefore, 10 μg/L B[a]P was selected to simulate the baseline of PAHs concentration in the natural environment, and also as the lowest concentration of toxicological tests to *C. muelleri* in the preliminary experiment of this study. Higher concentrations of 50, 100, and 150 μg/L B[a]P were set to simulate severely polluted areas. The preliminary results showed

TABLE 1 | Experimental design in this study.

Test	Pollutants	Concentration
Control	–	–
Single toxicity	mPS	200 mg/L
	mPET	200 mg/L
	B[a]P	10 and 150 μg/L
Combined toxicity	mPS + B[a]P	200 mg/L + 10 μg/L
		200 mg/L + 150 μg/L
	mPET + B[a]P	200 mg/L + 10 μg/L
		200 mg/L + 150 μg/L

"–" indicates that there is no contaminant.

that B[a]P at concentrations of 10, 50, and 100 μg/L did not significantly inhibit the growth of *C. muelleri*, while B[a]P at 150 μg/L reached an obvious inhibitory effect. Therefore, the concentration of B[a]P was set at 10 and 150 μg/L while microplastics at 200 mg/L (was determined by our previous study) were used for the following experiment. More details are presented in **Table 1**.

Completely dissolved B[a]P (Shanghai Aladdin Biochemical Technology Co., Ltd., AR) in dimethyl sulfoxide (DMSO, AR, Xilong Science Co., Ltd.) was used to produce a concentrated stock solution (2 g/L). The solution used for the toxicology test was obtained by adding an appropriate volume of the stocks into filtered seawater (0.45 μm). In the chronic toxicity test, the DMSO content is less than 0.005% and has no inhibition on microalgae (Gong et al., 2017). In addition, our preliminary experiments also demonstrated that the same volume of DMSO has no effect on the cell growth of *C. muelleri*.

The microplastics solution (200 mg/L) was prepared by weighing 0.03 g and adding them to the medium (150 mL) and then reaching evenly distributed state via ultrasonic treatment.

Toxicity Test of Single Microplastics and B[a]P on Microalgae

Microalgal inoculum was added to the medium supplemented with microplastics (i.e., mPS and mPET) and B[a]P, respectively, and then the cultures were placed in a light incubator for 15 days of cultivation. The experimental design is summarized in **Table 1**. All cultivation conditions were the same as those in Section "Microalgal Strain and Medium." All treatments were tested in replicates, and sterile conditions were maintained to avoid contamination in the test.

Combined Effects of Microplastics and B[a]P on Microalgae

The combined effects of mPS or mPET at 200 mg/L and B[a]P at concentrations of 10 and 150 μg/L were investigated (**Table 1**). All cultivation conditions were maintained the same as those in Section "Microalgal Strain and Medium."

Analytical Methods

Cell Number Density and Growth Inhibition Ratio

According to the guideline 201 of the Organization for Economic Cooperation and Development (OECD), the IR of *C. muelleri* was determined by counting cell numbers. The cell number density of *C. muelleri* was determined every 2 days, at 400× magnification using a hemocytometer under the microscope (OLYMPUS, DP71). Each sample was counted three times to obtain the mean value.

The microalgal growth inhibition ratio was calculated based on cell number density (Equation 1):

$$I_{gi}\ (\%) \ = \ \frac{C_{ci}-C_{ei}}{C_{ci}} \ \times \ 100\% \qquad (1)$$

where I_{gi} is the growth inhibition rate at the time *i*; C_{ci} and C_{ei} are the cell number density of the control and the treatment at the time *i*.

Assessment of Microplastics and B[a]P Interactive Effects on *C. muelleri* Growth

Abbott's model is commonly used to evaluate the potential interactions between microalgae and B[a]P combined system, which assumes the independent effects of components in the mixture. The model treats any deviation from this assumption as a symbol of the interaction between the mixture components (Gisi, 1996; Mwamba et al., 2016). Based on the measured individual toxicity of microplastics (T_{MPs}) and B[a]P ($T_{B[a]P}$), Abbott's model was used to predict their combined toxicity (T_{pre}), assuming an independent action of microplastics and B[a]P occurs in the mixture (Equation 2):

$$T_{pre} \ = \ T_{MPs} + T_{B[a]P} - \frac{\left(T_{MPs} \ \times \ T_{B[a]P}\right)}{100} \qquad (2)$$

where T_{pre} is the combined toxicity of microplastics and B[a]P predicted using Abbott's model; T_{MPs} and $T_{B[a]P}$ is the measured individual toxicity of microplastics and B[a]P, respectively.

Then, the ratio of the combined toxicity measured in the experiment (T_{obs}) and the value predicted by Abbott's model (T_{pre}) will be further calculated to check the existence of potential interaction between microplastics and B[a]P. For example, if the ratio of T_{obs} and T_{pre} (i.e., T_{obs}/T_{pre}) is equal to 1, indicating an additivity effect is achieved between microplastics and B[a]P, while the value of $T_{obs}/T_{pre} > 1$ or <1 indicates a synergistic or antagonistic effect is achieved for their combination, respectively.

Content of Photosynthetic Pigment

The content of photosynthetic pigment such as chlorophyll *a*, *b*, and carotenoid was measured by using the method of Song et al. (2020). Briefly, 2 mL of 90% methanol was added in some microalgal cells (2 mL) collected by centrifugation (10 min, 5,000 rpm). Then, the mixture was placed in the refrigerator overnight at 4°C for 24 h. Finally, the supernatant was obtained by centrifugation (10,000 rpm, 10 min) for measuring the absorbance at wavelengths of 470, 652, and 665 nm by using an ultraviolet-visible spectrophotometer (UV1800, Aoxi). The content of chlorophyll *a*, chlorophyll *b* and carotenoid was calculated according to the following formula.

$$C_a\ (\mathrm{mg/L}) \ = \ 16.82\mathrm{A}_{665} - 9.28\mathrm{A}_{652} \qquad (3)$$

$$C_b\ (\mathrm{mg/L}) \ = \ 36.92\mathrm{A}_{652} - 16.54\mathrm{A}_{665} \qquad (4)$$

TABLE 2 | Size distribution of microplastics used in this study.

Type	Distribution of size (μ m)		
	Dv10	Dv50	Dv90
mPS	173	258	376
mPET	177	281	425

Dv10, Dv50, and Dv90 indicates 10, 50, and 90% of particles with the size, respectively.

$$C_c\ (\mathrm{mg/L}) = \frac{1000A_{470} - 1.91C_a - 95.15C_b}{225} \quad (5)$$

where C_a, C_b, and C_c represents the content of chlorophyll *a*, chlorophyll *b* and carotenoid, respectively; A_{665}, A_{652}, and A_{470} indicate the absorbance of *C. vulgaris* at 470, 652, and 665 nm, respectively.

Antioxidant Enzyme

Antioxidant enzymes such as SOD and CAT of microalgae were determined using test kits (Solarbio Science & Technology Co., Ltd.). The samples were taken on the Days 1, 5, and 15. Briefly, some microalgal cells collected by centrifugation (10 min, 5,000 rpm) were added with extraction solution ($\sim 5 \times 10^6$ cells were added with 1 mL extraction solution) for further break cells by ultrasound (200 W, 3 s, 30 times). Finally, the supernatant was obtained by centrifugation (8,000 *g*, 10 min, 4°C) for measuring the absorbance at wavelength of 560 nm for SOD and 240 nm for CAT. The content of SOD and CAT was indicated as U/10^4 cells.

Interaction Between Microplastics and *C. muelleri*

The coexisting microplastics with microalgae in the culture were observed by naked eyes and recorded every day, while the surface structures of microplastics were measured using SEM at Day 15. Briefly, the microplastics were collected by centrifugation (8,000 rpm, 10 min) and resuspended in a phosphate buffer (0.05 M, pH 7.2) (Mao et al., 2018). Then, the microplastics were fixed using 2.5% glutaraldehyde for 24 h and were further observed and measured using SEM. Cell damage was determined by using the Calcein/PI cell viability and cytotoxicity test kit (Beyotime Biotechnology Co., Ltd.).

Statistical Analysis

Excel 2010 and Origin 2018 were used for data analysis and plotting. The data were expressed as average ± standard error in the study. Different treatments were tested significantly through one-way analysis of variance with Duncan comparisons (SPSS 23.0).

RESULTS

Properties of Microplastics

The size distribution of microplastics is shown in **Table 2**, and the average size of mPET was slightly greater than that of mPS. As shown in **Figures 1A,B**, mPS floated on the surface of culture, while mPET sank to the bottom. The precipitation of mPET results from a larger density as compared to mPS. **Figures 1C,D** showed that many microalgal cells adhered to the surface of microplastics and form heterogeneous aggregations. The coexisting microalgal cells may affect the structures and characteristics of microplastics (Endo and Koelmans, 2016). The mPS is a glassy polymer with a weakly polar and weak π electron donor, and concave structure can be observed via SEM (**Figure 1E**). By comparison, mPET is a crystalline polymer with more amorphous regions, and plenty of micro-pores can be observed on the rough surface (**Figure 1F**). Moreover, the functional groups of the two microplastics are different, for example, mPS has a stronger intensity of hydroxyl groups (−OH, ∼3,400 cm^{-1}), carbon-carbon double bond (C = C, ∼1,642 cm^{-1}), carbonyl group (C = O, ∼1,710 cm^{-1}) and C-O stretching of phenolic (C-O, ∼1,260 cm^{-1}), but with a weakened intensity of methylene (CH_2, ∼2,926 cm^{-1}) as compared with those of mPET (**Figure 2**).

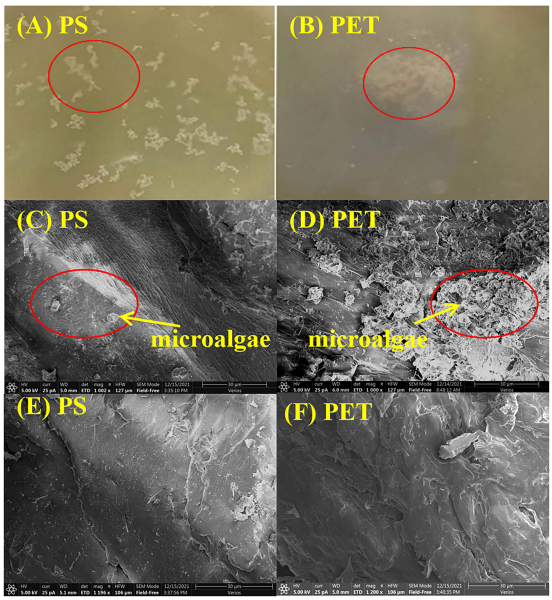

FIGURE 1 | Morphology of **(A)** mPS and **(B)** mPET in the culture of *Chaetoceros muelleri* observed by naked eyes; *C. muelleri* cells attached to **(C)** mPS and **(D)** mPET observed by SEM; SEM images of **(E)** mPS, and **(F)** mPET.

Effects of Microplastics and B[a]P on Microalgae

Effects of Microplastics on Cell Growth of *C. muelleri*

As shown in **Figures 3**, **4**, both microplastics have negative impacts on microalgae, with an increasing IR at the beginning of growth and then decreased in the later stage. The cell density of *C. muelleri* exposed to mPET (2.42×10^6 cells/mL) is less than mPS (2.55×10^6 cells/mL), and both were lower than the control (2.6×10^6 cells/mL). In addition, no significant difference ($P > 0.05$) was reached for the cell density of microalgae in the control

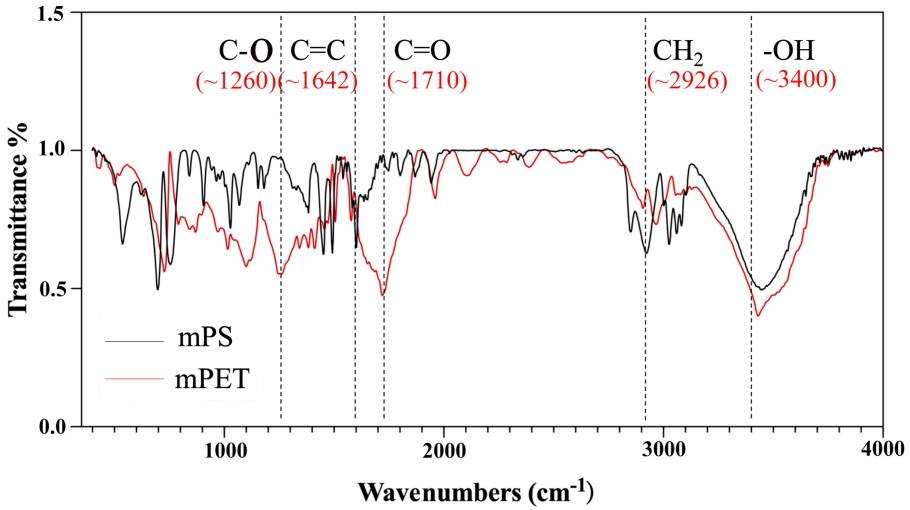

FIGURE 2 | Infrared absorption spectrum of mPS and mPET.

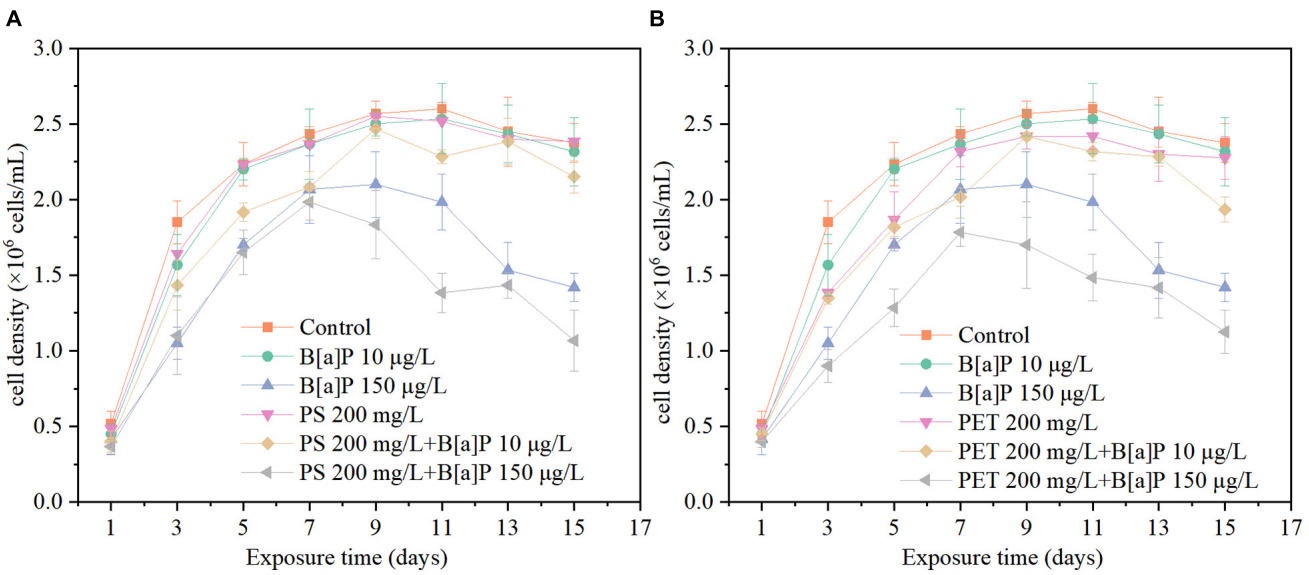

FIGURE 3 | The single and combined effects of microplastics [**(A)** mPS and **(B)** mPET] and B[a]P on the cell density of *C. muelleri*.

and the treatment with mPS. However, a significant difference ($P < 0.05$) was found with mPET as compared with the control.

Overall, mPET has stronger inhibition on the growth of microalgae than mPS, for example, the highest IR caused by mPET was 25.23% on the third day, which was significantly ($P < 0.05$) higher than that of mPS (11.17%) (**Figure 4**).

Effects of B[a]P on Cell Growth of *C. muelleri*

As also shown in **Figure 3**, in the 15 days of cultivation, the cell growth in terms of cell density (**Figure 3**) of *C. muelleri* was slightly inhibited by B[a]P at a concentration of 10 μg/L, but significantly inhibited at 150 μg/L ($P < 0.05$) compared to the control. The maximal cell density obtained in the treatment with B[a]P of 10 and 150 μg/L were 2.53×10^6 and 2.10×10^6 cells/mL (**Figure 3**), respectively. Correspondingly, the IR increased with the concentration of B[a]P on microalgae under the investigated condition, for instance, the IR caused by 10 and 150 μg/L B[a]P reached their own maximum value of 15.32 and 43.24% on Day 3, respectively (**Figure 4**).

Combined Effects of Microplastics and B[a]P on Cell Growth of *C. muelleri*

As shown in **Figures 3**, **4**, the cell density of all combined treatments of microplastics and B[a]P was lower than that of the single treatments. For instance, the highest IR of 55.18% was

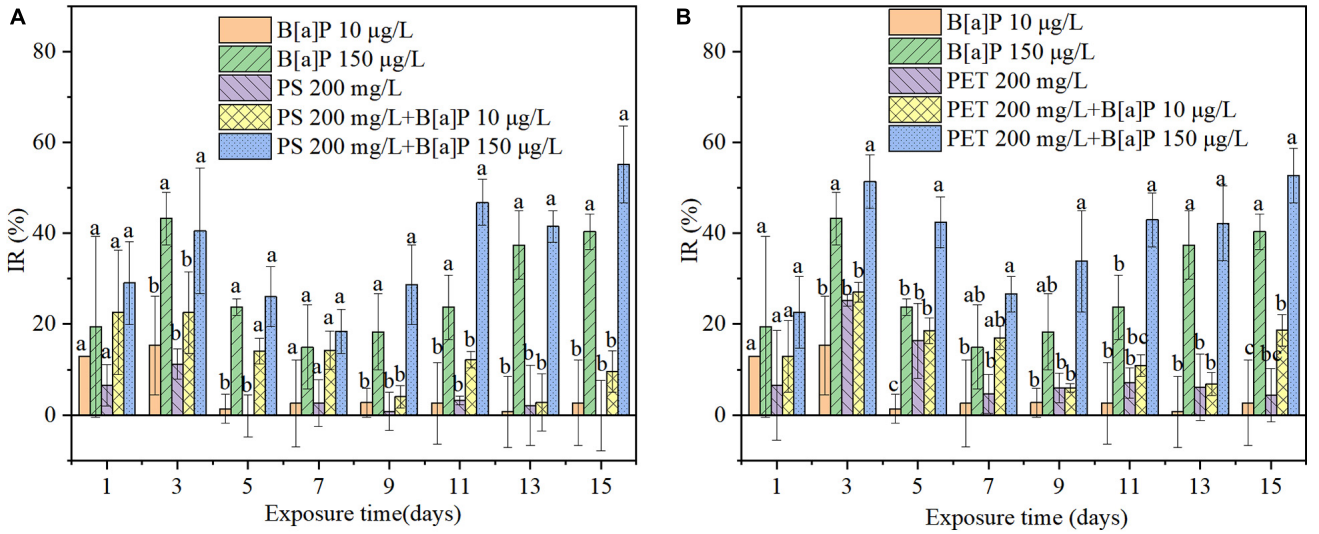

FIGURE 4 | The single and combined effects of microplastics [**(A)** mPS and **(B)** mPET] and B[a]P on the IR of *C. muelleri.* Different letters indicate significant differences among treatments ($P < 0.05$).

caused by the combined group of 150 μg/L B[a]P + 200 mg/L mPS, which was higher than that of single 150 μg/L B[a]P (IR = 40.34%) and mPS (IR = 1.26%) after 15-day cultivation, respectively (**Figure 4**). Similarly, the IR reached up to 52.66% in the combined group of 150 μg/L B[a]P + 200 mg/L mPET, which was also higher than that of single 150 μg/L B[a]P (IR = 40.34%) and mPET (IR = 4.36%) (**Figure 4**).

Furthermore, the combined toxicities of mPET and B[a]P on microalgae were greater than the combinations of mPS and B[a]P in terms of cell density and IR. It is consistent with the toxicity of microplastics to *C. muelleri* (**Figures 3**, **4**). Additionally, the combined inhibitory effects on the growth of *C. muelleri* increased with the concentration and single toxicity of pollutants (e.g., mPET, mPS, and B[a]P). For instance, the maximal cell density (1.98×10^6 cells/mL) achieved in the combined group of 150 μg/L B[a]P + 200 mg/L mPS, was significantly lower than that of combination of 10 μg/L B[a]P + 200 mg/L mPS (2.47×10^6 cells/mL) ($P < 0.05$). The IR of the combined group of B[a]P and mPS was less than the combined group of B[a]P and mPET.

Photosynthetic Pigment Content of Microalgae

Overall, the content of photosynthetic pigment was decreased when the microalgae exposed to either single or combined microplastics and B[a]P (**Figure 5** and **Supplementary Figure 1**). For single system, the inhibitory effect of high concentration of B[a]P was greater than that of low concentration of B[a]P. In addition, the inhibitory effect of PET was greater than that of PS. This is consistent with the results of growth inhibition. In the combined system, it is strange that the addition of microplastics alleviated the inhibitory effect of B[a]P on photosynthetic pigment of microalgae. For example, the photosynthetic pigment content of the culture exposed to single B[a]P (150 μg/L) was 1.97 mg/L, which was lower than that of cultures exposed to combined pollutants of PS + B[a]P 150 μg/L (2.19 mg/L) and PET + B[a]P 150 μg/L (3.36 mg/L) on Day 15 of cultivation.

Antioxidant Enzymes of Microalgae

The antioxidative defense system of *C. muelleri* in terms of SOD and CAT was also determined on the Days 1, 5, and 15 of cultivation in this study (**Figure 6**). In the early stage of pollutants exposure (Days 1 and 5), the pollutants stimulated the production of SOD and CAT of microalgae compared with the control group. As shown in a single toxicity test, the SOD and CAT content of the culture exposed to B[a]P increased with its concentration. For single microplastics, the SOD content of microalgal culture exposed to mPET was higher than that of mPS, but the CAT content of microalgal culture exposed to mPET was lower than that of mPS. The results may indicate that the type of microplastics was one of the important factors affecting the secretion of SOD and CAT by microalgae. As compared with the control, the SOD contents of the cultures exposed to the four combined treatments were significantly increased ($P < 0.05$) on Day 5, and the CAT on Day 1 was significantly increased ($P < 0.05$). Besides, the SOD and CAT content in the combined of microplastics and B[a]P was higher than that of single microplastics or B[a]P. Moreover, it should be mentioned that, for the combined treatment, the production of enzymes such as SOD and CAT was mainly affected by the concentration of B[a]P at the early period of pollutants exposure (Days 1–5), that is, the higher the concentration of B[a]P, the higher the enzyme content can be achieved.

On the contrary, in the late period of pollutants exposure (Day 15), the pollutants slightly inhibited the production of oxidative response kinase such as SOD and CAT, but no

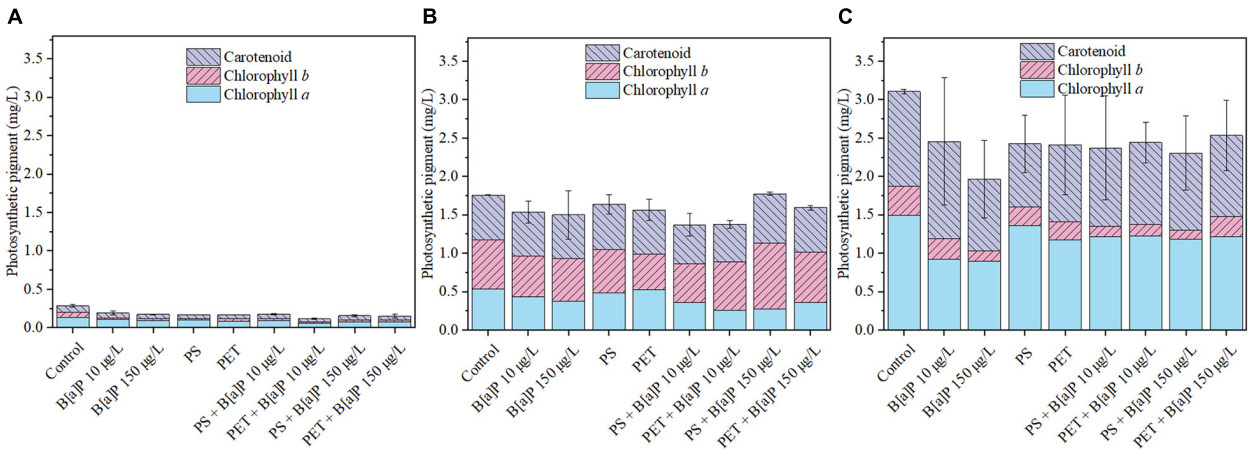

FIGURE 5 | The single and combined effects of microplastics (mPS and mPET) and B[a]P on the photosynthetic pigment of *C. muelleri* in **(A)** day 1, **(B)** day 5, and **(C)** day 15.

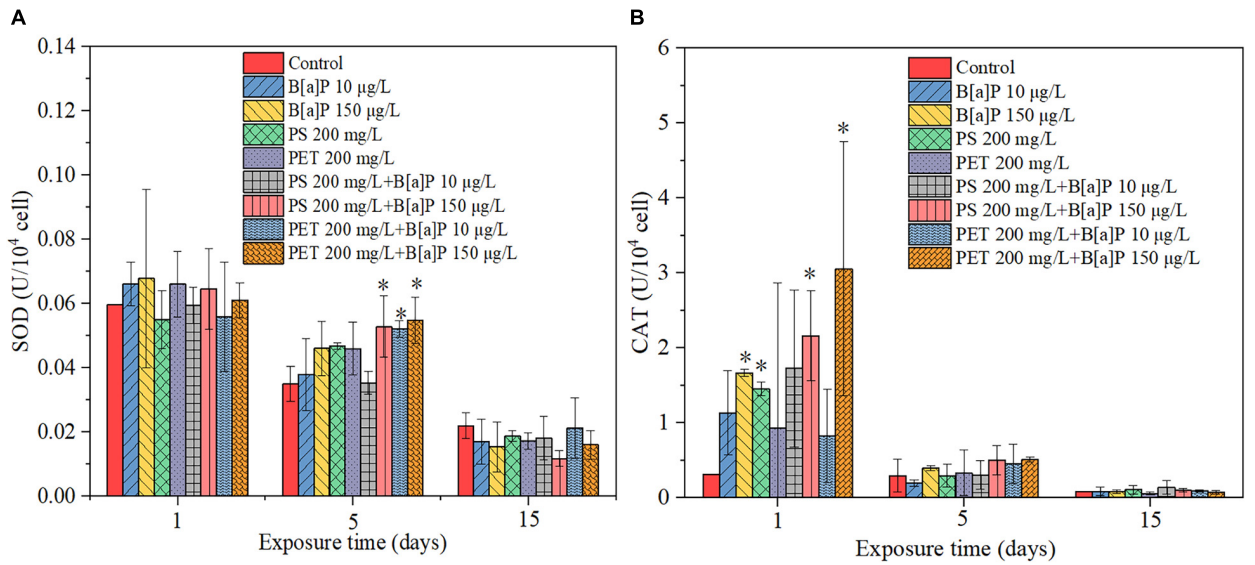

FIGURE 6 | (A) SOD and **(B)** CAT activity of *C. muelleri* to single microplastics, B[a]P, and their combinations. * indicates that significant differences compared to the control ($P < 0.05$).

significant difference ($P > 0.05$) was reached as compared with that of the control.

DISCUSSION

Effects of Microplastics and B[a]P on Cell Growth of Microalgae

Single Microplastics

The growth of *C. muelleri* exposed to microplastics can be generally divided into two stages. At the first stage (e.g., Days 1–3), the cell density of the cultures supplemented with microplastics decreased with time, corresponding to an increasing IR. This may be attributed to that unfavorable environmental conditions caused by microplastics (Zhang et al., 2017). Meanwhile, it can also result in damaged microalgal cell membrane in terms of some holes and hollows in this study (**Figure 7** and **Supplementary Figure 2**). At the second stage (e.g., Days 4–15), the IR of microalgae decreased since the cells gradually adapted to the existence of microplastics and the unfavorable environment. Therefore, the microalgal biomass and photosynthesis can be restored via thickening cell wall during the later exposure period of microplastics. These can effectively alleviate the cell damage caused by microplastics accordingly (Mao et al., 2018).

Meanwhile, this study found that mPET exhibited stronger inhibitory effect on microalgal growth compared to mPS. The toxicity may be derived from the differences in the physical and

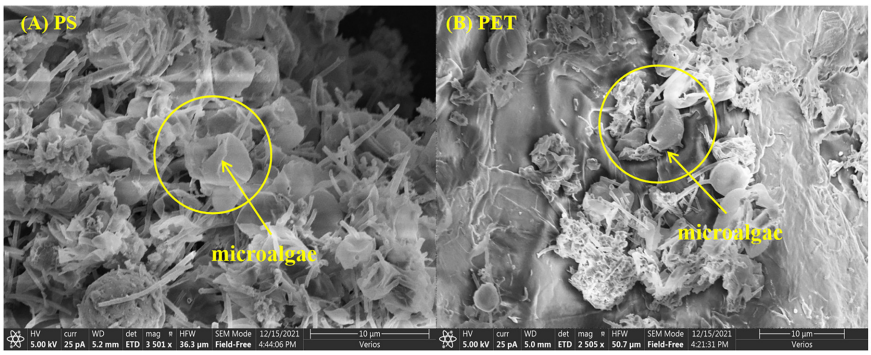

FIGURE 7 | (A) mPS and **(B)** mPET cause cell damage to microalgae.

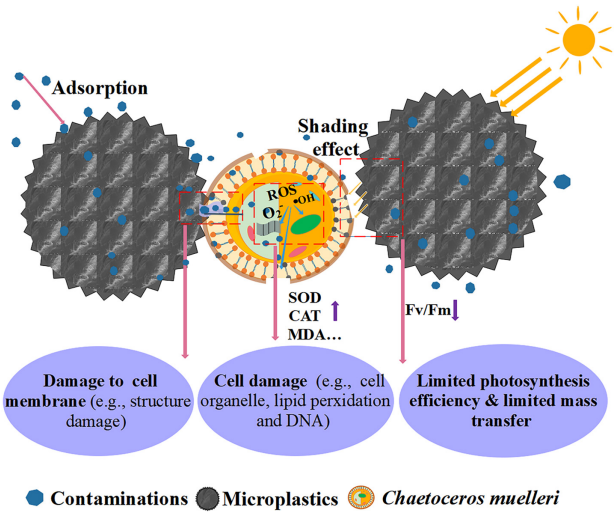

FIGURE 8 | Toxicity mechanism of microplastics on *C. muelleri*.

chemical properties of microplastics. For example, the mPET has greater surface roughness than that of mPS, and this would result in stronger toxic effects on microalgae. Previous study also reported that the surface roughness of microplastics can inhibit microalgal growth, and a rougher surface would lead to stronger inhibition to microalgae (Wang et al., 2021). Meanwhile, this study also found that mPET was completely immersed in the culture, offering a wider contact area to microalgal cells. This was confirmed by the intensive contact between microplastics with cells that can be observed via the SEM images (**Figure 1**). This would limit the mass transfer of microalgae with extracellular environment and further aggravate cell damage.

The main inhibition mechanism of microplastics on microalgae is shown in **Figure 8**. In general, microplastics may be led to damages to the cell wall and membrane structures, lipid peroxidation, toxicities to organelles and even DNA, which is commonly indicated by an increase of SOD enzyme, CAT enzyme, reactive oxygen species (ROS), malondialdehyde (MDA), respectively (Mao et al., 2018; Nava and Leoni, 2021).

Furthermore, it is reported that the presence of microplastics can increase the expression levels of microalgae genes involved in the sugar synthesis pathway, and trigger microalgal cells to secrete extracellular polymeric substances (EPS). Then, it can promote the heterogeneous aggregation between microalgae and microplastics, through establishing hydrogen bonds or electrostatic interactions (Chen et al., 2012; Fu et al., 2019). These aggregates would further limit the light transfer and mass transfer between cells and the environment. Thus, the photosynthesis of microalgae will be restricted in terms of a decreased chlorophyll fluorescence parameter (F_v/F_m) or photosynthesis pigment (Bhattacharya et al., 2010; Li S. et al., 2020; Lang et al., 2022). Additionally, the contaminants adsorbed or the additives released by microplastics can transfer to microalgal cells when they interact or aggregate. They can negatively impact the growth of microalgae particularly when the cell damage occurred (Prata et al., 2018).

Single B[a]P

In this study, B[a]P at low concentration (10 μg/L) did not inhibit the growth of *C. muelleri*, which may relate to that microalgal cells can adapt to the toxic environment with low concentration. Particularly, the cells in the growth stable period could gradually adapt to the presence of pollutants. For example, Olmos-Espejel et al. (2012) found that B[a]P was metabolized by *Selenastrum capricornutum* and the concentration of B[a]P in the solution gradually decreased with time. It may be inferred that the potential capacity of microalgae for detoxifying organic pollutants can be enhanced by bioabsorption, bio-uptake and biodegradation (Sutherland and Ralph, 2019). However, once reaching a high concentration of B[a]P, the ability of microalgae for alleviating pollutants (e.g., B[a]P) would be restricted and therefore the growth of microalgae can be inhibited (Wu et al., 2019). For example, B[a]P at high concentration (e.g., 150 μg/L) result in obvious inhibitory effects to *C. muelleri* in this study, which was consistent with the results of previous study (Shen et al., 2012).

Combined Toxicity of Microplastics and B[a]P

This study found that the presence of microplastics could enhance the toxicity of B[a]P on microalgae as compared with

TABLE 3 | Interactive effects of microplastics and B[a]P on cell density in 15 days treated in *C. muelleri*.

Treatment	Toxicity ratio (Tobs/Tpre)[a]
	Cell density
PS (200 mg/L) + B[a]P (10 μg/L)	−0.10 ± 1.25
PS (200 mg/L) + B[a]P (150 μg/L)	1.43 ± 0.34
PET (200 mg/L) + B[a]P (10 μg/L)	−1.50 ± 5.18
PET (200 mg/L) + B[a]P (150 μg/L)	1.19 ± 0.18

[a] *Toxic effects of metals mixture were measured experimentally (T_{obs}) and were predicted using Abbot's model (T_{pre}). T_{obs}/T_{pre} value = 1 indicated additivity of B[a]P and MPs individual effects, value >1 indicates synergism and value <1 indicates antagonism.*

the single toxicity caused by B[a]P. The results of Abbott's model indicated that the single pollutants (i.e., microplastics, B[a]P) and their combinations induced different toxicities to microalgae (**Table 3**). Synergistic effect (i.e., exceeding the additive effects of single pollutants that is predicted by Abbott's model) was observed between microplastics with B[a]P at high concentrations, but antagonistic effect was observed at low exposure level of B[a]P. In general, the degree of combined toxicity is associated with the amount of B[a]P accumulated in microalgae (Mwamba et al., 2016). Correspondingly, microplastics may also drive the toxic effect of B[a]P on microalgae.

On the one hand, microplastics can provide space for the colonization of microalgae, and meanwhile offer active sites for the adsorption of B[a]P (Gao et al., 2021). Under such circumstances, their coexistence may lead to close contact between microalgae and B[a]P on microplastics, resulting in cell damage to microalgae (Mao et al., 2018). Particularly, the absorption and/or toxicity of B[a]P to cells can be greatly aggravated when the cell structure is destroyed, owing to no protective shield to cells. Similar results were observed in some previous studies (Prata et al., 2018; Yi et al., 2019).

Furthermore, it should be mentioned that some studies reported that the combination of some organic pollutants with microplastics could decrease their combined toxicities on microalgae (Zhu et al., 2018) (**Table 4**). While the biotoxicity and bioaccumulation may be attributed to the tested species, polymer type, the type and concentration of pollutants (Bellas and Gil, 2020). Take the concentration of pollutants as an example, Li et al. (2019) demonstrated that the combined effect of mPS (0.1 μm) and dibutyl phthalate (DBP, 0.25–16 mg/L) on *Chlorella pyrenoidosa* varied with their concentration ranges, reaching an antagonistic effect between all the tested concentrations of mPS and DBP at low concentrations (e.g., 0.25 mg/L). However, the combined effects changed with the increasing concentrations of DBP, reaching synergistic effect between DBP and mPS less than 10 mg/L, while antagonistic effect for the combination of DBP with mPS exceeding 10 mg/L.

To further explore the toxicity mechanisms, the functional groups of microplastics were tested and analyzed, it is found that mPS is more aromatic and this would increase its affinity for pollutants (Fu et al., 2019). Other studies also reported that mPS offered a greater adsorption capacity of sulfamethoxazole (12 mg/L) than that of mPET, however, the mechanisms were not specified (Guo et al., 2019). This further explained the fact that mPS exhibited stronger toxicity to cells compared to mPET. Besides, it is interesting that the combined toxicity of mPET and B[a]P on cell growth of microalgae was more serious than that of mPS in this study. This may be attributed to that the weak adsorption capacity of mPET leading to a higher concentration of B[a]P in the environment (Fu et al., 2019), and therefore causing a strong inhibitory effect. It should be mentioned that the elucidation of specific toxic mechanisms requires further studies on other factors such as the crystallinity of microplastics, surface chemical structure and surface charge properties, and the types of pollutants.

Effects of Microplastics and B[a]P on Photosynthetic Pigment

Photosynthetic pigments play an important role in the photosynthesis of microalgae. In addition, the content of chlorophyll *a* can reflect environmental stress and toxicity (Lang et al., 2022). Therefore, this study determined the content of photosynthetic pigment (chlorophyll *a*, chlorophyll *b* and carotenoids) in microalgae. Previous studies have shown that the pollutants can inhibit the synthesis of chlorophyll *a*. For example, Lang et al. (2022) found that after 96 h of exposure, the inhibition ratio of PS (25–200 mg/L) on the content of chlorophyll *a* reached 20.11, 22.34, 22.10, and 25.45%, respectively. Triclosan (TCS) (0.7 μg/mL) significantly reduced the chlorophyll content of cyanobacterium (*Anabaena* sp. PCC7120) (Verdú et al., 2021). The above findings are consistent with this study. The inhibitory effect on the photosynthetic pigment of microalgae may also be the cause of the inhibitory effect on the microalgal growth.

For single microplastics or B[a]P, the content of photosynthetic pigment may be related to the concentration and type of pollutants, in other words, the higher the concentration of pollutants, the greater their inhibition on *C. muelleri*. Similar results were also reported in previous studies. For instance, Liu et al. (2021) found that triphenyl phosphate (TPhP, 0.08, 0.4, and 0.8 mg/L) have the greatest inhibition to chlorophyll *a* at high concentration (0.8 mg/L) on marine diatom *Phaeodactylum tricornutum*. In addition, the inhibition of PET on photosynthetic pigment was greater than PS, which may be because the light transmittance of PET is less than that of PS (Li, 1996), and this may be also weaken the synthesis of photosynthetic pigment. The combined of microplastics and B[a]P had a stronger inhibitory effect on *C. muelleri*, but their inhibitory effect on photosynthetic pigment was weakened compared with single microplastics or B[a]P. This may be attributed to that when the external pressure on the microalgae reaches a certain critical point, the microalgae cells would trigger a regulatory mode of defense to adapt to adverse conditions by reducing chlorophyll degradation or inhibiting biosynthesis (Agathokleous et al., 2020). Similarly, Chae et al. (2019) found that micro-sized polyethylene spheres had a slight inhibitory effect (no significant effect, $P > 0.05$) on the chlorophyll content of microalgae at low concentrations

TABLE 4 | The combined toxicity influence of microplastics and organic pollutants on microalgae.

Polymer	Polymer size (μm)	Polymer concentrations (mg/L)	Contaminations	Contaminations concentrations (mg/L)	Microalgae	Combined toxicities	References
PE, PA, PS, PE1000, PA1000	150,13	50	Nonylphenol	2	*Chlorella pyrenoidosa*	Antagonistic	Yang et al., 2020
PE, PS, PVC, PVC800	74 (PE, PS, PVC), 1 (PVC800)	50	Triclosan	0.3	*Skeletonema costatum*	Antagonistic	Zhu et al., 2018
Red fluorescent polymer microspheres	1–5	1.5	Pharmaceuticals procainamide and doxycycline	4–256	*Tetraselmis chuii*	Synergistic	Prata et al., 2018
mPS	0.1	10	Dibutyl phthalate	0.25–16	*Chlorella pyrenoidosa*	Antagonistic at low concentrations of DBP, synergistic at relatively high concentrations of DBP	Li et al., 2019
PS	0.55	0.05–5	Triphenyltin chloride	0.03	*Chlorella pyrenoidosa*	Synergistic	Yi et al., 2019
PE	2-6	5	Chlorpyrifos	0–3	*Isochrysis galbana*	Antagonistic	Garrido et al., 2019
PE, PVC	150 (PE), 250 (PVC)	1000	Phenanthrene	0.8	*Phaeodactylum tricornutum*	Antagonistic	Guo et al., 2019
nPS-NH_2	0.2	5	Glyphosate	5–15	*Microcystis aeruginosa*	Antagonistic	Zhang et al., 2018
mPS, mPET	173–376 (mPS), 177–425 (mPET)	200	B[a]P	0.01 0.15	*Chaetoceros muelleri*	antagonistic synergistic	In this study

(50–150 mg/L), but it significantly promoted ($P < 0.05$) the chlorophyll content at high concentrations (200–350 mg/L).

Effects of Microplastics and B[a]P on Antioxidant Enzymes

In general, SOD plays the role in antioxidant via transforming the O_2^- into H_2O_2 in cells (Mittler, 2002). The stimulatory effect results from short-term exposure to the low dosage of toxic substances (Calabrese et al., 2012), is commonly characterized as hormesis response in terms of increasing SOD activities. For instance, some studies reported that the SOD content of microalgae would increase when they were exposed to microplastics (Yang et al., 2020; Wang et al., 2021). This may be due to the production of ROS stimulated by rough surface structure of microplastics (Song et al., 2020). This study also found that the single or combined pollutants (e.g., mPS, mPET, and B[a]P) actually increased the SOD of microalgae as compared with the control in the first 5 days of cultivation. By comparison, the pollutants inhibited the SOD content on the last day of the experiment. This may be attributed to the stimulating effects to microalgae from the evolution of large amount of ROS under the stressed condition (Bellingeri et al., 2020). Once the accumulation of ROS in microalgal cells reached a super high level, the cellular ability to remove ROS via producing enough oxidative response kinases (i.e., SOD and CAT) would be restricted and even destroyed. Thus, the antioxidative enzymatic system may collapse accompanying with abnormal secretion of antioxidative enzymes. This was also demonstrated by a previous study that some organisms can eliminate excess ROS via increasing the production of SOD to cope with mild stress from copper, but the content of SOD would decrease when the stress is further aggravated (Papadimitriou and Loumbourdis, 2002).

Furthermore, CAT can be used to remove H_2O_2 from cells when H_2O_2 is at a high level (Mittler, 2002). Some studies pointed out that the CAT of microalgae can be increased when the cells being exposed to copper and microplastics (Manimaran et al., 2012; Zhang et al., 2021). However, the CAT content of microalgal cultures exposed to either single or combined pollutants increased in the first 5 ays, but decreased on Day 15 of cultivation compared with the control in this study, which was consistent with the results of SOD content. Similar results were observed in the study of Lozano et al. (2014), which the CAT activity in *Cylindrotheca closterium* was slightly decreased when being exposed to copper, but no details about the mechanisms. Overall, more profound studies are required to further elucidate the role of antioxidative enzymes and their fluctuations with the changes of stressed conditions in the future.

CONCLUSION

This study investigated the single and combined effects of microplastics (mPS and mPET) and B[a]P on microalgae *C. muelleri*. The results showed that single mPET or B[a]P at high concentration (i.e., 150 μg/L) have significantly inhibition on cell density of microalgae, but mPS or B[a]P at low concentration (i.e., 10 μg/L) have no significant inhibition to cells. The aggregation of mPET and microalgal cells was observed in the culture, which may be one of contributors to the negative impact on microalgae. The interaction between microplastics and B[a]P is closely related to the concentration and toxicity of single

pollutants. The synergistic effect of microplastics and B[a]P at high concentrations might be partially attributed to the ability of microplastics to be vector of B[a]P entering microalgal cells. This work would help to improve the understanding of the combined toxicity of microplastics and organic pollutants such as B[a]P in the marine environment. More studies regarding the interaction mechanisms of microplastics with B[a]P are required to be elucidated in the future.

DATA AVAILABILITY STATEMENT

The original contributions presented in the study are included in the article/**Supplementary Material**, further inquiries can be directed to the corresponding author.

AUTHOR CONTRIBUTIONS

YS and HQ provided the methodology, conducted the experiments, and wrote the manuscript. YH, MG, and JL performed the investigation. MC and XZ participated writing—review and editing. MC performed data processing. CG provided resources. DF and ZW provided the methodology. LP provided the resources, administrated the project, supervised the experiments, and participated in the writing original draft. All authors contributed to the article and approved the submitted version.

FUNDING

This study was supported by the Natural Science Foundation of Hainan Province, China (Grant No. 2019RC043), the National Natural Science Foundation of China (41766003), and Start-up funding from Hainan University [kyqd(zr)1719].

SUPPLEMENTARY MATERIAL

The Supplementary Material for this article can be found online at: https://www.frontiersin.org/articles/10.3389/fmars.2021.779321/full#supplementary-material

REFERENCES

Agathokleous, E., Feng, Z., and Peñuelas, J. (2020). Chlorophyll hormesis: are chlorophylls major components of stress biology in higher plants? *Sci. Total. Environ.* 726:138637. doi: 10.1016/j.scitotenv.2020.138637

Bellas, J., and Gil, I. (2020). Polyethylene microplastics increase the toxicity of chlorpyrifos to the marine copepod *Acartia tonsa*. *Environ. Pollut* 260:114059. doi: 10.1016/j.envpol.2020.114059

Bellingeri, A., Casabianca, S., Capellacci, S., Faleri, C., Faleri, C., Paccagnini, E., et al. (2020). Impact of polystyrene nanoparticles on marine diatom *Skeletonema marinoi* chain assemblages and consequences on their ecological role in marine ecosystems. *Environ. Pollut.* 262:114268. doi: 10.1016/j.envpol.2020.114268

Bhattacharya, P., Lin, S., Turner, J. P., and Ke, C. P. (2010). Physical adsorption of charged plastic nanoparticles affects algal photosynthesis. *J. Phys. Chem. C* 114, 16556–16561. doi: 10.1021/jp1054759

Calabrese, E. J., Iavicoli, I., and Calabrese, V. (2012). Hormesis: why it is important to biogerontologists. *Biogerontology* 13, 215–235. doi: 10.1007/s10522-012-9374-7

Chae, Y., Kim, D., and An, Y. (2019). Effects of micro-sized polyethylene spheres on the marine microalga *Dunaliella salina*: focusing on the algal cell to plastic particle size ratio. *Aquat. Toxicol.* 216:105296. doi: 10.1016/j.aquatox.2019.105296

Chen, P., Powell, B. A., Mortimer, M., and Ke, P. C. (2012). Adaptive interactions between Zinc Oxide nanoparticles and *Chlorella* sp. *Environ. Sci. Technol.* 46, 12178–12185. doi: 10.1021/es303303g

Derakhshesh, N., Salamat, N., Movahedinia, A., Hashemitabar, M., and Bayati, V. (2019). Exposure of liver cell culture from the orange-spotted grouper, *Epinephelus coioides*, to benzo[a]pyrene and light results in oxidative damage as measured by antioxidant enzymes. *Chemosphere* 226, 534–544. doi: 10.1016/j.chemosphere.2019.03.181

Endo, S., and Koelmans, A. A. (2016). "Sorption of hydrophobic organic compounds to plastics in the marine environment: equilibrium," in *Hazardous Chemicals Associated with Plastics in the Marine Environment. The Handbook of Environmental Chemistry*, Vol. 78, eds H. Takada and H. Karapanagioti (Cham: Springer), doi: 10.1007/698_2016_11

EuropePlastics (2019). *Plastics–The Facts 2019: An Analysis of European Plastics-Facts-2018. Production, Demand and Waste Data*. Belgium: Plastics Europe.

Fu, D., Chen, C. M., Qi, H., Fan, Z., Wang, Z., Peng, L., et al. (2020). Occurrences and distribution of microplastic pollution and the control measures in China. *Mar. Pollut. Bull.* 153:110963. doi: 10.1016/j.marpolbul.2020.110963

Fu, D., Zhang, Q., Fan, Z., Qi, H., Wang, Z., and Peng, L. (2019). Aged microplastics polyvinyl chloride interact with copper and cause oxidative stress towards microalgae *Chlorella vulgaris*. *Aquat. Toxicol.* 216:105319. doi: 10.1016/j.aquatox.2019.105319

Gao, L., Fu, D., Zhao, J., Wu, W., Wang, Z., Su, Y., et al. (2021). Microplastics aged in various environmental media exhibited strong sorption to heavy metals in seawater. *Mar. Pollut. Bull.* 169:112480. doi: 10.1016/j.marpolbul

Garrido, S., Linares, M., Campillo, J. A., and Albentosa, M. (2019). Effect of microplastics on the toxicity of chlorpyrifos to the microalgae *Isochrysis galbana*, clone t-ISO. *Ecotoxicol. Environ. Saf.* 173, 103–109. doi: 10.1016/j.ecoenv.2019.02.020

Gisi, U. (1996). Synergistic interaction of fungicides in mixtures. *Phytopathology* 86, 1273–1279.

Gong, W., Zhu, L., Jiang, T., and Han, C. (2017). The occurrence and spatial-temporal distribution of tetrabromobisphenol A in the coastal intertidal zone of Qingdao in China, with a focus on toxicity assessment by biological monitoring. *Chemosphere* 185, 462–467. doi: 10.1016/j.chemosphere.2017.07.033

Guillard, R. R. L. (1975). "Culture of phytoplankton for feeding marine invertebrates," in *Culture of Marine Invertebrate Animals*, eds W. L. Smith and M. H. Chanley (New York, NY: Plenum Press), 26–60. doi: 10.1007/978-1-4615-8714-9_3

Guo, X., Chen, C., and Wang, J. (2019). Sorption of sulfamethoxazole onto six types of microplastics. *Chemosphere* 228, 300–308. doi: 10.1016/j.chemosphere.2019.04.155

Guven, O., Bach, L., Munk, P., Dinh, K. V., Mariani, P., and Nielsen, T. G. (2018). Microplastic does not magnify the acute effect of PAH pyrene on predatory performance of a tropical fish (*Lates calcarifer*). *Aquat. Toxicol.* 198, 287–293. doi: 10.1016/j.aquatox.2018.03.011

Jambeck, J. R., Geyer, R., Wilcox, C., Siegler, T. R., Perryman, M., Andrady, A., et al. (2015). Plastic waste inputs from land into the ocean. *Science* 347, 768–771. doi: 10.1126/science.1260352

Kim, S., Shin, K., Moon, C. H., Park, D. W., and Chang, M. (2004). Effects of benzo(a)pyrene on growth and photosynthesis of phytoplankton. *Korean J. Environ. Biol.* 22, 54–62.

Lang, X., Ni, J., and He, Z. (2022). Effects of polystyrene microplastic on the growth and volatile halocarbons release of microalgae *Phaeodactylum tricornutum*. *Mar. Pollut. Bullet.* 174:113197. doi: 10.1016/j.marpolbul.2021.113197

Li, F., Jiang, L., Zhang, T., Qiu, J., Lv, D., Su, T., et al. (2021). Combined effects of seawater acidification and benzo(a)pyrene on the physiological performance of the marine bloom-forming diatom *Skeletonema costatum*. *Mar. Environ. Res.* 169:105396. doi: 10.1016/j.marenvres.2021.105396

Li, R. (1996). Research on the comprehensive utilization of PS plastics. *J. Chengde Teach. Coll. Natl.* 1, 136–139. doi: 10.16729/j.cnki.jhnun.1996.s1.063

Li, S., Wang, P., Zhang, C., Zhou, X., Yin, Z., Hu, T., et al. (2020). Influence of polystyrene microplastics on the growth, photosynthetic efficiency and aggregation of freshwater microalgae *Chlamydomonas reinhardtii*. *Sci. Total Environ.* 714:136767. doi: 10.1016/j.scitotenv.2020.136767

Li, Y., Wang, J., Yang, G., Lu, L., Zheng, Y., Zhang, Q., et al. (2020). Low level of polystyrene microplastics decreases early developmental toxicity of phenanthrene on marine medaka (*Oryzias melastigma*). *J. Hazard. Mater.* 385:121586. doi: 10.1016/j.jhazmat.2019.121586

Li, Z., Yi, X., Zhou, H., Chi, T., and Yang, K. (2019). Combined effect of polystyrene microplastics and dibutyl phthalate on the microalgae *Chlorella pyrenoidosa*. *Environ. Pollut* 257:113604. doi: 10.1016/j.envpol.2019.113604

Liu, Q., Tang, X., Zhang, X., Tong, X., Sun, Z., and Zhang, X. (2021). Mechanistic understanding of the toxicity of triphenyl phosphate (TPhP) to the marine diatom *Phaeodactylum tricornutum*: targeting chloroplast and mitochondrial dysfunction. *Environ. Pollut.* 295:118670. doi: 10.1016/j.envpol.2021.118670

Lozano, P., Trombini, C., Crespo, E., Blasco, J., and Moreno-Garrido, I. (2014). ROI-scavenging enzyme activities as toxicity biomarkers in three species of marine microalgae exposed to model contaminants (copper, Irgarol and atrazine). *Ecotox. Environ. Saf.* 104, 294–301. doi: 10.1016/j.ecoenv.2014.03.021

Ma, Y., Huang, A., Cao, S., Sun, F., Wang, L., Guo, H., et al. (2016). Effects of nanoplastics and microplastics on toxicity, bioaccumulation, and environmental fate of phenanthrene in fresh water. *Environ. Pollut.* 219, 166–173. doi: 10.1016/j.envpol.2016.10.061

Manimaran, K., Karthikeyan, P., Ashokkumar, S., Ashok Prabu, V., and Sampathkumar, P. (2012). Effect of copper on growth and enzyme activities of marine diatom, *Odontella mobiliensis*. *Bull. Environ. Contam. Toxicol.* 88, 30–37. doi: 10.1007/s00128-011-0427-4

Mao, Y., Ai, H., Chen, Y., Zhang, Z., Zeng, P., Kang, L., et al. (2018). Phytoplankton response to polystyrene microplastics: perspective from an entire growth period. *Chemosphere* 208, 59–68. doi: 10.1016/j.chemosphere.2018.05.170

Mittler, R. (2002). Oxidative stress, antioxidants and stress tolerance. *Trends Plant. Sci.* 7, 405–410. doi: 10.1016/S1360-1385(02)02312-9

Mwamba, T. M., Ali, S., Ali, B., Lwalaba, J. L., Liu, H., Farooq, M. A., et al. (2016). Interactive effects of cadmium and copper on metal accumulation, oxidative stress, and mineral composition in *Brassica napus*. *Int. J. Environ. Sci. Te.* 13, 2163–2174. doi: 10.1007/s13762-016-1040-1

Nava, V., and Leoni, B. (2021). A critical review of interactions between microplastics, microalgae and aquatic ecosystem function. *Water Res.* 188, 116476. doi: 10.1016/j.watres.2020.116476

Olmos-Espejel, J., García de Llasera, M. P., and Velasco-Cruz, M. (2012). Extraction and analysis of polycyclic aromatic hydrocarbons and benzo[a]pyrene metabolites in microalgae cultures by off-line/on-line methodology based on matrix solid-phase dispersion, solid-phase extraction and high-performance liquid chromatography. *J. Chromatogr. A* 1262, 138–147. doi: 10.1016/j.chroma.2012.09.015

Papadimitriou, E., and Loumbourdis, N. S. (2002). Exposure of the frog Rana ridibunda to Copper:impact on two biomarkers, lipid peroxidation, and gulathione. *Bull. Environ. Contam. Toxicol.* 69, 885–891. doi: 10.1007/s00128-002-0142-2

Prata, J. C., da Costa, J. P., Lopes, I., Duarte, A. C., and Rocha-Santos, T. (2019). Effects of microplastics on microalgae populations: a critical review. *Sci. Total. Environ.* 665, 400–405. doi: 10.1016/j.scitotenv.2019.02.132

Prata, J. C., Lavorante, B. R. B. O., Montenegro, B. S. M. M. D. C., and Guilhermino, L. (2018). Influence of microplastics on the toxicity of the pharmaceuticals procainamide and doxycycline on the marine microalgae *Tetraselmis chuii*. *Aquat. Toxicol.* 197, 143–152. doi: 10.1016/j.aquatox.2018.02.015

Qiu, Y. W., Zhou, J. L., Maskaoui, K., Hong, H. S., and Wang, Z. D. (2004). Distribution of polycyclic aromatic hydrocarbons in water and sediments from Daya bay and their ecological hazard assessment. *J. Tropic. Oceangr.* 23, 72–80. doi: 10.1016/S0269-7491(02)00215-4

Shen, C., Li, Y., and Pan, L. (2012). [Effects of benzo[α]pyrene on cell growth and characteristics in marine microalgae] in Chinese. *Mar. Environ. Sci.* 31, 510–514. doi: 10.3969/j.issn.1007-6336.2012.04.011

Song, C., Liu, Z., Wang, C., Li, S., and Kitamura, Y. (2020). Different interaction performance between microplastics and microalgae: the bio-elimination potential of *Chlorella* sp. L38 and *Phaeodactylum tricornutum* MASCC-0025. *Sci. Total. Enviro.* 723:138146. doi: 10.1016/j.scitotenv.2020.138146

Sutherland, D. L., and Ralph, P. J. (2019). Microalgal bioremediation of emerging contaminants – Opportunities and challenges. *Water Res.* 164, 114921. doi: 10.1016/j.watres.2019.114921

Verdú, I., González-Pleiter, M., Leganés, F., Rosal, R., and Fernández-Piñas, F. (2021). Microplastics can act as vector of the biocide triclosan exerting damage to freshwater microalgae. *Chemosphere* 266:129193. doi: 10.1016/j.chemosphere.2020.129193

Wang, Z., Fu, D., Gao, L., Qi, H., Su, Y., and Peng, L. (2021). Aged microplastics decrease the bioavailability of coexisting heavy metals to microalga *Chlorella vulgaris*. *Ecotoxicol. Environ. Saf.* 217:112199. doi: 10.1016/j.ecoenv

Wright, S. L., Thompson, R. C., and Galloway, T. S. (2013). The physical impacts of microplastics on marine organisms: a review. *Environ. Pollut.* 178, 483–492. doi: 10.1016/j.envpol.2013.02.031

Wu, Y., Guo, P., Zhang, X., Zhang, Y., Xie, S., and Deng, J. (2019). Effect of microplastics exposure on the photosynthesis system of freshwater algae. *J. Hazard. Mater.* 374, 219–227. doi: 10.1016/j.jhazmat.2019.04.039

Yang, W., Gao, X., Wu, Y., Wan, L., and Zhang, W. (2020). The combined toxicity influence of microplastics and nonylphenol on microalgae chlorella pyrenoidosa. *Ecotox. Environ. Saf.* 195:110484. doi: 10.1016/j.ecoenv.2020.110484

Yi, X., Chi, T., Li, Z., Wang, J., Yu, M., Wu, M., et al. (2019). Combined effect of polystyrene plastics and triphenyltin chloride on the green algae *Chlorella pyrenoidosa*. *Environ. Sci. Pollut. Res* 26, 15011–15018. doi: 10.1007/s11356-019-04865-0

Yu, N., Ding, Q., Li, E., Qin, J. G., Chen, L., and Wang, X. (2018). Growth, energy metabolism and transcriptomic responses in Chinese mitten crab (*Eriocheir sinensis*) to benzo[α]pyrene (BaP) toxicity. *Aquat. Toxicol.* 203, 150–158. doi: 10.1016/j.aquatox.2018.08.014

Zhang, C., Chen, X., Wang, J., and Tan, L. (2017). Toxic effects of microplastic on marine microalgae *Skeletonema costatum*: interactions between microplastic and algae. *Environ. Pollut.* 20, 1282–1288. doi: 10.1016/j.envpol.2016.11.005

Zhang, Q., Qu, Q., Lu, T., Ke, M. J., Zhu, Y. C., Zhang, M., et al. (2018). The combined toxicity effect of nanoplastics and glyphosate on microcystis aeruginosa growth. *Environ. Pollut.* 243, 1106–1112. doi: 10.1016/j.envpol.2018.09.073

Zhang, W., Sun, S., Du, X., Han, Y., Tang, Y., Zhou, W., et al. (2021). Toxic impacts of microplastics and tetrabromobisphenol A on the motility of marine microalgae and potential mechanisms of action. *Gondwana Res.* doi: 10.1016/j.gr.2021.08.011

Zhu, Z., Wang, S., Zhao, F., Wang, S., Liu, F., and Liu, G. (2018). Joint toxicity of microplastics with triclosan to marine microalgae *Skeletonema costatum*. *Environ. Pollut.* 246, 509–517. doi: 10.1016/j.envpol.2018.12.044

Conflict of Interest: The authors declare that the research was conducted in the absence of any commercial or financial relationships that could be construed as a potential conflict of interest.

frontiers in Marine Science

ORIGINAL RESEARCH
published: 03 February 2022
doi: 10.3389/fmars.2021.821008

Occurrence of Microplastic Pollution in the Beibu Gulf, the Northern South China Sea

Zuhao Zhu[1], Huihua Wei[1], Wei Huang[1,2], Xingxu Wu[3], Yao Guan[1] and Qiufeng Zhang[1]*

[1] Key Laboratory of Tropical Marine Ecosystem and Bioresource, Fourth Institute of Oceanography, Ministry of Natural Resources, Beihai, China, [2] Key Laboratory of Marine Ecosystem Dynamics, Second Institute of Oceanography, Ministry of Natural Resources, Hangzhou, China, [3] Central Cycle Ecological Technology Co., Ltd, Guangzhou, China

In this study, microplastics were sampled and analyzed from surface water and sediment samples from July to August in 2020, in the Beibu Gulf (the northern South China Sea [SCS]), a gulf with intensive fishery activities while the economy is less developed, compared with other coastal areas of China. The abundances of microplastics in seawater and sediment in the Beibu Gulf were 0.67 items/m^3 and 4.33 items/kg of dry weight, respectively. In seawater, the fragments (92.38%) contributed the most, and polystyrene (PS) was the dominant polymer (53.23%). In sediment, the most abundant microplastics were fiber (82.93%) and rayon (RY; 39.54%). The abundances of remarkably higher microplastics were found in the seawater and sediment adjacent to the urban area. The abundances of microplastics in far coastal sediment were only slightly lower than that in the coastal sediment, indicating that microplastics are ready to transport and bury in open area sediment. Significant positive correlations between the microplastic abundance and population density and per capita gross domestic product (GDP) were found in Chinese coastal seawater, with low population density and less developed economy, and the microplastic pollution in the Beibu Gulf was at a low level. This study provides preliminary data of microplastics in the Beibu Gulf, supporting further investigation of transportation fate and management of this emerging pollutant from the coastal zone to the SCS.

Keywords: microplastics, distribution, Beibu Gulf, long distance transportation, socioeconomic correlations

OPEN ACCESS

Edited by:
Xiaoshan Zhu,
Tsinghua University, China

Reviewed by:
Minggang Cai,
Xiamen University, China
Muhammad Reza Cordova,
Research Center for Oceanography,
Indonesian Institute of Sciences,
Indonesia

****Correspondence:***
Zuhao Zhu
zhuzuhao@4io.org.cn

Specialty section:
This article was submitted to Marine Pollution, a section of the journal Frontiers in Marine Science

Received: *23 November 2021*
Accepted: *17 December 2021*
Published: *03 February 2022*

Citation:
Zhu Z, Wei H, Huang W, Wu X, Guan Y and Zhang Q (2022) Occurrence of Microplastic Pollution in the Beibu Gulf, the Northern South China Sea. Front. Mar. Sci. 8:821008. doi: 10.3389/fmars.2021.821008

INTRODUCTION

As an emerging marine pollutant, microplastics (defined as those plastics with size < 5 mm) can be derived from the degradation of larger plastics in the ocean by sunlight, microbes and mechanical abrasion (Cózar et al., 2014; Khan, 2020; Cordova et al., 2021), or from discharge of wastewater that contains microplastics (Jambeck et al., 2015; Liu et al., 2017; Rochman, 2018; Naji et al., 2020; Nurhasanah et al., 2021). Due to the low density and stable properties, microplastics can be transported to a long distance in the ocean. For example, microplastics have been found in polar waters, deep seawaters, and ocean central island waters and can stably exist in seawater, sediments, and organisms (Cauwenberghe et al., 2013; Isobe et al., 2017; Waller et al., 2017;

Li et al., 2019; Wu et al., 2020). Microplastics will produce harmful additives and monomers and also carry heavy metals and persistent organic pollutants in the marine environment (Boyle et al., 2020; Catarino et al., 2021; Chen et al., 2021). Microplastics may be ingested by marine organisms, which could cause various adverse effects. Thus, they are potentially incorporated into the marine food web through trophic transfer and ultimately endanger human health through the consumption of contaminated seafood (Lusher et al., 2017; Pannetier et al., 2020; Philipp et al., 2021). Thus, monitoring microplastics in the ocean (especially the coastal zone) and exploring its biogeochemical cycle are the hot science topics in recent years (Everaert et al., 2018; Li Y. et al., 2020).

The Beibu Gulf, a semi-enclosed bay where microplastics are more likely to accumulate (Sharma et al., 2021; Zhou et al., 2021), is located in the northern South China Sea (SCS), surrounded by three major cities, such as Beihai, Qinzhou, and Fangchenggang, with a total population of 6.2 million (2020). As one of the world's largest fishing grounds in the SCS, mariculture is highly crowded in the coastal zone of the Beibu Gulf compared with other coastal areas of China. Intensive anthropogenic activities, including fishery and mariculture, have contributed a large amount of microplastics in the adjacent sea (Zhang et al., 2017; Cheung L. T. O. et al., 2018; Wang et al., 2018; Li Y. et al., 2020; Li Z. et al., 2020; Xue et al., 2020). Few studies reported microplastics in the coastal zones of the Beibu Gulf. Zhu et al. (2019) reported high levels of microplastics in the Maowei Sea (a bay of the Beibu Gulf), a traditional oyster farm bay. Xue et al. (2020) discovered that a large amount of microplastics derived from fishery activities were buried in deep sediment, suggesting that the microplastic storage worldwide might be underestimated because most of the previous studies examined only surface sediment. To date, still less is known of the abundance and distribution of microplastics in the coastal and far coastal zones of the Beibu Gulf.

At the same time, though Beibu Gulf is experiencing the economic development and rapid urbanization of the surrounded human land, still it is one of the least developed regions among the coastal areas of China, with per capita gross domestic product (GDP) of USD 8.56k, while for whole China is USD 11.3k (2020). The microplastic pollution should be at a low level according to the positive relationships found between microplastic abundance and factors, such as land use percentages (Kataoka et al., 2019), population density (Yonkos et al., 2014), and GDP (Fan et al., 2019) in some water bodies. However, the Beibu Gulf is also a microcosm of the fishery industry of China and Southeast Asian countries and fishery is one of the pillar industries. Therefore, the Beibu Gulf is a typical area to study the co-influence of socioeconomics and fishery industry to the microplastic pollution, understanding the status of microplastics in Beibu Gulf is helpful in taking measures and policymaking to reduce microplastics in China and Southeast Asian countries (Xue et al., 2020).

In this study, the characteristics and distributions of microplastics in the coastal zones of the Beibu Gulf were investigated, and socioeconomic indices, such as population density and per capita GDP, were chosen to assess the microplastic pollution status in the Beibu Gulf. To obtain more comparable data, a Manta net with a netmesh of 0.33 mm was used for surface seawater microplastic sampling (Yonkos et al., 2014; Chen et al., 2018; Xu et al., 2021). Sample preparation of microplastics in seawater and sediment was conducted according to the literature methods, i.e., wet oxidation (10% potassium hydroxide [KOH] for water; 30% hydrogen peroxide [H_2O_2] for sediment) and density separation (1.2 g/cm^3 sodium chloride [NaCl]) were employed (NOAA Marine Debris Program, 2015; Rocha-Santos and Duarte, 2015; Wang et al., 2020; Wu et al., 2020). Stereo microscope and micro-Fourier transform infrared spectrometer (μ-FTIR) were used to identify microplastics.

The aims of this study were to: (1) determine the microplastic abundance, size, color, and polymer composition in the Beibu Gulf, (2) analyze the differences of the microplastic status between Beibu Gulf and other comparable Chinese sea areas, (3) confirm the relationships between microplastic abundances and socioeconomic indices, and (4) provide preliminary data for further study of the transportation fate and management of microplastics in the Beibu Gulf and the SCS. The result of this study may be useful for the cooperation actions taken by the departments of marine environment protection, marine fishery, waste treatment, and public organizations to handle the microplastic pollution in the Beibu Gulf and other ocean waters.

MATERIALS AND METHODS

Field Sampling

Study Area

Sampling was conducted in the Beibu Gulf by two cruises, one was L cruise (coastal area) in July 2020 by the R/V Yueke 1, during which 59 stations were sampled for seawater and 43 stations for sediment. The other was B cruise (far coastal area) in August 2020 by the R/V Yuexiayuzhi 20028, during which 16 stations were sampled for seawater and 23 stations for sediment. The study area and sampling station distribution are shown in **Figure 1**.

Sampling Methods

Seawater samples were collected using a Manta trawl (330 μm mesh nylon net), while surface sediment (>5 cm) was collected using a Van Veen sediment collector. Detailed sampling methods were described in the **Supplementary Materials**.

Sample Preparation

The sample treatment for seawater was slightly modified according to Wang et al. (2020), and the sediments were analyzed according to Wu et al. (2020). Notably, 10% KOH and 30% H_2O_2 were used for the wet oxidation of seawater and sediment, respectively. Saturated NaCl (1.2 g/cm^3) was used for the density separation of microplastics in seawater and sediment. Sample pretreatment methods were detailed in the **Supplementary Materials**.

Characterization

The Shape, Color, and Size of Microplastics

A SteREO Discovery V8 microscope (Zeiss, Germany) equipped with a digital camera (C 33; OPLENIC, United States) and "ZEN lite" software was used to characterize the physical properties of

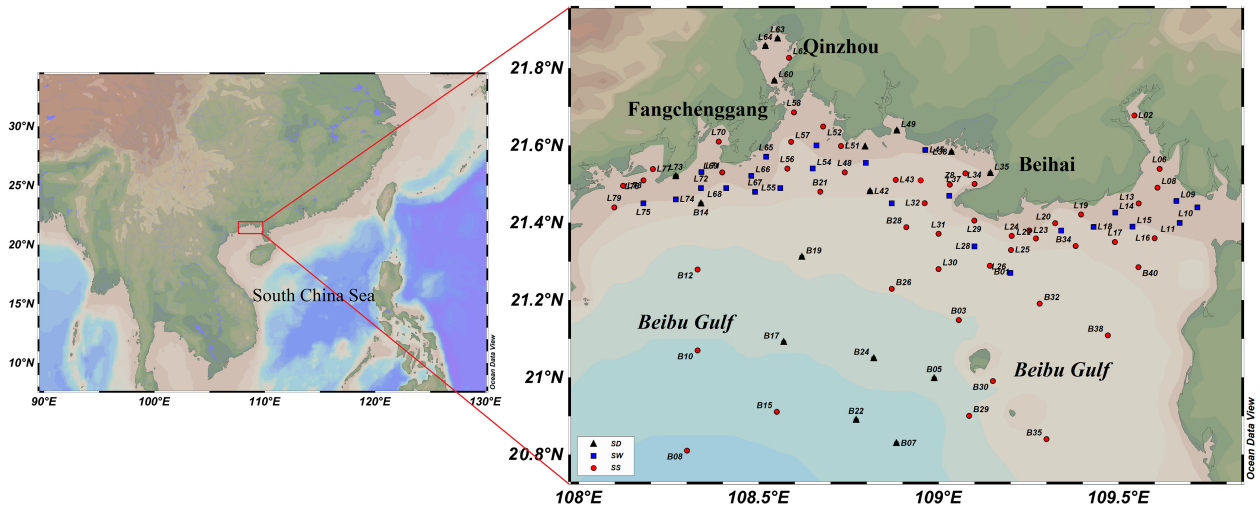

FIGURE 1 | Location of Beibu Gulf and sampling station distribution. L stations were sampled during L cruise, while B stations were sampled during B cruise. SD, sediment station, SW, seawater station, SS, sediment and seawater station.

the microplastics. Guidelines from Zhao et al. (2018) were used to identify the microplastics: (1) the particle cannot be easily broken with tweezers, (2) the color of the particle is uniform, and (3) the particle is free of biological tissues and cell structures. The size of each particle was measured along its longest axis (Wang et al., 2020).

The Composition of Microplastics

A μ-FTIR (Nicolet iN10; Thermo Fisher, United States) was used to determine the chemical composition of inspected materials, all suspected microplastics were examined, and only materials with polymers were successfully determined as microplastics (Cai et al., 2018; Wang et al., 2020). The sample was measured in the transmittance mode. The spectral range (650–4,000 cm^{-1}) and aperture range (from 50 × 50 mm to 150 × 150 mm) were selected according to particle size. The spectra obtained were matched with the OMNIC polymer spectral library (standard database) to identify the polymer types, and at least 70% similarity was assigned to the polymer conformation (Mecozzi et al., 2016).

Quality Control

All labware equipment used in the study were rinsed three times with Milli-Q water before use. All solutions and liquids used in the study were filtered by a glass fiber filter (GF/F Whatman, 47 mm diameter, and 0.7 μm pore size) before use. Procedural blank samples (n = 3) were analysed to correct the potential laboratory contamination in each batch sample treatment, and the recovery of the methods used was performed using standard reference materials (National Marine Environmental Monitoring Centre, China), with 95%. Other measures were taken in the lab to keep the contamination at the lowest level, such as using aluminum foil to cap the containers and wearing cotton clothes.

Data Analysis

Statistical analysis was carried out using the EXCEL 2010 (Microsoft Inc., United States) and SigmaPlot 12.5 (Systat Software Inc., United States) software. Figures were drawn using the SigmaPlot 12.5 software, while distribution maps were drafted using the Ocean Data View 4 (Alfred Wegener, Germany) software.

RESULTS

Abundance of Microplastics

Seawater Samples

A total of 75 stations of seawater samples were collected from the two (L + B) cruises. The mean abundance of microplastics in all seawater samples was 0.67 ± 1.09 items/m^3, while the mean abundances of 0.78 ± 1.20 and 0.26 ± 0.32 items/m^3 were obtained in seawater from L and B stations, respectively. These results were comparable with other studies, in which 0.3 mm trawl nets were used. The microplastic abundances reported in different Chinese sea areas are summarized in **Table 1**. The abundance observed in the Beibu Gulf was in the same order of magnitude as those in the Bohai Sea (0.79 items/m^3), Yellow Sea (0.33 ± 0.28 items/m^3), East China Sea (0.31 items/m^3), and Hangzhou Bay (0.14 ± 0.12 items/m^3) but much lower than those in Yangtze Estuary (67.5 ± 94.4 items/m^3), Jiaozhou Bay (46 ± 28 items/m^3), Xiangshan Bay (8.91 ± 4.7 items/m^3), Haizhou Bay (2.6 ± 1.4 items/m^3), Xiamen Bay (514.3 ± 520 items/m^3), and Hong Kong waters (3.973 ± 1.777 items/m^3). As expected, the mean abundance of microplastics in the Beibu Gulf was one order of magnitude higher than in the SCS (0.045 ± 0.093 items/m^3).

Sediment Samples

A total of 66 stations of sediment samples were collected from the two (L + B) cruises. The mean abundance of microplastics in sediment samples was 13.87 ± 9.9 items/kg of dry weight (d.w.), while mean abundances of 15.00 ± 10.74 items/kg d.w. and 12.21 ± 8.07 items/kg d.w. were obtained in sediment from L and B stations, respectively. The microplastic abundances in

TABLE 1 | Summary of microplastic abundances reported in surface water and sediment from various sea areas in China (data published within the last 3 years, revised from Wang et al., 2020).

Location	Abundance		References
	In seawater (items/m^3)	In sediment (items/kg d.w.)	
Bohai Sea	0.79	48.88	Xu et al., 2021
Jiaozhou Bay	46 ± 28	15 ± 6	Zheng et al., 2019
Yellow Sea	0.33 ± 0.28	2580 ± 1140	Wang et al., 2018
North Yellow Sea	ND	37.1 ± 42.7	Zhu et al., 2018
Haizhou Bay	2.6 ± 1.4	330 ± 260	Li Z. et al., 2020
East China Sea	0.31	ND	Liu et al., 2018
East China Sea	ND	142 ± 38	Zhang et al., 2019
Yangtze Estuary	67.5 ± 94.4	28.3 ± 14.4	Li Y. et al., 2020; Li Z. et al., 2020
Hangzhou Bay	0.14 ± 0.12	84.3 ± 56.6	Wang et al., 2020
Xiangshan Bay	8.91 ± 4.7	1740 ± 2150	Chen et al., 2018
Xiamen Bay	514.3 ± 520	181	Tang et al., 2018
Hong Kong waters	3.973 ± 1.777	–	Cheung P. K. et al., 2018
Beibu Gulf	ND	405 ± 336[a]	Xue et al., 2020
Qin River Estuary, Maowei Sea, Beibu Gulf	0.1–4.6	0-97	Zhang et al., 2020
Maowei Sea, Beibu Gulf	1200–10100	ND	Zhu et al., 2019
Beibu Gulf	0.67 ± 1.09	13.87 ± 9.9	This study
Coast area of Beibu Gulf (L)	0.78 ± 1.2	15 ± 10.74	
Far coast area of Beibu Gulf (B)	0.26 ± 0.32	12.21 ± 8.07	
South China Sea	0.045 ± 0.093	ND	Cai et al., 2018

ND, no data available.
[a]*Floating phase was potassium formate solution, with a density of 1.5 g/cm^3.*

sediments from other areas are also summarized in **Table 1**. The table shows that from the aspect of microplastics, the sediment quality in the Beibu Gulf was the best in China since the microplastic abundance was the lowest (13.87 ± 9.9 items/kg d.w.), while higher abundances (0–97 items/kg d.w.) were observed in the Qin River Estuary and Maowei Sea, which is a traditional oyster farm sea, indicating the contribution of mariculture. A much higher abundance (405 ± 336 items/kg d.w.) was discovered in the Beibu Gulf by Xue et al. (2020), in which a potassium formate solution with a density of 1.5 g/cm^3 was used as floating phase, yielding more microplastics from the sediments.

Microplastic Characteristics

Seawater Samples

Among all the seawater samples, the fragment was prevalent shape (91.0–92.6%), and no microplastic sphere was detected (**Figure 2A**). Only a small amount of fiber (4.9%), film (2.0%), and particle (0.8%) were found in L stations, whereas fiber (8.4%) and particle (0.6%) were found in the B station (**Figure 3**). Most of the microplastics were white (>50%), followed by transparent (33.0%) and green (6.4%) in L stations, whereas transparent (14.0%) and black (4.5%) in B stations (**Figure 2B**) were observed.

The size compositions of microplastics in seawater are shown in **Figure 2C**. In both L and B stations, microplastics with a diameter of 0.33–1 mm were the dominant polymers, accounting for 51.5 and 46.5%, respectively, followed by 1–2 mm (27.0 and 38.4%) and 2–3 mm (16 and 10.46%). Microplastics with a diameter of 3–5 mm were proportioned to less than 10% in the two sampling areas.

Typical polymer μ-FTIR spectra are shown in **Figure 4**. To identify the synthetic polymer, a relatively higher matching degree (>75%) was set to provide more accurate results. There was little shift of the main polymer absorption band according to the comparisons (Chen et al., 2018; Li Y. et al., 2020). Eleven polymers were detected in seawater samples, including polyethylene (PE), polypropylene (PP), PS, rayon (RY), cellulose (CE), polyethylene terephthalate (PET), polyester, polybutylene adipate glycol (PBA), polyoxymethylene (POM), and acrylic. The proportion of each polymer type in seawater is shown in **Figure 2D**. The main polymers in coastal seawater (L stations) were PS (51.1%), PP (25%), PE (18.6%), and RY (2.5%), while in far coastal areas (B stations), they were PS (73.7%), PE (10.6%), PP and RY (5.6%), and CE (1.1%).

Sediment Samples

As for microplastics in sediment (**Figure 2A**), the fiber was the prevalent shape (96.5 and 77.0% for L and B stations, respectively), and no microplastic film and sphere were detected. Only a small amount of fragment (22.5%) and particle (0.5%) were found in L stations, while fragment (1.2%) and particle (2.3%) were found in the B station. The microplastic color in sediment was dominated by black (both > 60.0%) (**Figure 2B**).

The size compositions of microplastics in sediment are shown in **Figure 2C**. In both L and B stations, microplastics with a diameter of 1–2 mm were the dominant, accounted for 43.8% and 41.3%, respectively, followed by 0–1 mm (24.2%), 2–3 mm (23.2%), 3–4 mm (6.9%), and 4–5 mm (2.2%) in L stations, and 2–3 mm (25.7%), 0–1 mm (16.7%), 3–4 mm (14.5%), and 4–5 mm (2.8%) in B stations.

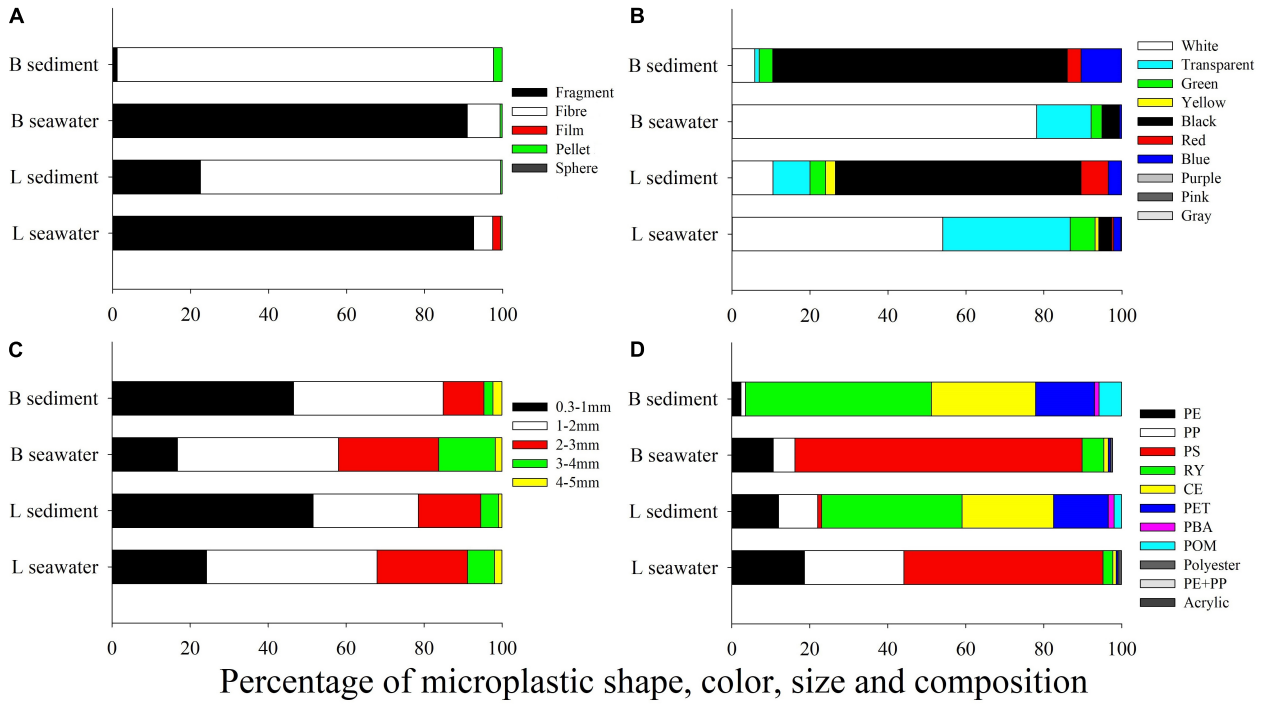

FIGURE 2 | Microplastic characteristics observed from the seawater and sediment samples in the Beibu Gulf (the northern South China Sea): shape **(A)**, color **(B)**, size **(C)**, and composition **(D)**.

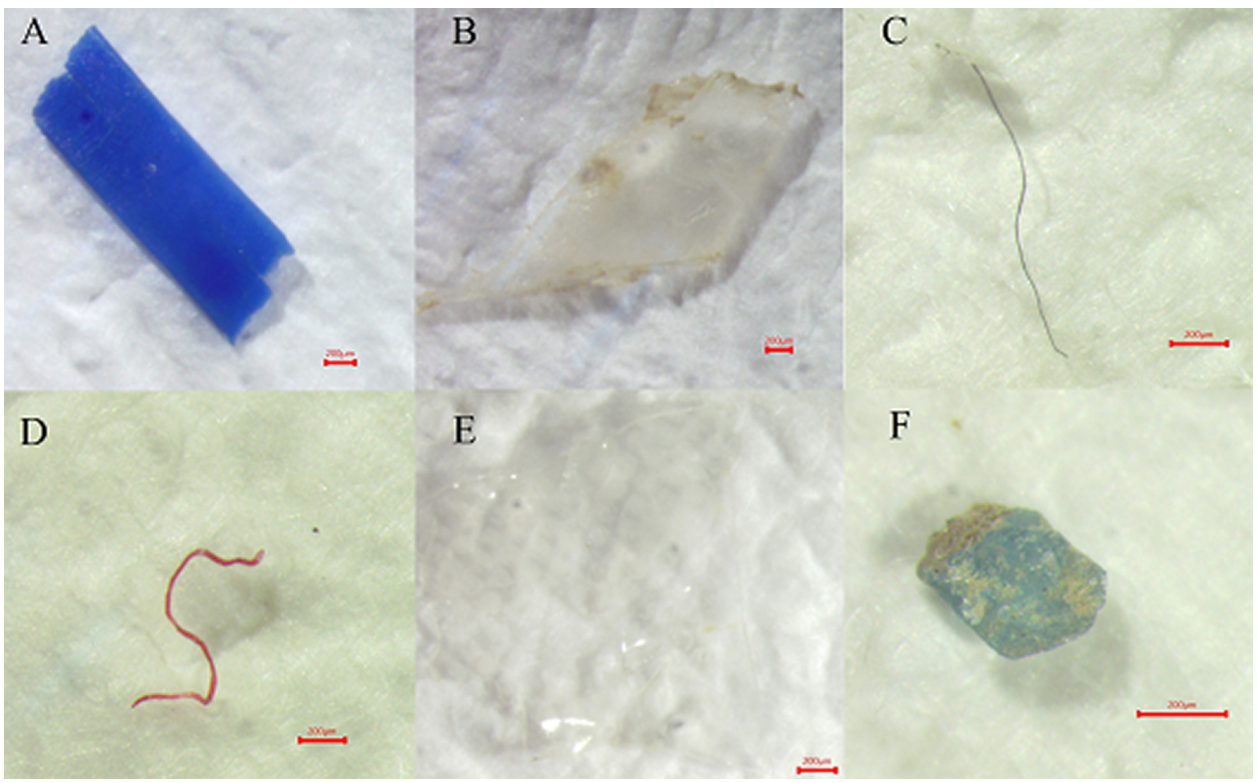

FIGURE 3 | Selected microplastic shapes inspected by SteREO microscope: fragment **(A,B)**, fiber **(C,D)**, film **(E)**, and pellet **(F)**.

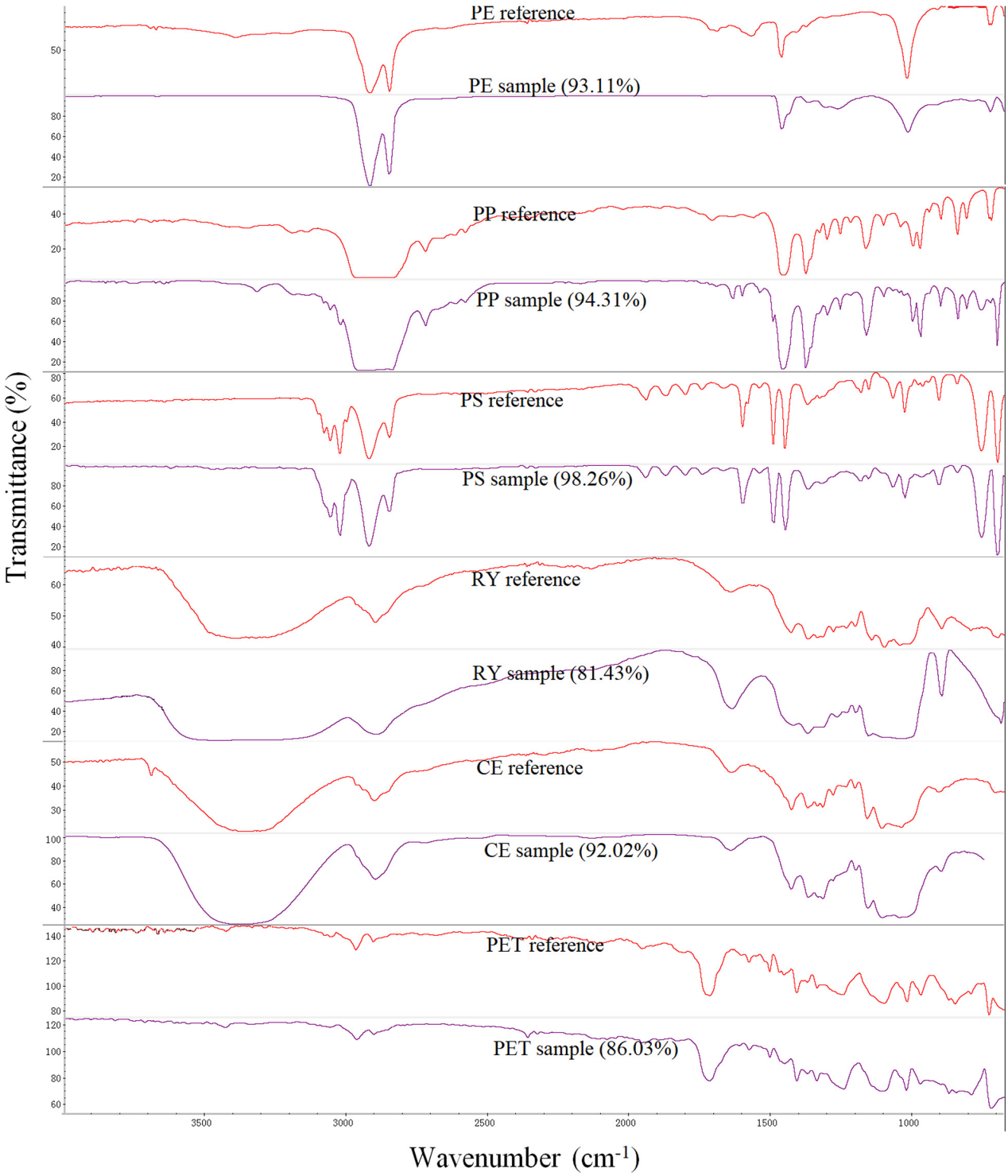

FIGURE 4 | Typical polymer spectra observed by micro-Fourier transform infrared spectrometer (numbers in brackets were the matching degree).

Eight polymers were detected in sediment samples, including PE, PP, PS, RY, CE, polyester, PET, and acrylic. The proportion of each polymer types in sediment is shown in **Figure 2D**. The main polymers in coastal sediment (L stations) were RY (36.0%), CE (23.5%), polyester (14.0%), PE (12.0%), PP (10%), acrylic (2.0%), PET (1.5%), and PS (1.0%), while in far coastal sediment (B stations) they were RY (47.6%), CE (26.7%), polyester (15.1%), acrylic (5.8%), PE (2.3%), and PP and PET (1.2%).

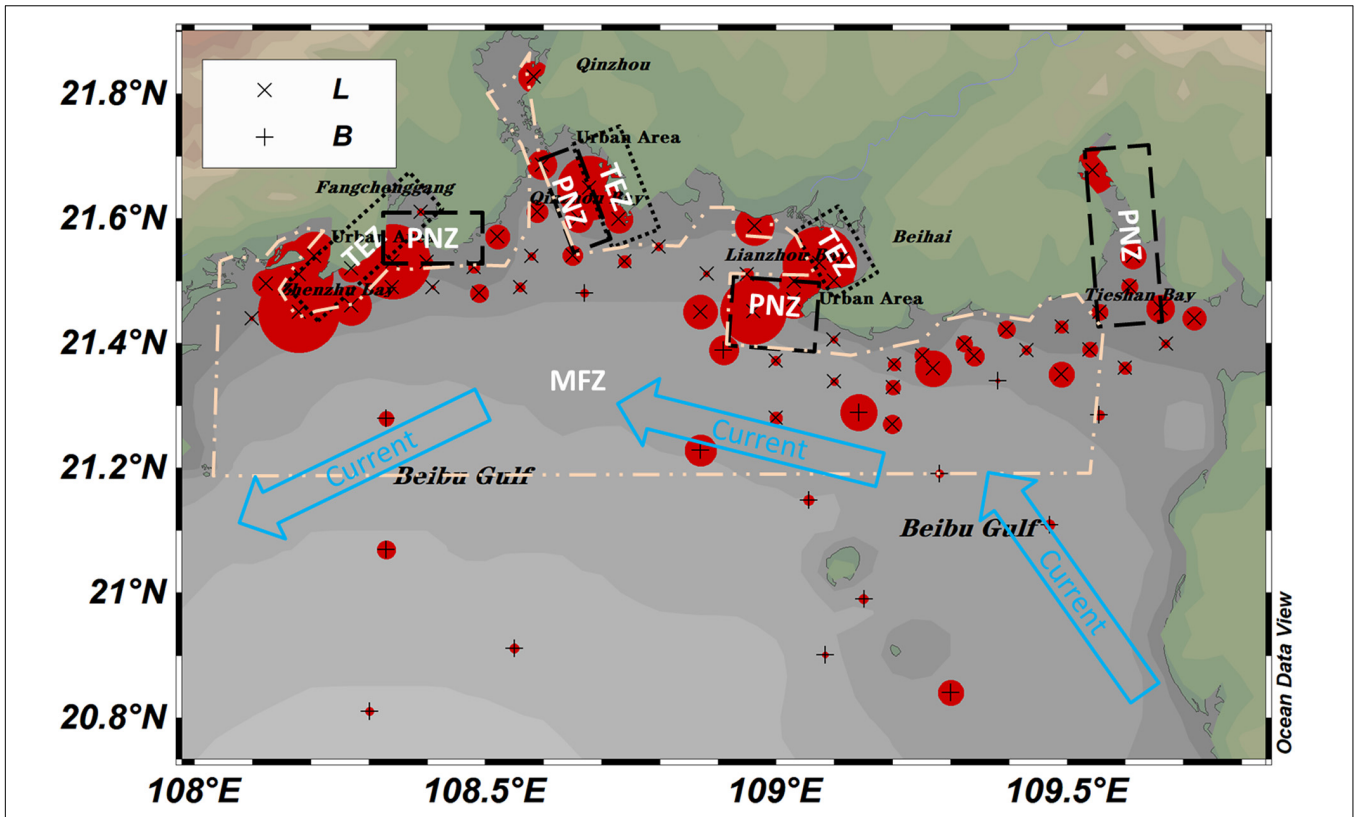

FIGURE 5 | Distributions of microplastics in seawater from L and B stations. MFZ, Mariculture and Fishery Zone; TEZ, Tourism and Entertainment Zone; PNZ, Port and Navigation Zone.

DISCUSSION

Distribution Characteristics of Microplastics

Seawater

The distribution of microplastics in seawater demonstrated the significant contributions of anthropogenic activities to the coastal seawater, especially the strong influence of fishery activities, such as oyster farming and fish culture occurred in the coastal area of the Beibu Gulf (Xue et al., 2020). As shown in **Figure 5**, the abundances of microplastics in L stations were remarkably higher than those in B stations, with an average abundance of 0.78 ± 1.20 and 0.26 ± 0.32 items/m^3, respectively. A large amount of microplastics were found in seawater close to urban areas, such as Zhenzhu Bay, Qinzhou Bay, and Lianzhou Bay, compared with other seawaters like Tieshan Bay. The stations in these bays with relatively higher microplastic abundances were coincidentally located in the Port and Navigation Zone (PNZ) and Tourism and Entertainment Zone (TEZ), according to the official marine functional zoning of Guangxi (2011–2020) (The People's Government of Guangxi, 2012). Seawaters adjacent to urban areas (especially PNZ and TEZ) receive a large amount of plastic litters and domestic sewage discharge, resulting in high abundant microplastics in these seawaters, as evident in **Figure 5**. However, the PNZ may not control the abundance of microplastics in seawater. For example, Tieshan Bay is the largest PNZ in the Beibu Gulf, while the abundances of microplastics in seawater were the lowest among the bays. One of the reasons was that Tieshan Bay is surrounded by rural area with a population density of 418 persons/km^2, presented the remarkably low microplastic abundance (0.39 ± 0.44 items/m^3), while Lianzhou Bay is surrounded by urban area with a population density of 4,272 persons/km^2, presented the highest microplastic abundance (2.49 ± 1.6 items/m^3). The other reason was that there is no TEZ in Tieshan Bay but the other three bays have, while the plastic litters produced by tourists were one of the main sources of microplastics in the seawater. Compared with the microplastic abundances in Zhenzhu Bay, Qinzhou Bay, and Lianzhou Bay with PNZ and TEZ, the microplastic abundances in the mariculture and fishery zone were quite small. These findings further confirmed that the relatively higher microplastic abundances found in seawater adjacent to the urban areas than the rural areas, and anthropogenic activities (i.e., domestic and industrial littering and sewage discharge) domain the microplastic distribution in seawater, rather than mariculture and fishery zone (Naidoo et al., 2015; Zhao et al., 2015; Tang et al., 2018).

It is known that current can influence microplastic distribution in the ocean (Eriksen et al., 2013; Pan et al., 2019); a case study in the Jiaozhou Bay reported by Zheng et al. (2019)

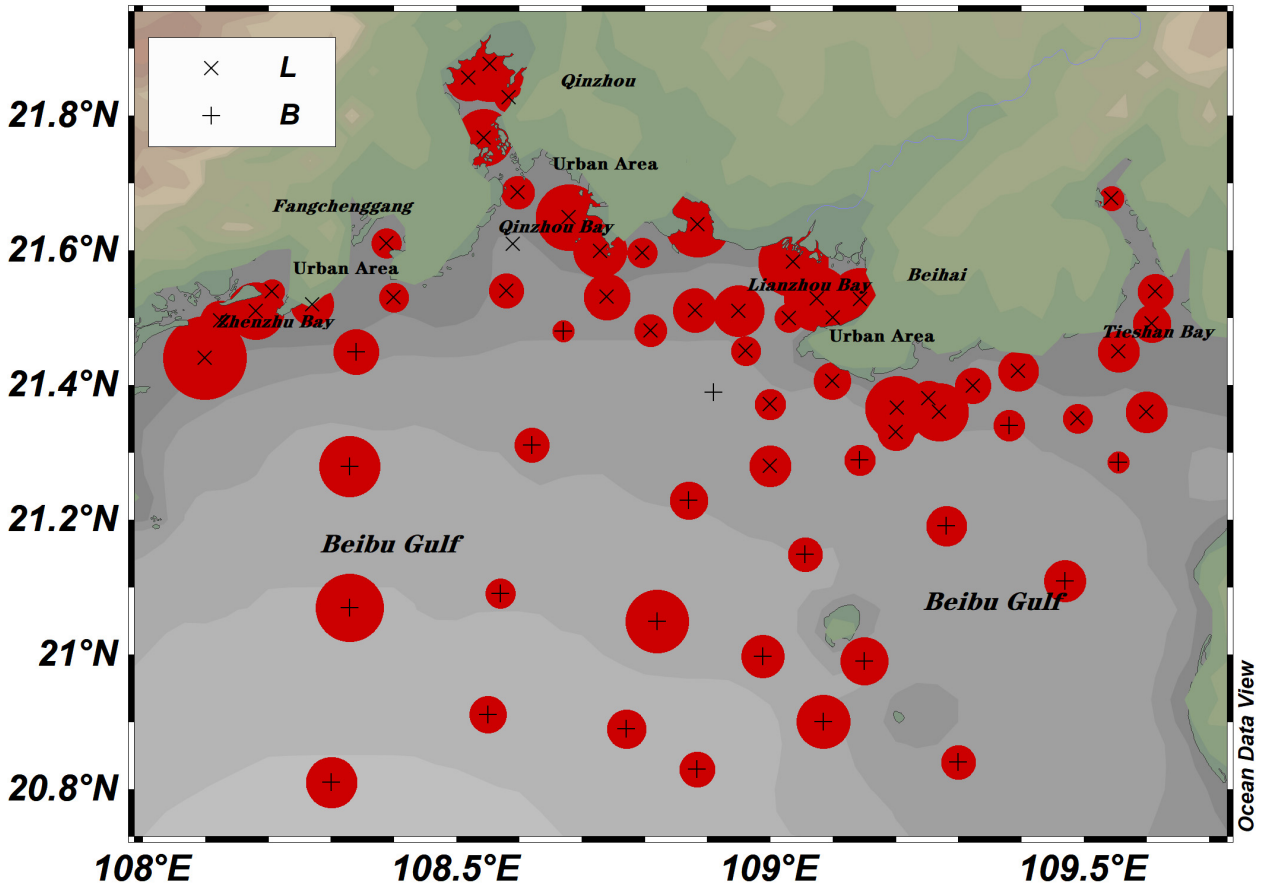

FIGURE 6 | Distributions of microplastics in sediment from L and B stations.

showed that residual currents seem to have a significant impact on the distribution and composition of microplastics. In this study, the abundance of microplastics in seawater increased from the east to the west (**Figure 5**), which was consistent with the current existed in the coastal areas of Beibu Gulf (Gao et al., 2014; Chen et al., 2019), showing that the current in the Beibu Gulf may have influence on the transportation of microplastics in the seawater.

Sediment

Similar to the distribution of microplastics in seawater, microplastic abundances in sediment samples from Zhenzhu Bay, Qinzhou Bay, and Lianzhou Bay were higher than those from Tieshan Bay and other stations, far away from urban areas (**Figure 6**; Vaughan et al., 2017). In addition, the intensive traditional oyster farm (floating row or pile) distributed in Zhenzhu Bay, Qinzhou Bay (Maowei sea), and Lianzhou Bay contributed a large proportion of microplastics in the sediment (Zhu et al., 2019, 2021; Xue et al., 2020). However, the average abundance of microplastics in L sediment stations (15.00 ± 10.74 items/kg d.w.) was only slightly higher than that of B sediment stations (12.21 ± 8.07 items/kg d.w.), indicating that a large amount of microplastics are readily transported to long distance, and sink down and bury in the sediment (Näkki et al., 2019).

TABLE 2 | Average microplastic abundances in seawater and sediment sample in this study.

	L	B
Seawater (items/m^3)	0.78	0.26
Sediment (items/kg d.w.)	15	12.21
Sediment/Seawater	19.23	46.96

Correlation Between Seawater and Sediment

Previous studies have shown that the abundance of microplastics in the seawater and sediment was positively correlated (Zheng et al., 2019; Li Z. et al., 2020; Wang et al., 2020); however, no significant correlations were observed between seawater and sediment in this study, probably related to mismatch in spatiotemporal distributions and variations in the characteristics, fate, and behavior of microplastics in the surface water and sediment (Xu et al., 2021). The average microplastic abundance ratio of sediment to seawater in L (19.23) and B (46.96) stations was obviously different, as shown in **Table 2**. Interestingly, it

TABLE 3 | Main microplastic characteristics observed in surface water and sediment in Chinese coastal seas and selected similar bays in other country with comparable data (data published within the last 3 years, revised from Xu et al., 2021).

	Sample	Shape	Color	Size	Composition	
Bohai Sea	Seawater	Fragment (67.4%)	Transparent (>24.9%)	0.4–2 mm (64.2%)	Alkyd resin	Xu et al., 2021
	Sediment	Fiber (54.9%)	Blue (>18.5%)	0–1 mm (69.3%)	RY	
Jiaozhou Bay	Seawater	Fiber (~85%)	Black (~40%)	1–2 mm (~40%)	PET (~55%)	Zheng et al., 2019
	Sediment	Fiber (~88%)	Black (~30%)	0–1 mm (55%)	PET (~50%)	
Yellow Sea offshore	Seawater	Fiber (75.4%)	Black (~40%)	1–3 mm (~30%)	–	Wang et al., 2018
	Sediment	Fiber (68.7%)	Transparent (~30%)	1–3 mm (~30%)	–	
North Yellow Sea	Seawater	Film (58.1%)	Transparent (~80%)	0.03–1 mm (~80%)	PE (77.8%)	Zhu et al., 2018
	Sediment	Film (61.4%)	Transparent (~70%)	0–1 mm (~80%)	PP (44.5%)	
Haizhou Bay	Seawater	Fiber (91.12%)	Blue (50.9%)	0.16–1 mm (~47%)	PET (41.71%)	Li Z. et al., 2020
	Sediment	Fiber (93.21%)	Blue (33.25%)	0.16–1 mm (~40%)	RY (~41.98%)	
East China Sea	Seawater	Foam (54.8%)	White (71.9%)	0.5–5 mm (88.6%)	PE (45.5%)	Liu et al., 2018
	Sediment	–	–	–	–	
East China Sea	Seawater	–	–	–	–	Zhang et al., 2019
	Sediment	Fiber (77%)	Blue (35%)	0.06–1 mm (89%)	Cellophane (37.2%)	
Yangtze Estuary	Seawater	Fragment (39.2%)	White (64.7%)	0–1 mm (~48.05%)	PE (37.3%)	Li Y. et al., 2020
	Sediment	Fiber (66.7%)	Transparent (16.2%)	0-1mm (88.5%)	PP (28.6%)	
Hangzhou Bay	Seawater	Pellet (46.4%)	–	0–1 mm (36.4%)	PE (52.3%)	Wang et al., 2020
	Sediment	Fiber (59.8%)	–	0–1 mm (38%)	RY (49.7%)	
Xiangshan Bay	Seawater	Foam	–	0.25–2 mm	PE (38.6%)	Chen et al., 2018
	Sediment	–	–	0.25–2 mm	RY (56.3%)	
Xiamen Bay	Seawater	Granule (~30%)	White (50%)	–	PE (50.4%)	Tang et al., 2018
	Sediment	Fiber (70%)	Black (26%)	–	PP	
Hong Kong waters	Seawater	Foam	–	0.3–0.7 mm	PS	Cheung P. K. et al., 2018
	Sediment	–	–	–	–	
Beibu Gulf	Seawater	–	–	–	–	Xue et al., 2020
	Sediment	Fiber (69.6%)	–	1–5 mm (~50%)	PP (68.7%)	
Qin River Estuary, Maowei Sea, Beibu Gulf	Seawater	Fiber (38.2%)	White (~28.5%)	1–5 mm (88.9%)	PP (39%)	Zhang et al., 2020
	Sediment	Film (62.8)	White (30%)	1–5 mm (76%)	PP (55.3%)	
Maowei Sea, Beibu Gulf	Seawater	Fiber (~80%)	White (~80%)	1–5 mm (4~0%)	PES(~40%)	Zhu et al., 2019
	Sediment	–	–	–	–	
In total (except Beibu Gulf)	Seawater	Fiber	White	0–1 mm	PE	
	Sediment	Fiber	Transparent	0–1 mm	RY	
Beibu Gulf	Seawater	Fragment (92.38%)	White (56.20%)	1–2 mm (44%)	PS (53.23%)	This study
	Sediment	Fiber (82.93%)	Black (66.83%)	0–1 mm (50.04%)	RY (39.54%)	

seems that the microplastic sedimentation in far coast area (B station) was much stronger than that in coastal area (L station); evidently, most of the microplastics were retained in the sediment of B stations while only a minimal amount in coastal area sediment. Furthermore, higher abundances of microplastics were found in coastal seawater, and a substantial part of them were sequestered into the far coast sediment, further confirming that the sediment is the sink of microplastics (Long et al., 2015; Martin et al., 2017; Zheng et al., 2019).

Dai et al. (2018) reported that the microplastic abundances were inversely correlated with the chlorophyll-*a* in surface water in the Bohai Sea; therefore, the algae aggregation might have an effect on the sinking of the microplastics into the sediment. In this study, no significant correlations were obtained between microplastics and chlorophyll-a or suspended particles, showing that the sedimentation of microplastics in the study area was controlled by multiple processes that remain further exploration, e.g., benthos might promote the burial of microplastics in the sediments (Gebhardt and Forster, 2018).

Comparison of Microplastic Characteristics

The main microplastic characteristics determined in the seawater and sediment samples in the sea areas of China are summarized in **Table 3**. Most identified microplastics existed were fragments (92.38%) in seawater, which is of great difference from other areas, e.g., fibers were the dominant components in most sea areas of China, such as Jiaozhou Bay, Haizhou Bay, and Yellow Sea offshore. The dominant polymer in seawater was PS, which is widely used to produce plastic foam applied in the mariculture and other packing materials, and usually, it is white. The dominant color of microplastics in seawater was found to be white (56.20%), inconsistent with the microplastic color

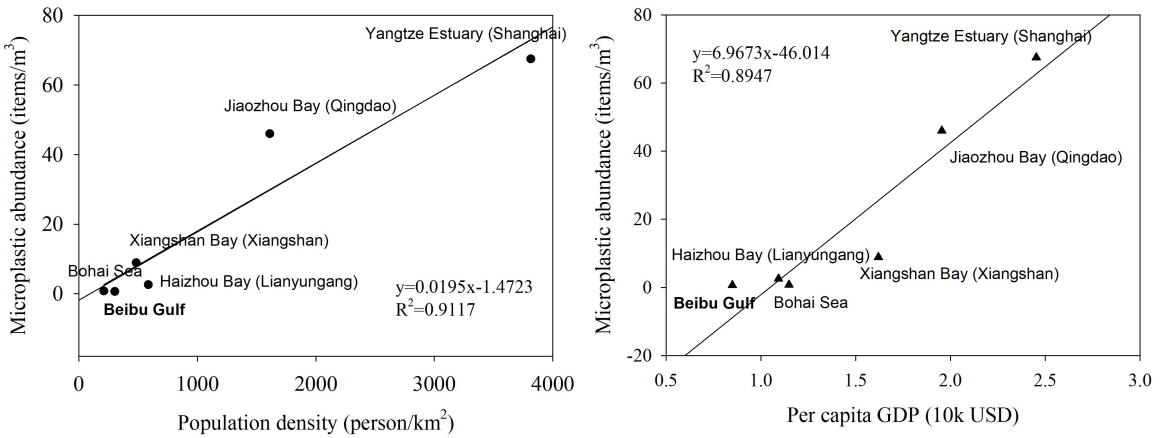

FIGURE 7 | Correlation between microplastic abundance in seawater and population density and per capita gross domestic product. Comparable data were selected from Bohai Sea, Jiaozhou Bay, Haizhou, Bay, Yangtze Estuary, Xiangshan Bay, and Beibu Gulf.

discovered in most seawaters reported in China. In addition, most colored microplastics are subjected to be decolored by sunlight (ultraviolet radiation), resulting in transformation to white. Since white microplastics are not as attractable as other colored microplastics, when missed to be eaten by marine organisms, they were likely to be retained in the water. The PS foam has more porous structures and then might be easily broken down into small plastics by sunlight, wind, and current, bringing much more fragments into the sea (Song et al., 2017), inconsistent with the dominant foams and fragments observed in the seawater in Hong Kong (Cheung P. K. et al., 2018), the north coast of Surabaya (Cordova et al., 2019), and this study, also inconsistent with the dominant PS foams (macroplastics), found in the beach and sediment of tourist spots in the coastal of Beihai, Qinzhou, and Fangchenggang according to the Marine Environment Bulletin (2017; Department of Ocean and Fishery of Guangxi). These findings provided clues for the mitigation of PS microplastic pollution such as the recycling of the PS foams used in mariculture.

The dominant size (1–2 mm) of microplastics measured in seawater in this study is larger than those (0–1 mm) in the other sea areas, possibly because that smaller microplastics tend to sink down to the sediment, and PS fragments need to be in relatively larger size to keep floating on the surface seawater. This further confirms that a large amount of microplastics are white PS foams (macro fragment) in samples collected in this field study, especially in the coastal area.

Similar to the most study areas, fibers were the dominant microplastics in the sediment in this study (**Table 3**). It is known that fibers were originated mainly from fabrics and were difficult to remove during sewage treatment. The Beibu Gulf is a semi-enclosed bay receiving all the sewage from the river and coastal cities, which supports the findings. This finding is also consistent with the high relative abundance of RY in the sediment in this study, a synthetic polymer largely used in the textile industry (Kauffman, 1993; De Falco et al., 2018). The density of RY is usually less than PS, but still acts as a high-density polymer. Furthermore, the RY detected in this study existed as very small size (0–1 mm), having large specific surface area for the microplastics, leading to more fiber microplastics settled and buried in the sediment. In addition, small microplastics tend not to retain in the water column and are likely to be deposited in sediments (Enders and Lenz, 2015; Wu et al., 2019; Xu et al., 2021), which was supported by the finding in this study that dominant microplastics were much smaller (0–1 mm, 50.04%) in sediments than in the surface water (1–2mm, 44%). These features were also discovered in Bohai and Yellow Seas (Dai et al., 2018; Zhao et al., 2018; Xu et al., 2021), Haizhou Bay, Hangzhou Bay, and Xiangshan Bay, indicating that more effective wastewater treatment technology should be adopted to remove the fibrous microplastic RY from domestic and industrial wastewater. Interestingly, the dominant color of fibers in the sediment in this study was black, and the same dominant color of microplastics discovered in Xiamen Bay (Tang et al., 2018) was quite different from the transparent in other sea area sediment, which need more exploration.

Comparison of Microplastic Abundances in Semi-Enclosed Bays

A semi-enclosed bay is likely to accumulate microplastics due to intensive anthropogenic activities and restricted water exchange (Li et al., 2018; Zhou et al., 2021). For example, up to 27.7 items/L of microplastic abundances were found in seawater of Bohai Sea (Dai et al., 2018), Maowei Sea (an inner bay of Beibu Gulf; Zhu et al., 2019, 2021), and Baltic Sea (Zhou et al., 2021), in which studies bulk water sampling was employed. However, significant lower microplastic abundance in seawater of Bohai Sea was reported using trawl net sampling by Xu et al. (2021), since much smaller filter pore size was used in the former method, theoretically resulted more microplastics were collected, and higher abundances were revealed than the trawl net sampling. Still, significantly higher microplastic abundances (>0.33 mm) in seawater were reported using bulk water sampling in those semi-enclosed bays than the Beibu Gulf. As a typical semi-enclosed bay, the Bohai Sea is surrounded by highly developed

regions in China compared with the Beibu Gulf. However, the microplastic abundance in seawater of Bohai Sea (0.79 items/m^3) and Beibu Gulf (0.67 items/m^3) was almost the same mainly because of the comparable population density, per capita GDP, and more relevantly, roughly the same water exchange time (406 days vs. 509 days; Cai, 2013; Fang, 2014). In contrast, the microplastic abundance in sediment of Bohai Sea (48.88 items/kg d.w.) was larger than Beibu Gulf (13.87 items/kg d.w.), indicating that the sediment in Bohai Sea accumulated more microplastics than Beibu Gulf since the Bohai Sea region was suffering much longer time economic development than the Beibu Gulf (Dai et al., 2018). Compared with the microplastics in Benoa Bay with similar ecosystems (i.e., mangroves and estuaries) (Suteja et al., 2021), the microplastic abundance (0.62 items/m^3) was nearly equal to the Beibu Gulf, suggesting that the indices influencing microplastic pollution, including population, GDP, and fishery between Beibu Gulf and Benoa Bay, were comparable, which provided clues for the applications of the microplastic pollution management in both waters.

Microplastic Abundance Links to Socioeconomics in China

Report showed that the plastic consumption was correlated with socioeconomic indices (Hossain et al., 2021). Therefore, the population density and other socioeconomic parameters are important when interpreting the occurrence of the microplastics (Lebreton et al., 2017; Wang, 2018; Mai et al., 2019; Chen B. et al., 2020; Wu et al., 2021). In this study, population density and per capita GDP were selected from districts with comparable microplastic data from **Table 1**; subsequently, we found positive correlations between microplastic abundance in seawater and population density and per capita GDP, respectively (**Figure 7**). Similarly, Yonkos et al. (2014) and Fan et al. (2019) found significant positive correlations between microplastic abundance in water and population density in four estuarine rivers in the Chesapeake Bay and the Pearl River catchment, indicating that large population areas released more microplastics. And Chen H. et al. (2020) reported a positive correlation between microplastic concentration in the global waterbodies and per capita GDP, indicating that increasing human living standards would accelerate the demand for plastic products, leading to the increase in the degree of microplastic pollution. However, Tang et al. (2018) and Chen H. et al. (2020) reported a positive correlation between microplastic abundance and population number (not population density), and Tang et al. (2018) reported a poor negative correlation between microplastic abundance and per capita GDP, which were contrary to the results of this study. These findings would play important roles in the first step of developing policy and regulations to mitigate the microplastic pollution risk (Xu et al., 2020).

CONCLUSION

In this study, microplastic distributions in seawaters and sediments in the Beibu Gulf were firstly investigated. Fiber and PE were the dominant microplastics in Chinese coastal seawater, while fragment and PS were the dominant microplastics in the seawater of Beibu Gulf. The abundances of microplastics in coastal seawater were much greater than that in far coastal seawater, indicating important contribution of human activities. In addition, a large amount of microplastics can be transported for long distance, and then sink down and bury in the sediment, since the microplastic abundances were comparable between coastal and far coastal sediments. Significant correlations between the microplastics abundance and population density and per capita GDP were found in Chinese coastal seawater, indicating that microplastics in the Beibu Gulf were at a low level. This study presented microplastics abundances and distributions in a semi-enclosed bay with increasing anthropogenic activities, which may provide reference methods and data for the microplastic research in the other ocean. Further studies need to be carried out to explain the transport and sink processes of microplastics in the water column of Beibu Gulf and SCS.

DATA AVAILABILITY STATEMENT

The original contributions presented in the study are included in the article/**Supplementary Material**, further inquiries can be directed to the corresponding author/s.

AUTHOR CONTRIBUTIONS

ZZ contributed for conceptualization, sampling, and writing – original draft preparation. HW contributed for sample preparation, characterization, and data management. WH contributed for characterization and draft modification. XW contributed for sample preparation and characterization. YG contributed for data management and editing. QZ contributed for conceptualization. All authors contributed to the article and approved the submitted version.

FUNDING

This work was supported by the National Natural Science Foundation of China (U20A20103), Guangxi Funding Project (304024XM20N0006, 2019GXNSFBA185036, and 2018AD19280), and Beihai Science and Technology Project (201995037, 202082031, and 202082022).

ACKNOWLEDGMENTS

The authors thank all the crews on the R/V Yueke 1 and R/V Yuexiayuzhi 20028 for the assistance of the microplastic sampling during the L and B cruises in the summer of 2020, and the reviewers for the revision of this manuscript.

SUPPLEMENTARY MATERIAL

The Supplementary Material for this article can be found online at: https://www.frontiersin.org/articles/10.3389/fmars.2021.821008/full#supplementary-material

REFERENCES

Boyle, D., Catarino, A. I., Clark, N. J., and Henry, T. B. (2020). Polyvinyl chloride (PVC) plastic fragments release Pb additives that are bioavailable in zebrafish. *Environ. Pollut.* 263(Pt A):114422. doi: 10.1016/j.envpol.2020.114422

Cai, M., He, H., Liu, M., Li, S., Tang, G., Wang, W., et al. (2018). Lost but can't be neglected: huge quantities of small microplastics hide in the South China Sea. *Sci. Total Environ.* 633, 1206–1216. doi: 10.1016/j.scitotenv.2018.03.197

Cai, Z. Y. (2013). *Modelling Average Residence Time of the Waterbody in Bohai and its Seasonal Variation*. Masteral dissertation. Qingdao: China Ocean University. (in Chinese).

Catarino, A. I., Kramm, J., Vlker, C., Henry, T. B., and Everaert, G. (2021). Risk posed by microplastics: scientific evidence and public perception. *Curr. Opin. Green Sust.* 29:100467. doi: 10.1016/j.cogsc.2021.100467

Cauwenberghe, L. V., Vanreusel, A., Mees, J., and Janssen, C. R. (2013). Microplastic pollution in deep-sea sediments. *Environ. Pollut.* 182, 495–499. doi: 10.1016/j.envpol.2013.08.013

Chen, B., Fan, Y., Huang, W., Rayhan, A., and Cai, M. (2020). Observation of microplastics in mariculture water of longjiao bay, southeast china: influence by human activities. *Mar. Pollut. Bull.* 160, 1–8.

Chen, B., Xu, Z., Ya, H., Chen, X., and Xu, M. (2019). Impact of the water input from the eastern qiongzhou strait to the beibu gulf on guangxi coastal circulation. *Acta Oceanol. Sin.* 38, 1–11. doi: 10.1007/s13131-019-1472-2

Chen, C. C., Zhu, X., Xu, H., Chen, F., Ma, J., and Pan, K. (2021). Copper adsorption to microplastics and natural particles in seawater: a comparison of kinetics, isotherms, and bioavailability. *Environ. Sci. Tech.* 55, 13923–13931.

Chen, H., Qin, Y., Huang, H., and Xu, W. (2020). A regional difference analysis of microplastic pollution in global freshwater bodies based on a regression model. *Water* 12:1889.

Chen, M., Jin, M., Tao, P., Wang, Z., Xie, W., Yu, X., et al. (2018). Assessment of microplastics derived from mariculture in Xiangshan Bay, China. *Environ. Pollut.* 242, 1146–1156. doi: 10.1016/j.envpol.2018.07.133

Cheung, L. T. O., Lui, C. Y., and Fok, L. (2018). Microplastic contamination of wild and captive Flathead Grey mullet (*Mugil cephalus*). *Int. J. Environ. Res. Public Health* 15:597. doi: 10.3390/ijerph15040597

Cheung, P. K., Fok, L., Hung, P. L., and Cheung, L. (2018). Spatio-temporal comparison of neustonic microplastic density in Hong Kong waters under the influence of the Pearl River Estuary. *Sci. Total Environ.* 628–629, 731–739. doi: 10.1016/j.scitotenv.2018.01.338

Cordova, M. R., Nurhati, I. S., Riani, E., Nurhasanah, A., and Iswari, M. Y. (2021). Unprecedented plastic-made personal protective equipment (ppe) debris in river outlets into Jakarta Bay during covid-19 pandemic. *Chemosphere* 268:129360. doi: 10.1016/j.chemosphere.2020.129360

Cordova, M. R., Purwiyanto, A., and Suteja, Y. (2019). Abundance and characteristics of microplastics in the northern coastal waters of Surabaya, Indonesia. *Mar. Pollut. Bull.* 142, 183–188. doi: 10.1016/j.marpolbul.2019.03.040

Cózar, A., Echevarría, F., González-Gordillo, J. I., Irigoien, X., Ubeda, B., Hernández-León, S., et al. (2014). Plastic debris in the open ocean. *Proc. Natl. Acad. Sci. U.S.A.* 111, 10239–10244. doi: 10.1073/pnas.1314705111

Dai, Z., Zhang, H., Zhou, Q., Tian, Y., Chen, T., Tu, C., et al. (2018). Occurrence of microplastics in the water column and sediment in an inland sea affected by intensive anthropogenic activities. *Environ. Pollut.* 242, 1557–1565. doi: 10.1016/j.envpol.2018.07.131

De Falco, F., Gullo, M. P., Gentile, G., Di Pace, E. D., Cocca, M., Gelabert, L., et al. (2018). Evaluation of microplastic release caused by textile washingprocesses of synthetic fabrics. *Environ. Pollut.* 236, 916–925.

Enders, K., and Lenz, R. (2015). *How to Find the Small Plastic in the Big Sea – the Identification and Characterisation of Microplastic ≥10 μm from the Atlantic Ocean*. Master thesis. Kgs. Lyngby: DTU Aqua.

Eriksen, M., Maximenko, N., Thiel, M., Cummins, A., Lattin, G., Wilson, S., et al. (2013). Plastic pollution in the South Pacific subtropical gyre. *Mar. Pollut. Bull.* 68, 71–76.

Everaert, G., Van Cauwenberghe, L., De Rijcke, M., Koelmans, A. A., Mees, J., Vandegehuchte, M., et al. (2018). Risk assessment of microplastics in the ocean: modelling approach and first conclusions. *Environ. Pollut.* 242(Pt B), 1930–1938. doi: 10.1016/j.envpol.2018.07.069

Fan, Y., Zheng, K., Zhu, Z., Chen, G., and Peng, X. (2019). Distribution, sedimentary record, and persistence of microplastics in the Pearl River catchment, China. *Environ. Pollut.* 251, 862–870. doi: 10.1016/j.envpol.2019.05.056

Fang, X. Y. (2014). *Numerical Simulation of Seasonally Circulation and Water Exchange in the Beibu Gulf*. Masteral dissertation. Qingdao: China Ocean University. (in Chinese).

Gao, J., Shi, M., Chen, B., Guo, P., and Zhao, D. (2014). Responses of the circulation and water mass in the Beibu Gulf to the seasonal forcing regimes. *Acta Oceanol. Sin.* 33:11.

Gebhardt, C., and Forster, S. (2018). Size-selective feeding of *Arenicola marina* promotes long-term burial of microplastic particles in marinesediments. *Environ. Pollut.* 242, 1777–1786. doi: 10.1016/j.envpol.2018.07.090

Hossain, K. B., Chen, K., Chen, P., Wang, C., and Cai, M. (2021). Socioeconomic relation with plastic consumption on 61 countries classified by continent, income status and coastal regions. *Bull. Environ. Contam. Toxicol.* 107, 786–792.

Isobe, A., Uchiyama-Matsumoto, K., Uchida, K., and Tokai, T. (2017). Microplastics in the southern ocean. *Mar. Pollut. Bull.* 114, 623–626.

Jambeck, J. R., Geyer, R., Wilcox, C., Siegler, T. R., Perryman, M., Andrady, A., et al. (2015). Plastic waste inputs from land into the ocean. *Science* 347, 768–771. doi: 10.1126/science.1260352

Kataoka, T., Nihei, Y., Kudou, K., and Hinata, H. (2019). Assessment of the sources and inflowprocesses of microplastics in the river environments of Japan. *Environ. Pollut.* 244, 958–965. doi: 10.1016/j.envpol.2018.10.111

Kauffman, G. (1993). Rayon: the first semi-synthetic fiber product. *J. Chem. Educ.* 70:887. doi: 10.1021/ed070p887

Khan, F. R. (2020). Prevalence, fate and effects of plastic in freshwater environments: new findings and next steps. *Toxics* 8:72.

Lebreton, L., Joost, V., Damsteeg, J. W., Slat, B., Andrady, A., and Reisser, J. (2017). River plastic emissions to the world's oceans. *Nat. Commun.* 8:15611.

Li, R., Yu, L., Chai, M., Wu, H., and Zhu, X. (2019). The distribution, characteristics and ecological risks of microplastics in the mangroves of southern China. *Sci. Total Environ.* 708:135025. doi: 10.1016/j.scitotenv.2019.135025

Li, Y., Lu, Z., Zheng, H., Wang, J., and Chen, C. (2020). Microplastics in surface water and sediments of Chongming island in the Yangtze Estuary, China. *Environ. Sci. Eur.* 32, 1–12. doi: 10.1016/j.csr.2005.10.003

Li, Y., Wolanski, E., Dai, Z., Lambrechts, J., Tang, C., and Zhang, H. (2018). Trapping of plastics in semi-enclosed seas: insights from the Bohai Sea, China. *Mar. Pollut. Bull.* 137, 509–517. doi: 10.1016/j.marpolbul.2018.10.038

Li, Z., Gao, C., Yang, J., Wu, L., Zhang, S., Liu, Y., et al. (2020). Distribution characteristics of microplastics in surface water and sediments of Haizhou Bay, Lianyungang. *Environ. Sci. J. Integr. Environ. Res.* 1, 1–17. (in Chinese), doi: 10.13227/j.hjkx.201910005

Liu, Q., Xu, X. D., Wei, H., Xu, X. Q., Shou, L., and Zeng, J. N. (2017). Research advances on the ecological effects of microplastic pollution on the marine environment. *Acta Ecol. Sin.* 37, 7397–7409.

Liu, T., Sun, X., Zhu, M., Liang, J., and Zhao, Y. (2018). Distribution and composition of microplastics in the surface water of the East China Sea. *Oceanol. Limnol. Sinica* 49, 62–69. (in Chinese),

Long, M., Moriceau, B., Gallinari, M., Lambert, C., Huvet, A., Raffray, J., et al. (2015). Interactions between microplastics and phytoplankton aggregates: impact on their respective fates. *Mar. Chem.* 175, 39–46. doi: 10.1016/j.marchem.2015.04.003

Lusher, A., Hollman, P., and Mendoza-Hill, J. (2017). *Microplastics in Fisheries and Aquaculture: Status of Knowledge on their Occurrence and Implications for Aquatic Organisms and Food Safety*, FAO Fisheries and AquacultureTechnical Paper: No. 615. Rome: FAO.

Mai, L., You, S., He, H., Bao, L., and Zeng, E. (2019). Riverine microplastic pollution in the Pearl River Delta, China: are modeled estimates accurate? *Environ. Sci. Tech.* 53, 11810–11817. doi: 10.1021/acs.est.9b04838

Martin, J., Lusher, A., Thompson, R., and Morley, A. (2017). The deposition and accumulation of microplastics in marine sediments and bottom water from the Irish continental shelf. *Sci. Rep.* 7:10772.

Mecozzi, M., Pietroletti, M., and Monhakova, Y. B. (2016). FTIR spectroscopy supported by statistical techniques for the structural characterization of plastic debris in the marine environment: application to monitoring studies. *Mar. Pollut. Bull.* 106, 155–161. doi: 10.1016/j.marpolbul.2016.03.012

Naidoo, T., Glassom, D., and Smit, A. J. (2015). Plastic pollution in five urban estuaries of KwaZulu-Natal, South Africa. *Mar. Pollut. Bull.* 101, 473–480. doi: 10.1016/j.marpolbul.2015.09.044

Naji, A., Azadkhah, S., Farahani, H., Uddin, S., and Khan, F. R. (2020). Microplastics in wastewater outlets of Bandar Abbas city (Iran): a potential point source of microplastics into the Persian Gulf. *Chemosphere* 262:128039.

Näkki, P., Setälä, O., and Lehtiniemi, M. (2019). Seafloor sediments asmicroplastic sinks in the northern Baltic Sea–negligible upwardtransport of buried microplastics by bioturbation. *Environ. Pollut.* 249, 74–81. doi: 10.1016/j.envpol.2019.02.099

NOAA Marine Debris Program (2015). *Laboratory Methods for the Analysis of Microplastics in the Marine Environment: Recommendations for Quantifying Synthetic Particles in Waters and Sediments*. Silver Spring, MD: NOAA Marine Debris Program.

Nurhasanah, A., Cordova, M. R., and Riani, E. (2021). Micro- and mesoplastics release from the indonesian municipal solid waste landfill leachate to the aquatic environment: case study in Galuga Landfill Area, Indonesia. *Mar. Pollut. Bull.* 163:111986. doi: 10.1016/j.marpolbul.2021.111986

Pan, Z., Guo, H., Chen, H., Wang, S., Sun, X., and Zou, Q. (2019). Microplastics in the Northwestern Pacific: abundance, distribution, and characteristics. *Sci. Total Environ.* 650, 1913–1922. doi: 10.1016/j.scitotenv.2018.09.244

Pannetier, P., Morin, B., Le Bihanic, F., Dubreil, L., Clérandeau, C., Chouvellon, F., et al. (2020). Environmental samples of microplastics inducesignificant toxic effects in fish larvae. *Environ. Int.* 134:105047. doi: 10.1016/j.envint.2019.105047

Philipp, C., Unger, B., Ehlers, S. M., Koop, J. H. E., and Siebert, U. (2021). First evidence of retrospective findings of microplastics in harbour porpoises (*Phocoena phocoena*) from German waters. *Front. Mar. Sci.* 8:682532.

Rocha-Santos, T., and Duarte, A. C. (2015). A critical overview of the analytical approaches to the occurrence, the fate and the behavior of microplastics in the environment. *TRAC Trend Anal. Chem.* 65, 47–53. doi: 10.1016/j.trac.2014.10.011

Rochman, C. M. (2018). Microplastics research from sink to source. *Science* 360, 28–29. doi: 10.1126/science.aar7734

Sharma, S., Sharma, V., and Chatterjee, S. (2021). Microplastics in the Mediterranean Sea: sources, pollution intensity, sea health, and regulatory policies. *Front. Mar. Sci.* 8:634934.

Song, Y. K., Hong, S. H., Jang, M., Han, G. M., Jung, S. W., and Shim, W. J. (2017). Combined effects of UV exposure duration and mechanical abrasion on microplastic fragmentation by polymer type. *Environ. Sci. Technol.* 52, 3831–3832. doi: 10.1021/acs.est.6b06155

Suteja, Y., Atmadipoera, A. S., Riani, E., Nurjaya, I. W., and Cordova, M. R. (2021). Spatial and temporal distribution of microplastic in surface water of tropical estuary: case study in Benoa Bay, Bali, Indonesia. *Mar. Pollut. Bull.* 163:111979. doi: 10.1016/j.marpolbul.2021.111979

Tang, G., Liu, M., Zhou, Q., He, H., Chen, K., Zhang, H., et al. (2018). Microplastics and polycyclic aromatic hydrocarbons (PAHs) in Xiamen coastal areas: implications for anthropogenic impacts. *Sci. Total Environ.* 634, 811–820.

The People's Government of Guangxi (2012). *Marine Function Zoning of Gunagxi (2011–2020)*.

Vaughan, R., Turner, S. D., and Rose, N. L. (2017). Microplastics in the sediments of a UK urban lake. *Environ. Pollut.* 229, 10–18. doi: 10.1016/j.envpol.2017.05.057

Waller, C. L., Griffiths, H. J., Waluda, C. M., Thorpe, S. E., Loaiza, I., Moreno, B., et al. (2017). Microplastics in the Antarctic marine system: an emerging area of research. *Sci. Total Environ.* 598, 220–227. doi: 10.1016/j.scitotenv.2017.03.283

Wang, M. (2018). Research on prediction of GDP per capita in China based on semi-parametric time series model. *Mark. Res.* 476, 23–25.

Wang, T., Hu, M., Song, L., Yu, J., Liu, R., Wang, S., et al. (2020). Coastal zone use influences the spatial distribution of microplastics in Hangzhou Bay, China. *Environ. Pollut.* 266:115137.

Wang, T., Zou, X., Li, B., Yao, Y., Li, J., Hui, H., et al. (2018). Microplastics in a wind farm area: a case study at the Rudong Offshore Wind Farm, Yellow Sea, China. *Mar. Pollut. Bull.* 128, 466–474. doi: 10.1016/j.marpolbul.2018.01.050

Wu, F., Wang, Y., Leung, S., Huang, W., and Cao, L. (2020). Accumulation of microplastics in typical commercial aquatic species: a case study at a productive aquaculture site in China. *Sci. Total Environ.* 708:135432. doi: 10.1016/j.scitotenv.2019.135432

Wu, N., Zhang, Y., Zhang, X., Zhao, Z., He, J., Li, W., et al. (2019). Occurrence and distribution of microplastics in the surface water and sediment of two typical estuaries in Bohai Bay, China. *Environ. Sci.: Process. Impacts* 21, 1143–1152. doi: 10.1039/C9EM00148D

Wu, Q., Liu, S., Chen, P., Liu, M., and Cai, M. (2021). Microplastics in seawater and two sides of the Taiwan Strait: reflection of the social-economic development. *Mar. Pollut. Bull.* 269:112588. doi: 10.1016/j.marpolbul.2021.112588

Xu, L., Cao, L., Huang, W., Liu, J., and Dou, S. (2021). Assessment of plastic pollution in the Bohai Sea: abundance, distribution, morphological characteristics and chemical components. *Environ. Pollut.* 278:116874. doi: 10.1016/j.envpol.2021.116874

Xu, Y., Chan, F., He, J., Johnson, M., and Zhu, Y. (2020). A critical review of microplastic pollution in urban freshwater environments and legislative progress in China: recommendations and insights. *Crit. Rev. Environ. Sci. Tech.* 6, 1–44. doi: 10.1080/10643389.2020.1801308

Xue, B., Zhang, L., Li, R., Wang, Y., and Wang, S. (2020). Underestimated microplastic pollution derived from fishery activities and "hidden" in deep sediment. *Environ. Sci. Tech.* 54, 2210–2217. doi: 10.1021/acs.est.9b04850

Yonkos, L. T., Friedel, E. A., Perez-Reyes, A. C., Ghosal, S., and Arthur, C. D. (2014). Microplastics in four estuarine rivers in the Chesapeake Bay, USA. *Environ. Sci. Technol.* 48, 14195–14202. doi: 10.1021/es5036317

Zhang, C., Zhou, H., Cui, Y., Wang, C., Li, Y., and Zhang, D. (2019). Microplastics in offshore sediment in the yellow sea and East China Sea, China. *Environ. Pollut.* 244, 827–833. doi: 10.1016/j.envpol.2018.10.102

Zhang, L., Liu, J., Xie, Y., Zhong, S., and Zhong, Q. (2020). Distribution of microplastics in surface water and sediments of Qin river in Beibu Gulf, China. *Sci. Total Environ.* 708:135176. doi: 10.1016/j.scitotenv.2019.135176

Zhang, W., Zhang, S., Wang, J., Wang, Y., Mu, J., Wang, P., et al. (2017). Microplastic pollution in the surface waters of the Bohai Sea, China. *Environ. Pollut.* 231, 541–548.

Zhao, J., Ran, W., Teng, J., Liu, Y., Liu, H., Yin, X., et al. (2018). Microplastic pollution in sediments from the Bohai Sea and the Yellow Sea, China. *Sci. Total Environ.* 640, 637–645. doi: 10.1016/j.scitotenv.2018.05.346

Zhao, S., Zhu, L., and Li, D. (2015). Microplastic in three urban estuaries, China. *Environ. Pollut.* 206, 597–604. doi: 10.1016/j.envpol.2015.08.027

Zheng, Y., Li, J., Cao, W., Liu, X., Jiang, F., Ding, J., et al. (2019). Distribution characteristics of microplastics in the seawater and sediment: a case study in Jiaozhou Bay, China. *Sci. Total Environ.* 674, 27–35. doi: 10.1016/j.scitotenv.2019.04.008

Zhou, Q., Tu, C., Yang, J., Fu, C., Li, Y., and Waniek, J. J. (2021). Trapping of microplastics in halocline and turbidity layers of the semi-enclosed Baltic Sea. *Front. Mar. Sci.* 8:761566.

Zhu, J., Zhang, Q., Huang, Y., Jiang, Y., and Lan, W. (2021). Long-term trends of microplastics in seawater and farmed oysters in the Maowei Sea, China. *Environ. Pollut.* 273:116450. doi: 10.1016/j.envpol.2021.116450

Zhu, J., Zhang, Q., Li, Y., Tan, S., Kang, Z., Yu, X., et al. (2019). Microplastic pollution in the Maowei Sea, a typical mariculture bay of China. *Sci. Total Environ.* 658, 62–68. doi: 10.1016/j.scitotenv.2018.12.192

Zhu, L., Bai, H. Y., Chen, B. J., Sun, X. M., Qu, K. M., and Xia, B. (2018). Microplastic pollution in North Yellow Sea, China: observations on occurrence, distribution and identification. *Sci. Total Environ.* 636, 20–29. doi: 10.1016/j.scitotenv.2018.04.182

Conflict of Interest: XW is employed by Central Cycle Ecological Technology Co., Ltd.

The remaining authors declare that the research was conducted in the absence of any commercial or financial relationships that could be construed as a potential conflict of interest.

Publisher's Note: All claims expressed in this article are solely those of the authors and do not necessarily represent those of their affiliated organizations, or those of the publisher, the editors and the reviewers. Any product that may be evaluated in this article, or claim that may be made by its manufacturer, is not guaranteed or endorsed by the publisher.

frontiers in Marine Science

ORIGINAL RESEARCH
published: 11 February 2022
doi: 10.3389/fmars.2022.830318

Spatial Distribution and Composition of Surface Microplastics in the Southwestern South China Sea

Jun Yu[1,2,3], Danling Tang[2,1,3], Sufen Wang[1,2]*, Lei He[4,5] and Kalani Randima Lakshani Pathira Arachchilage[1,2,3]*

[1] State Key Laboratory of Tropical Oceanography, Guangdong Key Laboratory of Ocean Remote Sensing, South China Sea Institute of Oceanology, Chinese Academy of Sciences, Guangzhou, China, [2] Southern Marine Science and Engineering Guangdong Laboratory (Guangzhou), Guangzhou, China, [3] University of Chinese Academy of Sciences, Beijing, China, [4] School of Marine Science, Sun Yat-sen University, Guangzhou, China, [5] Guangdong Provincial Key Laboratory of Marine Resources and Coastal Engineering, Guangzhou, China

Plastic pollution is one of the growing environmental problems in the world currently. The situation of microplastics (MPs) in the South China Sea (SCS) is not yet fully understood. This study investigated the spatial distribution, morphological characterization, and chemical composition of MPs in surface seawater in the southwestern SCS, based on cruise data in 2018. Our analysis shows that the average abundance of surface MPs in seawater was 0.072 ± 0.053 particles/m^3 and 88.4% of MPs were <2 mm. 97.3% of MPs were fibers and fragments. Polyethylene terephthalate (PET), polyvinyl chloride (PVC), and cellophane were predominant polymer components of surface MPs. Higher MPs abundance (0.083 ± 0.063 particles/m^3) and bigger MPs sizes were found at surface water in Nansha Islands than in Xisha Islands (0.032 ± 0.01 particles/m^3). In addition, more polymer types of MPs were found in Nansha Islands, while more MPs films were found in Xisha Islands. PET and cellophane dominated in Nansha Islands, while PVC dominated in Xisha Islands with no cellophane detected. The surface MPs were low in abundance and diverse in polymers in the southwestern SCS with apparent differences between islands and between onshore and offshore, owing to plastics wastes from vessel traffics and some inhabited islands.

Keywords: microplastics, spatial distribution, morphological characterization, chemical composition, the South China Sea

OPEN ACCESS

Edited by:
Xiaoshan Zhu,
Tsinghua University, China

Reviewed by:
Qipei Li,
Hainan University, China
Muhammad Reza Cordova,
Indonesian Institute of Sciences, Indonesia

***Correspondence:**
Danling Tang
lingzistdl@126.com
Sufen Wang
sufenwang1976@126.com

Specialty section:
This article was submitted to Marine Pollution, a section of the journal Frontiers in Marine Science

Received: *07 December 2021*
Accepted: *06 January 2022*
Published: *11 February 2022*

Citation:
Yu J, Tang D, Wang S, He L and Pathira Arachchilage KRL (2022) Spatial Distribution and Composition of Surface Microplastics in the Southwestern South China Sea. Front. Mar. Sci. 9:830318. doi: 10.3389/fmars.2022.830318

INTRODUCTION

Increasing quantities of waste debris originated from marine-based sources and land-based sources due to human activities have been gathered in the worldwide marine environment. Nearly 60–80% of marine debris is plastics (UNEP, 2005; GESAMP, 2010). Due to the difficulty of degrading, the oceans finally become one of the main sinks of waste plastics debris. Increasing input of waste plastics into the oceans has posed serious threats to the marine environment (Thompson et al., 2004; Li, 2019).

Microplastics (MPs) are defined as small plastics with particle sizes < 5 mm (Thompson et al., 2004; GESAMP, 2015). This debris is regarded as a threat to marine biota (Desforges et al., 2014). It has been reported that MPs present in all the types of aquatic environments around

the world (Cózar et al., 2014; Eriksen et al., 2014) such as terrestrial aquatic ecosystem (Lin et al., 2018), beaches and coastal areas (Cheung et al., 2016; Huang et al., 2021), offshore waters (Lusher et al., 2015; Reisser et al., 2015; Waller et al., 2017), sediments (Thompson et al., 2004; Qiu et al., 2015), marginal seas (Cai et al., 2018), and islands (Ding et al., 2019; Huang et al., 2019; Wang et al., 2019b). Coastal cities, ports, shipping, poorly regulated coastal landfills, and dumping sites are all the important sources of MPs worldwide (Jambeck et al., 2015; Hughes et al., 2017). Marine MPs can originate from marine-based sources or land-based sources. However, land-based sources are the primary sources of MPs (marine-based sources including fishing, aquaculture, and shipping so on; land-based sources including wastewater effluent, run-off, and rivers) (Andrady, 2011). Furthermore, MPs can easily be ingested and threatened the health of living things and the sustainable development of marine ecosystems (Vandermeersch et al., 2015; Sun et al., 2017). Being ingested, MPs can transfer toxic chemicals into organisms as a carrier, such as invertebrates, fish, birds, and mammals, which could cause adverse physical or chemical threats to the health of organisms (Teuten et al., 2007; Cole et al., 2011; Wright et al., 2013; Desforges et al., 2014; McCormick et al., 2014). Although more and more studies have been focused on the source, transport, and fate of MPs in the marine environment, the total status and mechanism are still unclear (Harris et al., 2021; Li et al., 2022).

The South China Sea (SCS) is the biggest semi-enclosed marginal seas in the west Pacific with seasonal monsoon climate. Being surrounded by several developing countries with large populations, intensive industrial, agricultural, and shipping activities have resulted in considerable anthropogenic pressure to the SCS. Most of Xisha Islands and Nansha Islands, which lie in the western and southern parts of the SCS, respectively, are original coral reefs and atolls. Due to the considerable distance from mainland China, the status of MPs pollution in Xisha Islands and Nansha Islands is still unclear (Huang et al., 2020; Tan et al., 2020). Therefore, microscopic observations and spectrum identification of MPs sampled from a cruise in the southwestern SCS were used to detect the abundance and diversity of MPs in these remote reefs and atolls and finally compare the differences of MPs pollution between Xisha Islands and Nansha Islands. The aims of this study were: (1) to examine and compare the abundances and distributions of MPs in surface water around Xisha Islands and Nansha Islands, southwestern of the SCS and (2) to discuss the potential sources of MPs in the uninhabited islands.

MATERIALS AND METHODS

Fields and Sampling

The major sampling sites were around Nansha Islands and another three sampling sites were around Zhongsha Island and Xisha Islands. Among the sites in Nansha Islands, three sampling sites were around Yongshu Islands and the rest were around southern reefs (**Figure 1**). Twenty two surface water samples were collected using a neuston trawl with a mesh size of 167 μm and an opening diameter of 60 cm from these remote reefs and atolls between March and April 2018. The meteorological conditions were stable in the SCS during this premonsoon period (Wang et al., 2009). Details of all the sampling sites are provided in **Supplementary Table 1**.

Extraction and Identification of Microplastics

In the laboratory, all the field samples were processed by filtration, elimination of organic matters, and refiltration (Su et al., 2016). Finally, the filter was placed into a clean petri dish and covered with aluminum foils for further observation (Lin et al., 2018). Careful visual sorting of residues is necessary to separate the plastic debris from other materials such as organic debris and other items (Hidalgo-Ruz et al., 2012). All the collected and processed filters were observed and identified carefully under a stereo light microscope (OLYMPUS SZX10, Tokyo, Japan) (Shaw and Day, 1994; Moore et al., 2002; Doyle et al., 2011). MPs images were taken with a digital camera (OLYMPUS DP80, Tokyo, Japan). The dominant color at surface of each MPs was recorded and their sizes were measured by the Image J software (1.46r, National Institutes of Health, Bethesda, Maryland, United States) (Lin et al., 2018; Tan et al., 2020). According to the external morphologies of MPs, shapes of MPs were categorized into fiber, fragment, and film. The abundance of MPs in this study was defined as the number of particles per cubic meter in surface water (particles/m^3).

Every suspected MP was transferred by tweezers to the objective table and detected the composition by attenuated total reflection Fourier transformed infrared reflection (ATR-μ-FTIR, Spotlight 200i, PerkinElmer, Waltham, MA, United States). Each particle was scanned at least three times in the IR spectrum ranging from 750 to 4,000 cm^{-1} to obtain better spectra. The acquired spectra were compared with the standard FTIR spectrum databases using PerkinElmer Spectrum software (Waltham, Massachusetts, United States). The MPs composition was confirmed and recorded when spectral similarity was >80%.

Quality Assurance and Quality Control

According to the floatation of MPs, extensive precaution was carried out along the field sampling and sample analysis in the laboratory to restrict background pollution. The filter and trawl were rinsed with clean seawater (filtered with a 2-μm membrane filter, GF/F, Whatman) before and after each use on board. All the containers and experimental tools were rinsed three times with Milli-Q water. All the openings of the analysis devices were covered with aluminum foil to avoid cross-pollution from the air and other materials. Before use, the liquid used in the experiment was filtered through glass fiber filter (0.2 μm, GF/F, Whatman). After detecting every specimen using ATR-μ-FTIR, the objective surface was thoroughly cleaned with filtered anhydrous ethanol to avoid cross-contamination (Ding et al., 2019). A total of two blank laboratory procedures were setup, one for the laboratory filtration process (blank 1) and one for the microscopy process (blank 2). The blanks were treated with 250 ml Milli-Q water as the field samples. No MPs were found in blank 1 and only

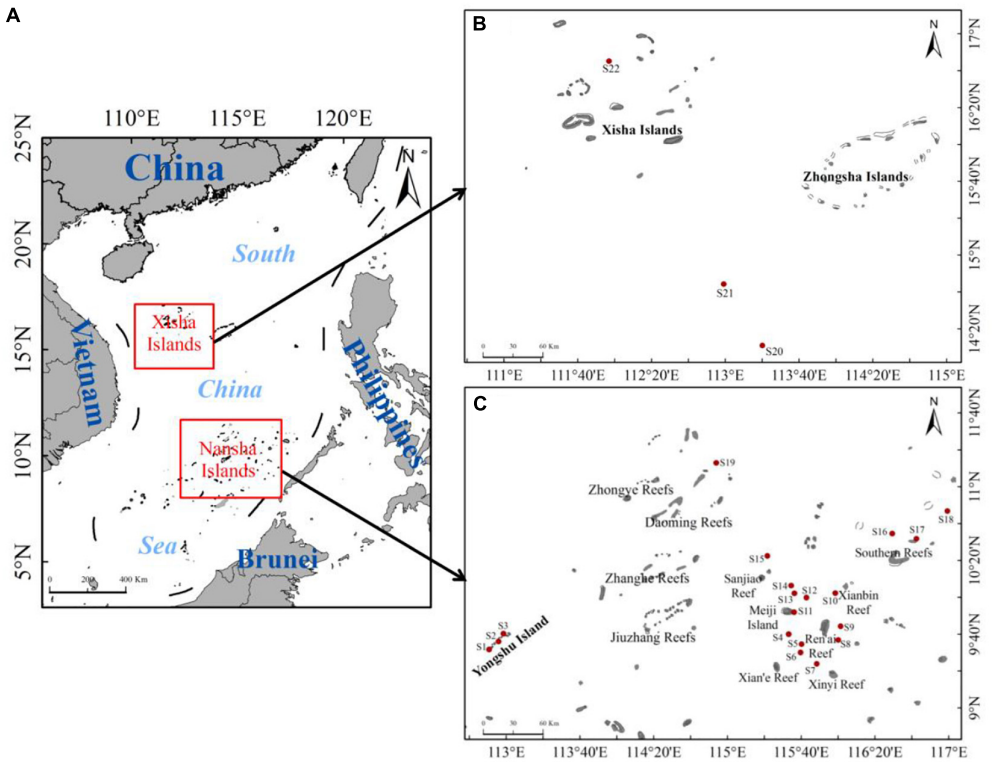

FIGURE 1 | (A) Location of sampling sites in the South China Sea (SCS). **(B)** Three sampling sites near Xisha Islands. **(C)** Sampling sites around Nansha Islands in detail.

one microfiber was found in blank 2, which were subsequently identified as cotton fibers from cotton laboratory coats by μ-FTIR (Cai et al., 2018; Lin et al., 2018). In this case, our environment in the laboratory was considered clean and appropriate to carry out MPs experiments.

Statistical Analysis

All the sites plots were drawn by ArcGIS 10 software. Data analyses were performed by SPSS software version 20.0 (SPSS Incorporation, Armonk, New York, United States) and Microsoft Excel 2013. Numerical data are all presented as the mean ± SD. The differences between the abundances of MPs were performed as the one-way ANOVA (Webb et al., 2012). In all the cases, $p < 0.05$ was set as statistically significant.

RESULTS

Abundance and Distribution of Microplastics

Microplastics were detected at all the sampling sites. Abundance of MPs varied widely and ranged from 0.015 to 0.239 particles/m^3, with an average of 0.072 ± 0.053 particles/m^3 (**Figure 2A**). The highest MPs abundance occurred in site S1 (0.239 particles/m^3), located on the southern fringe of Yongshu Island (**Figure 2C**). The MPs abundances at all the three sites around Yongshu Island were much higher than the average level of all the sample sites. The MPs abundance at sampling sites S4 and S6 exceeded 0.1 particles/m^3, surrounded by Ren'ai Reef, Meiji Island, and Xian'e Reef. Besides, the lowest MPs abundances were detected at S17 and S22, with 0.015 and 0.019 particles/m^3, respectively. S17 is located in Southern Reefs and S22 is located in the north-central part of Xisha Islands (**Figures 1A**, **2B**). The abundance at site S1 was almost 16 times greater than sites S17 and S22.

There were nine sites with higher MPs abundances than the average level (S1, S2, S3, S4, S5, S6, S8, S14, and S15). All these sites are located at the east of nearest islands/reefs and all these nine sites are around Nansha Islands (**Figure 2C**). The MPs abundances in sites S1, S4, and S6 were 2–3 times higher than the average MPs abundances. Among these nine sites, S1, S2, and S3 are closest to Yongshu Island, where site S1 is in the south, S2 is in the east, and S3 is in the west of Yongshu Island (**Figures 1C**, **2C**). MPs abundances of these three sites showed a decreasing trend from south to north. Sites S8 were located on the eastern waters of Meiji Island (**Figure 2C**). Both the Yongshu Island and Meiji Island are inhabited islands, which may account for the high MPs in these sites (Ministry of Civil Affairs of the People's Republic of China, 2020).[1]

[1]http://www.mca.gov.cn/article/xw/tzgg/202004/20200400026955.shtml

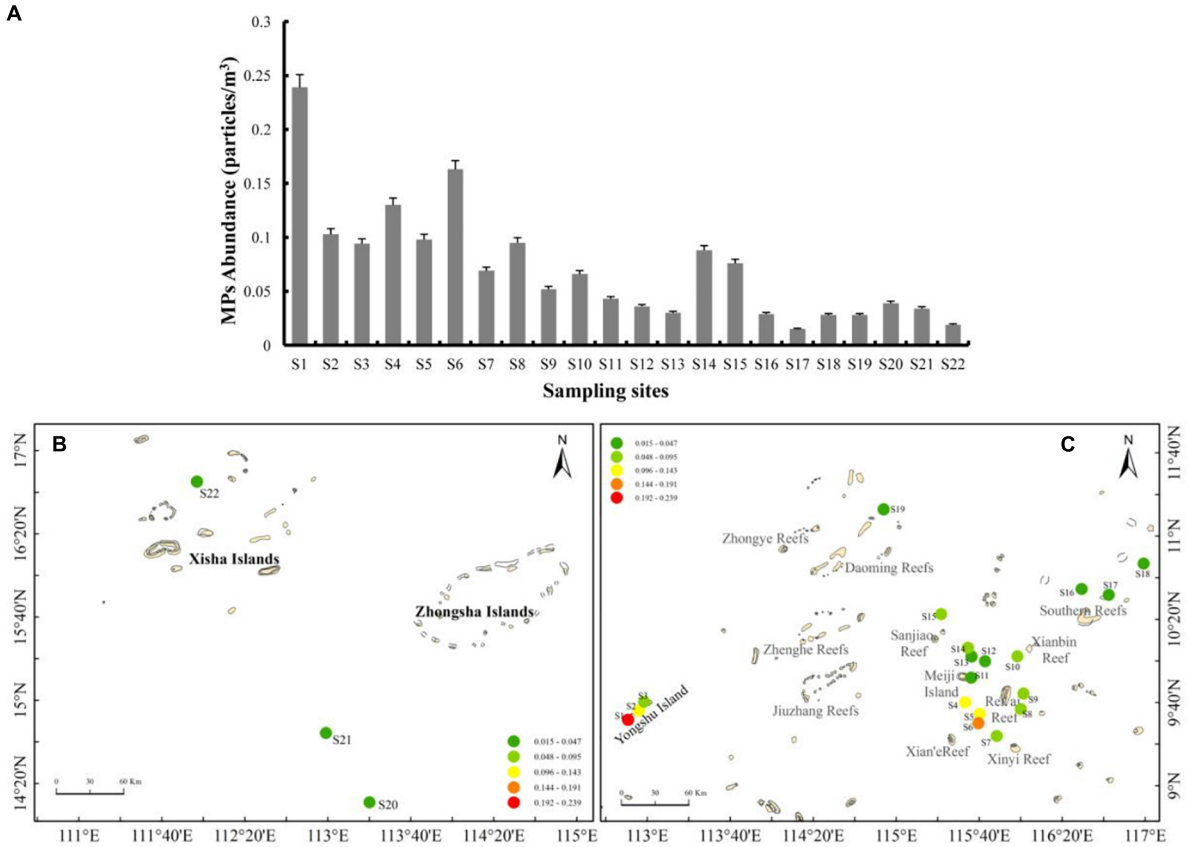

FIGURE 2 | (A) Abundance of surface microplastics (MPs) in the sampling sites around the southwestern SCS. **(B,C)** Spatial distribution of MPs abundances in the surface water surrounding southwestern SCS.

Sites S4–S15 are located around the scattered reefs in Nansha Islands such as Meiji Island and Xian'e Reef; sites S16–S18 are located in the Southern Reefs and S19 are located in the north of Daoming Reefs. The MPs abundances near these scattered reefs were higher than those near the Southern Reefs. Higher MPs abundances were mainly located in the south of reefs around Meiji Island or Ren'ai Reefs, with values larger than the average level (**Figures 1C**, **2C**). The rest three sites, S20, S21, and S22, were all in low MPs abundances, located away from Nansha Islands and near Zhongsha Island or Xisha Islands (**Figure 2B**).

Surface Morphology of Microplastics: Shape, Size, and Color

In this study, three irregular shapes of MPs were observed (**Figure 3**), which accounted for 67.1% (fibers), 30.2% (fragments), and 2.7% (films) for all the collected MPs. The MPs fibers accounted for a much higher proportion than fragments (ANOVA, $F = 8.594$, $p = 0.005$) and films (ANOVA, $F = 26.124$, $p < 0.001$).

More than 80% of MPs are fibers at several sampling sites in terms of number (92% at site S2, 82.4% at site S11, 82.6% at site S13, 87.3% at site S14, 89.5% at site S19, and 86.7% at site S22) indicating that MPs fibers dominated at these sites. It should be noted that the average MPs abundances of these sites were relatively low with values < 0.1 particles/m^3, except S2 and S14. MPs fragments were distributed in all the sites with percentages ranging from 6 to 50%, the highest proportion (50.2% at site S1) and the lowest proportion (6.6% at site S2) were near Yongshu Island. There were seven sites with more than 30% of MPs fragments, which were located near Yongshu Island (site S1), Ren'ai Reef and Xianbin Reef (sites S4, S6, S8, and S10), and Southern Reef (site S16 and S18). Although the fraction of films in all the three MPs shapes was only 2.7%, it distributed in ∼60% of the sampling sites. There were a few fragmentary distributions at sites S1–S9 near Yongshu Island, Meiji Island, and Ren'ai Reef, with the highest percentage at site S21 (28.6%), near Xisha Islands (**Supplementary Figure 1**).

The mean size of MPs particles was 991.46 ± 879.68 μm. The smallest particle size of all the MPs samples was 53.26 μm and the largest particle size of all the MPs samples was 4867.87 μm. Large plastic debris (>5 mm) was also found at more than half of the sampling sites. Their sizes ranged from 5.01 to 35.94 mm and accounted for 2.31% in the quantity of all the detected plastic debris. The MPs were categorized into six size classes based on their diameter (< 0.167, 0.167–1, 1–2, 2–3, 3–4, and 4–5 mm) (**Figure 3A**).

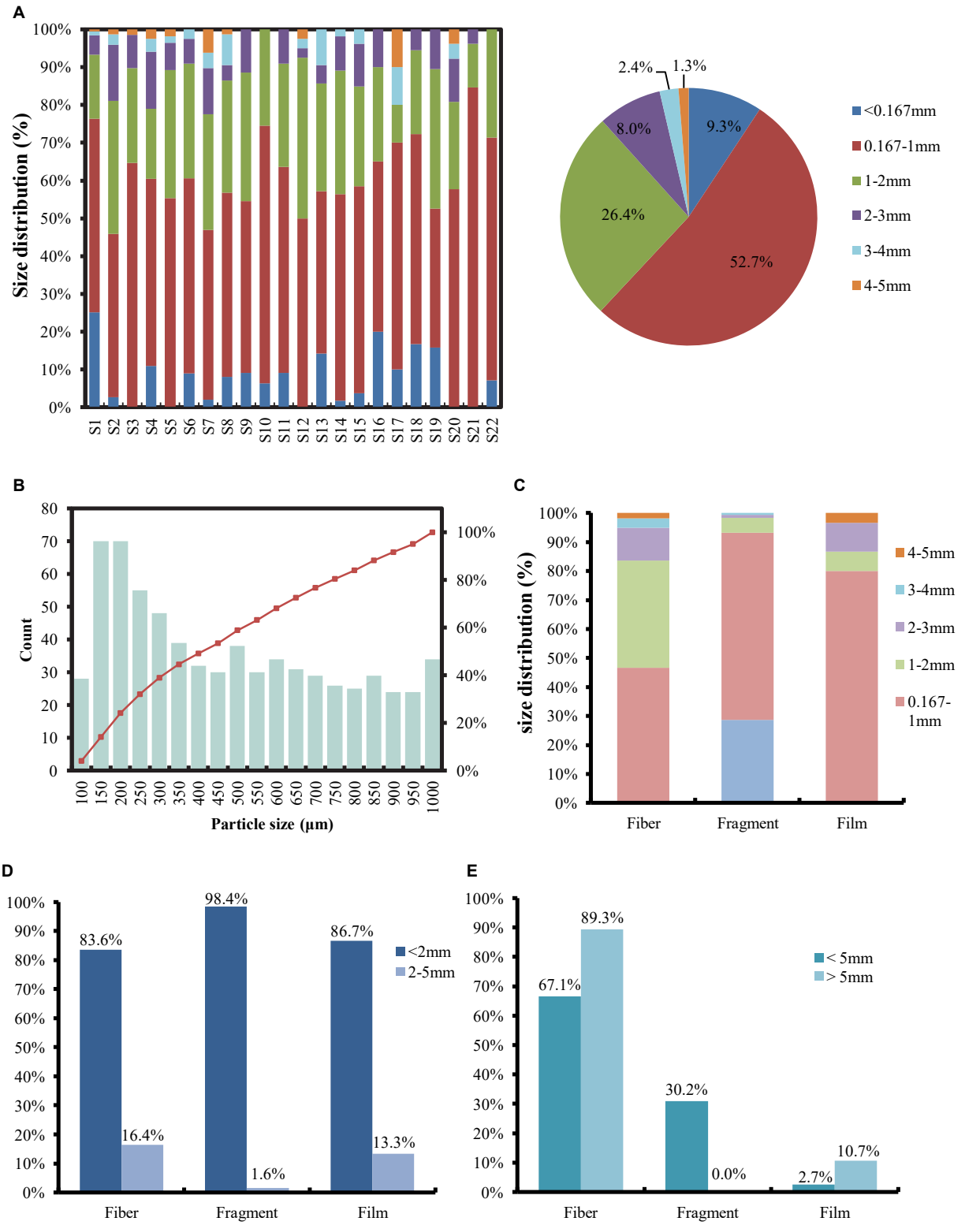

FIGURE 3 | (A) The size distribution of surface MPs around the southwestern SCS. S20, S21, and S22 were located around Zhongsha Island and Xisha Islands. **(B)** Frequency distribution and cumulative curve of MPs particles <1 mm (n = 696). **(C)** The size distribution of different MPs shapes: fibers, fragments, and films. **(D)** The percentages of different shapes between MPs <2 mm and 2–5 mm. **(E)** The percentages of different shapes between MPs (<5 mm) and plastic debris >5 mm.

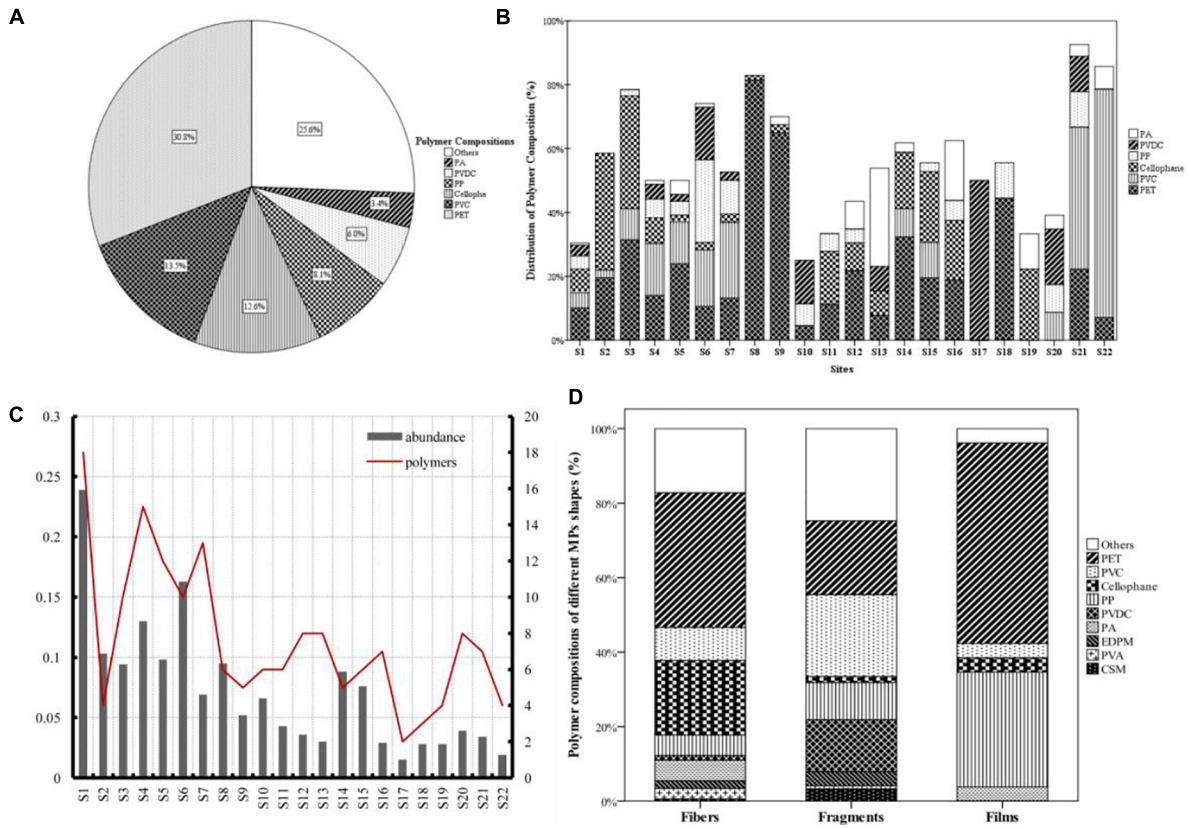

FIGURE 4 | (A,B) The proportions of six major polymer of surface MPs around the southwestern SCS. S20, S21, and S22 were located around Zhongsha Island and Xisha Islands. **(C)** MPs abundances and total polymer types at all the sampling sites. **(D)** The proportions of different shapes of MPs polymers: fibers, fragments, and films.

Microplastics with 0.167–1 mm accounted for the highest proportion in all the six classes (52.7%). 88.4% of the MPs were smaller than 2 mm, of which 26.4% of MPs were between 1 and 2 mm and 9.3% of MPs were < 0.167 mm (**Figure 3A**). The variations of MPs abundance with size < 1 mm from S1 to S22 presented a similar trend as that of total MPs abundances, with a significant positive correlation ($r = 0.97$, $p < 0.001$). Except for sites S2 and S7 with 45% of MPs < 1 mm, all the remaining sites contained 50% MPs with sizes < 1 mm. 44.5% of MPs particles with size of 0.167–1 mm were <350 μm and mainly concentrated in the range of 150–250 μm (**Figure 3B**). Thus, smaller-sized MPs (< 2 mm) dominated the MPs in our study area.

The population of MPs fibers with a size of 0.167–1 mm was the largest among all the MPs fibers followed by MPs fibers with the size of 1–2 mm and MPs fibers with size < 0.167 mm were low. The population of MPs fibers with size < 2 mm accounted for 83.6% of the total number of MP fibers (**Figures 3C,D**). ∼95% of MPs with size < 0.167 mm were MPs fragments and the diameter of MPs fragments was all < 3 mm. MPs fragments < 2 mm accounted for 98% of the total population of MPs fragments (**Figure 3D**). No MPs film with size < 0.167 mm was detected and 73% of MPs films were of size between 0.167 and 1 mm. Although fraction of MPs fibers in size of 4–5 mm was the lowest in the population of MPs fibers, the population of MPs fibers in size of 4–5 mm was larger than that of MPs fragments and films. In 4–5 mm, the proportion of MPs films was the highest (**Figure 3C**). The highest proportion of MPs particles < 2 mm was MPs fragments, followed by fibers and films (**Figure 3D**). Thus, size distribution of MPs fibers was the broadest and continuous, while MPs fragments and films were mainly concentrated in the size of < 2 mm. The MPs fragments were all < 5 mm compared to the other two shapes of MPs. Nearly 90% of the MPs particles > 5 mm were MPs fibers and the remaining small portion was MPs films (**Figure 3E**).

Several colors were observed from the surface of all the MPs samples. The dominant color of MPs is blue (45.6%), followed by black (24.2%), transparent (12.3%), red (10.1%), yellow (4.7%), green (2.9%), and white (0.2%) (**Supplementary Figure 2**). The blue and black MPs account for almost 70% of the observed MPs particles and the transparent and red MPs account for ∼22.4%. Transparent and yellow MPs accounted for a larger proportion of MPs > 3 mm and most of the plastic debris > 5 mm was transparent. The color distribution and proportion of MPs varied at each sampling site. Blue, black, and transparent MPs particles appeared at all the sampling sites. The proportion of white MPs particles in this study was only 0.2%, found at site S20 near Zhongsha Island and site S22 near Xisha

Islands. No white MPs particle was found at all the Nansha Islands sampling sites.

The proportions of the colors in the three different shapes of MPs particles were also diverse. All the seven colors were found in MPs fibers and fragments, but black, red, and white MPs films were not detected. The prominent colors of MPs fibers were black (35%), blue (30%), and red and transparent (13%, respectively). 84.4% of MPs fragments were blue and the rest ∼15% of MPs fragments were in the other five colors. 79% of the MPs films were transparent, while green, blue, and yellow accounted for the remaining 21% (**Supplementary Figure 2**).

Microplastics Composition and Diversity

According to μ-FTIR results of chemical characterization identification of MPs, 26.3% of the total suspected particles were removed because the matching spectral characteristics were <80% of standard polymers. There are 27 plastic polymers detected in the rest of the samples. The components of the six conventional plastic polymers accounted for ∼75% of all the MPs pieces including polyethylene terephthalate (PET) (30.8%), polyvinyl chloride (PVC) (13.5%), cellophane (12.6%), polypropylene (PP) (8.1%), vinylidene chloride/vinyl chloride copolymer (PVDC) (Saran, 6%), and polyamide 6 (PA6) (Nylon 6, 3.4%). The other 21 polymers accounted for 25.6% of the total MPs (**Figure 4A**). Combining the distribution of various polymers at all the sampling sites, ∼30% of the entire PET composition were detected at site S8. In comparison, about 17% of PVC, 42% of PP, and 35% of PVDC were documented at site S6. These two sites are located near Ren'ai Reef. 22% of cellophanes were gathered at site S3 near northern Yongshu Island (**Figure 4B**). There is a positive correlation between MPs abundances and the diversity of polymers types ($r = 0.730$, $p < 0.01$). For example, sites with much higher MPs abundance than averaged level also contained more MPs polymer types such as S1 (0.239 particles/m^3), S4 (0.13 particles/m^3), and S6 (0.163 particles/m^3) (**Figures 4B,C**). However, the MPs polymers did not present a significant spatial distribution, despite the correlation between MPs abundances and polymers types.

Five main polymer components of the MPs fibers were PET (36.2%), cellophane (20.1%), PVC (8.9%), PP, and PA (5.5%, respectively) (**Figure 4D**), which are all the common plastics used in clothing fabrics, industrial fabrics, engineering, and construction. The average diameter and median diameter of MPs fibers were 1.29 and 1.065 mm, respectively, which were much bigger than that of MP fibers (<0.5 mm) discharged from wastewater treatment systems. Only 13.4% of the MPs fibers in this study were < 0.5 mm, which indicated that clothing fiber shedding was not the primary source of fibers, but fishing activities and industrial fabrics on ships along their paths were the primary sources of MPs fibers in this region.

The average diameter of MPs fragments in this study was 0.37 mm, much smaller than those of MPs fibers and films. The MPs fragments were irregular in shape and hard in texture. PVC (21.9%), PET (19.8%), PVDC (14%), and PP (9.9%) accounted for 65.6% of total MPs fragments (**Figure 4D**). PVC is divided into two types, rigid PVC and soft PVC. Rigid PVC is commonly used for plastic profiles, pipes, and packaging materials, while soft PVC is used for hoses, cables wires, and various molds. PET and PVDC are mostly used for disposable packaging such as beverage bottles and food packaging. The average diameter of MPs films was 1.15 mm and 74.5% of MPs films were transparent. Nearly 85% of MPs films were composed of PET (53.8%) and PP (30.8%) (**Figure 4D**), both of which were mainly used for electrical insulation materials and packaging. MPs fibers and fragments had a wide variety of polymer compositions. They were mostly colored, while MPs films were relatively concentrated in a smaller number of polymers and were mostly transparent.

Microplastics Pollution in Nansha Islands and Xisha Islands

The abundance of floating MPs on the sea surface of Nansha Islands (0.083 ± 0.063 particles/m^3) was 2.5 times higher than that in Xisha Islands (0.032 ± 0.01 particles/m^3). It was also slightly higher than the average abundance of MPs in the southwestern SCS (0.072 ± 0.053 particles/m^3) in this study. MPs fibers and fragments dominated both the Xisha Islands and Nansha Islands, but percentage of MPs films in Xisha Islands (12.1%) was nearly six times higher than that in Nansha Islands (2%) ($F = 46.885$, $p = 0.005$).

A total of 88.1% of MPs were with size < 2 mm in Nansha Islands, of which 55.4% were MPs fibers, 31.1% were MPs fragments, and 1.6% were MPs films. Abundances of MPs with 2–5 mm accounted for 11.9% of total MPs, of which 11.1% were long MPs fibers. In contrast, 90.9% of MPs particles in Xisha Islands were < 2 mm with a vast majority of fibers (60.6%), while MPs fragments and MPs films together only accounted for the remaining 30.3%. MPs fibers, fragments, and films with 2–5 mm were all found in Nansha Islands, while no films larger than 2 mm were found in Xisha Islands (**Table 1**). In general, the diameters of MPs particles in Xisha Islands were relatively smaller, especially the MPs films which all the sizes were < 2 mm. MPs in Nansha Islands and Xisha Islands were mainly in blue, black, and transparent and the proportions of MPs in these three colors were slightly different. The blue MPs (42.7%) proportion was three times higher than that of transparent MPs (12.8%) in Nansha Islands. The ratio of MPs in these three main colors in Xisha Islands was relatively consistent and the ratio of transparent MPs in Xisha Islands (25.6%) was twice as high as that in Nansha Islands (12.8%).

The average abundances of the floating MPs of Xisha Islands and Nansha Islands were different. In addition, the MPs fibers was the dominant shape of MPs in Xisha Islands and Nansha Islands, while the proportion of MPs films was higher in Xisha Islands than that in Nansha Islands and the proportion of MPs fragments was higher in Nansha Islands than that in Xisha Islands. The MPs particles with size < 2 mm differed between Xisha Islands and Nansha Islands. There are more MPs films < 2 mm in Xisha Islands than Nansha Islands. The main components of MPs at Nansha Islands were PET (22.6%) and Cellophane

TABLE 1 | Comparison of the abundance and external morphological characteristics of microplastics (MPs) in Xisha Islands and Nansha Islands.

Abundance		Xisha		Nansha	
		0.032 particles/m^3		0.083 particles/m^3	
	Size	< 2 mm	2–5 mm	< 2 mm	2–5 mm
Shape	Fibers	60.60%	7.60%	55.40%	11.10%
	Fragments	18.20%	1.50%	31.10%	0.40%
	Films	12.10%	/	1.60%	0.40%
	Total	90.90%	9.10%	88.10%	11.90%
Color	Blue	27.60%		42.70%	
	Black	29.30%		25.90%	
	Transparent	25.60%		12.80%	
	the others	17.50%		18.60%	

"%" indicates the percentage in quantity.

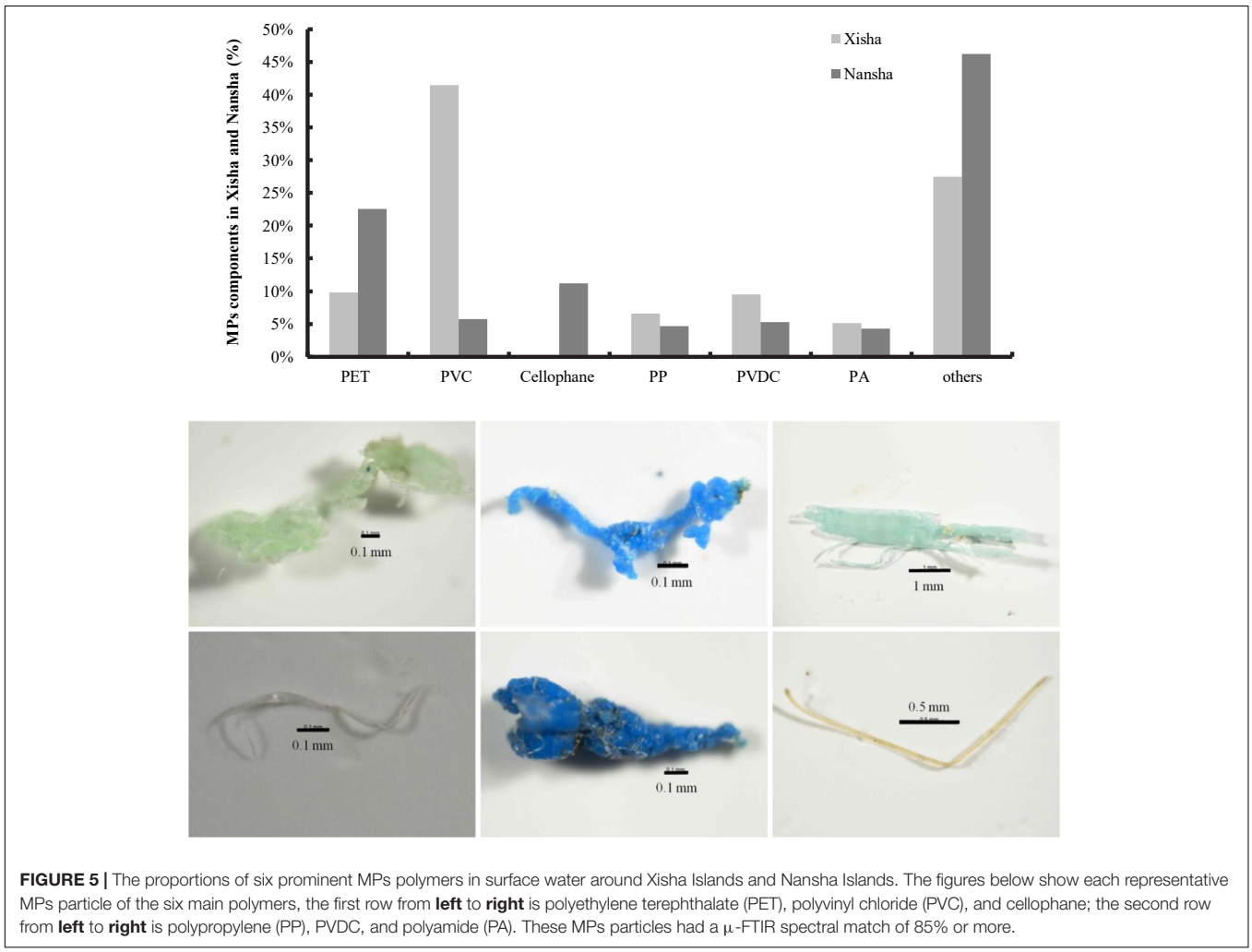

FIGURE 5 | The proportions of six prominent MPs polymers in surface water around Xisha Islands and Nansha Islands. The figures below show each representative MPs particle of the six main polymers, the first row from **left** to **right** is polyethylene terephthalate (PET), polyvinyl chloride (PVC), and cellophane; the second row from **left** to **right** is polypropylene (PP), PVDC, and polyamide (PA). These MPs particles had a μ-FTIR spectral match of 85% or more.

(11.2%), while PVC accounted for 41.5% at Xisha Islands and no cellophane was detected.

High proportion of suspected MPs particles in Xisha Islands (85.80%) were identified as polymers, while lower in Nansha Islands (60.6%). There was dominant polymer at Xisha Islands, with PVC accounting for > 40% of the six common polymers. No dominant polymer of MPs was observed at Nansha Islands, with the total percentages of six common polymers accounted for almost 50% of total MPs (**Figure 5**). However, the ANOVA results showed no statistically significant difference in the polymer

composition of MPs from Nansha Islands and Xisha Islands ($F = 2.135$, $p = 0.172$).

DISCUSSION

Microplastics Pollution Status in the Overall Southwestern South China Sea and Different Islands

Our results indicated varying degrees of MPs pollution in the southwestern SCS. The abundances of MPs collected by neuston trawl in this study were approximately similar to the plankton trawling sampling in previous studies (Cai et al., 2018; Wang et al., 2019b; Tan et al., 2020). The MPs abundance reported in this study was low in the global ocean (**Supplementary Table 2**). The MPs abundance in the southwestern SCS (0.072 ± 0.053 particles/m^3) was slightly higher than the overall MPs abundance in the SCS (0.045 ± 0.093 particles/m^3) (Cai et al., 2018). The average abundance of MPs in the SCS was one order of magnitude lower than that in the East China Sea and the Bohai Sea, while the East China Sea (0.167 ± 0.138 particles/m^3) was about 2.3 times higher and the Bohai Sea (0.33 ± 0.34 particles/m^3) was about 4.5 times higher than that in the southwestern SCS (Zhao et al., 2014; Zhang et al., 2017). Although there are lots of islands in the southwestern SCS, the input of MPs from land-based sources is limited due to sparse population, low human production, and livelihood activities (Browne et al., 2011; Cheung et al., 2016; Cai et al., 2018). Similarly, compared with the neighboring inshore waters in the western Pacific, the MPs abundance in the SCS is significantly lower than that of Korean (47 ± 192 pieces/m^3) (Song et al., 2014). The current reported MPs count in Japanese inshore waters was 1.72 pieces/m^3, which was calculated based on observed averaged concentration (3.7 pieces/m^3) (Isobe et al., 2015). The abundance of MPs in coastal waters in the northern SCS, such as Beibu Gulf (Zhu J. et al., 2019; Huang et al., 2021), Hainan Island (Qi et al., 2020), and the Pearl River Estuary (Fu et al., 2003; Zhou et al., 2011; Lin et al., 2018), is much higher than that in our study area. These observations indicated that MPs highly pollute the densely populated offshore areas with intensive human activities. The floating MPs in seawater also show an evident influence by land-based sources. In addition, the MPs abundance in the SCS was at a low level compared to the other oceans or seas in the world such as the Mediterranean Sea (Collignon et al., 2012), Atlantic Ocean (Lusher et al., 2014; Enders et al., 2015), northern Gulf of Mexico (Di Mauro et al., 2017), and Georgia Strait, Canada (Desforges et al., 2014; **Supplementary Table 2**).

The initial plastic forms can determine the MPs shapes, especially when the plastics enter the oceans as wastes or litter. Aging processes such as mechanical wear and tear, photo-oxidative aging, and biological contamination then change the shape of plastic debris. Although plastics degrade as soon as they come into contact with air, sunlight, and water, it takes time due to their resistance to degrade (Andrady, 2011). After entering the marine environment, seawater properties and movements such as waves and circulation can affect the weathering and fragmentation of plastics (Ter Halle et al., 2017). The comparative analysis of MPs showed that the external morphological characteristics of MPs were significantly different between Xisha Islands and Nansha Islands. Still, the abundances and polymer compositions of MPs were not quite different. The numbers of vessel activities in inhabited islands in Xisha Islans are much higher than that in Nansha Islands, which reveal that the current land-based emissions and sea-borne vessel activities are still the primary sources of plastic polymers entering the SCS. More data are needed to further elucidate the effects of the complex circulation and seawater movements on the degradation and aging of MPs in the SCS.

Due to the tremendous spatial heterogeneity of MPs in the ocean (Suaria et al., 2020; Zambrano et al., 2020), the different numbers and distributions of sampling sites in Xisha Islands and Nansha Islands may result in differences in area-averaged MPs abundance. The one-way ANOVA showed that the difference of the average MPs abundance between Xisha Islands and Nansha Islands was within the sampling error. Indeed, adding more sampling sites near Xisha Islands will help to improve the accuracy of this conclusion.

Effect of Different Sampling and Detection Methods on the Results

Different sampling methods can lead to variations in MPs abundances such as using different sampling devices with varying sizes of mesh, using different units to represent the abundances of MPs, and also different detection guidelines that can lead to variations in MPs compositions and MPs shapes.

At present, there are two methods for collecting MPs samples in sea surface water, namely, trawl sampling and pump water sampling. The results from these two methods are different from each other. Trawl sampling was used in this study and the various mesh sizes of the trawl nets may lead to several orders of magnitude differences in the measurement results. The main sampling sites in this study were near the islands and reefs of Nansha Islands and Xisha Islands. Compared with previous studies on MPs pollution near the islands and reefs in the SCS (**Supplementary Table 2**), the difference in MPs abundance between trawl sampling with a diameter of mesh ranged from 160 to 333 μm was within one order of magnitude (Wang et al., 2019b; Tan et al., 2020).

In contrast, the difference in MPs abundance between pumping and trawl sampling can be as high as 5–6 orders of magnitude because the range of membrane diameters used for pumped water sampling was generally less than 50 μm (Huang et al., 2019, 2020; Nie et al., 2019; Md Amin et al., 2020). These differences indicated that most sizes of the floating MPs are smaller than 160 μm or even 100 μm. Therefore, smaller pore sizes for pumping water sampling can provide a more comprehensive picture of the abundances and contamination of floating MPs at the sea surface. This study showed that the MPs abundance near Nansha Islands (0.083 ± 0.063 particles/m^3) was higher than that near Xisha Islands (0.032 ± 0.01 particles/m^3) through trawl sampling. However, only the MPs abundance data from pumping water sampling (filter membrane pore size 20–45 μm) in Xisha islands can be found in previous studies. Some previous studies found that MPs abundances were

higher in Nansha Islands than in Xisha Islands (Huang et al., 2019, 2020; Nie et al., 2019), but Ding et al. (2019) found that the MPs concentration in Xisha Islnads (6.3 particles/L) was higher than that in Terengganu Island (3.3 particles/L) in the southern SCS (Md Amin et al., 2020). Given high spatial and temporal heterogeneity of MPs in the environment, it requires various sample sizes and combined sampling methods to achieve statistically detectable changes in MPs abundances (Ryan et al., 2009).

In addition to the effect of different sampling methods, various detection methods will also affect MPs compositions and apparent features. For example, in some studies, the polymer identification was randomly selected from the microscopically examined suspected MPs particles (Cai et al., 2018; Lin et al., 2018; Wang et al., 2019b; Tan et al., 2020) instead of identifying all the suspected MPs, so the identification results may be biased and unable to fully reflect the real situation of the samples. In this study, all the suspected MPs were identified by μ-FTIR to avoid errors in the results caused by random sampling as much as possible. Nevertheless, there is still no adequate standard for MPs sampling and identification up to now and many efforts are needed to improve the accuracy of both the microscopic examination and μ-FTIR identification of MPs. Thus, it is necessary to develop a unified, efficient, and less error-prone standard for MPs experiments as soon as possible.

Shape recognition is another part of MPs detections. Three shapes were recognized in these MPs samples: fibers, fragments, and films. The percentages of MPs polymer were inconsistent for different shapes, with the highest percentage of 73.9% and 65.7% for MPs films and fragments, respectively. Although MPs fibers accounted for the highest total sample volume, only 38.7% of the microfibers were identified as polymers by μ-FTIR. MPs films and fragments had significantly higher polymer percentage because the surface characteristics of these two shapes of MPs were obvious and the accuracy of microscopic polymer detection was higher. It is more challenging to distinguish man-made recycled fibers, plant and animal fibers, and polymer fibers by microscope, so there is a substantial degree of uncertainty in the results of microscopic examination.

Relationship Between Each Characteristic of Microplastics and Comparisons of Their Regional Differences

In our results, the percentage of MPs fibers was the highest, the percentage of MPs fragments was the second, and the percentage of MPs films was the least. There were 88.4% of MPs with sizes smaller than 2 mm and 62% of MPs with sizes smaller than 1 mm in this study. The sharpness of the edges of plastic fragments is an indicator for the age of MPs in the sea (Shaw and Day, 1994; Hidalgo-Ruz et al., 2012; Rodríguez-Seijo and Pereira, 2016; Pan et al., 2019). In this study, there are few samples with sharp edges. MPs fibers, fragments, and films were all detected with relatively smooth edges and aged bifurcation appeared around the edge of some fibers, indicating that the aging fibers may split into much smaller microshapes.

Different proportions of MPs were in different colors and different shapes. However, the blue and black MPs were the most abundant, while 80% of MPs fragments were blue and 78.8% of MPs films were transparent. Various colors of MPs may show great similarity to the natural marine food, which may lead to ingestion by mistake by marine biota (Wright et al., 2013). Our results were inconsistent with early research (around Zhongye, Daoming, Jiuzhang, and Zhenghe Reefs) near Nansha Islands, where dominant colors were transparent and green (Tan et al., 2020). The blue and black MPs dominated our research area, which was different from the Pearl River surface water where the main colors of MPs were white and red (Lin et al., 2018). In addition, no microbeads (pellets) were observed in all the MPs samples in this study, which agreed with the results of previous studies in Pearl River (Lin et al., 2018) and in Nansha Islands (Tan et al., 2020). There were no significant spatial characteristics of different shapes of MPs. Twenty five plastic fibers and three plastic films were identified with the sizes > 5 mm (**Figure 3E**), which was much less than the 182 particles detected in a previous study (Tan et al., 2020).

Related findings from the other areas in the SCS showed that blue and transparent MPs were the most abundant near Zhubi Reef (Huang et al., 2019). Transparent MPs were more abundant than blue near Xisha Islands (Huang et al., 2020), while blue and white MPs were the most abundant near Nanxun Islands (Nie et al., 2019) and black MPs was the largest proportion in Haikou Bay (Qi et al., 2020). Moreover, blue MPs were the most abundant in the seabirds on Yongxing Island, followed by black MPs (Zhu C. et al., 2019). There were more transparent MPs in other areas of Nansha Islands, especially the transparent MPs films. In this study, colored MP fragments were the most abundant, followed by colored MPs fibers. The percentage of colored MPs fragments was consistent with previous studies mentioned above, except for the higher rate of transparent MPs films. Among the colored MPs, blue MPs fragments and black and red MPs fibers were the most abundant. Similar to the results of pumping water sampling (sampling mesh < 100 μm) in previous studies, this study also found a higher proportion of blue MPs particles. Results also revealed that MPs fragments had smaller particle diameters than MPs fibers and films, which may be related to long-distance transport and the greater susceptibility of hard plastics to abrasion (Tan et al., 2020).

According to Suaria et al. (2020), 92% of the floating microfibers on the sea surface were plant and animal fibers and regenerated fibers and only 8% were synthetic fibers. MPs fibers were mainly from fiber shedding during laundering of clothing, weathering, and shredding of industrial fabrics such as canvas, tarpaulins, fishing nets, and cables (Browne et al., 2011; Wang et al., 2019b). The proportion of polymers in all the three shapes of MPs particles in this study was much higher than that in global ocean surface (Suaria et al., 2020). This result may be related to the semi-enclosed characteristics of the SCS and the study of Suaria et al. (2020) is a global average abundance counting only microfibers polymers. In this study, longer MPs fibers (>2 mm) accounted for 16.4% of the total plastic fibers and shorter MPs fibers (<2 mm) accounted for the rest 83.6% of the total plastic fibers. The shorter MPs fibers may be derived

from the decomposition of longer plastic fibers or atmospheric deposition because of their small size (Liu et al., 2019; Suaria et al., 2020). The large proportion of shorter MPs fibers in this study suggested that the MPs fibers in this area may have been disintegrated in the ocean or deposited from the atmosphere for a long time. The overall particles sizes of MPs fragments were small in this study, with 90% less than 1 mm in diameter and 98.4% less than 2 mm in diameter, while 86.7% of the MPs films were less than 2 mm in diameter. Irregular, hard, and millimeter-sized pieces and particles of PE and PP may originate from decomposing larger hard plastic wastes (Wang et al., 2019b).

All the common plastic polymer components were found in the sea surface floating MPs. In this study, MPs fibers and films were mostly made of PET and cellophane and MPs fragments components were the most abundant in polymers of PVC, PET, and PVDC. Compared with the results from other waters in the SCS, the primary polymer components of MPs in surface seawater were PE, urethane alkyd/Alkyd resin (UA), PET, PP, PA, and PVC (Cai et al., 2018; Wang et al., 2019b; Tan et al., 2020). The most polymer components of MPs in the sand of some island in the SCS were PP, PE, and PET (Zhang et al., 2019) and the polymers of MPs in the surface water of Xisha Islands were PET and PP (Huang et al., 2020). Compared with other seas in China, the polymers of MPs in surface water of the Bohai Sea were mainly PE, PP, PS, and PET (Zhang et al., 2017);, while as PE, PP, and cellophane in the Yellow Sea (Li and Sun, 2020) and PE, PP, and polystyrene (PS)-poly(styrene:vinyl alcohol) (VA) copolymers in the East China Sea (Liu et al., 2018). These results showed that PE and PET were the main polymer components of MPs in the surface waters of the Chinese offshore and distant seas. The common polymer components of MPs in the Pearl River were PP, PE, and PET (Lin et al., 2018); PA and cellophane (Yan et al., 2019), which was different with PVC, are the most frequently detected polymers in MPs from Changjiang Estuary (Xu et al., 2018).

Due to the still unclear spatial heterogeneity of MPs, the main polymers of MPs near the southern coast of Korea were Alkyd Paint particles (Song et al., 2014). In contrast, the main polymers of MPs in the northern Gulf of Mexico were cellophane, PE, and Alkyd resin (Di Mauro et al., 2017), which were somewhat similar to the SCS (**Supplementary Table 3**). These polymers can be found almost everywhere in contemporary human production and life. Cellophane is an organic cellulose-based polymer that has been used in food packaging and cigarette wrappers. It is also used as a release agent in fiberglass and rubber products and is often used as a coating in combination with synthetic polymers (Yang et al., 2015; Zhu L. et al., 2019). Synthetic plastic fibers are mainly used in garment manufacturing and production tools (fishing nets, ropes, and threads, etc.). Fibers have been documented as the leading MPs pollutants in domestic wastewater from rivers, estuaries, marine aquatic systems, and wastewater treatment plants (Wang et al., 2019b; Suaria et al., 2020). The average and median diameter of MPs fibers in this study were 1.29 and 1.065 mm, respectively, and MPs fibers discharged from wastewater treatment systems were usually < 0.5 mm (Lin et al., 2018; Wang et al., 2019a). Only 13.4% of the MPs fibers in this study were < 0.5 mm, indicating that shedding clothing fibers from wastewater was not the primary source of MPs fibers. The industrial fabrics from fishing activities and marine vessels were the primary MPs sources in the southwestern SCS. Possible sources of PA include clothing, packaging, and fishing (Yan et al., 2019). PE is widely applied in food packaging bags and agricultural film (Zhu et al., 2018). PP is generally used in fishing tools (Nie et al., 2019). In addition, the proportion of MPs fibers > 2 mm was higher in Nansha Islands than in Xisha Islands, which may imply that more fishing nets or ropes or threads aged or abandoned in Nansha Islands. These may come from intentional or unintentional actions of fishermen in this region. The difference in MPs pollution in Xisha Islands and Nansha Islands indicated the need to strengthen control of plastic waste treatment from ships and fishing activities, raise the awareness of environmental protection in people, and reduce the man-made plastic waste at sea, especially at the open sea.

Overall, this study showed a high spatial heterogeneity of MPs and there is no obvious distribution pattern in the open sea. In addition to the significant influence of MPs from land-based emissions, atmospheric deposition is also a non-negligible source for marine MPs. Indeed, more data are necessary to further understand the life cycles and detailed distributions of MPs in the SCS.

CONCLUSION

This study highlighted that the low MPs abundance but diverse polymer types were found in the southwestern SCS. The mixed mixture of the various MPs particles resulted from long-distance transportation. The average MPs abundance in the southwest SCS was 0.072 ± 0.053 particles/m^3, more than 80% of MPs were < 2 mm, and the main polymer types were PET, PVC, and cellophane. There was spatial heterogeneity of MPs in the SCS. The MPs abundance in Nansha Islands is higher than that in Xisha Islands and the diameter of MPs in Xisha Islands is smaller than that in Nansha Islands, while the diversity of MPs polymers increased from Xisha Islands to Nansha Islands. In the southwestern SCS, MPs mainly originated from the weathering and decomposition of plastic waste from marine vessel activities and land-based sources.

In addition, the variability of external morphological characteristics of MPs in Nansha Islands and Xisha Islands may also be affected by marine environment through influencing weathering and decomposition of plastics and MPs. Different sampling and identification methods can cause significant differences in MPs abundances and characteristics. Establishing unified sampling methods and more adequate collection of *in situ* are crucial in eliminating artificial errors and systematic errors in future MPs studies, which will lead to a better understanding about the past and present of MPs.

DATA AVAILABILITY STATEMENT

The original contributions presented in the study are included in the article/**Supplementary Material**, further inquiries can be directed to the corresponding authors.

AUTHOR CONTRIBUTIONS

JY contributed to the conceptualization, methodology, investigation, writing—original draft preparation, and visualization. DT contributed to the resources, funding acquisition, project administration, conceptualization, supervision, and writing—review and editing. SW contributed to methodology, sampling, and investigation. LH contributed to the formal analysis, software, visualization, and methodology. KP contributed to the formal analysis and methodology. All authors contributed to the article and approved the submitted version of the manuscript.

FUNDING

This study was financially supported by grants by the Guangdong Key Special Supporting Team Project (2019BT02H594 and 2017B030301005), the National Natural Science Foundation of China (41876136), the Key Special Project of Southern Marine Science and Engineering Guangdong Laboratory (Guangzhou) (GML2019ZD0602), the Foundation of the South China Sea Institute of Ecological Environment Engineering Innovation of Chinese Academy of Sciences (ISEE2019ZR02), the Consulting Project for Academic of the Chinese Academy of Sciences: Development and Maritime Rights of Islands and Reefs in the South China Sea leading by Academician Wang Ying (2016ZWH005A-005), the National Science and Technology Fundamental Resources Investigation Program of China (2018FY100100), and The Research Fund Program of Guangdong Provincial Key Laboratory of Marine Resources and Coastal Engineering.

ACKNOWLEDGMENTS

We thank the Nansha Survey Cruise organized by the Academician Wang Ying, Nanjing University in March to April, 2018. We would like to thank Drs. Lang Lin, Hengxiang Li, and Prof. Xiangrong Xu of the UCAS (University of Chinese Academy of Sciences) Key Laboratory of Tropical Marine Bio-resources and Ecology, South China Sea Institute of Oceanology, Chinese Academy of Sciences, for their help and guidance during the laboratory experiments. We are thankful to Dr. Yupeng Liu of the South China Sea Institute of Oceanology, Chinese Academy of Sciences for his invaluable suggestion on writing and revising.

SUPPLEMENTARY MATERIAL

The Supplementary Material for this article can be found online at: https://www.frontiersin.org/articles/10.3389/fmars.2022.830318/full#supplementary-material

REFERENCES

Andrady, A. L. (2011). Microplastics in the marine environment. *Mar. Pollut. Bull.* 62, 1596–1605. doi: 10.1016/j.marpolbul.2011.05.030

Browne, M. A., Crump, P., Niven, S. J., Teuten, E., Tonkin, A., Galloway, T., et al. (2011). Accumulation of microplastic on shorelines woldwide: sources and sinks. *Environ. Sci. Technol.* 45, 9175–9179. doi: 10.1021/es201811s

Cai, M., He, H., Liu, M., Li, S., Tang, G., Wang, W., et al. (2018). Lost but can't be neglected: huge quantities of small microplastics hide in the South China Sea. *Sci. Total Environ.* 633, 1206–1216. doi: 10.1016/j.scitotenv.2018.03.197

Cheung, P. K., Cheung, L. T. O., and Fok, L. (2016). Seasonal variation in the abundance of marine plastic debris in the estuary of a subtropical macro-scale drainage basin in South China. *Sci. Total Environ.* 562, 658–665. doi: 10.1016/j.scitotenv.2016.04.048

Cole, M., Lindeque, P., Halsband, C., and Galloway, T. S. (2011). Microplastics as contaminants in the marine environment: a review. *Mar. Pollut. Bull.* 62, 2588–2597. doi: 10.1016/j.marpolbul.2011.09.025

Collignon, A., Hecq, J.-H., Glagani, F., Voison, P., Collard, F., and Goffart, A. (2012). Neustonic microplastic and zooplankton in the North Western Mediterranean Sea. *Mar. Pollut. Bull.* 64, 861–864. doi: 10.1016/j.marpolbul.2012.01.011

Cózar, A., Echevarria, F., Gonzalez-Gordillo, J. I., Irigoien, X., Ubeda, B., Hernandez-Leon, S., et al. (2014). Plastic debris in the open ocean. *Proc. Natl. Acad. Sci. U.S.A.* 111, 10239–10244. doi: 10.1073/pnas.1314705111

Desforges, J.-P. W., Galbraith, M., Dangerfield, N., and Ross, P. S. (2014). Widespread distribution of microplastics in subsurface seawater in the NE Pacific Ocean. *Mar. Pollut. Bull.* 79, 94–99. doi: 10.1016/j.marpolbul.2013.12.035

Di Mauro, R., Kupchik, M. J., and Benfield, M. C. (2017). Abundant plankton-sized microplastic particles in shelf waters of the northern Gulf of Mexico. *Environ. Pollut.* 230, 798–809. doi: 10.1016/j.envpol.2017.07.030

Ding, J., Jiang, F., Li, J., Wang, Z., Sun, C., Wang, Z., et al. (2019). Microplastics in the coral reef systems from xisha islands of south china sea. *Environ. Sci. Technol.* 53, 8036–8046. doi: 10.1021/acs.est.9b01452

Doyle, M. J., Watson, W., Bowlin, N. M., and Sheavly, S. B. (2011). Plastic particles in coastal pelagic ecosystems of the Northeast Pacific ocean. *Mar. Environ. Res.* 71, 41–52. doi: 10.1016/j.marenvres.2010.10.001

Enders, K., Lenz, R., Stedmon, C. A., and Nielsen, T. G. (2015). Abundance, size and polymer composition of marine microplastics =10μm in the Atlantic Ocean and their modelled vertical distribution. *Mar. Pollut. Bull.* 100, 70–81. doi: 10.1016/j.marpolbul.2015.09.027

Eriksen, M., Lebreton, L. C., Carson, H. S., Thiel, M., Moore, C. J., Borerro, J. C., et al. (2014). Plastic Pollution in the World's Oceans: more than 5 Trillion Plastic Pieces Weighing over 250,000 Tons Afloat at Sea. *PLoS One* 9:e111913. doi: 10.1371/journal.pone.0111913

Fu, J., Mai, B., Sheng, G., Zhang, G., Wang, X., Peng, P., et al. (2003). Persistent organic pollutants in environment of the Pearl River Delta. *Chemosphere* 52, 1411–1422. doi: 10.1016/s0045-6535(03)00477-6

GESAMP (2010). *Proceedings of the GESAMP International Workshop on Plastic Particles as a Vector in Transporting Persistent*. Italy: FAO.

GESAMP (2015). "Sources, Fate and Effects of Microplastics in the Marine Environment: a Global Assessment. IMO/FAO/UNESCO-IOC/UNIDO/-WMO/ IAEA/UN/UNEP/UNDP," in *Joint Group of Experts on the Scientific Aspects of Marine Environmental Protection Reports and Studies*, ed. P. J. Kershaw, (Italy: FAO).

Harris, P. T., Tamelander, J., Lyons, Y., Neo, M. L., and Maes, T. (2021). Taking a mass-balance approach to assess marine plastics in the South China Sea. *Mar. Pollut. Bull.* 171:112708. doi: 10.1016/j.marpolbul.2021.112708

Hidalgo-Ruz, V., Gutow, L., Thompson, R. C., and Thiel, M. (2012). Microplastics in the marine environment: a review of the methods used for identification and quantification. *Environ. Sci. Technol.* 46, 3060–3075. doi: 10.1021/es2031505

Huang, L., Li, Q., Xu, X., Yuan, X., Lin, L., and Li, H. (2020). Composition and distribution of microplastics in the surface seawater of Xisha Islands. *Chinese. Sci. Bull.* 65, 2627–2635. doi: 10.1360/tb-2020-0220

Huang, Y., Xiao, X., Effiong, K., Xu, C., Su, Z., Hu, J., et al. (2021). New Insights into the Microplastic Enrichment in the Blue Carbon Ecosystem: evidence from Seagrass Meadows and Mangrove Forests in Coastal South China Sea. *Environ. Sci. Technol.* 55, 4804–4812. doi: 10.1021/acs.est.0c07289

Huang, Y., Yan, M., Xu, K., Nie, H., Gong, H., and Wang, J. (2019). Distribution characteristics of microplastics in Zhubi Reef from South China Sea. *Environ. Pollut.* 255:113133. doi: 10.1016/j.envpol.2019.113133

Hughes, T. P., Barnes, M. L., Bellwood, D. R., Cinner, J. E., Cumming, G. S., Jackson, J. B. C., et al. (2017). Coral reefs in the Anthropocene. *Nature* 546, 82–90. doi: 10.1038/nature22901

Isobe, A., Uchida, K., Tokai, T., and Iwasaki, S. (2015). East Asian seas: a hot spot of pelagic microplastics. *Mar. Pollut. Bull.* 101, 618–623. doi: 10.1016/j.marpolbul.2015.10.042

Jambeck, J. R., Geyer, R., Wilcox, C., Siegler, T. R., Perryman, M., Andrady, A., et al. (2015). Plastic waste inputs from land into the ocean. *Science* 347, 768–771. doi: 10.1126/science.1260352

Li, C., Zhu, L., Wang, X., Liu, K., and Li, D. (2022). Cross-oceanic distribution and origin of microplastics in the subsurface water of the South China Sea and Eastern Indian Ocean. *Sci. Total Environ.* 805:150243. doi: 10.1016/j.scitotenv.2021.150243

Li, Q., and Sun, X. (2020). Progress on microplastics research in the Yellow Sea *China*. *Anthropocene Coasts* 3, 43–52. doi: 10.1139/anc-2018-0033

Li, D. (2019). Research Advance and Countermeasures on Marine Microplastic Pollution (in Chinese). *Res. Environ. Sci.* 32, 197–202. doi: 10.13198/j.issn.1001-6929.2018.11.25

Lin, L., Zuo, L. Z., Peng, J. P., Cai, L. Q., Fok, L., Yan, Y., et al. (2018). Occurrence and distribution of microplastics in an urban river: a case study in the Pearl River along Guangzhou City. *China Sci. Total Environ.* 644, 375–381. doi: 10.1016/j.scitotenv.2018.06.327

Liu, K., Wu, T., Wang, X., Song, Z., Zong, C., Wei, N., et al. (2019). Consistent Transport of Terrestrial Microplastics to the Ocean through Atmosphere. *Environ. Sci. Technol.* 53, 10612–10619. doi: 10.1021/acs.est.9b03427

Liu, T., Sun, X., Zhu, M., Liang, J., and Zhao, Y. (2018). Distribution and composition of microplastics in the surface water of the East China Sea (In Chinese). *Oceanol. Limnol. Sin.* 49, 62–69. doi: 10.11693/hyhz20170100021

Lusher, A. L., Burke, A., O'Connor, I., and Officer, R. (2014). Microplastic pollution in the Northeast Atlantic Ocean: validated and opportunistic sampling. *Mar. Pollut. Bull.* 88, 325–333. doi: 10.1016/j.marpolbul.2014.08.023

Lusher, A. L., Tirelli, V., O'Connor, I., and Officer, R. (2015). Microplastics in Arctic polar waters: the first reported values of particles in surface and sub-surface samples. *Sci. Rep.* 5:14947. doi: 10.1038/srep14947

McCormick, A., Hoellein, T. J., Mason, S. A., Schluep, J., and Kelly, J. J. (2014). Microplastic is an Abundant and Distinct Microbial Habitat in an Urban River. *Environ. Sci. Technol.* 48, 11863–11871. doi: 10.1021/es503610r

Md Amin, R., Shazira Sohaimi, E., Tuan Anuar, S., and Bachok, Z. (2020). Microplastic ingestion by zooplankton in Terengganu coastal waters, southern South China Sea. *Mar. Pollut. Bull.* 150:110616. doi: 10.1016/j.marpolbul.2019.110616

Ministry of Civil Affairs of the People's Republic of China (2020). Announcement by the Ministry of Civil Affairs on the State Council's approval of the establishment of a municipal district in Sansha City, Hainan Province, PRC. (In Chinese). Available online at: http://www.mca.gov.cn/article/xw/tzgg/202004/20200400026955.shtml [accessed on April 18, 2020]

Moore, C. J., Moore, S. L., Weisberg, S. B., Lattin, G. L., and Zellers, A. F. (2002). A comparison of neustonic plastic and zooplankton abundance in southern California's coastal waters. *Mar. Pollut. Bull.* 44, 1035–1038. doi: 10.1016/S0025-326X(02)00150-9

Nie, H., Wang, J., Xu, K., Huang, Y., and Yan, M. (2019). Microplastic pollution in water and fish samples around Nanxun Reef in Nansha Islands. *South China Sea. Sci. Total Environ.* 696:134022. doi: 10.1016/j.scitotenv.2019.134022

Pan, Z., Guo, H., Chen, H., Wang, S., Sun, X., Zou, Q., et al. (2019). Microplastics in the Northwestern Pacific: abundance, distribution, and characteristics. *Sci. Total Environ.* 650, 1913–1922. doi: 10.1016/j.scitotenv.2018.09.244

Qi, H., Fu, D., Wang, Z., Gao, M., and Peng, L. (2020). Microplastics occurrence and spatial distribution in seawater and sediment of Haikou Bay in the northern South China Sea. *Estuar. Coastal Shelf Sci.* 239:106757. doi: 10.1016/j.ecss.2020.106757

Qiu, Q., Peng, J., Yu, X., Chen, F., Wang, J., and Dong, F. (2015). Occurrence of microplastics in the coastal marine environment: first observation on sediment of China. *Mar. Pollut. Bull.* 98, 274–280. doi: 10.1016/j.marpolbul.2015.07.028

Reisser, J., Slat, B., Noble, K., du Plessis, K., Epp, M., Proietti, M., et al. (2015). The vertical distribution of buoyant plastics at sea: an observational study in the North Atlantic Gyre. *Biogeosciences* 12, 1249–1256. doi: 10.5194/bg-12-1249-2015

Rodríguez-Seijo, A., and Pereira, R. (2016). "Chapter 3: morphological and physical characterization ofmicroplastics," in *Comprehensive Analytical Chemistry*, Vol. 75, eds T. A. P. Rocha-Santos and A. C. Duarte (Netherlands: Elsevier), 49–65.

Ryan, P. G., Moore, C. J., van Franeker, J. A., and Moloney, C. L. (2009). Monitoring the abundance of plastic debris in the marine environment. *Philos. Trans. R Soc. Lond. B Biol. Sci.* 364, 1999–2012. doi: 10.1098/rstb.2008.0207

Shaw, D. G., and Day, R. H. (1994). Colour- and form-dependent loss of plastic micro-debris from the North Pacific Ocean. *Mar. Pollut. Bull.* 28, 39–43. doi: 10.1016/0025-326x(94)90184-8

Song, Y. K., Hong, S. H., Jang, M., Kang, J. H., Kwon, O. Y., Han, G. M., et al. (2014). Large accumulation of micro-sized synthetic polymer particles in the sea surface microlayer. *Environ. Sci. Technol.* 48, 9014–9021. doi: 10.1021/es501757s

Su, L., Xue, Y., Li, L., Yang, D., Kolandhasamy, P., Li, D., et al. (2016). Microplastics in Taihu Lake. *China*. *Environ. Pollut.* 216, 711–719. doi: 10.1016/j.envpol.2016.06.036

Suaria, G., Achtypi, A., Perold, V., Lee, J. R., Pierucci, A., Bornman, T. G., et al. (2020). Microfibers in oceanic surface waters: a global characterization. *Sci. Adv.* 6:eaay8493. doi: 10.1126/sciadv.aay8493

Sun, X., Li, Q., Zhu, M., Liang, J., Zheng, S., and Zhao, Y. (2017). Ingestion of microplastics by natural zooplankton groups in the northern South China Sea. *Mar. Pollut. Bull.* 115, 217–224. doi: 10.1016/j.marpolbul.2016.12.004

Tan, F., Yang, H., Xu, X., Fang, Z., Xu, H., Shi, Q., et al. (2020). Microplastic pollution around remote uninhabited coral reefs of Nansha Islands. *South China Sea. Sci. Total Environ.* 725:138383. doi: 10.1016/j.scitotenv.2020.138383

Ter Halle, A., Ladirat, L., Martignac, M., Mingotaud, A. F., Boyron, O., and Perez, E. (2017). To what extent are microplastics from the open ocean weathered? *Environ. Pollut.* 227, 167–174. doi: 10.1016/j.envpol.2017.04.051

Teuten, E. L., Rowland, S. J., Galloway, T. S., and Thompson, R. C. (2007). Potential for plastic to transport hydrohobic contaminants. *Environ. Sci. Technol.* 41, 7759–7764. doi: 10.1021/es071737s

Thompson, R. C., Olsen, Y., Mitchell, R. P., Davis, A., Rowland, S. J., John, A. W., et al. (2004). Lost at sea: where is all the plastic? *Science* 304:838. doi: 10.1126/science.1094559

UNEP (2005). *Marine Litter, An Analytical Overview*. Kenya: UNEP.

Vandermeersch, G., Van Cauwenberghe, L., Janssen, C. R., Marques, A., Granby, K., Fait, G., et al. (2015). A critical view on microplastic quantification in aquatic organisms. *Environ. Res.* 143, 46–55. doi: 10.1016/j.envres.2015.07.016

Waller, C. L., Griffiths, H. J., Waluda, C. M., Thorpe, S. E., Loaiza, I., Moreno, B., et al. (2017). Microplastics in the Antarctic marine system: an emerging area of research. *Sci. Total Environ.* 598, 220–227. doi: 10.1016/j.scitotenv.2017.03.283

Wang, B., Huang, F., Wu, Z., Yang, J., Fu, X., and Kazuyoshi Kikuchi. (2009). Multi-scale climate variability of the South China Sea monsoon: a review. *Dyn. Atmos. Oceans* 47, 15–37. doi: 10.1016/j.dynatmoce.2008.09.004

Wang, T., Zou, X., Li, B., Yao, Y., Zang, Z., Li, Y., et al. (2019b). Preliminary study of the source apportionment and diversity of microplastics: taking floating microplastics in the South China Sea as an example. *Environ. Pollut.* 245, 965–974. doi: 10.1016/j.envpol.2018.10.110

Wang, T., Li, B., Zou, X., Wang, Y., Li, Y., Xu, Y., et al. (2019a). Emission of primary microplastics in mainland China: invisible but not negligible. *Water Res.* 162, 214–224. doi: 10.1016/j.watres.2019.06.042

Webb, H. K., Arnott, J., Crawford, R. J., and Ivanova, E. P. (2012). Plastic Degradation and Its Environmental Implications with Special Reference to Poly(ethylene terephthalate). *Polymers* 5, 1–18. doi: 10.3390/polym5010001

Wright, S. L., Thompson, R. C., and Galloway, T. S. (2013). The physical impacts of microplastics on marine organisms: a review. *Environ. Pollut.* 178, 483–492. doi: 10.1016/j.envpol.2013.02.031

Xu, P., Peng, G., Su, L., Gao, Y., Gao, L., and Li, D. (2018). Microplastic risk assessment in surface waters: A case study in the Changjiang Estuary. *China*, *Mar. Pollut. Bull.* 133, 647–654. doi: 10.1016/j.marpolbul.2018.06.020

Yan, M., Nie, H., Xu, K., He, Y., Hu, Y., Huang, Y., et al. (2019). Microplastic abundance, distribution and composition in the Pearl River along Guangzhou city and Pearl River estuary. *China*, *Chemosphere* 217, 879–886. doi: 10.1016/j.chemosphere.2018.11.093

Yang, D., Shi, H., Li, L., Li, J., Jabeen, K., and Kolandhasamy, P. (2015). Microplastic Pollution in Table Salts from China. *Environ. Sci. Technol.* 49, 13622–13627. doi: 10.1021/acs.est.5b03163

Zambrano, M. C., Pawlak, J. J., Daystar, J., Ankeny, M., Goller, C. C., and Venditti, R. A. (2020). Aerobic biodegradation in freshwater and marine environments of textile microfibers generated in clothes laundering: effects of cellulose and polyester-based microfibers on the microbiome. *Mar. Pollut. Bull.* 151:110826. doi: 10.1016/j.marpolbul.2019.110826

Zhang, L., Zhang, S., Wang, Y., Yu, K., and Li, R. (2019). The spatial distribution of microplastic in the sands of a coral reef island in the South China Sea: comparisons of the fringing reef and atoll. *Sci. Total Environ.* 688, 780–786. doi: 10.1016/j.scitotenv.2019.06.178

Zhang, W., Zhang, S., Wang, J., Wang, Y., Mu, J., Wang, P., et al. (2017). Microplastic pollution in the surface waters of the Bohai Sea. *China. Environ. Pollut.* 231, 541–548. doi: 10.1016/j.envpol.2017.08.058

Zhao, S., Zhu, L., Wang, T., and Li, D. (2014). Suspended microplastics in the surface water of the Yangtze Estuary System, China: first observations on occurrence, distribution. *Mar. Pollut. Bull.* 86, 562–568.

Zhou, P., Huang, C., Fang, H., Cai, W., Li, D., Li, X., et al. (2011). The abundance, composition and sources of marine debris in coastal seawaters or beaches around the northern South China Sea (China). *Mar. Pollut. Bull.* 62, 1998–2007. doi: 10.1016/j.marpolbul.2011.06.018

Zhu, C., Li, D., Sun, Y., Zheng, X., Peng, X., Zheng, K., et al. (2019). Plastic debris in marine birds from an island located in the South China Sea. *Mar. Pollut. Bull.* 149:110566. doi: 10.1016/j.marpolbul.2019.110566

Zhu, J., Zhang, Q., Li, Y., Tan, S., Kang, Z., Yu, X., et al. (2019). Microplastic pollution in the Maowei Sea, a typical mariculture bay of China. *Sci. Total Environ.* 658, 62–68. doi: 10.1016/j.scitotenv.2018.12.192

Zhu, L., Wang, H., Chen, B., Sun, X., Qu, K., and Xia, B. (2019). Microplastic ingestion in deep-sea fish from the South China Sea. *Sci. Total Environ.* 677, 493–501. doi: 10.1016/j.scitotenv.2019.04.380

Zhu, L., Bai, H., Chen, B., Sun, X., Qu, K., and Xia, B. (2018). Microplastics pollution in North Yellow Sea, China: observations on Occurrence, distribution and identification. *Sci. Total Environ.* 636, 20–29. doi: 10.1016/j.scitotenv.2018.04.182

Conflict of Interest: The authors declare that the research was conducted in the absence of any commercial or financial relationships that could be construed as a potential conflict of interest.

Publisher's Note: All claims expressed in this article are solely those of the authors and do not necessarily represent those of their affiliated organizations, or those of the publisher, the editors and the reviewers. Any product that may be evaluated in this article, or claim that may be made by its manufacturer, is not guaranteed or endorsed by the publisher.

frontiers in Marine Science

ORIGINAL RESEARCH
published: 25 March 2022
doi: 10.3389/fmars.2022.863652

Microplastic Contamination on the Beaches of South China

Bingwen Chai[1,2†], Yanping Li[1†], Li Wang[3], Xiao-Tan Zhang[4], Yi-Ping Wan[2], Fengyuan Chen[1], Jie Ma[1], Wenlu Lan[5] and Ke Pan[1]*

[1] Shenzhen Key Laboratory of Marine Microbiome Engineering, Institute for Advanced Study, Shenzhen University, Shenzhen, China, [2] School of Environment and Energy, South China University of Technology, Guangzhou, China, [3] Bureau of Hydrology and Water Resources, Pearl River Water Resources Commission of Ministry of Water Resources, Guangzhou, China, [4] Department of Clinical Pathology, The First Affiliated Hospital of Jinan University, Guangzhou, China, [5] Marine Environmental Monitoring Center of Guangxi, Beihai, China

Microplastics (MPs) have emerged as a pollutant of significant global concern. The sandy beach is a fragile environment that deserves our special attention with regard to MP contamination, as this area is a hotspot that accumulates large quantities of plastic waste. Notably, our current understanding of the MP distribution on beaches and the scale of contamination is far from sufficient. Hence, this study investigated the occurrence and characteristics of MPs on 14 beaches along the coast of South China. The MPs were ubiquitously distributed in the sand, most were small, less than 1 mm. A total of 18 types of polymers were identified in the sand, suggesting that diverse types of MPs are present on the beaches. Polyethylene, polypropylene, and polystyrene were the dominant types of MPs in most of our sampling sites. The MP abundance was higher in the upper layers (0–20 cm) of the beach than in the deeper layers (20–40 cm) of the sampling site when characterized by depth (Yangjiang beach). Our study demonstrates the extent and severity of MP pollution on the beaches of South China and provides implications for future remediation measures. More effort is needed to clarify the vertical distribution of MPs on beaches, especially for those MPs less than 1 μm.

Keywords: microplastics, contamination, beach, μ-FTIR, South China

OPEN ACCESS

Edited by:
Xiangrong Xu,
South China Sea Institute of Oceanology (CAS), China

Reviewed by:
Bin Xia,
Chinese Academy of Fishery Sciences (CAFS), China
Huifeng Wu,
Yantai Institute of Coastal Zone Research (CAS), China

***Correspondence:**
Ke Pan
panke@szu.edu.cn

† These authors have contributed equally to this work

Specialty section:
This article was submitted to Marine Pollution, a section of the journal Frontiers in Marine Science

Received: *27 January 2022*
Accepted: *25 February 2022*
Published: *25 March 2022*

Citation:
Chai B, Li Y, Wang L, Zhang X-T, Wan Y-P, Chen F, Ma J, Lan W and Pan K (2022) Microplastic Contamination on the Beaches of South China. Front. Mar. Sci. 9:863652. doi: 10.3389/fmars.2022.863652

INTRODUCTION

Microplastics (MPs) and nanoplastics (NPs), respectively, defined as synthetic solid particles or polymeric matrices ranging in size from 1 μm to 5 mm and less than 1 μm (Frias and Nash, 2019), have emerged as a pollutant of significant global concern (Thompson et al., 2004; Ivar do Sul and Costa, 2014). The sources, transport, and fates of MPs have been intensively studied in the past decade (Burns and Boxall, 2018; Beiras and Schönemann, 2020; Wang et al., 2021). Evidence has shown that they are ubiquitous in the environment, including in remote areas such as the polar regions and deep ocean (Lusher et al., 2015; Li et al., 2020). However, due to constraints in the sampling, identification, and quantification techniques (Hidalgo-Ruz et al., 2012), our understanding of the mechanisms underlying MP distribution and their scale of contamination is still limited. Much more effort is needed to understand the impacts of MPs on different ecosystems.

The sandy beach is one of those ecosystems that deserves our attention with regard to MP contamination. The beach ecosystem is an extremely dynamic environment where the physical structure of the habitat is determined by interactions between the sand, waves, and tides

(McLachlan and Defeo, 2017). This dynamic habitat is home to a diversity of species which are extremely mobile and adaptable to changing conditions (Brown and McLachlan, 2002). Sandy beach ecosystems make up almost half of the world's ice-free ocean coastline and function as a social–ecological system (Defeo et al., 2021). It is also a fragile environment facing many threats including erosion and anthropogenic disturbance. Millions of tons of plastic waste enter the ocean every year from rivers, with many of them ending up in coastal areas (Galgani et al., 2015; Jambeck et al., 2015; Peng et al., 2021). In addition, beaches are a leisure hotspot and subject to intense recreational activities that generate large amounts of plastic litter. Inadequate waste management, littering, and illegal dumping result in build-ups of plastic litter on beaches (Silva-Cavalcanti et al., 2009). The aging and weathering of this plastic litter can generate a substantial amount of MPs which could then be transported to the sea or deposited in the sand (Andrady, 2015). Meanwhile, the sublittoral zone of beach areas is subject to strong wave action, where huge volumes of seawater spread on the beach surface and then rapidly drain back to the sea due to the high permeability of the sand (McLachlan and Defeo, 2017). During this process, MPs in the seawater could be trapped and accumulate in the sand, making sandy beaches a sink for MPs.

There have been reports of MP contamination on beach surfaces worldwide, and alarming levels of MPs have been reported (Li et al., 2018; Tiwari et al., 2019; De-la-Torre et al., 2020; Mazariegos-Ortíz et al., 2020; Patchaiyappan et al., 2021). While abundance and distribution of MPs have been characterized in beach sand, vertical distribution of MPs on beaches has received relatively less attention. Investigating vertical distribution is important to understand the migration of MPs in the beach environment. In addition, it should be noted that most of previous studies have identified the MPs by visual identification under a microscope on the basis of plastic color and shape. Such a method is labor intensive and inefficient for counting MPs, especially micro-sized MPs. An overestimation of MP contamination is also possible when using these techniques due to false positive identifications (Shim et al., 2017). Due to the limitations of traditional methods, early studies only focused on large-sized MPs and were limited to a few common plastics such as polyethylene (PE), polypropylene (PP), polyamide, polyethylene terephthalate (PET), polystyrene (PS), and polyvinyl chloride (Li et al., 2018; Yaranal et al., 2021). The abundance of MPs beyond these polymer types has thus far rarely been reported for beaches. Therefore, our understanding of the MP distribution and fate on beaches is far from adequate.

In this study, we aimed to assess the distribution and characteristics of MPs on the beaches of South China. Sand samples were collected from 14 beaches along the coast of South China. Large MPs (usually > 800 μm) were characterized using Fourier transform infrared-attenuated total reflection (FTIR-ATR) spectroscopy. Smaller-sized MPs (<800 μm) were enumerated using a cutting-edge μ-FTIR technique combined with a Wizards feature that characterizes micron-sized plastics in an automatic, direct, and continuous way (Chai et al., 2020). To gain a better understanding of the MP distribution on beaches, we also examined the vertical distribution of MPs at one of the sampling sites. Our study demonstrates the extent and severity of MP pollution on the beaches of South China and provides implications for future remediation measures.

MATERIALS AND METHODS

Study Sites

Sand samples were collected at ebb tide from 14 beaches along the southeast coast of China from December 2020 to March 2021. The locations of the sampling sites are shown in **Figure 1**, and detailed information for each site is provided in **Supplementary Table 1**. The investigated sand beach included Lianhuafeng (LHF), Nansha (NS), Shayuchong (SYC), Xiaomeisha (XMS), Jiaochangwei (JCW), Dongchong (DC), Youganwan (YGW), Xiangluwan (XLW), Wanweijintan (WWJT), Yintan (YT), Nanjicun (NJC), Yerong (YR), Yudaitan (YDT), and Beiluowan (BLW). At each site, surface sands (<5 cm depth) were sampled from three sublittoral locations that were at least 5 m apart from each other using a pre-cleaned glass beaker. To observe the vertical distribution of the MPs, a stainless-steel corer was used on the Yangjiang beach (Site 14; **Figure 1** and **Supplementary Table 1**) to collect sand samples from different layers (0–10, 10–20, 20–30, and 30–40 cm depths). All sand samples were wrapped in aluminum foil before transport to the laboratory. The samples were dried in an oven at 60°C for 24 h before sieving through 5 mm stainless-steel mesh to remove large particles.

Extraction of Microplastics From the Sand

A two-step air-induced overflow extraction procedure was used to separate the MPs from the sand as described by Nuelle et al. (2014). A continuous flow and floating separation apparatus, which is composed of an air-induced overflow and a 1,200-mesh stainless steel sieve (c.a. 11 μm), was set up following Nuelle et al.'s descriptions. The extraction was performed without oxidation as the samples contained little organic material. The separation of the MPs was performed based on the fluidization of the sediments in a saturated sodium chloride (NaCl, $\rho = 1.2$ g·cm^{-3}) solution and passed through the 1,200-mesh stainless steel sieve. This reduced the sample mass for the second density separation step by flotation. The particles retained in the sieve were resuspended by a saturated sodium iodide solution (NaI, $\rho = 1.6$ g·cm^{-3}) and again filtered through the 1,200-mesh sieve. The collected particles were rinsed with distilled water to remove salts, dried at 60°C, and transferred to a clean glass petri dish. All samples were wrapped in aluminum foil and stored in a drying cabinet until further analysis in the laboratory.

Enumeration, Classification, and Characterization of the Microplastics

Large MPs (usually > 800 μm) were selected and examined under a stereomicroscope (SteREO Discovery.V20, Zeiss, Germany).

FIGURE 1 | Map showing the locations of the 14 sampled beaches. Detailed information for each sampling site is given in **Supplementary Table 1**.

TABLE 1 | Size distribution and abundance of microplastics (MPs; n kg^{-1}) in the surface sand (0–5 cm) collected from the beach along the coasts of South China.

Site no.	Site name	4–5 mm	3–4 mm	2–3 mm	1–2 mm	<1 mm	Total
1	ST-LHF	6.7 ± 11.5	20.0 ± 20.0	40.0 ± 40.0	0.0 ± 0.0	546.7 ± 758	613.3 ± 823.7
2	GZ-NS	120.0 ± 17.3	143.3 ± 41.6	183.3 ± 23.1	100.0 ± 36.1	1096.7 ± 270.2	1643.3 ± 285.9
3	SZ-SYC	0.0 ± 0.0	0.0 ± 0.0	0.0 ± 0.0	0.0 ± 0.0	2160.0 ± 485.4	2160.0 ± 485.4
4	SZ-XMS	6.7 ± 11.5	13.3 ± 15.3	23.3 ± 40.4	46.7 ± 80.8	1286.7 ± 465.8	1376.7 ± 611.6
5	SZ-JCW	0.0 ± 0.0	0.0 ± 0.0	0.0 ± 0.0	0.0 ± 0.0	4433.3 ± 4822.5	4433.3 ± 4822.5
6	SZ-DC	0.0 ± 0.0	0.0 ± 0.0	0.0 ± 0.0	0.0 ± 0.0	606.7 ± 670.0	606.7 ± 670.0
7	SZ-YGW	0.0 ± 0.0	0.0 ± 0.0	0.0 ± 0.0	0.0 ± 0.0	93.3 ± 90.2	93.3 ± 90.2
8	ZH-XLW	6.7 ± 11.5	46.7 ± 64.3	20.0 ± 34.6	26.7 ± 46.2	266.7 ± 246.8	366.7 ± 181.5
9	FCG-WWJT	140.0 ± 207.8	146.7 ± 133.2	113.3 ± 120.6	86.7 ± 61.1	560.0 ± 275.0	1046.7 ± 291.4
10	BH-YT	0.0 ± 0.0	0.0 ± 0.0	0.0 ± 0.0	0.0 ± 0.0	526.7 ± 397.2	526.7 ± 397.2
11	ZJ-NJC	0.0 ± 0.0	0.0 ± 0.0	0.0 ± 0.0	0.0 ± 0.0	2586.7 ± 2773.6	2586.7 ± 2773.6
12	DZ-YR	13.3 ± 23.1	6.7 ± 11.5	0.0 ± 0.0	0.0 ± 0.0	526.7 ± 704.7	546.7 ± 739.3
13	QH-YDT	0.0 ± 0.0	0.0 ± 0.0	0.0 ± 0.0	0.0 ± 0.0	565.0 ± 798.7	565.0 ± 798.7

These particles were analyzed by Axio Vision SE64 Rel.49 software and classified into five size categories: <1 mm, 1–2 mm, 2–3 mm, 3–4 mm, and 4–5 mm. The MPs were further analyzed using a FTIR spectrometer (NicoletiS50, Thermo Fisher, Waltham, MA, United States) equipped with a built-in ATR accessory. The FTIR spectra were recorded

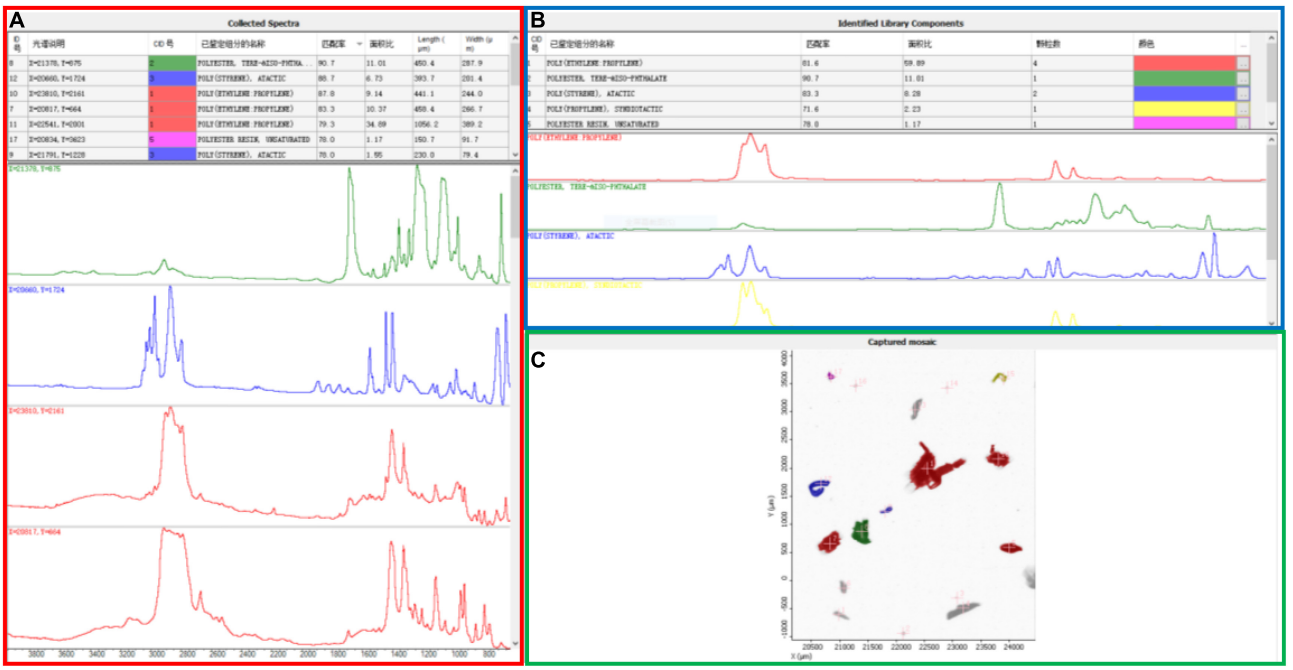

FIGURE 2 | Representative analysis results for MPs collected from beach. The same color indicates the information from the same particle. **(A)** Collected spectra and information of each particle under the μ-Fourier transform infrared (μ-FTIR) spectroscopy, including particle position, identified component name, matching degree, and the length and width of the particle; **(B)** identified library components of these particles, reporting the number of particles; **(C)** scan results for gold-coated microslide with micron-size particles.

between 500 and 4000 cm^{-1} with 16 scans per sample and a resolution of 4 cm^{-1}. All spectra were compared with a database (HR Hummel Polymer and Additives) to identify the texture of the MPs.

Small MPs (<800 μm) were identified with a μ-FTIR (Nicolet iN10 MX, Thermo Fisher, United States) spectrometer equipped with a deuterated triglycine sulfate detector. The spectrum was set in the range of 675–4,000 cm^{-1} and the collection time was set at 3 s. The MPs were evenly spread across a gold-coated microslide and scanned 16 times at a resolution of 8 cm^{-1}. The results were analyzed with the Particles Wizards in OMNIC Picta software (Thermo Fisher, United States).

Quality Control

To minimize sample contamination, all sampling containers and labware for extractions were cleaned with Milli-Q water and dried before use. The samples, solution, and labware were covered or immediately wrapped with aluminum foil when they were not in use.

To test the recovery of our analytical procedure, PE, PP, PET, and polyformaldehyde with a size range of 100 μm to 5 mm were prepared and homogenized with a sand sample. The mixture was analyzed with the described procedure, and recoveries of between 93.4 and 96.8% were obtained.

Statistical Analysis

Microplastic abundance is presented as the number of MP particles per dry mass of sand [numbers (n)·kg^{-1}]. Data analysis was performed using SPSS 18.0 for Windows (SPSS Inc., Chicago, IL, United States).

RESULTS AND DISCUSSION

Size Distribution and the Abundance of Microplastics on the Beach Surface

The MP concentrations in the sand samples are shown in **Table 1**. MPs were detected in all beach samples and ranged from 93.3 to 4433.3 n·kg^{-1} (dry weight basis). The lowest MP concentration (93.3 n·kg^{-1}) was observed at the SZ-YGW site, a private beach with much less tourist activity, while the highest MP concentration was detected in SZ-JCW (4433.3 n·kg^{-1}), a famous tourist region in the Greater Bay Area in China. As suggested by the large standard deviations for the data, the MP concentrations in the samples were highly variable, even in those collected from the same site (**Table 1**). The concentrations also varied by two orders of magnitude (**Table 1**), reflecting the different human disturbances and MP inputs at these sites. Overall, our data indicates that the spatial distribution of MPs is rather heterogeneous on the beaches.

While the presence and abundance of MPs on beaches have been investigated worldwide, the reported values have varied greatly (Li et al., 2018; Tiwari et al., 2019; De-la-Torre et al., 2020; Mazariegos-Ortíz et al., 2020; Patchaiyappan et al., 2021). This reflects not only the degree of MP contamination, but also the bias of different methodologies. Dekiff et al. (2014)

TABLE 2 | Types and abundance of MPs (n kg^{-1}) in the surface sand (0–5 cm) collected from the beach along the coasts of South China.

Site no.	Site name	PE	PS	PVC	PP	PP + PE	epoxy resin	PA	ABS	POM	PET	PU	AB	PTFE	AS	A	EVA	PBT	PMMA
1	ST-LHF	146.7 ± 204.3	413.3 ± 612.3	6.7 ± 11.5	0.0 ± 0.0	0.0 ± 0.0	6.7 ± 11.5	13.3 ± 11.5	0.0 ± 0.0	0.0 ± 0.0	26.7 ± 30.6	6.7 ± 11.5	0.0 ± 0.0	0.0 ± 0.0	0.0 ± 0.0	0.0 ± 0.0	0.0 ± 0.0	0.0 ± 0.0	0.0 ± 0.0
2	GZ-NS	646.7 ± 105.0	556.7 ± 205.0	63.3 ± 50.3	116.7 ± 20.8	53.3 ± 35.1	140.0 ± 149.3	40.0 ± 45.8	3.3 ± 5.8	3.3 ± 5.8	16.7 ± 15.3	3.3 ± 5.8	0.0 ± 0.0	0.0 ± 0.0	0.0 ± 0.0	0.0 ± 0.0	0.0 ± 0.0	0.0 ± 0.0	0.0 ± 0.0
3	SZ-SYC	613.3 ± 144.7	140.0 ± 69.3	106.7 ± 80.8	280.0 ± 260.0	0.0 ± 0.0	693.3 ± 541.2	233.3 ± 387.0	13.3 ± 11.5	0.0 ± 0.0	60.0 ± 0.0	6.7 ± 11.5	0.0 ± 0.0	6.7 ± 11.5	0.0 ± 0.0	6.7 ± 11.5	0.0 ± 0.0	0.0 ± 0.0	0.0 ± 0.0
4	SZ-XMS	286.7 ± 210.1	473.3 ± 380.7	173.3 ± 102.1	116.7 ± 73.7	10.0 ± 17.3	180.0 ± 105.8	56.7 ± 41.6	10.0 ± 17.3	3.3 ± 5.8	26.7 ± 20.8	6.7 ± 11.5	10.0 ± 10.0	16.7 ± 28.9	6.7 ± 11.5	0.0 ± 0.0	0.0 ± 0.0	0.0 ± 0.0	0.0 ± 0.0
5	SZ-JCW	1093.3 ± 731.1	420.0 ± 539.3	26.7 ± 30.6	2300.0 ± 3724.6	0.0 ± 0.0	53.3 ± 30.6	133.3 ± 41.6	0.0 ± 0.0	0.0 ± 0.0	380.0 ± 363.9	20.0 ± 34.6	0.0 ± 0.0	0.0 ± 0.0	0.0 ± 0.0	0.0 ± 0.0	6.7 ± 11.5	0.0 ± 0.0	0.0 ± 0.0
6	SZ-DC	460.0 ± 624.8	6.7 ± 11.5	0.0 ± 0.0	33.3 ± 11.5	0.0 ± 0.0	0.0 ± 0.0	6.7 ± 11.5	0.0 ± 0.0	0.0 ± 0.0	93.3 ± 41.6	0.0 ± 0.0	0.0 ± 0.0	0.0 ± 0.0	0.0 ± 0.0	0.0 ± 0.0	0.0 ± 0.0	6.7 ± 11.5	0.0 ± 0.0
7	SZ-YGW	53.3 ± 50.3	0.0 ± 0.0	0.0 ± 0.0	13.3 ± 11.5	0.0 ± 0.0	0.0 ± 0.0	0.0 ± 0.0	0.0 ± 0.0	0.0 ± 0.0	26.7 ± 30.6	0.0 ± 0.0	0.0 ± 0.0	0.0 ± 0.0	0.0 ± 0.0	0.0 ± 0.0	0.0 ± 0.0	0.0 ± 0.0	0.0 ± 0.0
8	ZH-XLW	73.3 ± 11.5	160.0 ± 111.4	0.0 ± 0.0	93.3 ± 113.7	0.0 ± 0.0	0.0 ± 0.0	0.0 ± 0.0	0.0 ± 0.0	0.0 ± 0.0	33.3 ± 41.6	0.0 ± 0.0	0.0 ± 0.0	6.7 ± 11.5	0.0 ± 0.0	0.0 ± 0.0	0.0 ± 0.0	0.0 ± 0.0	0.0 ± 0.0
9	FCG-WWJT	246.7 ± 220.3	440.0 ± 610.2	40.0 ± 20.0	233.3 ± 253.2	0.0 ± 0.0	0.0 ± 0.0	20.0 ± 34.6	0.0 ± 0.0	0.0 ± 0.0	46.7 ± 80.8	0.0 ± 0.0	0.0 ± 0.0	20.0 ± 20.0	0.0 ± 0.0	0.0 ± 0.0	0.0 ± 0.0	0.0 ± 0.0	0.0 ± 0.0
10	BH-YT	320.0 ± 290.5	46.7 ± 23.1	26.7 ± 46.2	33.3 ± 41.6	0.0 ± 0.0	0.0 ± 0.0	6.7 ± 11.5	0.0 ± 0.0	0.0 ± 0.0	86.7 ± 50.3	6.7 ± 11.5	0.0 ± 0.0	0.0 ± 0.0	0.0 ± 0.0	0.0 ± 0.0	0.0 ± 0.0	0.0 ± 0.0	0.0 ± 0.0
11	ZJ-NJC	2260.0 ± 2605.9	20.0 ± 20.0	20.0 ± 20.0	240.0 ± 140.0	0.0 ± 0.0	0.0 ± 0.0	0.0 ± 0.0	0.0 ± 0.0	0.0 ± 0.0	33.3 ± 11.5	0.0 ± 0.0	6.7 ± 11.5	6.7 ± 11.5	0.0 ± 0.0	0.0 ± 0.0	0.0 ± 0.0	0.0 ± 0.0	0.0 ± 0.0
12	DZ-YR	133.3 ± 197.3	146.7 ± 236.9	0.0 ± 0.0	100.0 ± 100.0	0.0 ± 0.0	0.0 ± 0.0	0.0 ± 0.0	0.0 ± 0.0	0.0 ± 0.0	26.7 ± 46.2	113.3 ± 196.3	0.0 ± 0.0	0.0 ± 0.0	0.0 ± 0.0	0.0 ± 0.0	0.0 ± 0.0	0.0 ± 0.0	26.7 ± 46.2
13	QH-YDT	375.0 ± 513.9	20.0 ± 23.1	5.0 ± 10.0	140.0 ± 228.0	0.0 ± 0.0	0.0 ± 0.0	0.0 ± 0.0	0.0 ± 0.0	0.0 ± 0.0	15.0 ± 30.0	0.0 ± 0.0	0.0 ± 0.0	5.0 ± 10.0	0.0 ± 0.0	0.0 ± 0.0	0.0 ± 0.0	0.0 ± 0.0	5.0 ± 10.0

Abbreviations for the MPs: PE, polyethylene; PS, polystyrene; PVC, polyvinyl chloride; PP, polypropylene; PP + PE, the mixture of PP + PE; PA, polyamide; ABS, the copolymer of acrylonitrile-butadiene-styrene; POM, polyoxymethylene; PET, polyethylene terephthalate; PU, polyurethane; AB, the copolymer of acrylonitrile-butadiene; PTFE, polytetrafluoroethylene; AS, the copolymer of acrylonitrile- styrene; A, acrylonitrile; EVA, ethylene-vinyl acetate; PBT, polybutylene terephthalate; PMMA, polymethyl methacrylate.

FIGURE 3 | Pictures of microplastics (MPs) observed on the beaches of South China.

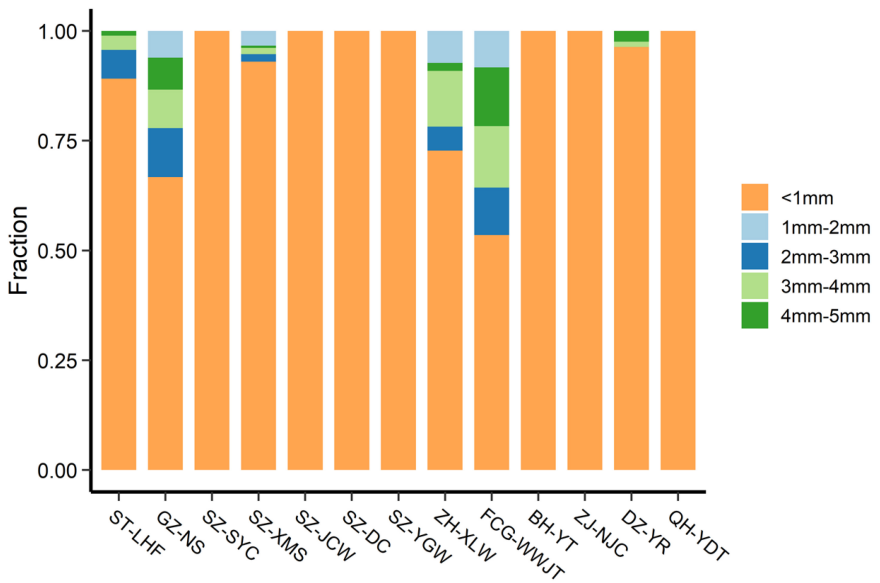

FIGURE 4 | Proportion of MPs in different size at each sampling site.

examined the spatial distribution of small potential MPs by optical analysis and only detected 1.0–2.0 n·kg^{-1} in the beach sand. Also using an optical microscope, Laglbauer et al. (2014) investigated the quality, size, and quantity of MPs in the shoreline and sublittoral sands from six beaches in Slovenia. They reported that the median MP density was higher in the infralittoral zone (155.6 n·kg^{-1}) than on the shoreline (133.3 n·kg^{-1}). Combining microscopic and FTIR methods, Yu et al. (2016) reported that

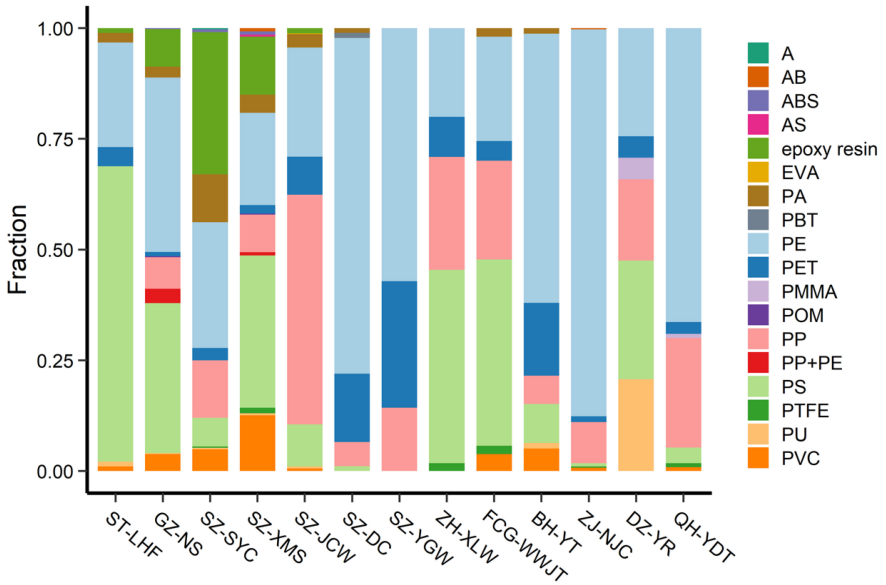

FIGURE 5 | Percentage of different MPs at each sampling site. Abbreviations for the MPs: PE, polyethylene; PS, polystyrene; PVC, polyvinyl chloride; PP, polypropylene; PP + PE, the mixture of PP + PE; PA, polyamide; ABS, the copolymer of acrylonitrile-butadiene-styrene; POM, polyoxymethylene; PET, polyethylene terephthalate; PU, polyurethane; AB, the copolymer of acrylonitrile-butadiene; PTFE, polytetrafluoroethylene; AS, the copolymer of acrylonitrile- styrene; A, acrylonitrile; EVA, ethylene-vinyl acetate; PBT, polybutylene terephthalate; PMMA, polymethyl methacrylate.

the abundance of MPs on the Bohai Sea beach (located in north China) was in the range of 102.9–163.3 n·kg^{-1}, whereas the mean concentration of MPs on several sandy beaches in south China has been reported to be 3,266.0 ± 6,390.8 n·kg^{-1} (Li et al., 2018). However, the identification of MPs in the latter study was based only on a magnifier with 10 × magnification. Using a combination of FTIR and a staining method, Godoy et al. (2020) detected 45.0 ± 24.7 n·kg^{-1}, 31.5 ± 21.5 n·kg^{-1}, and 22.0 ± 23.2 n·kg^{-1} at the La Herradura, Motril, and La Rábita beaches, respectively, in Spain. Using optical fluorescence microscopy, Raman spectroscopy, and field emission scanning electron microscopy with energy dispersion spectroscopy, Yaranal et al. (2021) found that the MP concentrations on five beaches in the Indian state of Karnataka ranged from 264 ± 62 to 1002 ± 174 n·kg^{-1}, for an average MP abundance on the beaches of 664 ± 114 n·kg^{-1}. MP contamination in sediments can be a suitable reference for beach sand, and Phuong et al. (2018) have provided a detailed summary of MP concentrations in sediments around the world. A range of 50–2,000 n·kg^{-1} is commonly observed in marine sediments, although results up to several thousand n·kg^{-1} have also been reported.

Our data are relatively higher than those reported above for beach and sediment environments. However, a direct comparison with earlier results is rough or not statistically feasible due to the different performances of the techniques applied in these studies. Differences in the minimum size dimensions of the MPs captured by various studies is one fundamental constraint to comparing across studies (Ross et al., 2021). In our study, large-sized particles were observed and classified with a stereomicroscope (SteREO Discovery.V20, Zeiss, Germany), while the micron-sized plastics were characterized individually with μ-FTIR. A novel Wizard function quickly located all particles and determined the optimal aperture size for each particle. The length, width, number, and best materials matching the MP specimens were automatically collected by the software (**Figure 2**), providing a quick and effective identification of the small MPs in the sand. This could be the reason the range (93.3–4,433.3 n·kg^{-1}) reported here is on the high end of previously reported MP concentrations in sediments and beach sand. It should be noted that the application of μ-FTIR spectroscopy for MP identification is generally limited to MPs larger than 10 μm. For those MPs smaller than this limit, the irregular shape of the particles may produce reflection errors, making the spectrum matching more challenging (Zarfl, 2019).

Characterization of Microplastics in the Beach Sand

Representative pictures of the MPs are shown in **Figure 3**. The MPs varied in size, color, shape, and texture, and some were coated or attached to unknown materials, possibly biofilms or organic debris. The abundance and size distribution of the total MPs and the different types of MPs are provided in **Tables 1**, **2**, respectively. Smaller-sized MPs were much more abundant than larger ones (**Table 1**). In fact, most of the MPs detected in the sand were sized at less than 1 mm (**Figure 4**). All of the MPs were in this size class at the SZ-YC, SZ-JCW, SZ-YGW, BH-YT, ZJ-NJC, and QH-YDT sites. In GZ-NS, ZH-XLW, and FCG-WWJT, 3–4 mm sized MPs contributed around 5–10% of the total MPs. Such skewed size distributions are commonly observed for MPs in different environments (Liu et al., 2018; Scheurer and Bigalke, 2018; Zhang and Liu, 2018). Due to its good water permeability, beach sand can also act as a filter to retain small

TABLE 3 | Vertical distribution of different MPs on the beach of Yangjiang (n kg^{-1}).

Depth	PE	PS	PVC	PP	PP + PE	epoxy resin	PA	ABS	POM	PET	PU	AB	PTFE	AS	A	EVA	PBT	PMMA	Total
0–10 cm	12.3 ± 7.5	2.0 ± 2.0	0.3 ± 0.6	1.0 ± 1.7	0.0 ± 0.0	0.33 ± 0.58	0.3 ± 0.6	0.0 ± 0.0	0.0 ± 0.0	6.7 ± 6.4	0.0 ± 0.0	0.0 ± 0.0	2.3 ± 1.5	0.0 ± 0.0	0.7 ± 0.6	0.0 ± 0.0	0.0 ± 0.0	0.0 ± 0.0	26.0 ± 1.7
10–20 cm	37.3 ± 51.1	1.0 ± 1.0	2.0 ± 2.7	4.3 ± 2.9	0.0 ± 0.0	0.0 ± 0.0	0.0 ± 0.0	0.0 ± 0.0	0.0 ± 0.0	5.3 ± 1.2	0.3 ± 0.6	0.0 ± 0.0	3.0 ± 3.6	0.0 ± 0.0	0.0 ± 0.0	0.0 ± 0.0	0.0 ± 0.0	0.0 ± 0.0	53.3 ± 45.2
20–30 cm	1.3 ± 1.5	1.3 ± 1.5	0.7 ± 0.6	1.0 ± 1.0	0.0 ± 0.0	0.0 ± 0.0	0.0 ± 0.0	0.0 ± 0.0	0.0 ± 0.0	0.7 ± 1.2	0.0 ± 0.0	0.0 ± 0.0	0.3 ± 0.6	0.0 ± 0.0	0.0 ± 0.0	0.0 ± 0.0	0.0 ± 0.0	0.0 ± 0.0	5.3 ± 5.0
30–40 cm	7.7 ± 7.0	0.0 ± 0.0	0.7 ± 1.2	0.7 ± 0.6	0.0 ± 0.0	0.0 ± 0.0	0.0 ± 0.0	0.0 ± 0.0	0.0 ± 0.0	1.7 ± 1.5	0.0 ± 0.0	0.0 ± 0.0	0.7 ± 1.2	0.0 ± 0.0	0.3 ± 0.6	0.0 ± 0.0	0.0 ± 0.0	0.0 ± 0.0	11.7 ± 10.6

Abbreviations for the MPs: PE, polyethylene; PS, polystyrene; PVC, polyvinyl chloride; PP, polypropylene; PP + PE, the mixture of PP + PE; PA, polyamide; ABS, the copolymer of acrylonitrile-butadiene-styrene; POM, polyoxymethylene; PET, polyethylene terephthalate; PU, polyurethane; AB, the copolymer of acrylonitrile-butadiene; PTFE, polytetrafluoroethylene; AS, the copolymer of acrylonitrile- styrene; A, acrylonitrile; EVA, ethylene-vinyl acetate; PBT, polybutylene terephthalate; PMMA, polymethyl methacrylate.

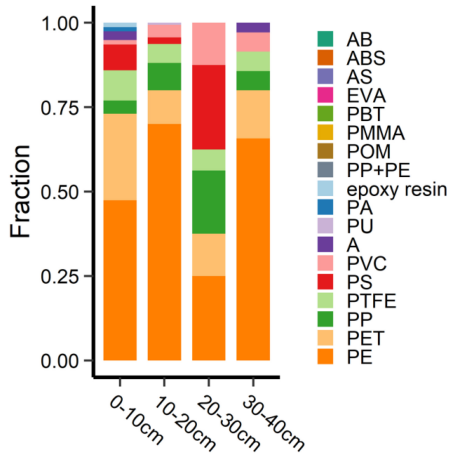

FIGURE 6 | Depth-dependent percentage of different MPs at the Yangjiang beach. Abbreviations for the MPs: PE, polyethylene; PS, polystyrene; PVC, polyvinyl chloride; PP, polypropylene; PP + PE, the mixture of PP + PE; PA, polyamide; ABS, the copolymer of acrylonitrile-butadiene-styrene; POM, polyoxymethylene; PET, polyethylene terephthalate; PU, polyurethane; AB, the copolymer of acrylonitrile-butadiene; PTFE, polytetrafluoroethylene; AS, the copolymer of acrylonitrile- styrene; A, acrylonitrile; EVA, ethylene-vinyl acetate; PBT, polybutylene terephthalate; PMMA, polymethyl methacrylate.

plastic particles in seawater. In addition, MPs can be continuously generated from the weathering of larger plastic debris on the beach. Their exposure to sunlight, frequent wave disturbance, and sand abrasion might also make the disintegration of plastic debris more common here than in other environments. Although the beach is a place accumulating substantial amounts of plastic waste and MPs from both the land and sea, much remains unknown about the effects of the plastic fragments and MPs on beach organisms. There is evidence that small MPs can be potentially ingested by sand-dwelling organisms such as crabs, polychaetes, and bivalves (Van Cauwenberghe and Janssen, 2014; Horn et al., 2020; Knutsen et al., 2020), which could be further transferred along food chains and affect human health (Mercogliano et al., 2020).

Previous studies have only reported a few types of MPs, most of which were mainly based on size, color, or shape, while others have mainly focused on PE, PP, polyamide, PET, PS, and polyvinyl chloride (Li et al., 2018; Zhou et al., 2019; Yaranal et al., 2021). In our study, the texture of the MPs was analyzed by both FTIR-ATR and μ-FTIR analyses. A total of 18 polymers was detected in the sand samples, including various engineering plastics and modified plastics (**Table 2** and **Figure 5**). Besides the above common plastics, acrylonitrile butadiene styrene, epoxy resin, polyformaldehyde, polytetrafluoroethylene, and poly (butylene terephthalate) were also detected in the sand, although their abundances were much lower. To the best of our knowledge, this is the most comprehensive report of MP diversity in beach environments.

Generally, PE, PP, and PS comprised a major portion of the MPs on the beaches (**Figure 5**). The abundance of PE, PP, and PS was 53.3–2,260.0 n·kg^{-1}, 0–2,300 n·kg^{-1}, 0–556.7 n·kg^{-1}, respectively. Polyethylene accounted for 19–86% of the total

counts, while PS contributed 26–66% at the ST-LHF, GZ-NS, SZ-XMS, ZH-XLW, FCG-WWJT, and DZ-YRST sites. Polypropylene was another important type of MP contamination at the SZ-JCW, ZH-XLW, FCG-WWJT, DZ-YRST, and QH-YDT sites, contributing 18–51% of the total MPs. At SZ-YC, epoxy resin, a class of reactive prepolymers and polymers that contain epoxide groups contributed nearly 30% of the total MPs. This kind of polymer was generally absent at most other sites, suggesting a point source could exist nearby. Overall, our study demonstrated that the MPs on the beaches were much more diverse than previous reports suggest.

Vertical Profile of Microplastics in the Beach Sand

The vertical distribution of MPs on the YJ-BLW beach is shown in **Table 3** and **Figure 6**. The MP abundances were 26.0 ± 1.7, 53.3 ± 45.2, 5.3 ± 5.0, and 11.7 ± 10.6 $n \cdot kg^{-1}$ at the 0–10, 10–20, 20–30, and 30–40 cm depths, respectively. There was no significant difference between the 0–10 and 10–20 cm layers. However, the MP concentration was significantly higher in the two surface layers (0–20 cm) than in the deeper layers (20–40 cm, $p < 0.01$), suggesting a slow migration of the MPs downward. **Figure 6** shows the depth-dependent abundance of the different MPs. Again, the largest proportion was PE. The MPs in the uppermost layer appeared more diverse than those in the other layers. As all of the MPs here were less than 1 mm, there was no significant difference in terms of the size distribution among the four layers. Because μ-FTIR is more effective in identifying MPs larger than 10 μm (Zarfl, 2019), much remains unknown about the vertical distribution of MPs smaller than this limit, especially for nanoplastics which are smaller than 1 μm. Whether the deeper layers of beaches are a sink for nanoplastics deserves further study in the future.

CONCLUSION

This study described the distribution and characteristics of MPs on 14 beaches located on the coast of South China. Our results detected a ubiquitous distribution of MPs in the sand from the surface layers to a depth of 40 cm. Most of the beach MPs were small in size, particularly less than 1 mm. A total of 18 types of polymers were identified in the sand, suggesting that the types of MPs on beaches are much more diverse than indicated in previous reports. Polyethylene and PS comprised a major portion of the MPs on the beach, and at the site examined by depth, they were more abundant in the upper layers of the beach than in the deeper layers. More efforts are needed to clarify the vertical distribution of MPs in beach sand, especially for those MPs less than 1μ m.

DATA AVAILABILITY STATEMENT

The original contributions presented in the study are included in the article/**Supplementary Material**, further inquiries can be directed to the corresponding author.

AUTHOR CONTRIBUTIONS

BC: field sampling, conceived and designed the research, performed the experiments, analyzed data, and wrote the manuscript. YL: performed the experiments, analyzed data, and wrote the manuscript. LW, X-TZ, FC, and JM: field sampling and analyzed data. Y-PW: performed the experiments and analyzed data. KP: conceived and designed the research and wrote the manuscript. All authors contributed to the article and approved the submitted version.

FUNDING

This work was supported by the Shenzhen Science and Technology Innovation Commission of China (JCYJ20180507182227257 and KQTD20180412181334790), the Guangxi Key R&D Program of China (GUIKE AB20297018), Guangdong Basic and Applied Basic Research Foundation (2019A1515011630), the Fundamental Research Funds for the Central Universities of China (21621054), and Medical Scientific Research Foundation of Guangdong Province of China (20191118142729581).

SUPPLEMENTARY MATERIAL

The Supplementary Material for this article can be found online at: https://www.frontiersin.org/articles/10.3389/fmars.2022.863652/full#supplementary-material

REFERENCES

Andrady, A. L. (2015). "Persistence of plastic litter in the oceans," in *Marine anthropogenic litter*, eds M. Bergmann, L. Gutow, and M. Klages (Cham: Springer), 57–72. doi: 10.1007/978-3-319-16510-3_3

Beiras, R., and Schönemann, A. M. (2020). Currently monitored microplastics pose negligible ecological risk to the global ocean. *Sci. Rep.* 10:22281.

Brown, A. C., and McLachlan, A. (2002). Sandy shore ecosystems and the threats facing them: some predictions for the year 2025. *Environ. Conserv.* 29, 62–77. doi: 10.1017/s037689290200005x

Burns, E. E., and Boxall, A. B. (2018). Microplastics in the aquatic environment: evidence for or against adverse impacts and major knowledge gaps. *Environ. Toxicol. Chem.* 37, 2776–2796.

Chai, B., Wei, Q., She, Y., Lu, G., Dang, Z., and Yin, H. (2020). Soil microplastic pollution in an e-waste dismantling zone of China. *Waste Manag.* 118, 291–301. doi: 10.1016/j.wasman.2020.08.048

Defeo, O., McLachlan, A., Armitage, D., Elliott, M., and Pittman, J. (2021). Sandy beach social–ecological systems at risk: regime shifts, collapses, and governance challenges. *Front. Ecol. Environ.* 19, 564–573. doi: 10.1002/fee.2406

Dekiff, J. H., Remy, D., Klasmeier, J., and Fries, E. (2014). Occurrence and spatial distribution of microplastics in sediments from Norderney. *Environ. Pollut.* 186, 248–256. doi: 10.1016/j.envpol.2013.11.019

De-la-Torre, G. E., Dioses-Salinas, D. C., Castro, J. M., Antay, R., Fernández, N. Y., Espinoza-Morriberón, D., et al. (2020). Abundance and distribution of microplastics on sandy beaches of Lima, Peru. *Mar. Pollut. Bull.* 151:110877. doi: 10.1016/j.marpolbul.2019.110877

Frias, J. P. G. L., and Nash, R. (2019). Microplastics: finding a consensus on the definition. *Mar. Pollut. Bull.* 138, 145–147. doi: 10.1016/j.marpolbul.2018.11.022

Galgani, F., Hanke, G., and Maes, T. (2015). "Global distribution, composition and abundance of marine litter," in *Marine anthropogenic litter*, eds M. Bergmann, L. Gutow, and M. Klages (Cham: Springer), 29–56. doi: 10.1007/978-3-319-16510-3_2

Godoy, V., Prata, J. C., Blázquez, G., Almendros, A. I., Duarte, A. C., Rocha-Santos, T., et al. (2020). Effects of distance to the sea and geomorphological characteristics on the quantity and distribution of microplastics in beach sediments of Granada (Spain). *Sci. Total Environ.* 746:142023. doi: 10.1016/j.scitotenv.2020.142023

Hidalgo-Ruz, V., Gutow, L., Thompson, R. C., and Thiel, M. (2012). Microplastics in the marine environment: a review of the methods used for identification and quantification. *Environ. Sci. Technol.* 46, 3060–3075. doi: 10.1021/es2031505

Horn, D. A., Granek, E. F., and Steele, C. L. (2020). Effects of environmentally relevant concentrations of microplastic fibers on Pacific mole crab (Emerita analoga) mortality and reproduction. *Limnol. Oceanogr. Lett.* 5, 74–83. doi: 10.1002/lol2.10137

Ivar do Sul, J. A., and Costa, M. F. (2014). The present and future of microplastic pollution in the marine environment. *Environ. Pollut.* 185, 352–364. doi: 10.1016/j.envpol.2013.10.036

Jambeck, J. R., Geyer, R., Wilcox, C., Siegler, T. R., Perryman, M., Andrady, A., et al. (2015). Plastic waste inputs from land into the ocean. *Science* 347, 768–771. doi: 10.1126/science.1260352

Knutsen, H., Cyvin, J. B., Totland, C., Lilleeng, Ø, Wade, E. J., Castro, V., et al. (2020). Microplastic accumulation by tube-dwelling, suspension feeding polychaetes from the sediment surface: a case study from the Norwegian Continental Shelf. *Mar. Environ. Res.* 161:105073. doi: 10.1016/j.marenvres.2020.105073

Laglbauer, B. J., Franco-Santos, R. M., Andreu-Cazenave, M., Brunelli, L., Papadatou, M., Palatinus, A., et al. (2014). Macrodebris and microplastics from beaches in Slovenia. *Mar. Pollut. Bull.* 89, 356–366. doi: 10.1016/j.marpolbul.2014.09.036

Li, D., Liu, K., Li, C., Peng, G., Andrady, A. L., Wu, T., et al. (2020). Profiling the vertical transport of microplastics in the West Pacific Ocean and the East Indian Ocean with a novel in situ filtration technique. *Environ. Sci. Technol.* 54, 12979–12988. doi: 10.1021/acs.est.0c02374

Li, J., Zhang, H., Zhang, K., Yang, R., Li, R., and Li, Y. (2018). Characterization, source, and retention of microplastic in sandy beaches and mangrove wetlands of the Qinzhou Bay, China. *Mar. Pollut. Bull.* 136, 401–406. doi: 10.1016/j.marpolbul.2018.09.025

Liu, M., Lu, S., Song, Y., Lei, L., Hu, J., Lv, W., et al. (2018). Microplastic and mesoplastic pollution in farmland soils in suburbs of Shanghai, China. *Environ. Pollut.* 242, 855–862. doi: 10.1016/j.envpol.2018.07.051

Lusher, A. L., Tirelli, V., O'Connor, I., and Officer, R. (2015). Microplastics in Arctic polar waters: the first reported values of particles in surface and sub-surface samples. *Sci. Rep.* 5, 1–9. doi: 10.1038/srep14947

Mazariegos-Ortíz, C., de los Ángeles Rosales, M., Carrillo-Ovalle, L., Cardoso, R. P., Muniz, M. C., and Dos Anjos, R. M. (2020). First evidence of microplastic pollution in the El Quetzalito sand beach of the Guatemalan Caribbean. *Mar. Pollut. Bull.* 156:111220. doi: 10.1016/j.marpolbul.2020.111220

McLachlan, A., and Defeo, O. (2017). *The ecology of sandy shores*. Cambridge, Massachusetts: Academic press.

Mercogliano, R., Avio, C. G., Regoli, F., Anastasio, A., Colavita, G., and Santonicola, S. (2020). Occurrence of microplastics in commercial seafood under the perspective of the human food chain. A review. *J. Agric. Food Chem.* 68, 5296–5301. doi: 10.1021/acs.jafc.0c01209

Nuelle, M. T., Dekiff, J. H., Remy, D., and Fries, E. (2014). A new analytical approach for monitoring microplastics in marine sediments. *Environ. Pollut.* 184, 161–169. doi: 10.1016/j.envpol.2013.07.027

Patchaiyappan, A., ZakiAhmed, S., Dowarah, K., Khadanga, S. S., Singh, T., Jayakumar, S., et al. (2021). Prevalence of microplastics in the sediments of Odisha beaches, southeastern coast of India. *Mar. Pollut. Bull.* 167:112265. doi: 10.1016/j.marpolbul.2021.112265

Peng, Y., Wu, P., Schartup, A. T., and Zhang, Y. (2021). Plastic waste release caused by COVID-19 and its fate in the global ocean. *Proc. Natl. Acad. Sci. U. S. A.* 118:e2111530118. doi: 10.1073/pnas.2111530118

Phuong, N. N., Poirier, L., Lagarde, F., Kamari, A., and Zalouk-Vergnoux, A. (2018). Microplastic abundance and characteristics in French Atlantic coastal sediments using a new extraction method. *Environ. Pollut.* 243, 228–237. doi: 10.1016/j.envpol.2018.08.032

Ross, P. S., Chastain, S., Vassilenko, E., Etemadifar, A., Zimmermann, S., Quesnel, S. A., et al. (2021). Pervasive distribution of polyester fibres in the Arctic Ocean is driven by Atlantic inputs. *Nat. Commun.* 12, 1–9. doi: 10.1038/s41467-020-20347-1

Scheurer, M., and Bigalke, M. (2018). Microplastics in Swiss floodplain soils. *Environ. Sci. Technol.* 52, 3591–3598. doi: 10.1021/acs.est.7b06003

Shim, W. J., Hong, S. H., and Eo, S. E. (2017). Identification methods in microplastic analysis: a review. *Anal. Methods* 9, 1384–1391. doi: 10.1039/c6ay02558g

Silva-Cavalcanti, J. S., Barbosa de Araujo, M. C., and Ferreira da Costa, M. (2009). Plastic litter on an urban beach—a case study in Brazil. *Waste Manag. Res.* 27, 93–97. doi: 10.1177/0734242X08088705

Thompson, R. C., Olsen, Y., Mitchell, R. P., Davis, A., Rowland, S. J., John, A. W., et al. (2004). Lost at sea: where is all the plastic? *Science* 304, 838–838.

Tiwari, M., Rathod, T. D., Ajmal, P. Y., Bhangare, R. C., and Sahu, S. K. (2019). Distribution and characterization of microplastics in beach sand from three different Indian coastal environments. *Mar. Pollut. Bull.* 140, 262–273. doi: 10.1016/j.marpolbul.2019.01.055

Van Cauwenberghe, L., and Janssen, C. R. (2014). Microplastics in bivalves cultured for human consumption. *Environ. Pollut.* 193, 65–70. doi: 10.1016/j.envpol.2014.06.010

Wang, C., Zhao, J., and Xing, B. (2021). Environmental source, fate, and toxicity of microplastics. *J. Hazard. Mater.* 407:124357. doi: 10.1016/j.jhazmat.2020.124357

Yaranal, N. A., Subbiah, S., and Mohanty, K. (2021). Distribution and characterization of microplastics in beach sediments from Karnataka (India) coastal environments. *Mar. Pollut. Bull.* 169:112550. doi: 10.1016/j.marpolbul.2021.112550

Yu, X., Peng, J., Wang, J., Wang, K., and Bao, S. (2016). Occurrence of microplastics in the beach sand of the Chinese inner sea: the Bohai Sea. *Environ. Pollut.* 214, 722–730. doi: 10.1016/j.envpol.2016.04.080

Zarfl, C. (2019). Promising techniques and open challenges for microplastic identification and quantification in environmental matrices. *Anal. Bioanal. Chem.* 411, 3743–3756. doi: 10.1007/s00216-019-01763-9

Zhang, G. S., and Liu, Y. F. (2018). The distribution of microplastics in soil aggregate fractions in southwestern China. *Sci. Total Environ.* 642, 12–20.

Zhou, Y., Liu, X., and Wang, J. (2019). Characterization of microplastics and the association of heavy metals with microplastics in suburban soil of central China. *Sci. Total Environ.* 694:133798. doi: 10.1016/j.scitotenv.2019.133798

Conflict of Interest: The authors declare that the research was conducted in the absence of any commercial or financial relationships that could be construed as a potential conflict of interest.

Advantages of publishing in Frontiers

OPEN ACCESS
Articles are free to read for greatest visibility and readership

FAST PUBLICATION
Around 90 days from submission to decision

HIGH QUALITY PEER-REVIEW
Rigorous, collaborative, and constructive peer-review

TRANSPARENT PEER-REVIEW
Editors and reviewers acknowledged by name on published articles

Frontiers
Avenue du Tribunal-Fédéral 34
1005 Lausanne | Switzerland

Visit us: www.frontiersin.org
Contact us: frontiersin.org/about/contact

REPRODUCIBILITY OF RESEARCH
Support open data and methods to enhance research reproducibility

DIGITAL PUBLISHING
Articles designed for optimal readership across devices

FOLLOW US
@frontiersin

IMPACT METRICS
Advanced article metrics track visibility across digital media

EXTENSIVE PROMOTION
Marketing and promotion of impactful research

LOOP RESEARCH NETWORK
Our network increases your article's readership